ABSTRACT

Title of Dissertation:	SOIL-PILE INTERACTION UNDER VERTICAL DYNAMIC LOADING
	Ghassan Sutaih, Doctor of Philosophy, 2018
Dissertation directed by:	Professor M. Sherif Aggour (Chair/Advisor), Department of Civil and Environmental Engineering.

Improper foundation designs for machine vibrations can result in machine failure, severe discomfort to workers around the machine or excessive settlement. The goal of foundation design for machine vibrations is to minimize vibration amplitude. In poor soil conditions, pile foundations are used to support the machine. Soil-pile stiffness and damping must be known at the level of the pile head. Since piles are used mostly in a group, it is also necessary to determine the interaction of the piles within the group. This study uses a 3D finite element method to study the response of pile foundations subjected to vertical dynamic loading. It uses Lysmer's analog where the pile is replaced by a single degree of freedom dynamic system that provides frequency independent parameters.

A parametric study is performed to obtain the value of the stiffness and the damping of a single pile for different soil properties and for both homogeneous and

nonhomogeneous soils. Floating and end-bearing piles were also studied. Pile group response is influenced by the soil-pile-soil interaction. The interaction is obtained by varying both the spacing and the soil properties around the pile. Interaction between the piles causes reduction in the stiffness and damping of the soil-pile system compared to an isolated pile. The study provided the interaction factors as a function of pile spacing and properties of the soil. Using the interaction factors, the response of a group of piles can be determined from the response of a single pile.

SOIL-PILE INTERACTION UNDER VERTICAL DYNAMIC LOADING

By

Ghassan Hassan Sutaih

Dissertation submitted to the Faculty of the Graduate School of the
University of Maryland, College Park, in partial fulfillment
of the requirements for the degree of
Doctor of Philosophy
2018

Advisory Committee:
Professor M. Sherif Aggour, Chair
Professor Amde M. Amde
Professor Chung C. Fu
Professor Dimitrios G. Goulias
Professor Amr Baz

Dedication

To my mother and my sisters for their contineous support during my graduates studies.

To the government of Saudi Arabia represented by Kng Abdul Aziz University for their financial support and giving me this opputrtuinity to pursue a graduate degree.

Acknowledgements

I would like to thanks Professor M.S. Aggour who supervised my research. I would like to thank him for his contneous support and guidance during my graduate studies. I would like to thank Professors Amde M. Amde, Chung Fu, Dimitrios G. Goulias and Amr Baz for kindly serving on my thesis committee. I would like to thanks the government of Saudi Arabia represented by Kng Abdul Aziz University for their financial support and giving me this opputrtuinity to pursue a graduate degree.

Table of Contents

List of Tables

List of Figures

1. Introduction

Vibration from operating machines generates cyclic stresses within the soil. The stresses will cause deformation within the soil. Due to the dynamic nature of the stresses, deformations will be amplified if the machine operates at the foundation-soil resonant frequency. Machine foundation design involves analyzing and optimizing the foundation to determine foundation type (shallow or deep) and geometry. Selection of foundation type and geometry control parameters that influence the motion of the foundation under the applied dynamic load such as natural frequency, geometric damping, and stiffness. The goal of the design is to minimize vibration so that the machine can operate smoothly. One design criteria is Suggested by Richart, F. E. et al. (1970) and is shown in Figure.1.1. It is based on the maximum allowable amplitude of dynamic displacement for a certain operating frequency. The cristerion gives human comfort around the machine for a certain frequency and amplitude. Another criterion given by Baxter & Bernhard (1967) is shown in Figure 1.2 which is based on how smooth the machine will run based on amplitude and vibration frequency.

Examples of machines include Gas turbine Generators, wind turbine generators, industrial machines, etc. The foundation can be designed to support loadings in different directions (i.e., vertical, horizontal, rocking and rotational) and different Loading type (e.g., sinusoidal vibration and sudden loads).

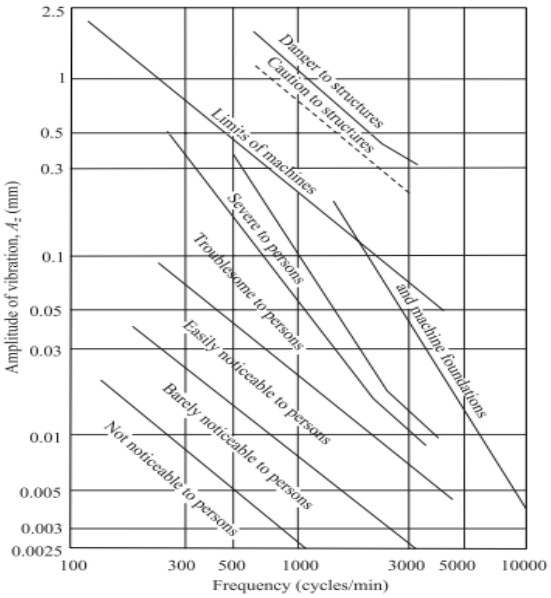

Figure 1.1: Criterion for Foundation Vibration after Richart F.E. et al. (1970).

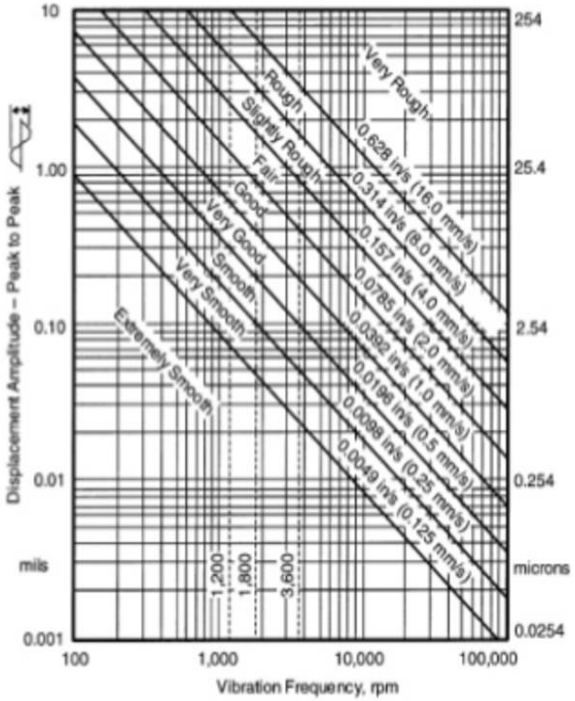

Figure 1.2: Criterion for foundation vibration after Baxter & Bernhard (1967).

Design of machine foundations requires working with the available soil either at site conditions, if suitable, or improved soil. Foundation type needs to be considered (i.e., shallow or deep foundation). Is the soil conditions near the surface is good, shallow foundations are used, if poor soil conditions exists near the surface, pile foundations are used to carry the load to a deeper stronger strata. After selecting the foundation, its dimensions need to be adjusted to meet design requirements. Many variables influence the design of the foundation. These variables include soil elastic properties (usually Young's modulus and Poisson's ratio), soil density, the mass of supported machine and the mass of the supporting foundation, the shape of the foundation and dimensions of the foundation. Common analytical design method for shallow foundations involves reducing the problem into a single degree of freedom dynamic problem which includes a mass, a spring, and a dashpot. This is known as Lysmer's analog (Lysmer & Richart, 1966). The three parameters are sufficient to describe the foundation motion corresponding to the applied dynamic loading. The mass is the sum of the footing and the machine mass. The spring constant describes the stiffness of the foundation-soil system. The damper describes energy loss due to damping. Different soil conditions and foundation types and dimensions control the values of these three parameters. Also, stiffness and damping could be frequency dependent. A schematic drawing that describes Lysmer's Analogue is shown in Figure 1.3.

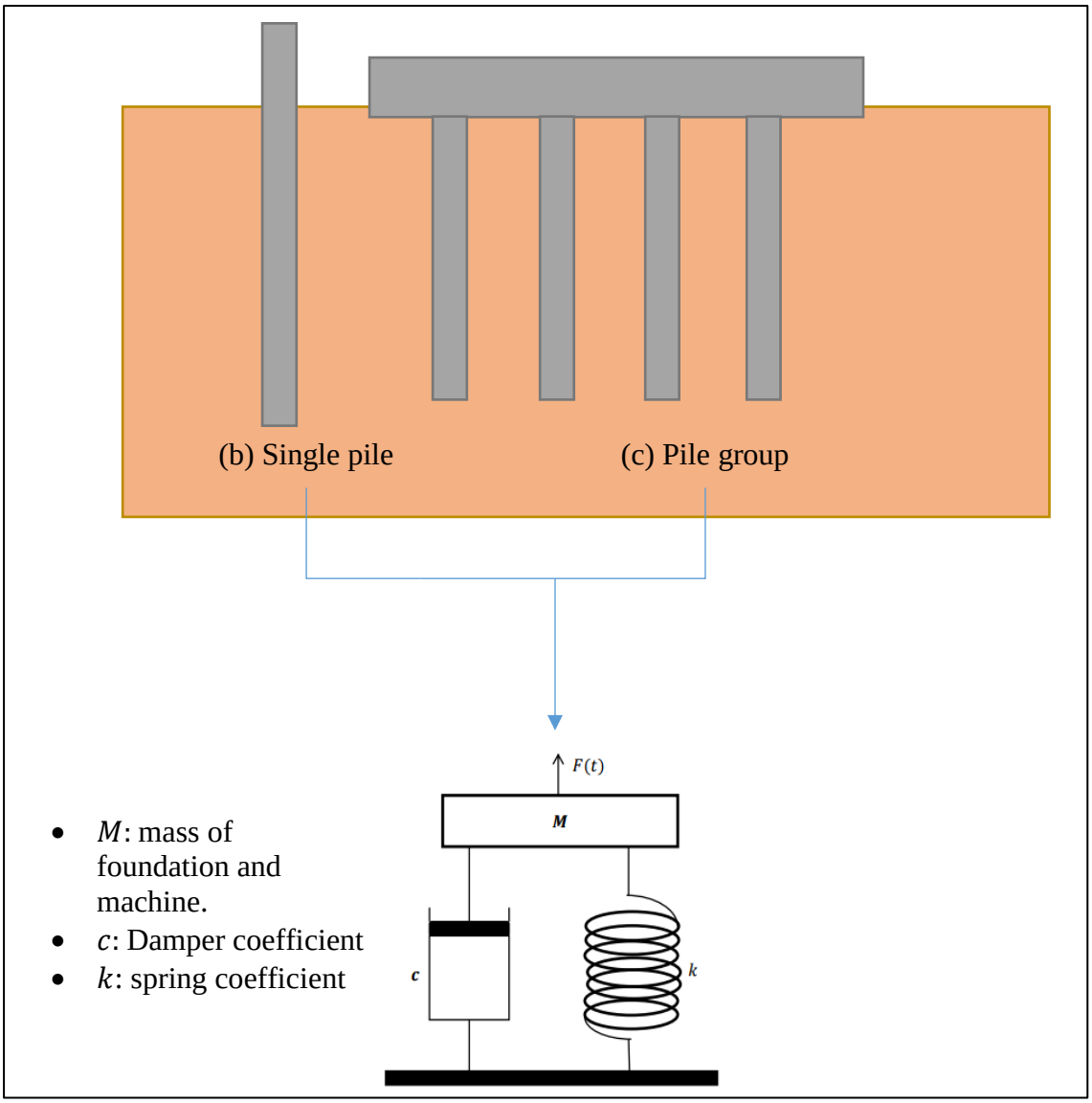

Figure 1.3: Simplified single degree of freedom problem for Different Types of Foundations subjected to Vertical Dynamic Loading.

Figure 1.3 shows a single pile (a), and a pile group (b) that can be converted to a single degree of freedom dynamic problem which consists of a spring with a spring constant, k, a dashpot with a damping, c, and a mass, M, which is the sum of masses of the machine and the foundation. Depending on the condition of the problem, k and c may vary.

Solution provided by Novak (1974) for single pile subjected to vertical dynamic loading is an analytical method used to design single piles subjected to

dynamic loading. It gives the spring and damper coefficients that describe the motion at the top of the pile. Another approach in design of piles subjected to dynamic loading is a one dimensional finite element approach where the pile is modeled as a bar element divided into segments. Side soil is modeled as a discrete set of springs and dampers. Soil at the base is also modeled using a spring and damper. This approach is approximate and better in modeling pile embedded in layered soil profiles.

Since piles are used in groups, the values of the stiffness and damping of the group are needed. Pile groups subjected to dynamic loading are designed by using interaction factors. A single pile stiffness and damping are obtained analytically using Novak's solution. After obtaining stiffness and damping of a single pile, the values of the stiffness and damping of the single piles are adjusted for group behavior using interaction factors provided by Poulos (1968).

1.1. Limitations in current design methods

- Current available analytical solution regarding pile subjected to vertical dynamic load is the one provided by Novak (1974) and is accurate at α certain value of dimensionless frequency, $a_0 = 0.3$. where $a_0 = \omega\, r_p/v_s$. ω is the frequency of the load in radians per seconds, r_p is the pile radius and v_s is the shear wave velocity of the soil.
- Novak's (1974) Solution is also limited to homogeneous soil profiles (i.e., constant soil elastic modulus with depth). This means that if inhomogeneous soil exists in the field, properties must be averaged for the engineer to be able to design the foundation using Novak's Solutions. Averaging soil properties

might yield an erroneous design that would require a high factor of safety. This would render the design to be inefficient and costly.

- One dimensional finite element approach is fast compared to 3D continuum finite element modeling. However, the approach ignores the continuity of the problem due to the soil being modeled as discrete separate sets of springs and dampers. Piles interact with surrounding soil as continuum. Layers of soil around the pile interact with each other and reflection, and refraction between layers will alter the behavior of the soil around the pile. Discrete springs and dampers might not represent real layered soil behavior.
- Another limitation in current design methods is that static interaction factors provided by Poulos (1968) are the ones used in design for pile groups subjected to dynamic loading. The interaction factors are applied to both, stiffness and damping of the group.

1.2. The need for research

- Currently, available codes for machine foundation lack provisions for machine foundation supported on piles. These codes include ACI 351.3R-04: Foundations for Dynamic Equipment, 2004, DIN 4024: Machine Foundations, 1955, SAES-Q-007: Foundations and Supporting Structures for Heavy Machinery, 2009s. An extensive review of codes provision for machine foundations is given by Bharathi, Dhiraj, & Dubey (2014).
- Novak accuracy is limited to dimensionless frequency, $a_0 = 0.3$. studying piles subjected to dynamic loading at dimensionless frequencies far from 0.3 is needed.

- To study single piles in inhomogeneous soils. In many cases, field conditions of soils are far from being homogeneous and averaging soil properties might not represent field conditions properly. In many cases, field studies on soil show that soil elastic modulus calculated by shear wave velocity measurements tend to increase with depth. See Figure 1.4. In Figure 1.4, a typical linear increase of soil elastic modulus with depth is shown. Using such soil profile would be better than averaging soil properties.
- There is a need to study the dynamic interaction between piles in a group. Since piles are mostly used in groups, the stiffness and damping of the individual piles within the group are less than the stiffness and damping of an isolated pile in the same soil. This is due to the interaction between the piles within the group; However, currently only static interaction factors are used in design for dynamic problems.

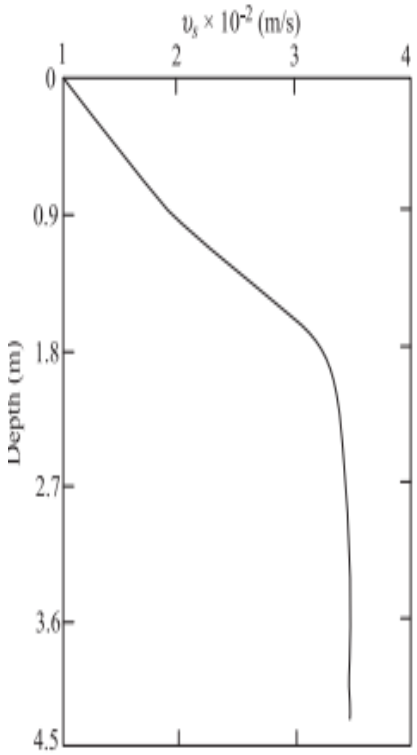

Figure 1.4: Typical variation of soil shear wave velocity with depth after Stokoe & Woods (1972).

1.3. Problem Statement and Objectives

The problem studied here generally considers circular pile foundations subjected to vertical dynamic loading. A mass is attached on top of the pile. The soil material properties are varied but in general remain linearly elastic. Inhomogeneous and homogeneous soil profiles are studied. The pile is either a floating pile or and end bearing pile. In addition to single pile behavior under dynamic loading, pile-to-pile interaction is studied. In pile-to-pile interaction study, two piles are equally loaded dynamically and spaced at different distances to study the effect of spacing. Soil material properties are also varied at each spacing. Each variable studied has an influence on the stiffness and damping of the pile. Comparison of available design methods is discussed. The finite element method is

used to determine the stiffness and damping of the pile for the different cases. Figure 1.4 shows a graphical representation of the cases considered.

In summary, the cases to be studied are

1- Study of a single pile foundation (floating and end bearing piles) subjected to vertical dynamic loading in a homogeneous soil.
2- Study of a single pile foundation (floating and end bearing pile) subjected to vertical dynamic loading in an inhomogeneous soil.
3- Study of pile-to-pile interaction at different spacing in a homogeneous soil.

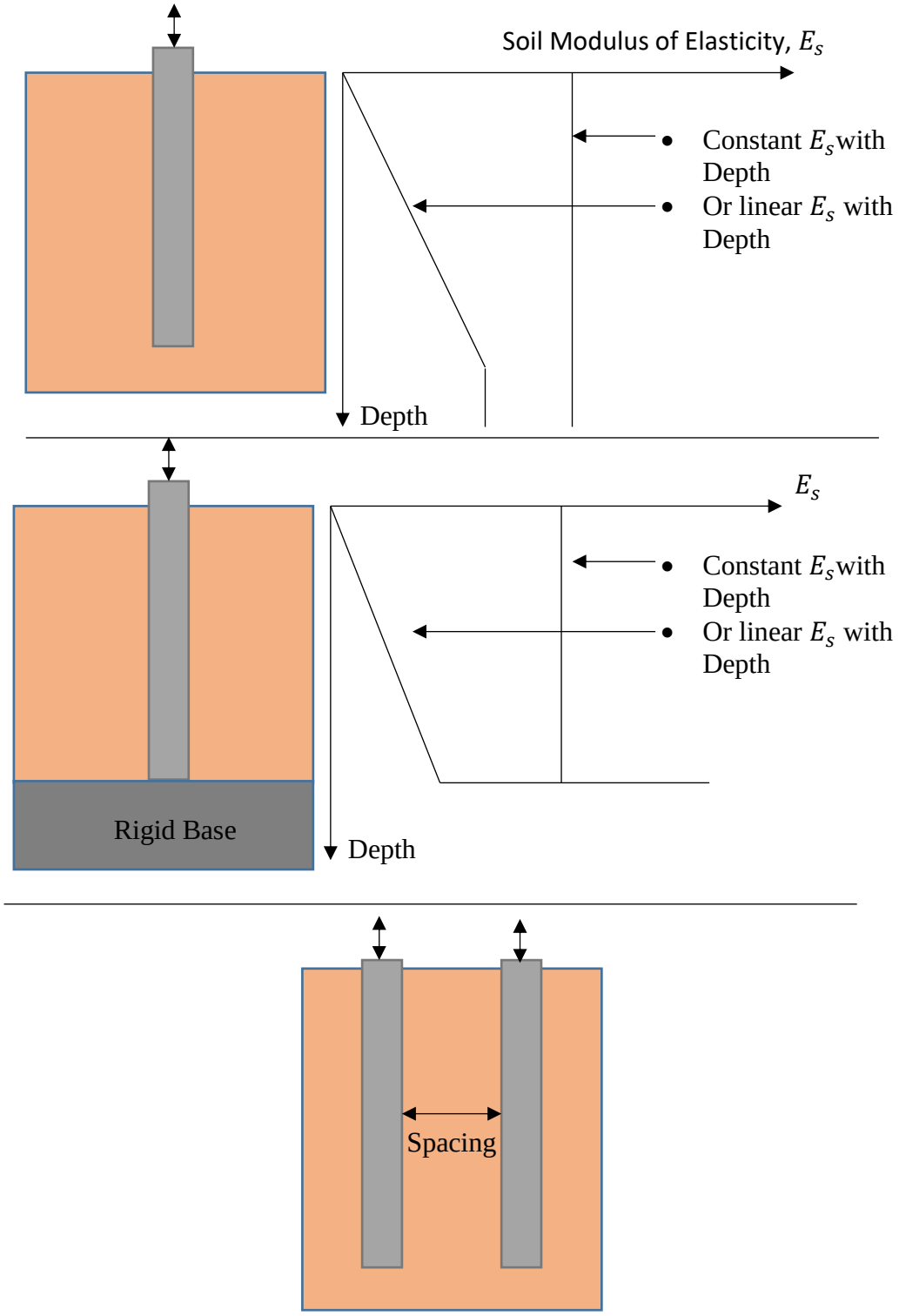

Figure 1.5: Graphical Representation of studied cases.

In Figure 1.5, a floating pile in a homogeneous or an inhomogeneous soil is shown (top). An end bearing pile in homogeneous or inhomogeneous soil is shown (middle). Finally, pile-to-pile interaction is shown at the bottom.

1.4.Thesis Organization

The thesis is divided into 6 chapters (including this one). Starting from chapter 2 these chapters are:

- Chapter 2: Literature Review. This chapter gives an introduction to available design methods for single pile foundations. Both analytical and numerical methods are discussed. A discussion of the design of pile groups subjected to vertical dynamic loading is also provided.
- Chapter 3: Introduction to the Finite Element Method. The chapter gives an introduction to the finite element method and its application in dynamic problems. A discussion of the math involved in finite element analysis is provided. Discussion of element matrices formulation, assembly of global matrices is provided. Static and dynamic solvers are discussed.
- Chapter 4: Modeling and Finite Element Method Implementation. The chapter describes how the finite element method is applied to current research. It also discusses the research procedure from modeling the geometry, performing the analysis to obtaining and interpreting the results.
- Chapter 5: Results and Discussion. This chapter presents the results of this research and discuss their interpretation. It also compares research results with the work of others when applicable.

- Chapter 6: Design Charts and Conclusion. The chapter summarizes the research work, its results, and outcomes. Practical design recommendations are provided based on outcomes of this research.

2. Literature Review

This chapter covers previous studies on piles under dynamic vertical loads. It covers design methods and research related to pile dynamics. Several studies are undertaken on piles subjected to vertical dynamic loading. These studies vary greatly in their approach to the problem. Some studies provide a closed-form solution to the differential Equations that describe the behavior of piles. This type of study is limited to 1) the case considered in describing the problem. 2) the assumptions made to simplify the problem in order to obtain the solution. Other studies provide a simplified 1-Dimensional numerical solution to the problem. These studies are limited due to the inherent error in using 1-Dimensional solution to a 3D problem. Advancements have been made for these studies to account for this error. Other studies provide the use of finite element method and varying the variables that affect the response of the pile to the applied load. This chapter provides a summary on these studies from the closed-form solutions to the numerical analysis.

2.1. Machines and machine vibration

Proper machine foundation design is an integral part of machine operation. The machines discussed are those related to industrial machines and power plants machines. These machines operate at a certain frequency, and they generate vibratory loads. The vibration can be amplified if the machine operate at the soil-foundation resonance frequency. Amplification of machine vibration can hinder the machine productivity, be very uncomfortable to people working next to the

machine, and in severe cases might break the machine or cause failure in the systems connected to that machine.

Based on the frequency of operations, machines can be classified to 4 classes: 1) very low-speed machines that operate at 500 cycles per minute or less, 2) low-speed machines which operate at frequencies between 500 and 1500 cycles per minute. 3) medium speed machines which operate at frequencies between 1500 and 3000 cycles per minute and 4) high-speed machines that operate at frequencies higher than 3000 cycles per minute. Examples of machines include wind turbines, printing machines, steam mills, boiler feed pumps, small fans used in power industry and turbomachines such as gas turbines and compressors.

The goal of the design is to limit vibration. The design involves working with existing field or improved soil condition and selecting the optimal foundation type suitable for those conditions. From this definition, the variables of the design are soil profile and soil properties (mainly elastic modulus, density and Poisson's ratio), foundation type: shallow or deep foundations and foundation Geometry (shape, dimensions, and mass). The foundation serves two purposes: static stability which means that foundation should carry the weight of the machine at acceptable settlement and dynamical stability which means low vibration amplitude so that the machine can operate smoothly.

This dissertation covers pile foundations, which are categorized as deep foundations. This type of foundation is used when shallow foundations are not an option due to poor soil conditions near the surface. The piles are used then to carry the load into deeper more stronger soil strata or to rock base. Using piles increases the value of the natural frequency of the system, and decreases the geometric

damping of the system. Design of piles for machine foundation also means working with pile groups since piles are mostly used in groups. Piles in a group interact with each other. This means that the stiffness and damping of a pile group is not simply the sum of the stiffness and damping of individual piles within the group. It is less than the sum due to the interaction between piles in the group. The following sections in this chapter discuss pile foundation design and analysis techniques with more detail. For more on machines and machine foundation the reader is referred to Chowdhury & Dasgupta, (2008), Das & Ramana, (2010) and Richart, F.E. et al., (1970).

2.2. Closed form solutions for single pile subjected to dynamic loading

Closed form solutions simplify the problem into a mathematical model consisting of differential Equations. A solution to these Equations is then provided. Assumptions are made on the original problem to simplify the complexity of the differential Equations to be solved.

2.2.1. Richart (1970) solution for single pile resting on rock

Richart, F. E. et al., (1970) presented a closed form solution for a pile resting on a rock base. The pile supports a weight at its top. The problem is simplified into a fixed free rod with a mass attached at the free end. See Figure 2.1 for illustration of the actual problem and the corresponding simplified model.

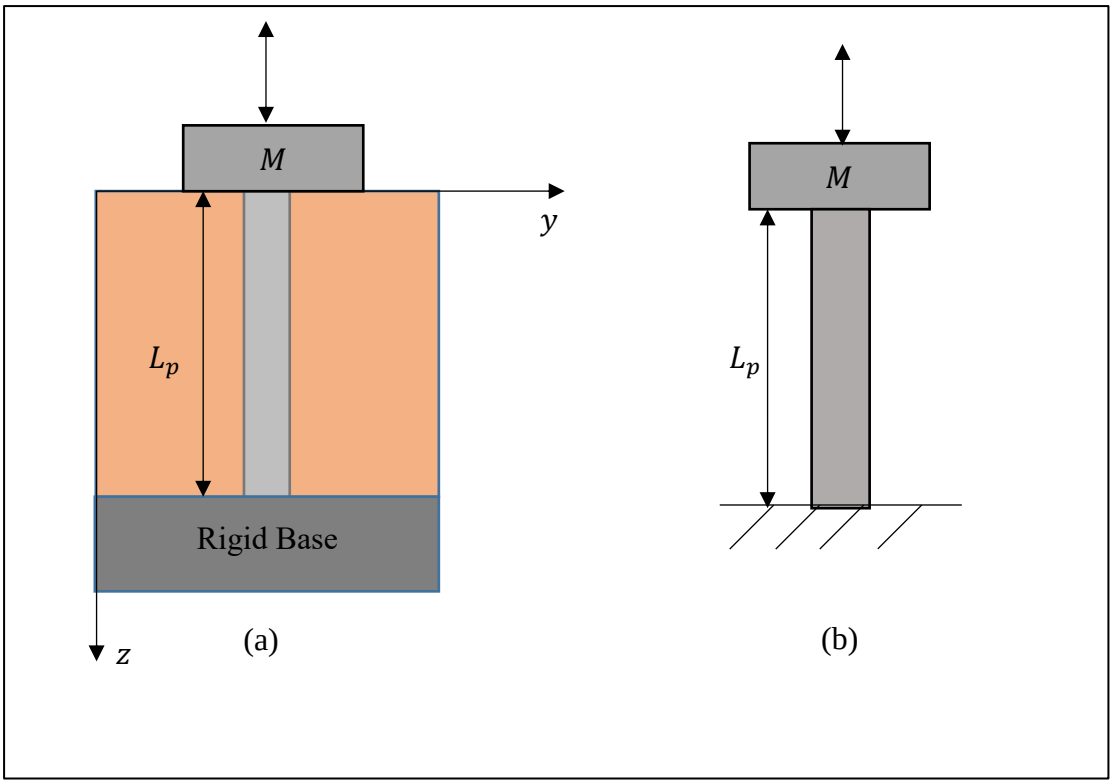

Figure 2.1: Model for pile resting on rock (a) Pile resting on rock base supporting weight on top. (b) Simplified model as a fixed-free rod with a mass at the free end Richart, F. E. et al. (1970).

For a free-fixed rod, The displacement at the fixed end is equal to zero. At the free end ($z = 0$) an excitation force is applied which is equal to the inertia of the mass at the top.

Mathematically this is expressed by:

$$F = \frac{\partial u}{\partial z} A_p E_p = -M \frac{\partial^2 u}{\partial t^2} \tag{2.1}$$

Where F is the Force, u is the displacement at top of the rod in z direction, t is the time, M is the mass supported, A_p is the pile cross-sectional area and E_p is the pile modulus of elasticity.

The amplitude of the displacement, $U = u_d/u_s$ can be expressed as

$$U = \frac{u_d}{u_s} = C_4 \, sin\left(\frac{\omega_n \, z}{v_c}\right) \tag{2.2}$$

Where u_d is the dynamic displacement at a certain frequency, u_s is the static displacement if the load applied was static, C_4 is a constant, ω_n is the natural frequency in $radians/second$ and v_c is the compressional wave velocity of the pile. At the fixed end ($z = L_p$), the following Equations apply

$$\frac{\partial u}{\partial z} = \frac{\partial U}{\partial z} \, (C_1 \, cos(\omega_n \, t) + C_2 \sin(\omega_n \, t)) \tag{2.3}$$

$$\frac{\partial^2 u}{\partial t^2} = \, - \omega_n^2 \, U \, \, (C_1 \, cos(\omega_n \, t) + C_2 \sin(\omega_n \, t) \tag{2.4}$$

Substituting Equation 2.3 and 2.4 in Equation 2.1 gives the following expression

$$A_p \, E_p \, \frac{\partial U}{\partial z} = M \, \omega_n^2 \, U \tag{2.5}$$

Also substituting Equation 2.2 in Equation 2.5 gives

$$A_p E_p \, \frac{\omega_n}{V_c} \cos(\frac{\omega_n \, L_p}{V_c}) = m \, \omega_n^2 \, U \, \sin(\frac{\omega_n \, L_p}{V_c}) \tag{2.6}$$

Equation 2.6 can be rearranged to become

$$\frac{A \, L_p \, \gamma_p}{W} = \frac{\omega_n \, L_p}{V_c} \, \tan(\frac{\omega_n \, L_p}{V_c}) \tag{2.7}$$

γ_p is the unit weight of the pile material, W is the weight of the mass on top of the pile. A plot of $\omega_n L_p / V_c$ against $A_p L_p \gamma_p \, / W$ is given in Figure 2.2 while the natural frequency in cycles per minute is given in Figure 2.3 for different pile materials.

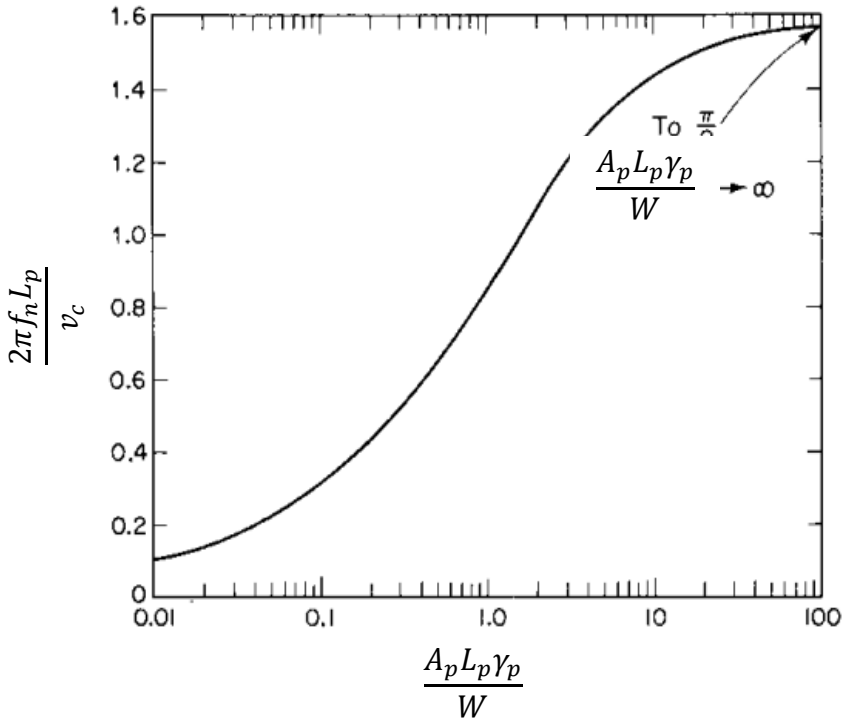

Figure 2.2: plot of $\omega_n \, L_p/v_c$ against $A_p L_p \gamma_p \, /W$ after Richart, F.E. et al (1970).

In Richart's solution, only the natural frequency is obtained. The static stiffness is assumed to be the same as a bar (i.e., $k = E_p A_p / L_p$). Richart also mentions that Geometrical damping is non-existent in cases of piles resting on rock.

The limitation of this solution is that it is only applicable to a foundation supported by a pile resting on rock bases and it assumes the soil along the pile shaft provides no support and no geometrical damping.

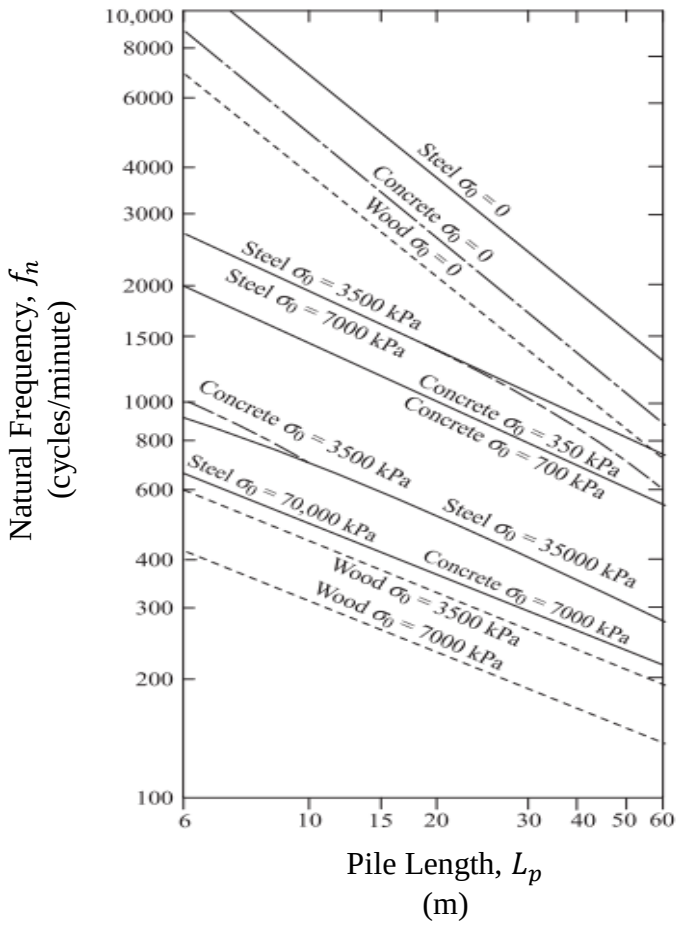

Figure 2.3: Natural frequency for different pile materials after Richart, F. E. et al. (1970).

2.2.2. Novak (1974) Solution for a single pile under dynamic loading

Novak in 1974 presented a closed form solution for floating and end bearing pile in homogeneous soil. Novak Solution gives stiffness and damping constants of single piles in homogeneous elastic soils. The pile can be either an end-bearing pile or a floating pile.

The Equations that govern the pile behavior under dynamic loading are:

$$k = \left(\frac{E_p A_p}{r_p}\right) f_{z1} \tag{2.8}$$

$$c = \left(\frac{E_p A_p}{\sqrt{G_s/\rho_s}}\right) f_{z2} \tag{2.9}$$

Where k is the stiffness of the pile, c is the damping of the pile, E_p is the pile modulus of elasticity, A_p is the pile cross-sectional area, r_p is the pile radius, G_s is the shear modulus of the soil, ρ_s is the density of the soil material and $f_{z1}$and f_{z2} are factors depending on pile slenderness ratio, L_p/r_p , relative rigidity E_p/G_s of the pile material related to the surrounding soil. f_{z1} and f_{z2} also depend on whether the pile is a friction pile or an end bearing pile resting on rock. Plots of f_{z1} and f_{z2} are given in Figures 2.4 and 2.5 for friction piles and 2.6 and 2.7 for end bearing pile.

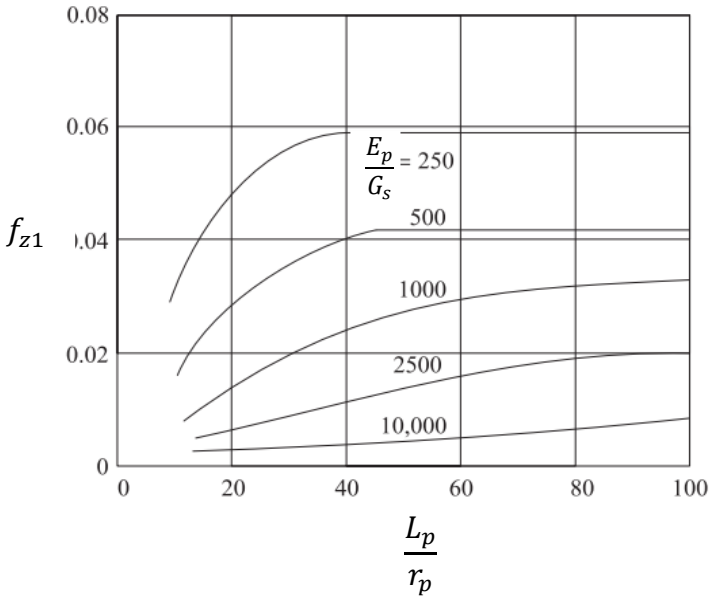

Figure 2.4: Plot of f_{z1} values for friction piles.

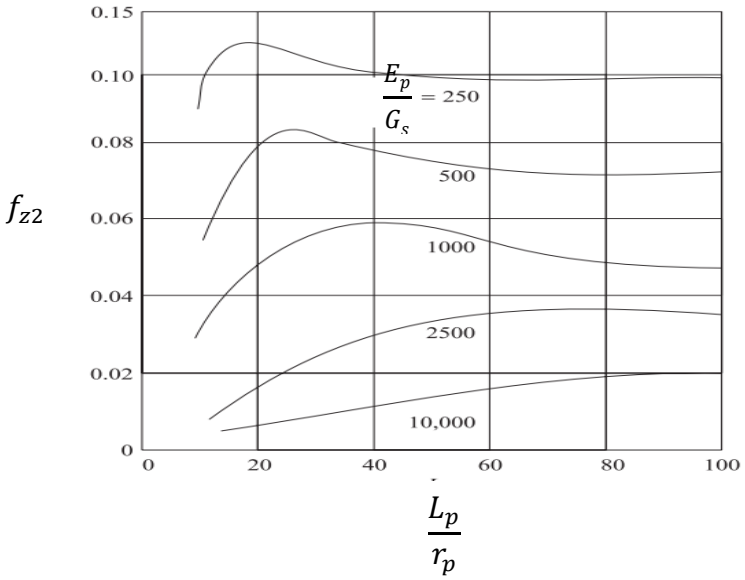

Figure 2.5: Plot of f_{z2} for friction piles.

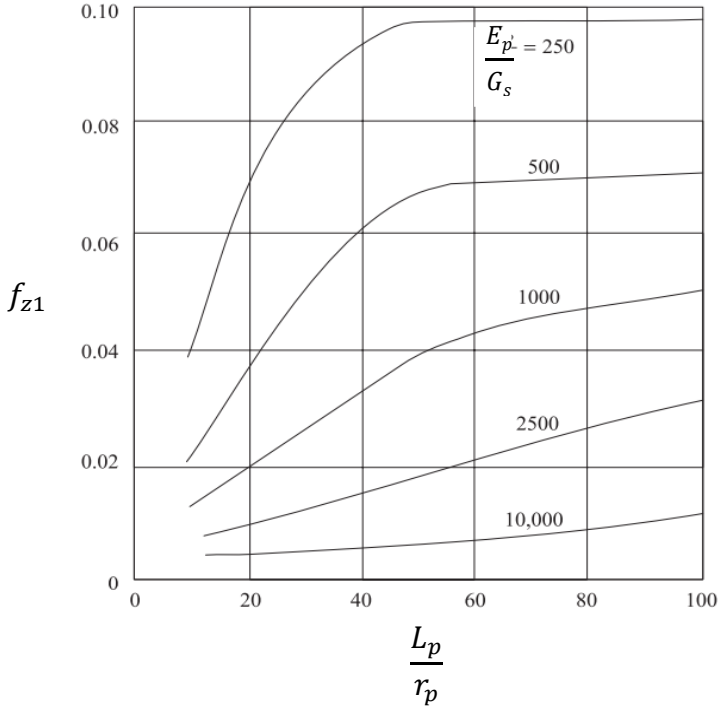

Figure 2.6: Plot of f_{z1} for end bearing piles.

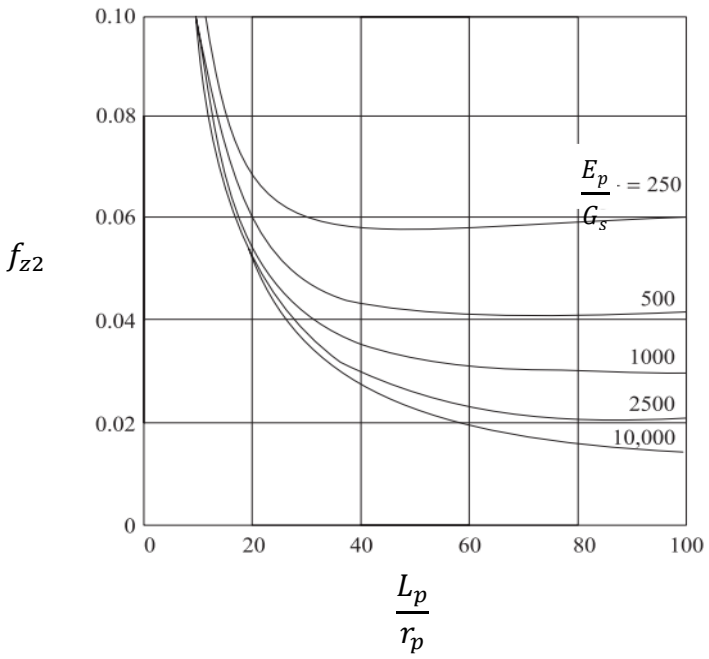

Figure 2.7: Plot of f_{z2} for end bearing piles.

Using Figures 2.4-2.7, f_{z1} and f_{z2}can be determined for the case at hand. From there, the values of stiffness, k and damping, c can be obtained using Equations 2.8 and 2.9. The damping ratio, natural frequency, amplitude of displacement at the natural frequency and at any other frequency can be obtained as:

After finding k and c, the damping ratio D can be found as

$$D = \frac{c}{2\sqrt{kM}} \tag{2.10}$$

Where M is the mass supported by the pile.

The natural frequency in Hz, f_n can be obtained by the following Equation

$$f_n = \frac{1}{2\pi}\sqrt{\frac{k}{M}} \tag{2.11}$$

The static displacement, u_s is obtained by dividing the applied force, F over the static stiffness, k

$$u_s = \frac{F}{k} \tag{2.12}$$

the amplitude of displacement, $U = u_d/u_s$ can be found using the following Equation

$$U = \frac{u_d}{u_s} = \frac{1}{\sqrt{\left(1 - \frac{f^2}{f_n^2}\right)^2 + 4D^2\frac{f^2}{f_n^2}}} \tag{2.13}$$

$u_d$is the dynamic displacement, u_s is the static displacement, f is the frequency in Hz and f_n is the natural frequency in Hz and $D$is the damping ratio. Once U is found, u_d can be found as $u_d = U\, u_s$.

It is worth mentioning that Novak's solution is only accurate at dimensionless frequency, $a_0 = 0.3$. where $a_0 = \omega r_p/v_s$. Where ω is the frequency in radians/sec, r_p is the pile radius and v_s is the shear wave velocity of the soil.

Novak's Solution provides an easy and a fast method for the analysis and design of pile foundations under vertical dynamic load. This solution is subject to certain assumptions and limitations. Assumptions include linearity of the problem, the pile and soil being in perfect contact (no slippage at the pile-soil interface), the pile is circular, vertical and elastic. Finally the soil at the side of the pile is assumed to behave as very thin independent layers (Plane strain condition).

Comparisons with field tests by Novak (1977) found good agreement with theory in cases where shear wave velocity at an end bearing pile base is twice that at the side of the pile. In other cases, the theory overestimates the response of the pile.

Elkasabgy & El Naggar (2013) compared Novak (1974) with the response of helical and driven steel piles. It was found that theory gives highly overestimated predictions while incorporating soil nonlinearity in the analysis provided better predictions with field tests.

2.2.3. Chowdhury & Dasgupta (2008) analytical solution for single pile

It is a modification of Novak's solution for embedded rigid cylinder Novak & Beredugo (1972). In this method, the stiffness of a friction pile is calculated as

$$k = \frac{G_S S_1 L_p}{2} \tag{2.14}$$

Where G_s is the soil shear modulus, L_p is the pile length and S_1 is calculated as

$$S_1 = \frac{9.553(1+\mu_s)}{\left(\frac{L_P}{r_p}\right)^{1/3}} \tag{2.15}$$

Where r_p is the pile radius.

Damping of a friction pile is calculated as

$$c = \frac{1}{2} r_p \sqrt{\rho_s G_s} S_2 L_p + r_p \sqrt{\rho_b G_b} C_b \tag{2.16}$$

Where c is the damping of the pile, r_p is the pile radius, ρ_s is the density of the soil at the side of the pile, G_s is the side soil shear modulus, S_2 a constant, L_p is the pile length, ρ_b is the density of the soil at the base of the pile, G_b is the shear modulus of the soil at pile base and C_b is a constant

In the case of an end bearing pile the static stiffness and damping are calculated using the following Equation respectively:

$$k = \frac{E_p A_p}{8L_p} + \frac{G_s S_1 L_p}{2} \tag{2.17}$$

$$c = \frac{1}{2} r_p \sqrt{\rho_s G_s} S_2 L_p \tag{2.18}$$

2.3. Finite Element solution for Pile subjected to dynamic loading

The finite element method is a numerical method used to solve differential Equations. For more on the general finite element method, see Bathe (2006). References specifically oriented towards geotechnical engineering include Potts & Zdravkovic (1999, 2001) and Desai & Zaman (2013). A brief introduction is also given in chapter 3 while application to the finite element method to current research is covered in chapter 4. Usage of the finite element method in geotechnical engineering is becoming the norm. This is due to the finite element method reliability to get accurate results and its ability to connect lab and field tests to computer simulations through material modeling. However, this accuracy is highly dependable on the accuracy of the user input. Another limitation of the finite element method is the need for high computing power and time to get results. This is true in 3D geotechnical problems which involve non-linearity or dynamic problems. Geotechnical problems also require large geometry and require fine mesh. Another limitation is the absence of guidelines and codes that govern modeling in geotechnical engineering. This makes the modeling process different from a user to another and makes modeling subject to individual judgment. Improvement on these limitations has been undertaken and as a result, it is a widely

used method in geotechnical engineering research and practice in different areas. Current and future improvement in computer processors and parallel computing will make it even easier, faster and more accurate.

2.3.1. One-dimensional finite element approach

The early approach to finite element modeling of pile dynamic problems was to discretize the pile to Beam elements attached to springs and dashpots at the sides and at the base. The method was first suggested by Smith (1960). The springs and dashpots describe the soil behavior around the pile and at the base. Pile and soil material could be linear or non-linear. The model is shown in Figure 2.8.

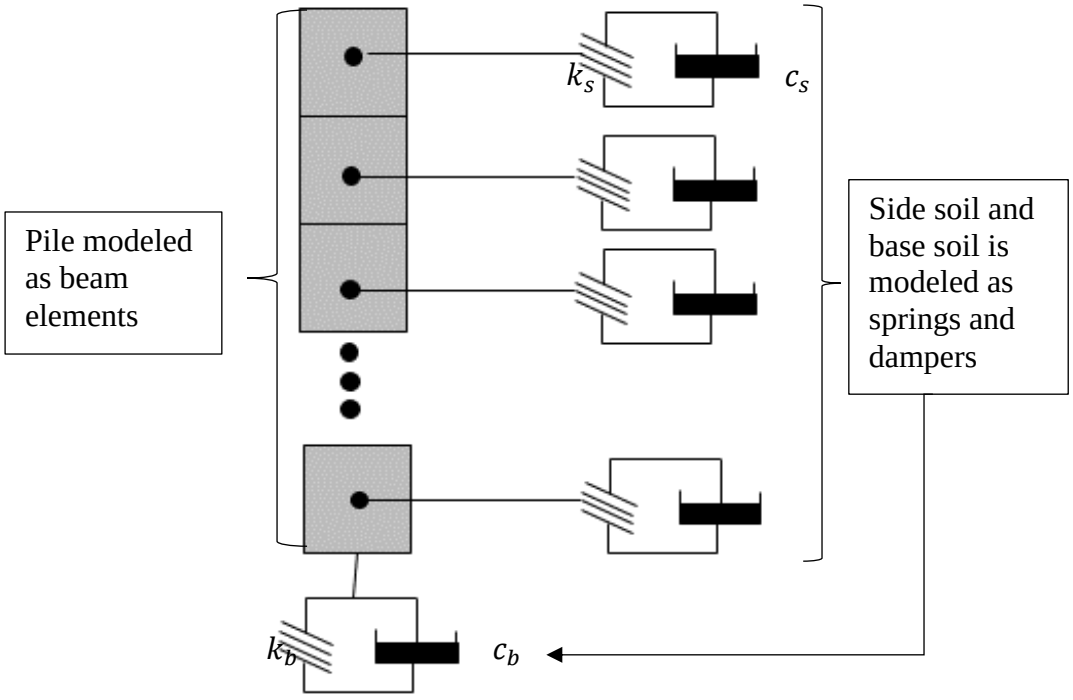

Figure 2.8: Model for soil-pile interaction.

Figure 2.8, shows how the pile is discretized into several beams segments and how each segment is connected to a set of a spring and dashpot damper. In

Figure 2.8, k is the spring coefficient and c is the dashpot damping while the subscript s stands for side and b stands for base. Values of k_s, can be obtained from static t-z curves (side friction vs. displacement curve) and values of k_b can be obtained from q-z curves (base load vs base settlement curve). Figure 2.9 shows an idealized t-z and q-z curves and how to obtain k at side and base of the pile.

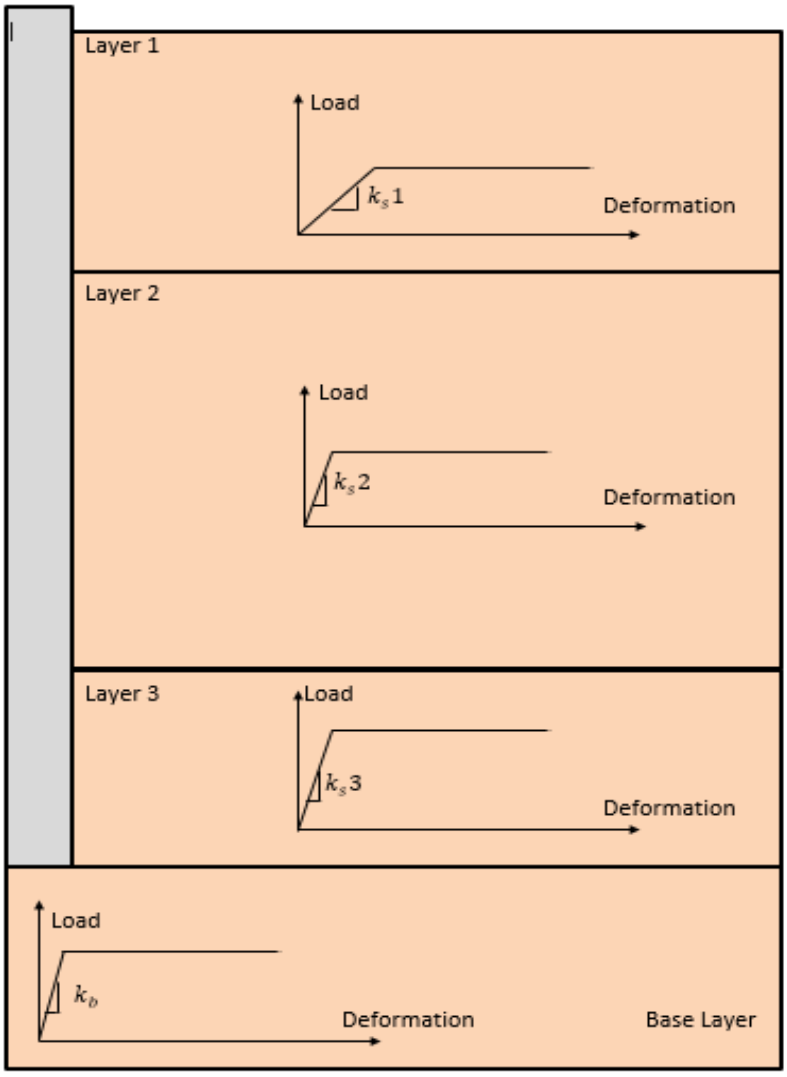

Figure 2.9 Idealized t-z and q-z curves and value of $k_s$and k_b.

Values of side damping can be taken as 0.5 sec/ft for sand while clay should have 0.2 sec/ft. For base damper c_b should be taken as 0.15 sec/ft for sand and 0.01 sec/ft for clay (Coyle, Lowery, & Hirsch , 1977).

Randolph & Simons, (1986) suggested the following Equations for side spring, k_s and side damper, c_s

$$k_s = 1.375\frac{G_s}{\pi r_p} \tag{2.19}$$

$$c_s = \frac{G_s}{v_s} \tag{2.20}$$

Where G_s is soil shear modulus at the spring location, r_p is the pile radius and v_s is the soil shear wave velocity at the spring location.

Lysmer & Richart (1966) proposed a static stiffness and dampings at of a circularly loaded area on a surface of an elastic half-space. Based on this model the values of the stiffness and dampings at the base of a circular area are given by the following Equations respectively:

$$k_b = \frac{4G_s r_p}{1-\mu_s} \tag{2.21}$$

$$c_b = \frac{3.4r_p^2}{1-\mu_s}\sqrt{G_s\rho_s} \tag{2.22}$$

In the previous Equations, G_s is the soil shear modulus, r_p is the pile radius, μ_s is soil Poisson's ratio and ρ_s is the soil mass density.

Holeyman (1988) suggested adding another damper to side and base soil to account for soil material damping. The configuration is shown in Figure 2.10.

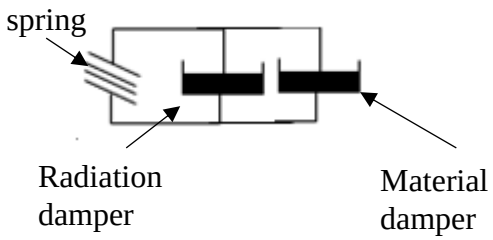

Figure 2.10 Model to account for material damping for side and base Soil.

. The method is further modified and refined by researchers to account for shortcomings, to produce more accurate results and to expand applicability to different cases. Kagawa (1991) proposed a nonlinear model that doesn't use dampers. The model relies only on the nonlinear behavior of the soil using dynamic t-z (shaft resistance vs. displacement) and q-z curves (base resistance vs. displacement). Seidel & Coronel (2011) formulated a model that takes into account the degradation resulting from cyclic loading to predict long-term response of piles

The method described here (one-dimensional soil pile interaction) is advantageous over analytical method as it is better in modeling layering of the soil profile since the set of dashpots and springs around the pile can have different coefficients. Care should be taken when choosing values of spring and dashpot coefficients for the soil beneath the pile and the soil surrounding the pile. The values should resemble field conditions and are obtained through field testing or available literature. This model is flawed in that it ignores the continuity of the problem. Reflections and interaction between soil layers cannot be accounted for. There is also difficulty in choosing appropriate and reliable spring and damping values for the soil.

2.3.2. 3D Finite element modeling

In this approach the soil is modeled as solid elements, the pile is modeled as solid elements or beams with interface elements that connect the pile to the soil. The method accuracy depends on the selected element size, time step and boundary of the problem. The method is very time consuming and requires great computational power due to a large number of elements. Several general purpose computer programs are created for finite element simulation. Some programs are more tailored to geotechnical engineering applications.

Ali, O. (2015) implemented 3D finite element method to study end bearing piles subjected to a vertical dynamic load. The study calculated the dynamic stiffness and damping of the pile. The soil along the pile shaft was homogeneous and elastic. At the base, the soil shear modulus was 100 times that of the soil along the pile shaft. In addition, a group of 3 by 3 piles are studied at different spacing.

2.4. Design of pile groups and pile to pile interaction

Piles are mostly used in groups. Groups of piles consist of a cap that connects the piles together. This cap could be flexible or rigid. The difference between rigid and flexible caps is that flexible caps allow for deformation of the cap and thus the load is distributed unequally on the piles within the group. This means that displacement is different between the piles. Rigid caps however distribute the loads on the piles equally and displacement is uniform across the piles in the group.

In static and dynamic problems, the stiffness and dampings of a single pile don’t translate simply into a group of piles. Group stiffness and damping is not

simply the sum of the stiffness and damping of individual piles. The interaction between the piles results in a reduction in the stiffness and dampings of individual piles. Mathematically this is described by the following Equations

$$k_G = \frac{\sum_{i=1}^{n} k_i}{\sum_{i=1}^{n} \alpha_i} \tag{2.23}$$

$$c_G = \frac{\sum_{i=1}^{n} c_i}{\sum_{i=1}^{n} \alpha_i} \tag{2.24}$$

Where $k_G$is the group stiffness, $k_i$is the stiffness of a pile i in the group, $\alpha_i$is the interaction factor of pile i with a reference pile within the group. The interaction factor is defined as the increase of settlement of a pile i due to loading on an adjacent pile j over the settlement of pile i if it were isolated.

Mathematically this is written as:

$$\alpha = \frac{u_{ij} - u_i}{u_i} \tag{2.25}$$

Where u_{ij} is the total settlement of pile i (settlement because of its own load and added settlement due to loading on an closely spaced pile), u_i is the settlement of pile i due to its own loading and if it were isolated. The interaction factor,α is a function of pile dimensions (i.e. length and diameter), its stiffness, soil properties around the piles and spacing between the piles in the group.

2.4.1. Poulos (1968) static interaction factors

In this study, two piles of the same characteristics embedded in an elastic half-space are analyzed. The analysis is based on Elasticity theory. Equal loads are applied on each pile. The increase of settlement on the piles due to the interaction between them is calculated. This system despite having two piles, it is considered a pile group by definition (The simplest form of a pile group). The analysis assumes

incompressibility of the piles and that the piles and the soil are perfectly contacted and move together with no slippage at the pile-soil interface. This limits the solution to cases where the stresses in the soil are within the elastic capacity of the soil and not have reached yield strength of the soil. This doesn't limit the solution from being applicable to design since the investigation of pile groups load-settlement behavior shows that the group settles linearly up to one third or one-half of its maximum load capacity (Poulos, 1968). The solution gives values of the interaction factor, α that ranges between 1 for 0 spacing and 0 for pile spaced at an infinite distance. Figure 2.11 gives a plot of the values of α against s/d_p for different L_p/d_p. Where s is the spacing between the piles (center to center), d_p is the pile diameter, L_p is the pile length.

In Figure 2.11, values of α are plotted for Poisson's ratio, μ_s of 0.5 and 0 for the case of $L_p/d_p = 25$. The author states that influence of Poisson's ratio is just 0.06 of difference in α at maximum. This means that μ_s has little effect on interaction between piles. The analysis is extended to group of 3 and 4 piles. The results of the analysis shows that superposition can be assumed and holds true for group of piles subjected to static load. This means that the total interaction factor for a group is equal to the sum of the interaction factor for each pile added to the group.

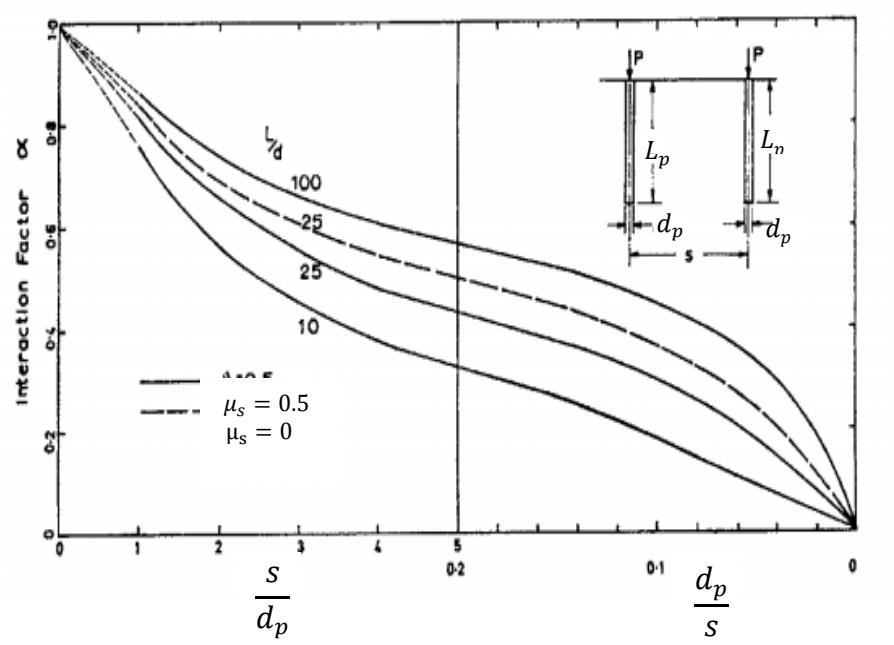

Figure 2.11: Interaction factors between two piles after Poulos (1968).

To illustrate the principle of superposition consider an example like that shown in Figure 2.12 where the reference pile is the black pile while the interacting piles are 3 gray piles. Let α_1 be the interaction factor of two piles spaced at spacing s and α_2 is the interaction factor between two piles spaced at $\sqrt{2}s$. This means that the total static stiffness of the group is reduced by $1 + 2\alpha_1 + \alpha_2$.

Poulos states that superposition holds true for symmetrical pile groups and it may be assumed in general pile groups analyses. Symmetrical pile groups are any group that has its piles spaced equally around the circumference of a circle. The piles should be loaded equally and settlement is equal among the piles. Figure 2.13 shows solution for 2, 3 and 4 pile group at $L_p/d_p = 25$.

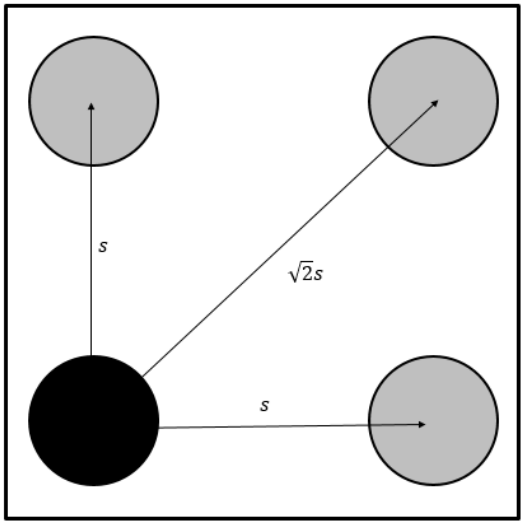

Figure 2.12: layout of 4 pile group.

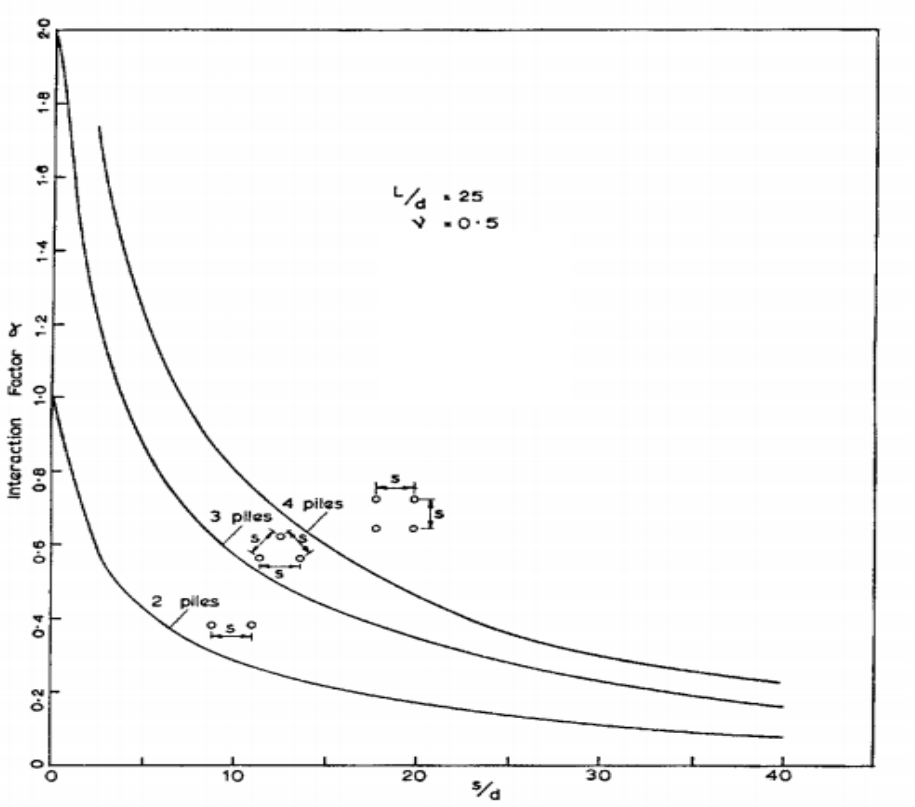

Figure 2.13 Interaction factors for 2, 3 and 4 symmetrical pile groups after Poulos (1968).

Advancements are made on pile-to-pile interaction by Poulos and other researchers. Butterfield & Banerjee (1971) presented an analysis to a group of piles while

considering the cap of the group being in contact with the ground. The results of the analysis demonstrated that a contacting cap increased the stiffness of the pile group by 5-15%. This increase in stiffness depends on the group size and spacing between the piles. The portion of the load carried by the piles is different from that of a group with a non-contacting cap. The range of difference is between 20% and 60%. The larger the group, the higher the difference is. Chow & Teh (1992) studied groups in a nonhomogeneous elastic soil where the soil's Young's modulus increases linearly with depth till it reaches rock base. They found that using homogeneous soil profile underestimates the stiffness of the pile group. They provided field case studies in which results are in agreement with their studies. In these case studies, the soil was of clayey nature and the cap of the group was in contact with the ground. More research in this area is being conducted to account for more cases and different soil conditions.

2.4.2. Studies on dynamic interaction factors

Novak (1974) provided a comparison of pile groups against footing under dynamic loading. The response is given in Figure 2.14. From Figure 2.14, Novak concluded that due to increased stiffness of the pile group, the natural frequency increases. The pile group had more amplitude of displacement at the natural frequency which means that it is less damped than shallow block foundations. A footing might have a higher amplitude at lower frequencies than a group of piles. This is apparent at frequencies between 0 and 60 radians per seconds. Embedment of the cap increased damping of the pile group so did embedment of the footing. In this comparison interaction between the piles was considered by applying

interaction factors provide by Poulos (1968). It was presented to show the difference between pile groups and shallow foundations under dynamic loading.

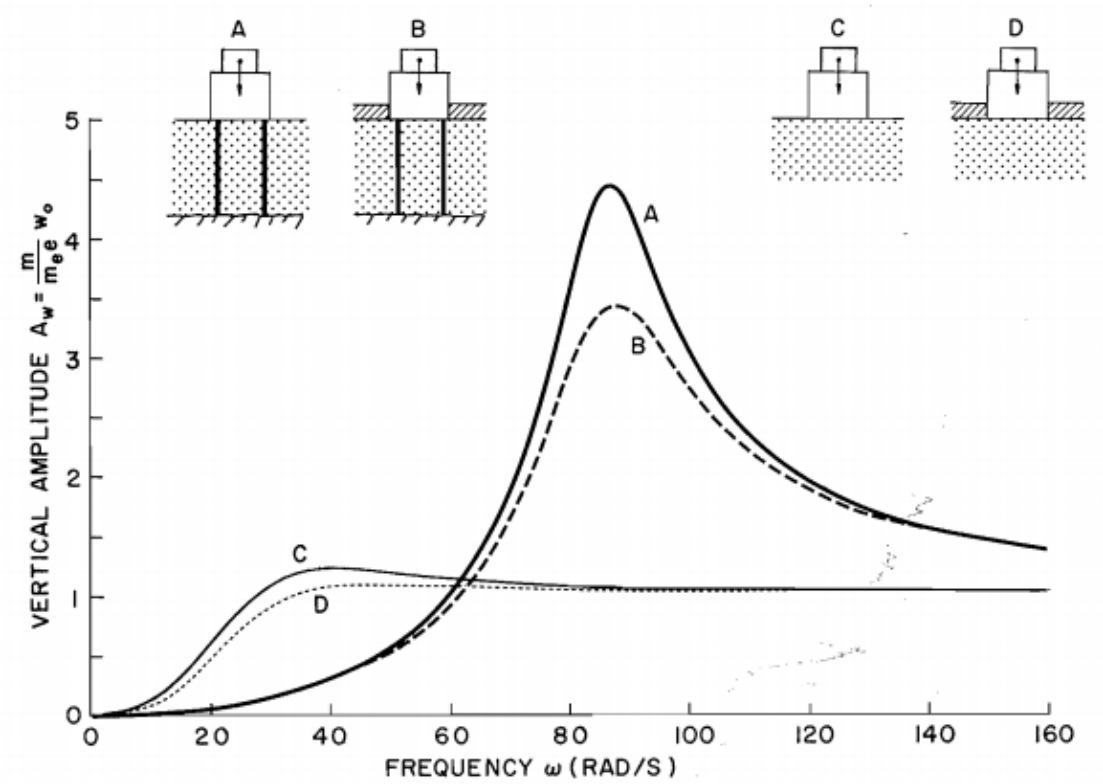

Figure 2.14 Comparison between pile group and footing under vertical dynamic loading after Novak (1974).

Sharnouby & Novak (1985) studied pile groups under low frequency using a numerical approach. They found that using static interaction factors provided by Poulos (1968) gives a response in agreement with their method at low frequencies. Dobry & Gazetas (1988), Gazetas & Makris (1991) presented dynamic interaction factors for pile groups. The interaction factors were frequency dependent. El Naggar & El Naggar (2007) presented a simplified method in which the stiffness and damping of single piles are calculated as described in section 2.2.2 using Novak's

solution. The next step is to obtain interaction factor for a group that has been solved for in the paper (2 by 2, 3 by 3, and 4 by 4 up to 9 by 9).

The presented studies in this section give some insight into the interaction factor of dynamic loading on pile groups. Due to lack of analytical solutions on the dynamic pile to pile interaction, references of soil dynamics refer to interaction factors given by Poulos (1968) for dynamic analysis and it is the one used in design for pile groups subjected to dynamic loading. See Prakash & Puri (1988) and Das & Ramana (2010).

3. The Finite element method, an introduction

The finite element method (might be referred to as FEM or FEA throughout the rest of this text) is a numerical method that discretizes a continuum into small finite sub-structures. The sub-structure element is mathematically defined in how it transports a certain quantity (e.g., stress, temperature, or fluid) to the adjacent element. Boundary conditions and material models are to be defined in order for the solution of the differential Equations to be solved. Basically, FEM is a numerical method used to solve differential Equations of field problems. The field problem can be one, two or three dimensional of any shape and configuration.

In this research, the finite element method is used to study the dynamic behavior of pile foundations under vertical dynamic loading. Five different studies are performed. 4 of those studies are on single piles. Since the piles in these studies have circular cross sections, axisymmetric finite elements are used to discretize the problem. Use of axisymmetric element is time efficient when simulating solids of revolution. These solids are formed by revolving a planar shape around an axis. The method would yield the same results as a full 3D simulation but with significantly less number of elements. A smaller number of elements means a smaller stiffness matrix and much less amount of time to solve the system of Equations. This is of great importance in this research since the analysis is dynamic. Dynamic analysis requires the system of linear Equations to be solved at each time step of the analysis. The fifth study, however, is on the pile-to-pile interaction. This study requires a full 3D model to be set up for the analysis in order to properly capture the behavior of the two piles. This means that full 3D analysis is run on this case and the analysis time is very high compared to 2D analysis.

This chapter serves as an introduction to the finite element method based on Bathe, (2006) and Logan (2007). In this chapter, 2D axisymmetric elements and 3D tetrahedron elements are briefly introduced. The process of obtaining the stiffness matrix and other matrices for each type of element is covered. A solution of linear Equations systems is discussed. In particular, the sparse and iterative solvers are discussed. Integration schemes in time for dynamic analysis are discussed.

3.1. Mathematical preliminaries for the finite element method

In a linear elastic material, the stress-strain relationship is defined by

$$\{\sigma\} = [C]\{\varepsilon\} \tag{3.1}$$

Where $\{\sigma\}$ is the stress matrix, $[C]$ is a constitutive matrix that relates the stress to the strain and $\{\varepsilon\}$ is the strain matrix.

From the constitutive matrix, a local elemental stiffness matrix $[k]$ can be calculated as

$$\{k\} = \int [B]^T [C][B] dV \tag{3.2}$$

The matrix $[B]$ depends on the geometry and coordinates of the finite element and is defined by

$$[B] = \{\partial\}[N] \tag{3.3}$$

In 3.3, $\{\partial\}$is a differential operator of the shape functions matrix $[N]$.

The final equilibrium Equation for a static problem is

$$\{F\} = [K]\{D\} \tag{3.4}$$

Where $[F]$ is the global nodal forces matrix and $[U]$ is the global nodal displacement matrix. They are defined by

$$\{F\} = \sum_{i=0}^{n} f_i \tag{3.5}$$

$$\{D\} = \sum_{i=0}^{n} d_i \tag{3.6}$$

f_i and u_i are the force and displacement at node i respectively. n is the total number of nodes in the problem.

$[K]$ is the global stiffness matrix and is obtained by

$$\{K\} = \sum_{j=0}^{n} \sum_{i=0}^{n} k_{ij} \tag{3.7}$$

$\{F\}$ and $\{U\}$ depends on the boundary conditions of the problem (i.e. applied loads and prescribed displacements). After defining all the required matrices Equation 3.4 can be solved to obtain unknown forces or displacements at any node in the continuum. All the above Equations depend on the problem at hand.

3.2. Axisymmetric elements

An axisymmetric element is a finite element used to model a three-dimensional body that is symmetrical around an axis in regards to geometry and boundary conditions. Due to symmetry around the z-axis, as shown in Figure 3.1, the stresses and strains are independent of the value of θ. The stresses are dependent on the coordinates of the plane $z - r$. The following is a derivation of

the matrices required to solve a finite element problem with a triangular axisymmetric element. See Figure 3.2 for the triangular element with vertices $i, j, and\ m$; each has the coordinates (z, r). The element has two degrees of freedom per node ($u\ and\ w$). Let the element have the following displacement functions

$$u(r, z) = a_1 + a_2 r + a_3 z \tag{3.8}$$

$$w(r, z) = a_4 + a_5 r + a_6 z \tag{3.9}$$

Note that the total number of the coefficients a is the same as the number of the degrees of freedom. (6 $a_i's$ for 6 degrees of freedom).

The nodal displacement matrix is

$$\{d\} = \begin{Bmatrix} d_i \\ d_j \\ d_m \end{Bmatrix} = \begin{Bmatrix} u_i \\ w_i \\ u_j \\ w_j \\ u_m \\ w_m \end{Bmatrix} \tag{3.10}$$

At any node i, u and w are evaluated as

$$u(r_i, z_i) = a_1 + a_2 r_i + a_3 z_i \tag{3.11}$$

$$w(r_i, z_i) = a_4 + a_5 r_i + a_6 z_i \tag{3.12}$$

In matrix form, the displacement function is represented as

$$\{\psi\} = \begin{bmatrix} 1 & r & z & 0 & 0 & 0 \\ 0 & 0 & 0 & 1 & r & z \end{bmatrix} \begin{Bmatrix} a_1 \\ a_2 \\ a_3 \\ a_4 \\ a_5 \\ a_6 \end{Bmatrix} \tag{3.13}$$

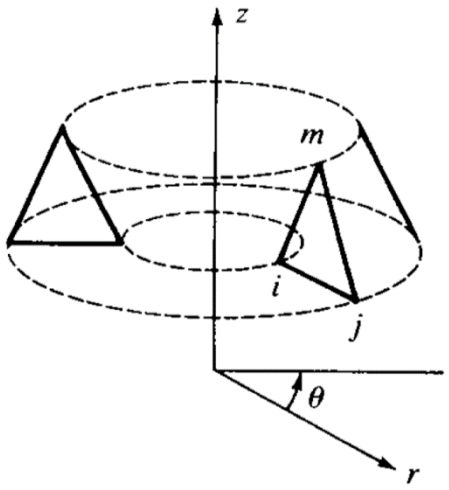

Figure 3.1: Axisymmetric element used to model solids of revolution.

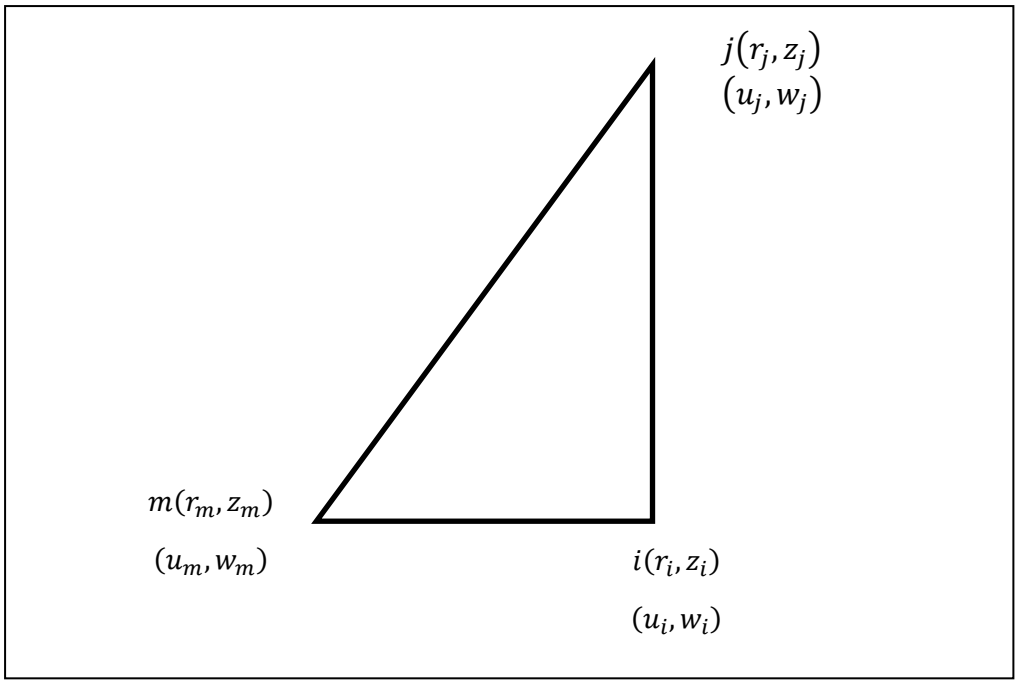

Figure 3.2 Triangular axisymmetric element.

Rearranging Equation 3.13 and substituting the coordinates of each vertex on the element yields:

$$\begin{Bmatrix} a_1 \\ a_2 \\ a_3 \end{Bmatrix} = \begin{bmatrix} 1 & r_i & z_i \\ 1 & r_j & z_j \\ 1 & r_m & z_m \end{bmatrix}^{-1} \begin{Bmatrix} u_i \\ u_j \\ u_m \end{Bmatrix} \tag{3.14}$$

$$\begin{Bmatrix} a_4 \\ a_5 \\ a_6 \end{Bmatrix} = \begin{bmatrix} 1 & r_i & z_i \\ 1 & r_j & z_j \\ 1 & r_m & z_m \end{bmatrix}^{-1} \begin{Bmatrix} w_i \\ w_j \\ w_m \end{Bmatrix} \tag{3.15}$$

After performing the inversion in Equations 3.14 and 3.15, they become

$$\begin{Bmatrix} a_1 \\ a_2 \\ a_3 \end{Bmatrix} = \frac{1}{2A} \begin{bmatrix} \alpha_\iota & \alpha_j & a_m \\ \beta_\iota & \beta_j & \beta_m \\ \gamma_i & \gamma_j & \gamma_m \end{bmatrix} \begin{Bmatrix} u_i \\ u_j \\ u_m \end{Bmatrix} \tag{3.16}$$

$$\begin{Bmatrix} a_4 \\ a_5 \\ a_6 \end{Bmatrix} = \frac{1}{2A} \begin{bmatrix} \alpha_\iota & \alpha_j & a_m \\ \beta_\iota & \beta_j & \beta_m \\ \gamma_i & \gamma_j & \gamma_m \end{bmatrix} \begin{Bmatrix} w_i \\ w_j \\ w_m \end{Bmatrix} \tag{3.17}$$

Where:

$$\begin{array}{lll} \alpha_\iota = r_j z_m - z_j r_m & \alpha_j = r_m z_i - z_m r_i & \alpha_m = r_i z_j - z_i r_j \\ \beta_i = z_j - z_m & \beta_j = z_m - z_i & \beta_m = z_i - z_j \\ \gamma_i = r_m - r_j & \gamma_j = r_i - r_m & \gamma_m = r_j - r_i \end{array} \tag{3.18}$$

The shape functions are then defined as:

$$N_i = \frac{1}{2A}(\alpha_i + \beta_i r + \gamma_i z) \tag{3.19}$$

$$N_j = \frac{1}{2A}(\alpha_j + \beta_j r + \gamma_j z) \tag{3.20}$$

$$N_m = \frac{1}{2A}(\alpha_m + \beta_m r + \gamma_m z) \tag{3.21}$$

The displacement matrix of the element is:

$$\begin{Bmatrix} u(z,r) \\ w(z,r) \end{Bmatrix} = \begin{bmatrix} N_i & 0 & N_j & 0 & N_m & 0 \\ 0 & N_i & 0 & N_j & 0 & N_m \end{bmatrix} \begin{Bmatrix} u_i \\ w_i \\ u_j \\ w_j \\ u_m \\ w_m \end{Bmatrix} \tag{3.22}$$

From continuum mechanics and elasticity the strains can be defined as

$$\varepsilon_r = \frac{\partial u}{\partial r} \qquad \varepsilon_\theta = \frac{u}{r} \qquad \varepsilon_z = \frac{\partial w}{\partial z} \qquad \gamma_{rz} = \frac{\partial u}{\partial z} + \frac{\partial w}{\partial r} \quad (3.23)$$

Using Equations 3.8 and 3.9 with 3.23 the following is obtained

$$\{\varepsilon\} = \begin{Bmatrix} a_2 \\ a_6 \\ \frac{a_1}{r} + a_2 + \frac{a_3 z}{r} \\ a_3 + a_5 \end{Bmatrix} \quad (3.24)$$

Equation 3.24 can be rewritten as

$$\begin{Bmatrix} \varepsilon_r \\ \varepsilon_z \\ \varepsilon_\theta \\ \gamma_{rz} \end{Bmatrix} = \begin{bmatrix} 0 & 1 & 0 & 0 & 0 & 0 \\ 0 & 0 & 0 & 0 & 0 & 1 \\ \frac{1}{r} & 1 & \frac{z}{r} & 0 & 0 & 0 \\ 0 & 0 & 1 & 0 & 1 & 0 \end{bmatrix} \begin{Bmatrix} a_1 \\ a_2 \\ a_3 \\ a_4 \\ a_5 \\ a_6 \end{Bmatrix} \quad (3.25)$$

Substituting Equations 3.16 and 3.17 in 3.25 with simplification, the following Equation is obtained

$$\{\varepsilon\} = \underbrace{\frac{1}{2A} \begin{bmatrix} \beta_i & 0 & \beta_j & 0 & \beta_m & 0 \\ 0 & \gamma_i & 0 & \gamma_j & 0 & \gamma_m \\ \frac{\alpha_i}{r} + \beta_i + \frac{\gamma_i z}{r} & 0 & \frac{\alpha_j}{r} + \beta_j + \frac{\gamma_j z}{r} & 0 & \frac{\alpha_m}{r} + \beta_m + \frac{\gamma_m z}{r} & 0 \\ \gamma_i & \beta_i & \gamma_j & \beta_j & \gamma_m & \beta_m \end{bmatrix}}_{[B]} \begin{Bmatrix} u_i \\ w_i \\ u_j \\ w_j \\ u_m \\ w_m \end{Bmatrix} \quad (3.26)$$

The stresses are given by Equation 3.1 where the constitutive matrix $[C]$ is according to the following Equation

$$[C] = \frac{E}{(1+\mu)(1-2\mu)} \begin{bmatrix} 1-\mu & \mu & \mu & 0 \\ \mu & 1-\mu & \mu & 0 \\ \mu & \mu & 1-\mu & 0 \\ 0 & 0 & 0 & \frac{1-2\mu}{2} \end{bmatrix} \tag{3.27}$$

The axisymmetric element stiffness matrix is calculated according to the volume integral in Equation 3.2 and in the cylindrical coordinates Equation 3.2 becomes

$$[k] = 2\pi \iint [B]^T [C][B]\, r\, dr\, dz \tag{3.28}$$

So far the element stiffness matrix of an axisymmetric element is derived. Boundary conditions (i.e., nodal forces and prescribed displacements) are applied on each node and placed in the proper location in the forces and displacement matrices. In the case of surface forces (i.e., surface traction and/or pressure), the process is more involved in obtaining equivalent nodal forces. The process is explained with the aid of Figure3.3. In Figure 3.3, an axisymmetric element is presented with forces acting on the surface of the element. One force is a pressure force and the other is a surface traction force. In general, surface forces can be found by

$$\{f_s\} = \iint [N_s]^T \{T\}\, dS \tag{3.29}$$

Where $\{f_s\}$ is the element forces matrix and $[N_s]$ is the shape function matrix evaluated along the surface where the surface forces are applied. In the case of the element presented in Figure 3.3, Equation 3.29 becomes

$$\{f_s\} = \iint [N_s]^T \begin{Bmatrix} p_r \\ p_z \end{Bmatrix} dS \tag{3.30}$$

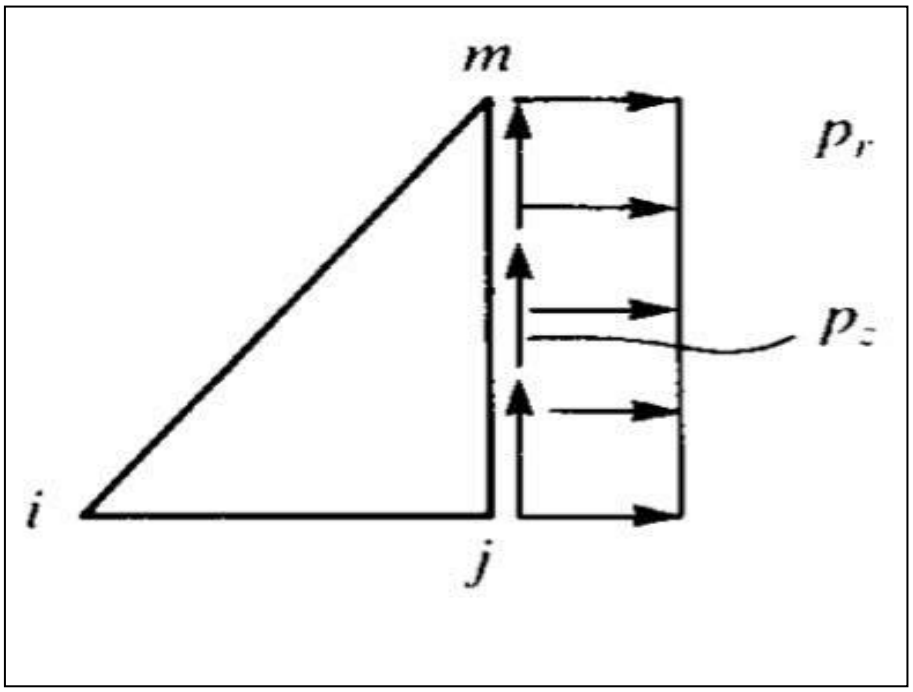

Figure 3.3 Example of surface forces acting on an axisymmetric element (Logan, 2007).

The evaluation of $[N_s]$ is obtained from Equations 3.19, 3.20, and 3.21 for each node and the integral is evaluated individually to obtain the equivalent forces at the node. For example at node j the integral in Equation 3.30 and with the aid of Equation 3.20 becomes

$$\{f_{sj}\} = \int_{z_j}^{z_m} \frac{1}{2A} \underbrace{\begin{bmatrix} \alpha_j + \beta_j r + \gamma_j z & 0 \\ 0 & \alpha_j + \beta_j r + \gamma_j z \end{bmatrix}}_{\text{Evaluated at } r = r_j \text{ and } z = z} \begin{Bmatrix} p_r \\ p_z \end{Bmatrix} 2\pi r_j \, dz \tag{3.31}$$

After performing the integration at each node, the forces matrix can be calculated and at each node the final force matrix becomes

$$\{f_s\} = \frac{2\pi r_j(z_m - zj)}{2}\begin{Bmatrix} 0 \\ 0 \\ p_r \\ p_z \\ p_r \\ p_z \end{Bmatrix} \tag{3.32}$$

Finally the global stiffness, forces, and displacements are formed by the summation of the values at each node according to Equations 3.5, 3.6, and 3.7.

The discussion presented here on axisymmetric elements applied to 3D elements with several modifications on the matrices size and entries within the matrices to allow for 3D analysis. The core concept, however, applies. Shape functions are used to describe the element nodal coordinates, a stress-strain relationship matrix is extended to include x, y and z directions, the stiffness matrix is a 9 by 9 matrix and force and displacements matrix are 9 by 1. Stress and strains matrices are 6 by 1.

3.3. Solution of the static equilibrium Equations

For static analysis, Equation 3.4 needs to be solved. Several techniques are available to solve the Equation. The software used here is capable of using two methods. The first is a sparse solver and the second is an iterative solver. The following sections gives an in-depth look at each technique.

3.3.1. Direct solution of the static equilibrium Equation in linear analysis (sparse solver)

Gauss Elimination method is used in the direct solution to the equilibrium Equations in linear elastic finite elements. The process of the Gauss elimination is better explained with the aid of the following Equation

$$\begin{bmatrix} k_{11} & k_{12} & k_{13} & k_{14} \\ k_{21} & k_{22} & k_{23} & k_{24} \\ k_{31} & k_{32} & k_{33} & k_{34} \\ k_{41} & k_{42} & k_{43} & k_{44} \end{bmatrix} \begin{Bmatrix} u_1 \\ u_2 \\ u_3 \\ u_4 \end{Bmatrix} = \begin{Bmatrix} f_1 \\ f_2 \\ f_3 \\ f_4 \end{Bmatrix} \tag{3.33}$$

The mathematical steps to solve the system of Equations above are:

1. For the second row get

$$k_{2,j} - \frac{k_{2,1}k_{1,j}}{k_{1,1}}$$

This means that for $i = 2\ and\ j = 1$ the entry will be $k_{2,1} - \frac{k_{2,1}k_{1,1}}{k_{1,1}} = 0$

For the third row get

$$k_{3,j} - \frac{k_{3,1}k_{1,j}}{k_{1,1}}$$

This means that for $i = 3\ and\ j = 1$ the entry will be $k_{3,1} - \frac{k_{2,1}k_{1,1}}{k_{1,1}} = 0$

The process is then repeated for all the rows and columns until the first column of entries in the matrix $= 0$ and in one Equation step one is summarized is summarized as

$$k_{i,j} - \frac{k_{i,1}k_1,j}{k_{1,1}} \quad i = 2,3,\ldots.to\ the\ number\ of\ rows \tag{3.34}$$

Where $j = 1,2,3,$ ... to the number of columns

2. Starting from the third row apply the following Equation

$$k_{i,j} - \frac{k_{i,2}k_{2},j}{k_{2,2}} \quad i = 3,4,\ldots . to\ the\ number\ of\ rows$$
$$j = 2,3,4 \ldots \ldots to\ the\ number\ of\ columns \tag{3.35}$$

3. The process is repeated for the fourth row until a triangle of zeros is made below the diagonal of the matrix similar to Equation 3.36

$$\begin{bmatrix} k_{11} & k_{12} & k_{13} & k_{14} \\ 0 & k'_{22} & k'_{23} & k'_{24} \\ 0 & 0 & k'_{33} & k'_{34} \\ 0 & 0 & 0 & k'_{44} \end{bmatrix} \begin{Bmatrix} u_1 \\ u_2 \\ u_3 \\ u_4 \end{Bmatrix} = \begin{Bmatrix} f_1 \\ f_2 \\ f_3 \\ f_4 \end{Bmatrix} \tag{3.36}$$

$k'_{i,j}$ is the new entry calculated as per steps $1\ to\ 3$.

4. A simultaneous solution can now be obtained as

$$u_4 = \frac{f_4}{k'_{44}}$$
$$u_3 = \frac{f_3 - k'_{34}u_4}{k'_{33}}$$
$$u_2 = \frac{f_2 - k'_{23}u_3 - k'_{24}u_4}{k'_{22}} \tag{3.37}$$
$$u_1 = \frac{f_1 - k_{12}u_2 - k_{13}u_3 - k_{14}u_4}{k_{11}}$$

The process of obtaining the solution is then made directly until all unknowns are identified. This solution yields the exact solution for the set of equilibrium Equations given that the problem is defined correctly. Considering the sparsity of the stiffness matrix (i.e., many entries are zeros in the matrix) programming algorithms are built with consideration to take advantage of this sparsity and solve

fewer Equations since the zero entries in the stiffness matrix do not affect the solution of the Equations.

3.3.2. Iterative solution of the static equilibrium Equation in linear analysis

The Iterative solution presented here is based on that developed by Varga (2009). Basically, the solution to Equations of static equilibrium is calculated iteratively by trial and error as

$$U_i^{t+1} = K_{ii}^{-1}\left(F_i - \sum_{j=1}^{i-1} K_{ij}\, U_j^{t+1} - \sum_{j=i+1}^{n} k_{ij} U_j^{t} \right) \tag{3.38}$$

Where U_i^{t+1} and F_i are the i^{th} component of U and F and t represents the trial number. The trials are continued until the following Equation is satisfied

$$\frac{|U^{t+1} - U^{t}|}{|U^{s+1}|} < tolerance \tag{3.39}$$

Tolerance is a preset value depends on the user choice.

3.4. Dynamic Analysis

The following sections covers dynamic finite element analysis and the solution to equilibrium Equations in dynamic analysis.

3.4.1. Mass matrix of an axisymmetric element

The mass matrix divides the total element mass on its nodes. It is of importance in dynamic problems since inertia forces are part of the dynamic Equation of equilibrium as shown later and they (i.e. inertia forces) play an important role in the dynamic response of any structure. The mass matrix of an axisymmetric element is obtained using the following Equation

$$[M] = \iiint \rho [N]^T [N] dV \tag{3.40}$$

This mass matrix is called the consistent mass matrix, and it is a full and symmetric matrix. By using the shape functions given in Equations 3.19, 3.20 and 3.21, the mass matrix can be obtained for the axisymmetric element. The same concept applies to a 3D elements and the shape functions used are related to the 3D element.

3.4.2. Integration of dynamic Equation of equilibrium in time

The following integration schemes are summarized from Bathe (2006) and Logan (2007) textbooks.

If no viscous damping is applied, the Equation of equilibrium in dynamics is

$$\{F(t)\} = \{K\}\{d\} + [M]\{\ddot{d}\} \tag{3.41}$$

In 3.41, the force is transient and is a function of time, $[M]$ is the global mass matrix and $\{\ddot{d}\}$ is the acceleration. The acceleration is defined as the second derivative of the displacement over time. Several methods are used to integrate Equation 3.41 over time. The methods are called direct integration methods and under the direct integration method there is the explicit method which is known as the central difference method and there are the implicit methods such as Newmark-Beta (to be referred to as Newmark's method) and the Wilson-Theta method (to be referred to as Wilson's method). Each method has its advantages and disadvantages. A brief description is given in the upcoming sections.

3.4.2.1 The central difference method

The finite difference Equations for velocity is

$$\{\dot{d}_i\} = \frac{\{d_{i+1}\} - \{d_{i-1}\}}{2(\Delta\tau)} \tag{3.42}$$

And for acceleration

$$\{\ddot{d}\} = \frac{\{\dot{d}_{i+1}\} - \{\dot{d}_{i-1}\}}{2(\Delta t)} \tag{3.43}$$

In 3.43 and 3.42 the subscripts indicate the current time step for a time increment Δt. This means that $d\{(t)\} = \{d_i\}$ and $\{d(t + \Delta t)\}$.

With 3.42 and 3.43 an Equation that relates the displacement with the acceleration can be obtained as

$$\{\ddot{d}\} = \frac{\{d_{i+1}\} - 2\{d_i\} + \{d_{i-1}\}}{(\Delta t)^2} \tag{3.44}$$

Given those previous two Equations, the procedure for the solution is

1- To start solving, $\{d_0\}$, $\{\dot{d}_i\}$, $\{\ddot{d}\}$, and $\{F_i(t)\}$ must be known

2- If $\{\ddot{d}\}$ is not known, it should be calculated by rearranging Equation 3.41 as

$$\{\ddot{d}_0\} = [M]^{-1}(\{F_0\} - [K]\{d_0\}) \tag{3.45}$$

3- After obtaining $\{\ddot{d}_0\}$, $\{d_{-1}\}$ is calculated as

$$\{d_{-1}\} = \{d_0\} - (\Delta t)\{\dot{d}_0\} + \frac{(\Delta t)^2}{2}\{\ddot{d}_0\} \tag{3.46}$$

4- $\{d_1\}$ is now needed to be calculated as

$$\{d_1\} = [M]^{-1}\{ (\Delta t)^2\{F_0\} + \left[2[M] - (\Delta t)^2[K]\right]\{d_0\} - [M]\{d_{-1}\}\} \quad (3.47)$$

5- $\{d_2\}$ can now be calculated as

$$\{d_2\} = [M]^{-1}\{ (\Delta t)^2\{F_1\} + \left[2[M] - (\Delta t)^2[K]\right]\{d_1\} - [M]\{d_0\}\} \quad (3.48)$$

6- $\{\ddot{d}_1\}$ is calculated as

$$\{\ddot{d}_1\} = [M]^{-1}(\{F_1\} - [K]\{d_1\}) \quad (3.49)$$

7- The velocity is calculated as

$$\{\dot{d}_1\} = \frac{\{d_2\} - \{d_0\}}{2(\Delta t)} \quad (3.50)$$

Repeating steps 5 to 7 for all other time steps while increasing the subscripts in Equations 3.48, 3.49, and 4.50 by 1 to complete the integration in time.

3.4.2.2 Newmark's method

Newmark's Equations that are used to solve finite element problems in dynamics are

$$\{\dot{d}_{i+1}\} = \{\dot{d}_i\} + (\Delta t)[(1-\gamma)\{\ddot{d}_i\} + \gamma\{\ddot{d}_{i+1}\}] \quad (3.51)$$

And

$$\{d_{i+1}\} = \{d_i\} + (\Delta t)\{\dot{d}_i\} + (\Delta t)^2[\left(\frac{1}{2} - \beta\right)\{\ddot{d}_i\} + \beta\{\ddot{d}_{i+1}\}] \quad (3.52)$$

In Newmark's Equations the parameters γ and β are selected by the analyzer. The steps to solve a dynamic problem using Newmark's method are:

1- With the load varying in time and known at every time step, proceed to calculate the displacements, velocity, and acceleration for every time step.

2- Initially at $t = 0$, $\{d_0\}$ and $\{\dot{d_0}\}$ are know from the boundary conditions.

3- The initial acceleration $\{\ddot{d}_0\}$; unless it is also know; is calculated as

$$\{\ddot{d}_0\} = [M]^{-1}(\{F_0\} - [K]\{d_0\}) \tag{3.53}$$

4- Using $\{d_0\}$, $\{\dot{d}_0\}$, and $\{\ddot{d}_0\}$, $\{d_1\}$ is calculated as

$$[K']\{d_1\} = \{F_1'\} \tag{3.54}$$

Where

$$[K'] = [K] + \frac{1}{\beta(\Delta t)^2}[M] \tag{3.55}$$

And

$$\{F_1'\} = \{F_1\} + \frac{[M]}{\beta(\Delta t)^2}[\,\{d_0\} + (\Delta t)\{\dot{d}_0\} + \left(\frac{1}{2} - \beta\right)(\Delta t)^2\{\ddot{d}_0\}\,] \tag{3.56}$$

5- $\{\ddot{d}_1\}$ is calculated by rearranging Equation 3.52 as

$$\{d_1\} = \frac{1}{\beta(\Delta t)^2}[\,\{d_1\} - \{d_0\} - (\Delta t)\{\dot{d}_0\} - (\Delta t)^2\left(\frac{1}{2} - \beta\right)\{\ddot{d}_0\}] \tag{3.57}$$

6- The velocity at $i = 1$, is calculated from Equation 3.51

With the results from steps 5 and 6, the steps are repeated starting from step 4 while increasing the subscript i by a 1.

3.4.2.3 Wilson's method

Wilson Equations that are used are

$$\{\dot{d}_{i+1}\} = \{\dot{d}_i\} + \frac{\theta(\Delta t)}{2}\left(\{\ddot{d}_{i+1}\} + \{\ddot{d}_i\}\right) \tag{3.58}$$

And

$$\{d_{i+1}\} = \{d_i\} + \theta(\Delta t)\{\dot{d}_i\} + \frac{\theta^2(\Delta t)^2}{6}\left(\{\ddot{d}_{i+1}\} + 2\{\ddot{d}_i\}\right) \tag{3.59}$$

The steps for integration in time using Wilson's method are

1- From initial boundary and velocity conditions at time $t = 0$, the displacement $\{d_0\}$ and the velocity $\{\dot{d}\}$ are known.

2- If the initial acceleration $\{\ddot{d}_0\}$ is not known, it is calculated as

$$\{\ddot{d}_0\} = [M]^{-1}(\{F_0\} - [K]\{d_0\}) \tag{3.60}$$

3- $\{d_1\}$ is calculated a s

$$[K']\{d_1\} = \{F_1'\} \tag{3.61}$$

Where

$$[K'] = [K] + \frac{6}{(\theta\Delta t)^2}[M] \tag{3.62}$$

And

$$\{F_1'\} = \{F_1'\} + \frac{[M]}{(\theta \Delta t)^2}[6\{d_0\} + 6\theta(\Delta t)\{\dot{d}_1\} + 2(\theta \Delta t)^2\{\ddot{d}_0\}] \qquad (3.63)$$

4- $\{\ddot{d}_1\}$ is calculated as

$$\{\ddot{d}_1\} = \frac{6}{\theta^2(\Delta t)^2}(\{d_1\} - \{d_0\}) - \frac{6}{\theta(\Delta t)}\{\dot{d}_0\} - 2\{\ddot{d}_0\} \qquad (3.64)$$

5- $\{\dot{d}_1\}$ is calculated as

$$\{\dot{d}_1\} = \frac{3}{\theta(\Delta t)}(\{d_1\} - \{d_0\}) - 2\{\dot{d}_0\} - \frac{\theta(\Delta t)}{2}\{\ddot{d}_0\} \qquad (3.65)$$

6- Steps 3 to 5 are repeated with the subscript increased by one each time a repetition is made.

Notes on Dynamic analysis solvers

Solving the dynamic finite element is more involved than solving static problems. The time step size is essential to the accuracy of the results and in case of using Newmark's method, the variables β and γ affect the solution accuracy and stability. Usually, β is selected from between 0 and $\frac{1}{4}$; while γ is selected as $\frac{1}{2}$. If β is set as 0 and γ is set as $\frac{1}{2}$, Newmark's Equations 3.51 and 3.52 become similar to the central difference Equations. Similarly, If Wilson's method is used; the choice of the variable θ also has an impact on the accuracy of the solution. Bathe (2006) gives a discussion about the stability and the accuracy of the integration schemes discussed in the previous sections.

4. Modeling and finite element method implementation

In this chapter, the process of modeling the geometry of the problem, its boundary conditions, time step choice, element size are discussed. In order to verify proper modeling of the problem and proper choice of modeling parameters, a verification study is performed on the model. The verification study compares the model of a single pile in homogeneous linear elastic soil with the analytical solution of Novak (1974) at $a_0 = 0.3$. His solution is given in more details in chapter 2.

The problem of a pile under a vibrating vertical load is shown in Figure 4.1. the pile is considered a floating pile in this case (or friction pile). The black part on top of the pile represents the mass the pile is carrying. A force Q is acting on top of the pile. Q varies with time in a sinusoidal manner. The force applied (sinusoidal load) has an amplitude of 22000 N therefore, $Q(t) = 22000\, Sin(\omega t)$. Where ω is the frequency of the load in $radians/sec$, t is the time in seconds.

Finite element modeling of this problem utilizes axisymmetric elements for discretizing the model. The solution parameters need to be optimized for accuracy include mesh size, time step, and boundary conditions. Choice of these parameters is based on recommendations from the literature. Once these parameters are set, a verification study is performed to verify that the modeling process is applicable to the modeling of the research cases.

Although most of the discussion here is limited to the 2D axisymmetric modeling of a single pile, the concepts and assumptions can be extended to the 3D modeling of two piles for the dynamic interaction study.

Autodesk simulation was used in this research. It has the capability to perform the linear static and dynamic finite element analysis required by this

research. It can mesh 2D regions and 3D solids automatically. Furthermore, the license of this software was given for free for the author as a Ph.D. student. The license grants full access to the software with no limitations.

4.1. Research assumptions

The following assumptions are applied to the research studied:

1- Pile and soil material is linearly elastic.

2- Pile and soil are in perfect contact and slippage and separation aren't allowed between the pile and the soil.

3- The pile in this research is circular in cross-section.

4- No material damping is applied.

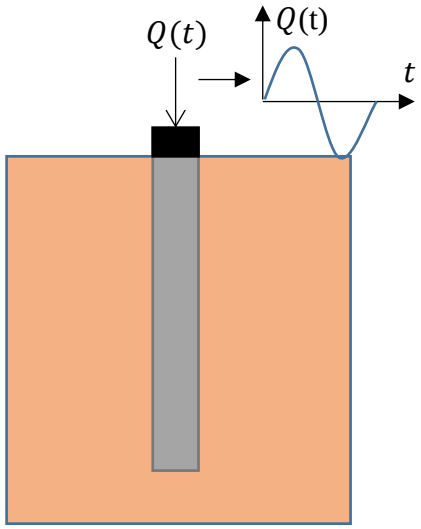

Figure 4.1: Pile subjected to vertical dynamic loading.

4.2. Geometry Modeling

Figure 4.1 showed the basic problem. A single pile subjected to vertical dynamic loading. Two types of analysis are carried in this research, 2D and 3D. This requires creating 2D and 3D geometries that represent the actual problem. The

2D axisymmetric geometry was created by drawing planes that represent the problem. for 3D modeling of the pile to pile interaction, 3D solids were created and assembled using Autodesk Inventor 2015 and then imported into Autodesk simulation mechanical for meshing and analysis.

The problem geometry consists of a mass on top of pile (rectangular region for 2D axisymmetric and 3D cylinder for 3D analysis), the pile (rectangular region for 2D axisymmetric and 3D cylinder for 3D analysis), and the soil (rectangular regions for 2D axisymmetric and 3D brick shape with hole to place pile in for 3D analysis). See Figure 4.2 for geometry modeling details with dimensions. Although the Figure shows 1 pile in the 3D model, the 3D model was used to model two piles to study the interaction between them.

4.2.1. Additional geometry modeling considerations

For piles in nonhomogeneous soils, geometry modeling of this study is slightly different than that of a pile in a homogeneous soil. Since Autodesk simulation doesn't have a built-in feature to set soil modulus of elasticity as a function of depth, it was done manually. The soil adjacent to the pile was divided into 10 segments each segment is 1 m in height. The modulus of elasticity of each segment is the average modulus of elasticity at the top of the segment and at the end of the segment. See Figure 4.3.

For end Bearing Pile, the bottom layer at which the pile rests is removed and fixed boundaries are placed along the bottom line of the model. This is because rock base deformation is almost non-existent and negligible compared to the pile and the soil. See Figure 4.3.

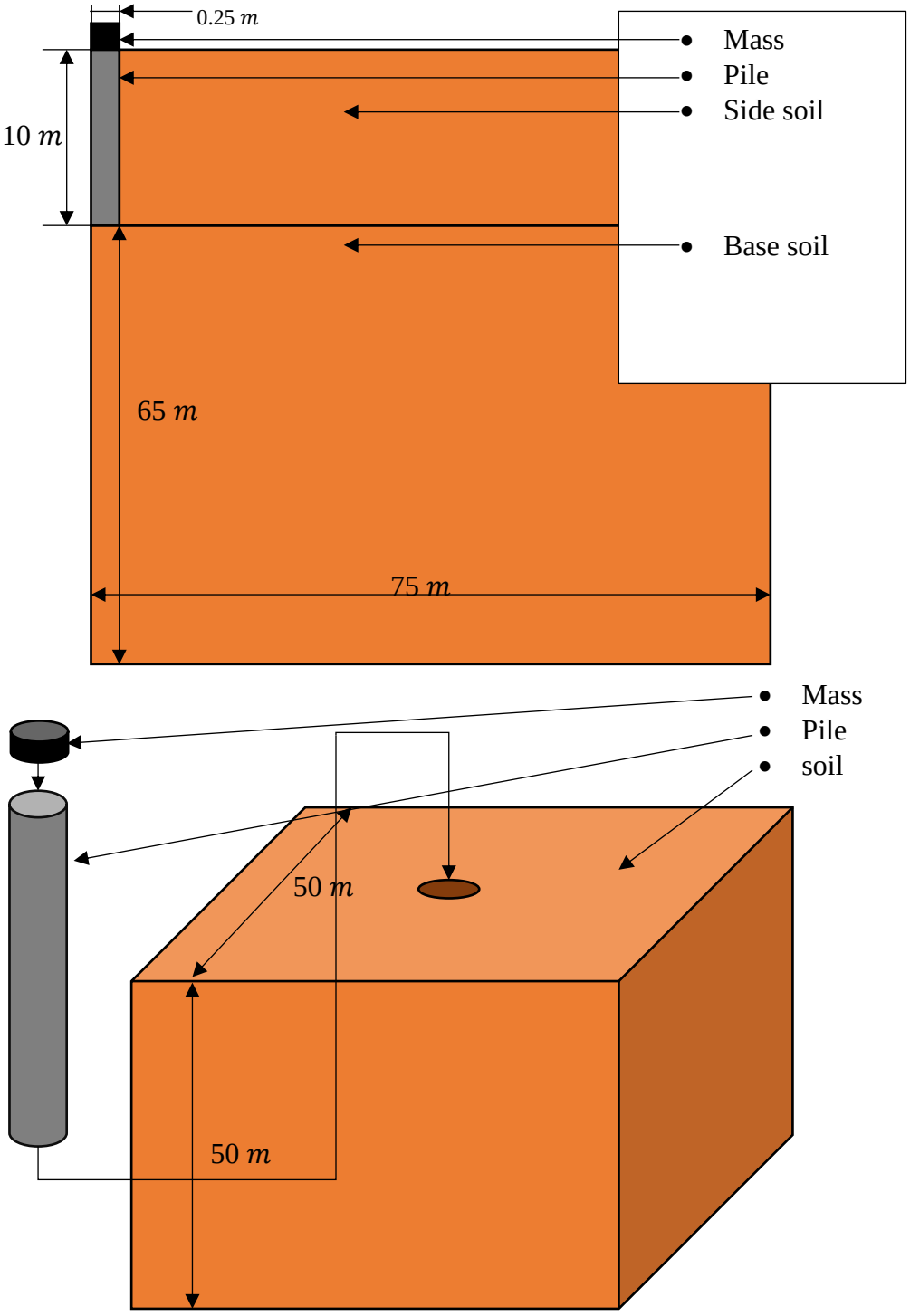

Figure 4.2: Details of geometry modeling. 2D axisymmetric model (top) and 3D model (bottom).

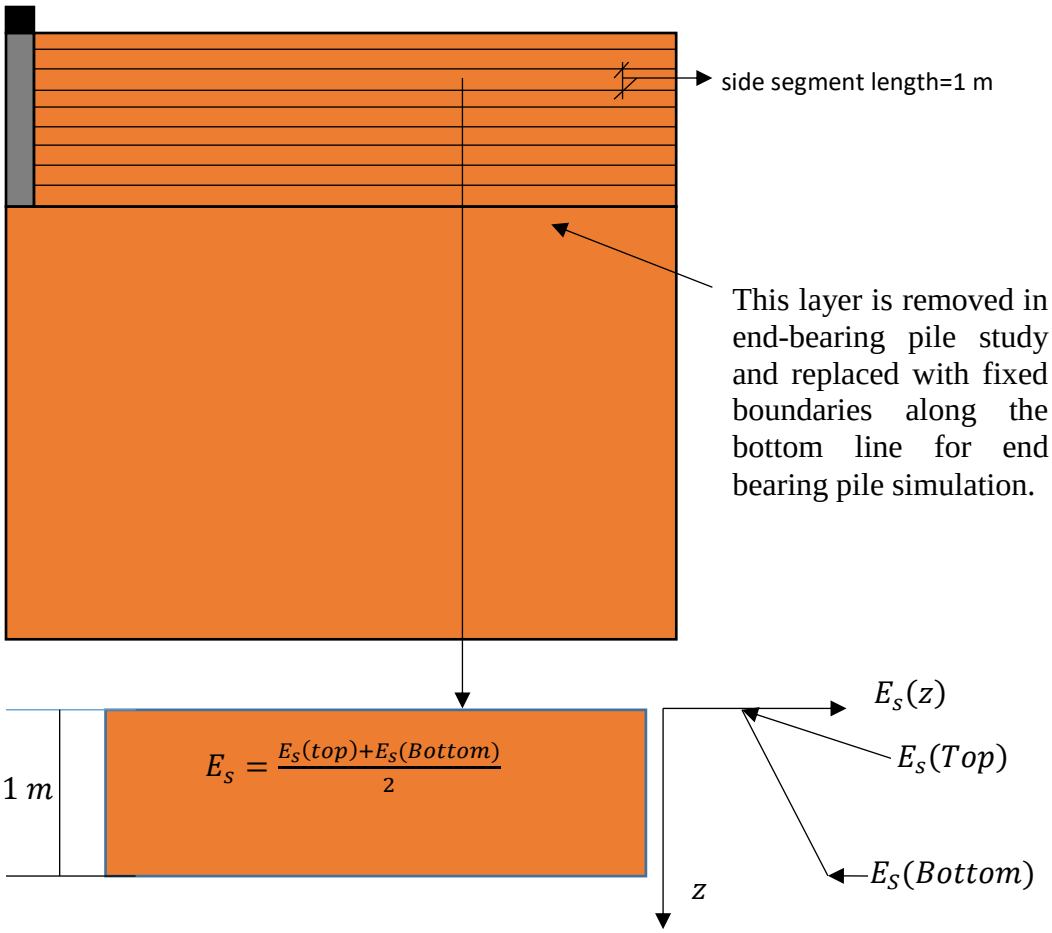

Figure 4.3: Additonal modeling considerations.

4.3. Finite element solution parameters

4.3.1. Element size

One of the major parameters in obtaining an accurate finite element solution is the mesh element size. The element size has to be chosen as small as possible to obtain accurate results while not being too small that the model has a huge number of elements and consequently consume more time to be solved.

Recommendations in literature by Lysmer (1978) and Zhang & Tang (2007) suggest that the following Equation governs the element size for dynamic soil problems

$$Element\ size, l_e = \frac{1}{8} \sim \frac{1}{5}\lambda_s \tag{4.1}$$

In Equation 4.1, λ_s is the shear wave length which is equal to v_s/f. Where v_s is the shear wave velocity and f is the frequency in Hz. Note that in an elastic continuum, the shear wave velocity v_s is $\sqrt{G_s/\rho_s}$. Where G_s is the shear modulus of the soil and ρ_s is the soil mass density. Based on Equation 4.1, if the soil has a shear wave velocity of 300 m/s and the frequency of the load is 6 Hz, the element size should be between 8.33 and 10 m. In this study the upper limit ($l_e = 1/5\ \lambda_s$) was chosen for the element size. See Figure 4.4 that shows how 2D and 3D elements sizes is defined. Two types of elements were used in this research, triangular axisymmetric elements for single piles and 3D tetrahedrons for 3D pile to pile interaction analysis. For the 2D axisymmetric model the Z-axis is the axis of symmetry.

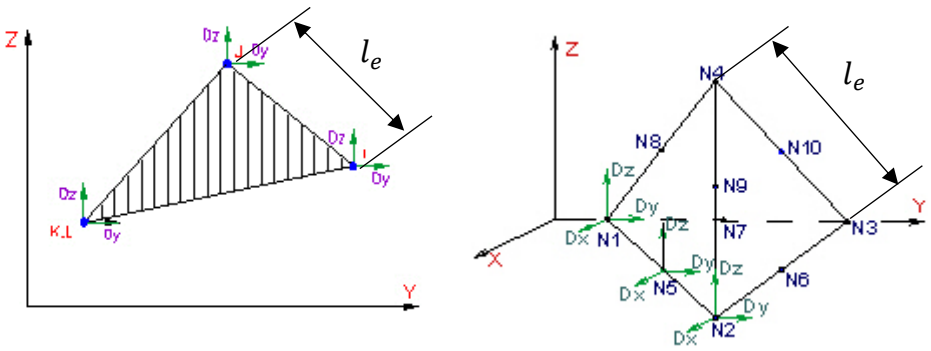

Figure 4.4: Definition of element length for a) Autodesk Simulation Axisymmetric element and b) Autodesk Simulation 3D tetrahedron.

4.3.2. Time step

Another important parameter in finite element solution is the time step. Wave propagation problems are dynamic and dynamic analysis is carried through integration in time at consecutive time steps. In choosing time step, the wave must

not travel more than one element length each time step (Bathe, 2006). The following Equation then governs the time step size

$$time\ step = l_e/v_p \tag{4.2}$$

Where l_e is the element length and v_p is the compressional wave velocity and it is calculated as

$$v_p = \frac{\lambda + 2G_s}{\rho_s} \tag{4.3}$$

In Equation 4.3, λ is Lame's parameter, G_s is the shear modulus and ρ_s is the mass density of the continuum. The integration scheme used in the analysis was Newmark's Integration in time.

4.3.3. Boundary conditions

Since the model needs to simulate an elastic half-space, it needs to be infinite. The program used Autodesk simulation (2017) doesn't have infinite elements. Because of this, the boundaries needed to be far away from the pile so that displacement amplitudes near the boundaries are very small and do not cause any significant reflection. In case of 3D analysis, the boundaries were much closer but needed to be composed of dashpot elements that absorb the upcoming waves and prevent reflection. Using far fixed boundaries and absorbing boundaries prevent significant reflection of the waves at the boundary and back to the pile for the 2D and 3D model. It is needed so that the reflected waves do not corrupt analysis results. Figure 4.5 shows a complete 2D axisymmetric model with fixed boundaries. Figure 4.6 shows the 3D model with absorbing boundaries. Figure 4.7 shows the amplitude of displacement at the pile and near side boundaries for a 2D

axisymmetric model and in Figure 4.8 amplitude of displacement is shown near bottom boundaries for a 2D axisymmetric model. From these Figures, it can be seen the displacement is small near fixed boundaries and any reflection won't corrupt results of dynamic displacement at the pile. The dashpot used at the boundary of 3D model has a coefficient calculated using the following Equations (Wilson, 2002)

$$c_v = \rho_s v_p A_e \tag{4.4}$$

$$c_h = \rho_s v_s A_e \tag{4.5}$$

Where c_v is the dashpot (vertical to element side) coefficient to absorb compressional waves, $c_h$is coefficient of dashpots (parallel to element side) absorbing shear waves, ρ_s is the soil density v_p is the compressional wave velocity, v_s is the shear wave velocity and A_e is the element area.

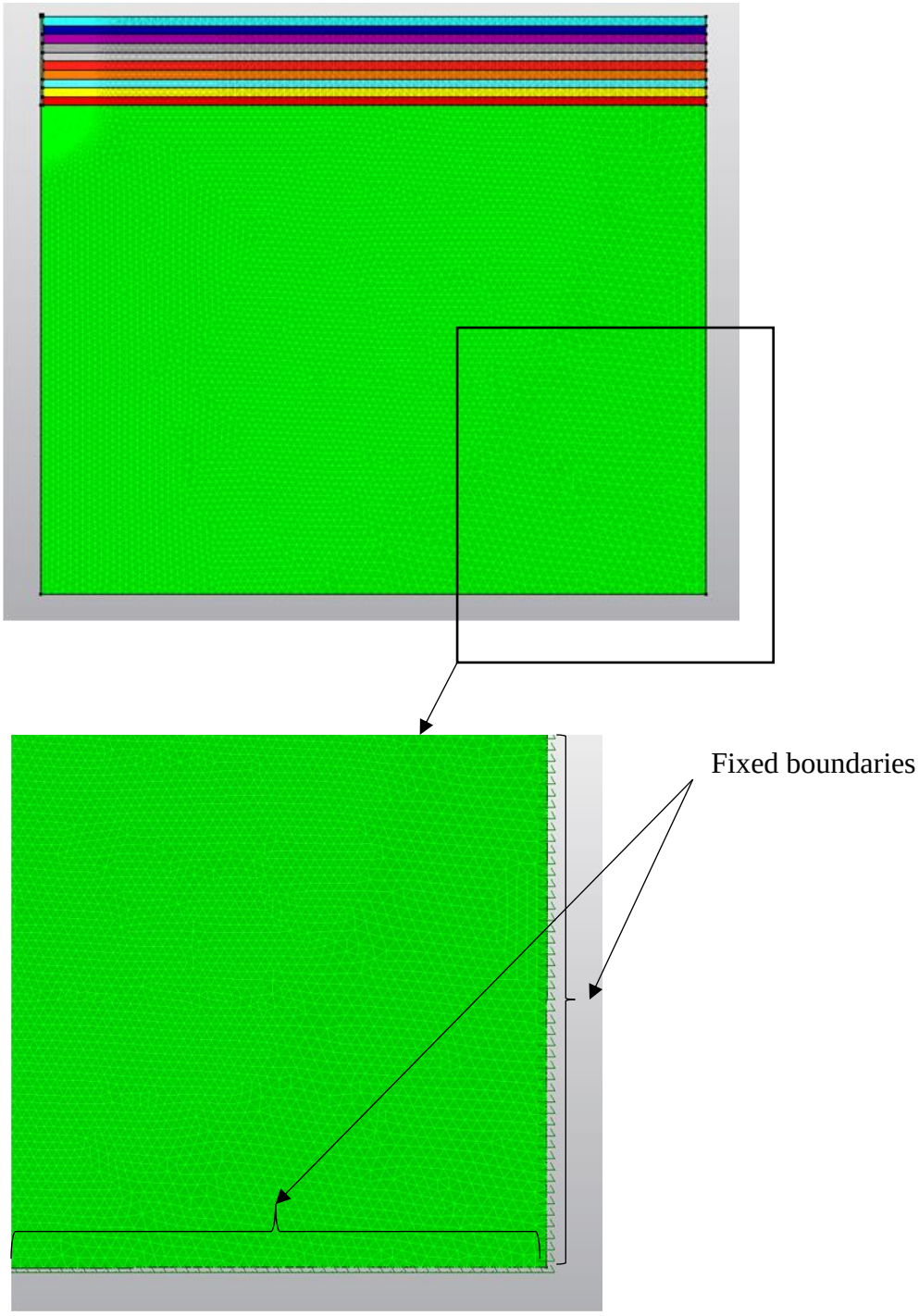

Figure 4.5: 2D axisymmetric model (meshed) with fixed boundaries placed far from the pile.

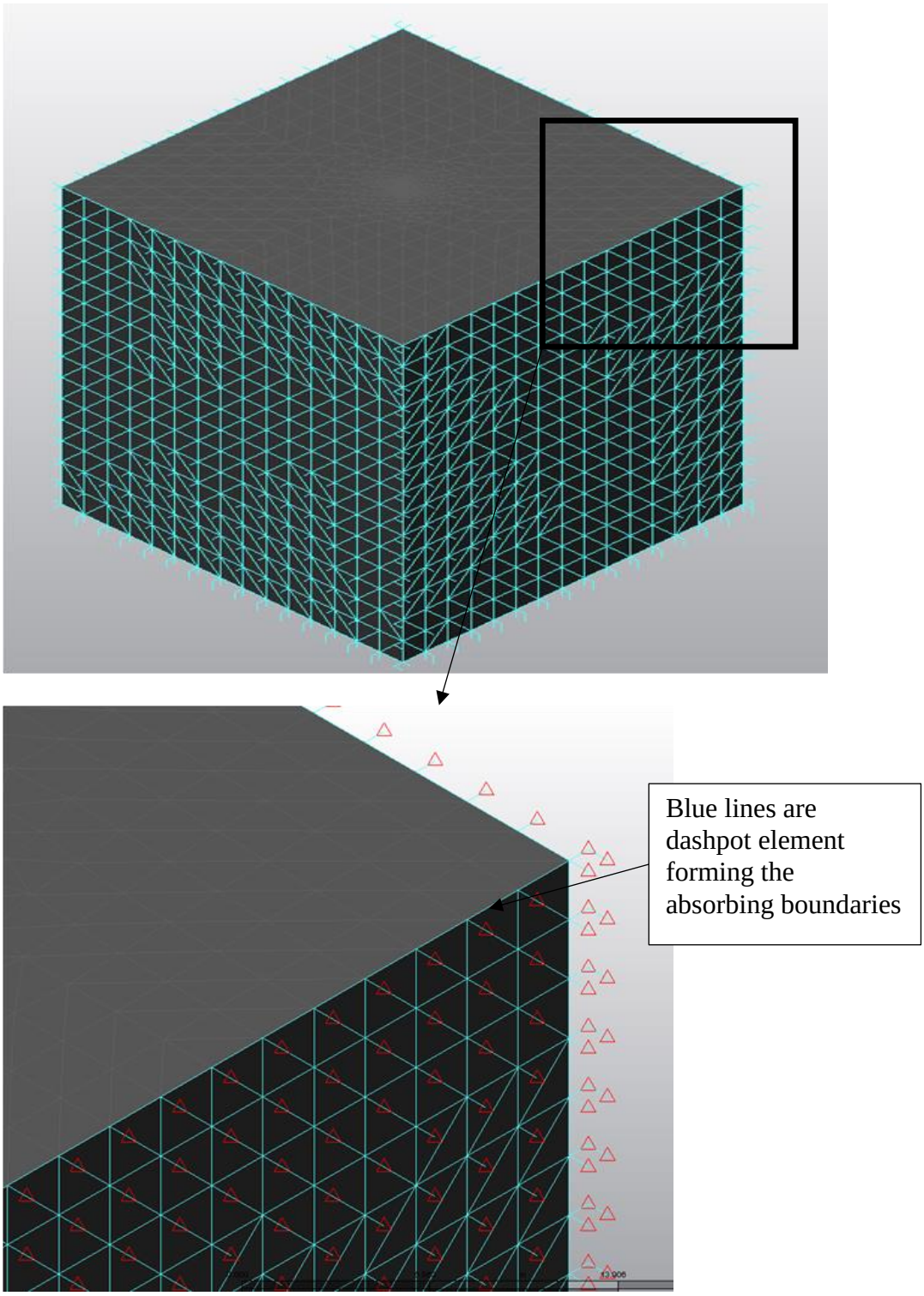

Figure 4.6: 3D model with dashpots as absorbing boundaries.

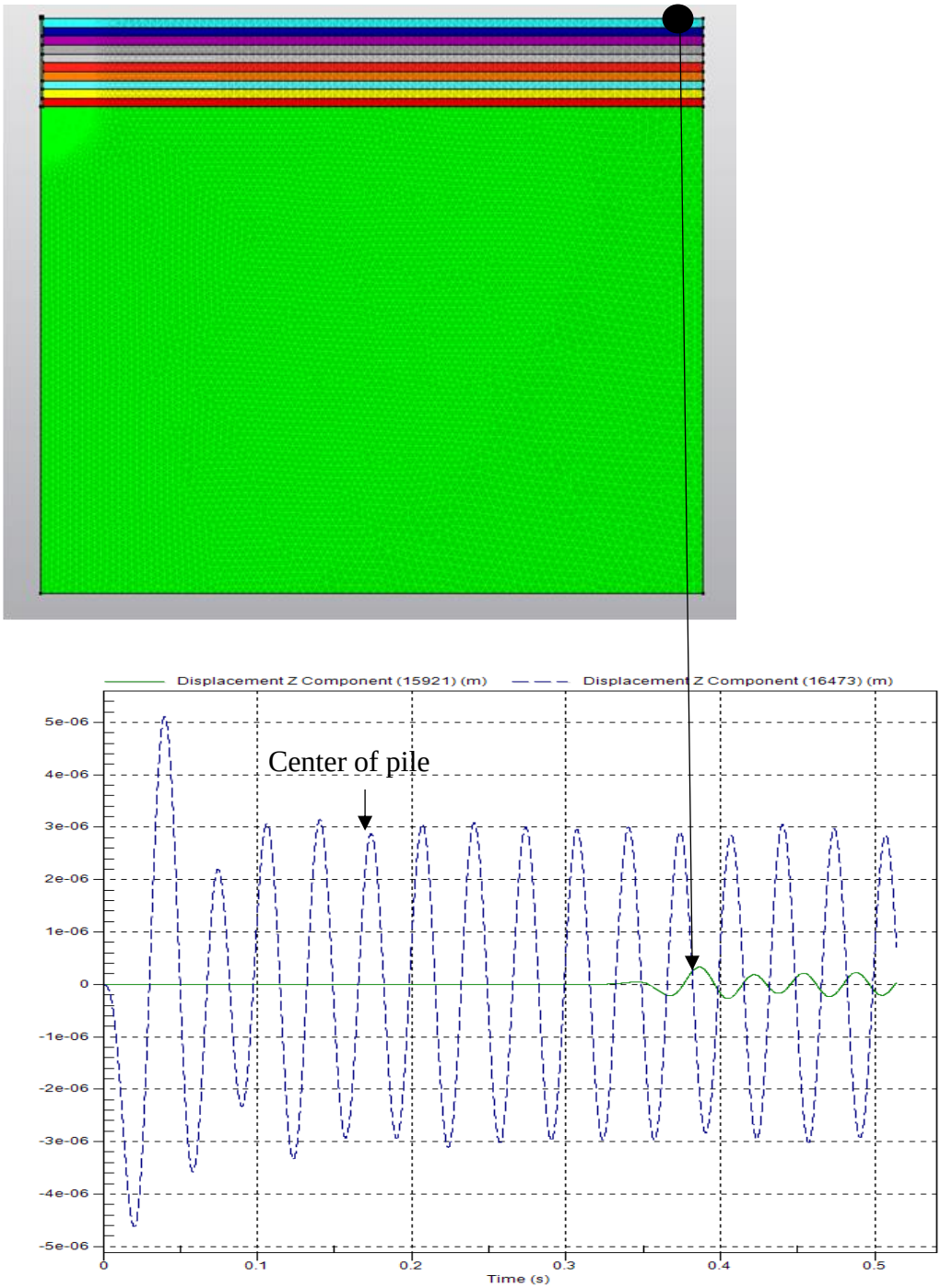

Figure 4.7: Amplitude of dynamic displacement near side boundary (green) compared to amplitude of dynamic displacement at pile(blue).

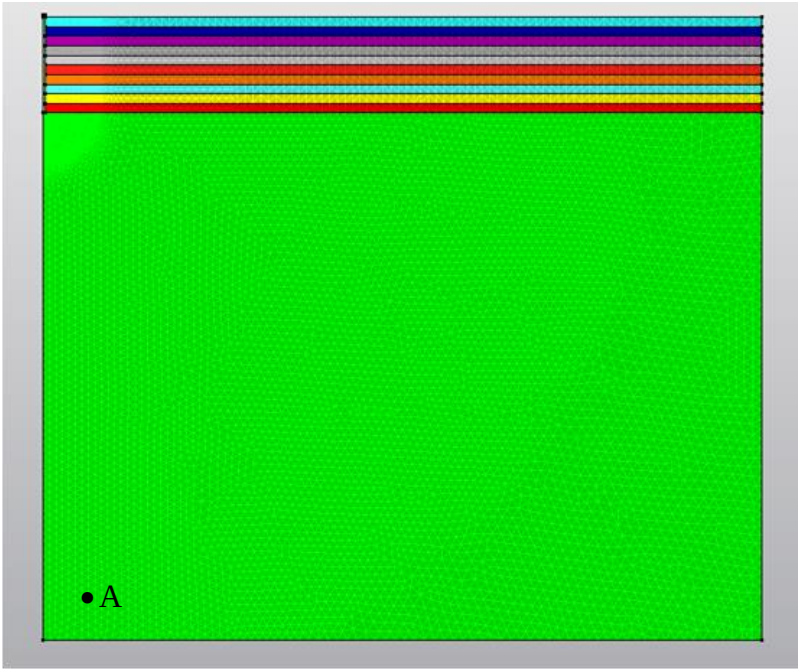

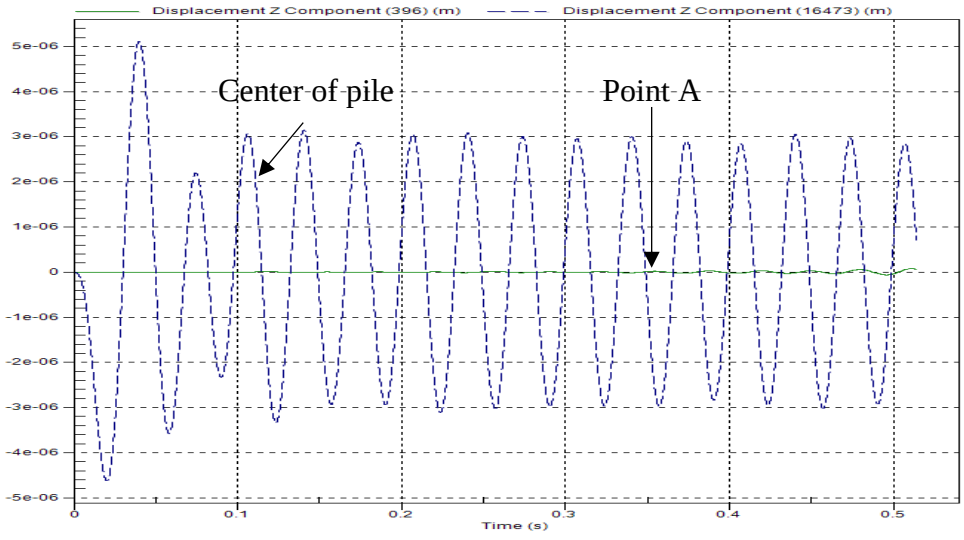

Figure 4.8: Amplitude of dynamic displacement near bottom boundary (green) compared to amplitude of dynamic displacement at pile (blue).

4.4. Analysis, obtaining results and interpretation procedure

The following is a step by step procedure for applying solution parameters, performing the analysis and obtaining results and interpretation of these results.

1- Parameters of study are set. This includes: Soil material Properties (Young's modulus, E_s , Poisson's ratio, μ_s and mass density, ρ_s), Pile Material Properties (Young's modulus,E_p and Poisson's ratio $\mu_p$and mass density, ρ_p).

2- Depending on the case, mesh element size, time step and boundaries are set.

3- A mass, M = 65000 kg is applied on top of the pile.

4- A static pressure , $Q_s = 22000\ Newton/m^2$ is applied on top of the pile and a static analysis is run. From static analysis, the static pile displacement,u_s is determined. From static analysis, the static stiffness, k is calculated as:

$$k = \frac{Q_S\, A_p}{u_s} \tag{4.6}$$

Where A_p is the area of the pile.

Also the natural frequency, f_n can be calculated as

$$f_n = \frac{1}{2\pi}\sqrt{\frac{k}{M}} \tag{4.7}$$

Where k is the static stiffness of the pile and M is the mass applied on top of the pile.

5- A load frequency, f is set and the dynamic load-time curve is prepared. (see Figure 4.9 for an example of a load-time curve)

6- The dynamic pressure $Q_d = 220000Sin(2\pi ft)Newton/m^2$ is applied on top of the pile and the dynamic analysis is run until steady state vibration is reached. Note that t in the previous Equation is the time in seconds.

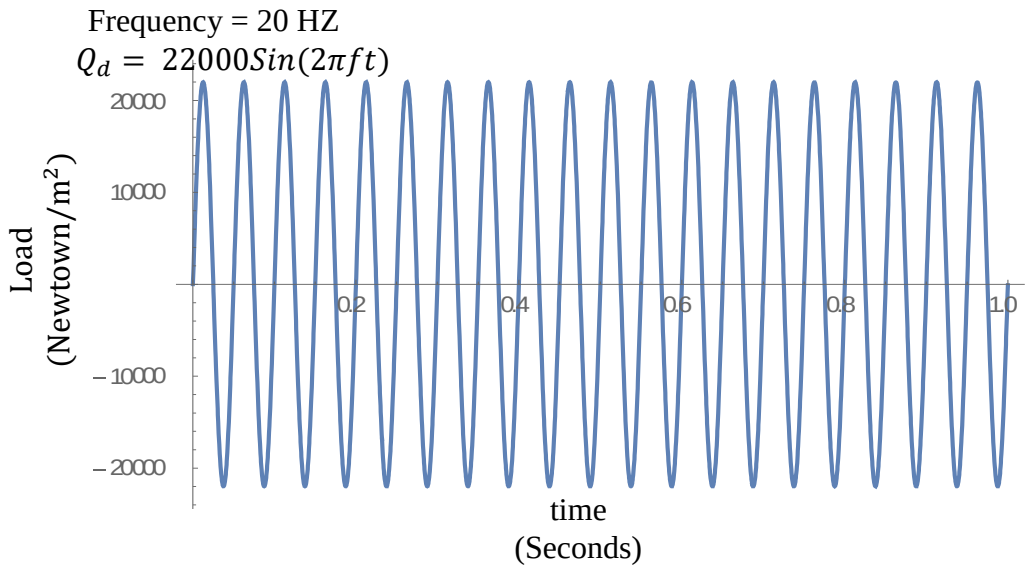

Figure 4.9: Example of applied load-time curve.

7- From dynamic analysis the pile dynamic displacement, u_d is determined. Note that dynamic displacement is the maximum amplitude of displacement at the steady state vibration.

8- The frequency is changed and steps 5 to 7 are repeated for several frequencies.

9- A curve of normalized dynamic displacement over static displacement is plotted against frequency. See Figure 4.10 for example.

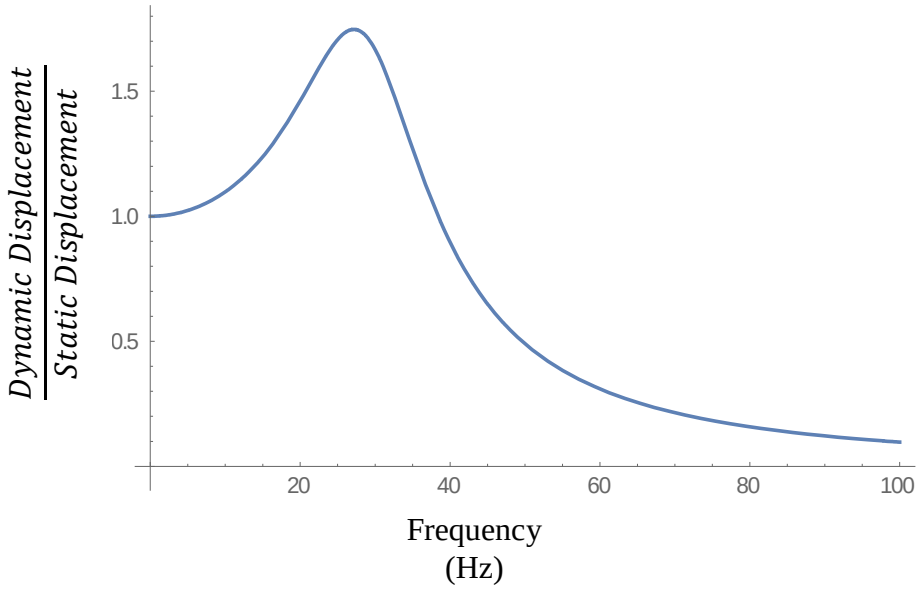

Figure 4.10: Example of pile response curve under different frequencies.

10- A curve similar to that shown in Figure 4.10 is described mathematically as

$$\frac{u_d}{u_s} = \frac{1}{\sqrt{\left(1 - \frac{f^2}{f_n^2}\right)^2 + \left(2D\frac{f}{f_n}\right)^2}} \tag{4.8}$$

Where $u_d$is the dynamic displacement, u_s is the static displacement, f is the frequency in Hz, f_n is the system natural frequency in Hz, D is the geometrical damping ratio.

In Equation 4.8, all the parameters of the Equation are known except for the geometrical damping ratio, D. It is the goal of the dynamic analysis is to determine D that describes the curve. Excel solver is used to determine D with the least error across all frequencies.

The process of determining the stiffness and damping ratio, D is illustrated by the following sample calculation.

Sample calculation of stiffness and damping: Floating pile in homogeneous elastic soil

For soil, $E_s = 2.5x10^8\ N/m^2$, μ_s = 0.45 and $\rho_s = 1800\ kg/m^3$.

For pile, $E_p = 2.1x10^{10} N/m^2$, μ_p = 0.25, $\rho_p = 2400\ kg/m^3$, $d_p = 0.5\ m$, $L_p = 10\ m$. Pressure applied on top of pile and amplitude of dynamic pressure $Q = 22000\ Newton/m^2$. Mass, M attached on top of pile = $65000\ kg$.

Where E is elastic modulus, μ is Poisson's ratio and ρ is the mass density. Subscript s designate soil property while subscript p designate pile property. d_p is the pile diameter and L_p is the length of the pile. For the specified case, results of finite element analysis are shown in Table 4.1. The results are obtained from static and dynamic analysis performed with accordance to sections 4.1, 4.2 and 4.3.

Table 4.1: Sample results for static and dynamic analysis.

$Frequnecy^1$	$Displacement^2$	$\frac{Dynamic\ Displacement}{Static\ Displacement}$
Hz	$meter$	
0	5.70E-06	1.00
10	8.00E-06	1.40
17.2	1.80E-05	3.16
25	5.00E-06	0.88
30	3.00E-06	0.53

Note in Table 4.1:

1- For frequency = 0, displacement is the static displacement.

2- $xx\ E - xx$ means $xx \times 10^{-xx}$ example: $5.70E - 06 = 5.7 \times 10^{-6}$.

The static stiffness can be calculated using

$$k = \frac{Q_S\, A_p}{u_s} = \frac{(22000)\left(\pi\left(\frac{d_p}{2}\right)^2\right)}{5.7X10^{-6}} = 7.6X10^8\ Newton/m \tag{4.9}$$

The system natural frequency can be calculated using

$$f_n = \frac{1}{2\pi}\sqrt{\frac{k}{M}} = \frac{1}{2\pi}\sqrt{\frac{7.6X10^8}{65000}} = 17.2\ Hz \tag{4.10}$$

An arbitrary value of the geometrical damping ratio D is chosen, let $D = 0.1$. Table 4.2 can be prepared using the value of assumed D and Equation 4.8.

Table 4.2: Calculated Dynamic Displacement/Static Displacement using assumed D value.

$Frequnecy^1$	$\frac{Dynamic\ Displacement^2}{Static\ Displacement}$	$Error^3$
Hz		
0	1.00	0.00
10	1.49	0.09
17.2	5.00	1.84
25	0.87	-0.01
30	0.48	-0.04

Sum of Errors = 1.87

Note in Table 4.2:

1- For frequency = 0, displacement is the static displacement.

2- The values in column 2 are calculated using Equation 4.6 with the assumed value of $D = 0.1$.

3- $Error = Column\ 2\ of\ Table\ 4.2 - Column\ 3\ of\ Table\ 4.1$

Using Excel Solver, the actual value of D that would minimize the sum of the errors is obtained. Table 4.2 values are adjusted. The new results of u_d/u_d are show in Table 4.3. The value of D that would minimize the errors is 0.16.

Table 4.3: Table generated after solving for D that would minimize the sum of errors.

$FrequnecY$	$\frac{Dynamic\ Displacement^2}{Static\ Displacement}$	$Error$
Hz		
0	1.00	0.00
10	1.46	0.05
17.2	3.12	-0.04
25	0.83	-0.05
30	0.47	-0.06

It can be seen from Table 4.3 that the error is at around 0.05 across all frequencies. The value of $D = 0.16$ is the best that describes the system response for the current set of analysis parameters. Plot of finite element results with results predicted using calculated geometric damping, D value is shown in Figure 4.11.

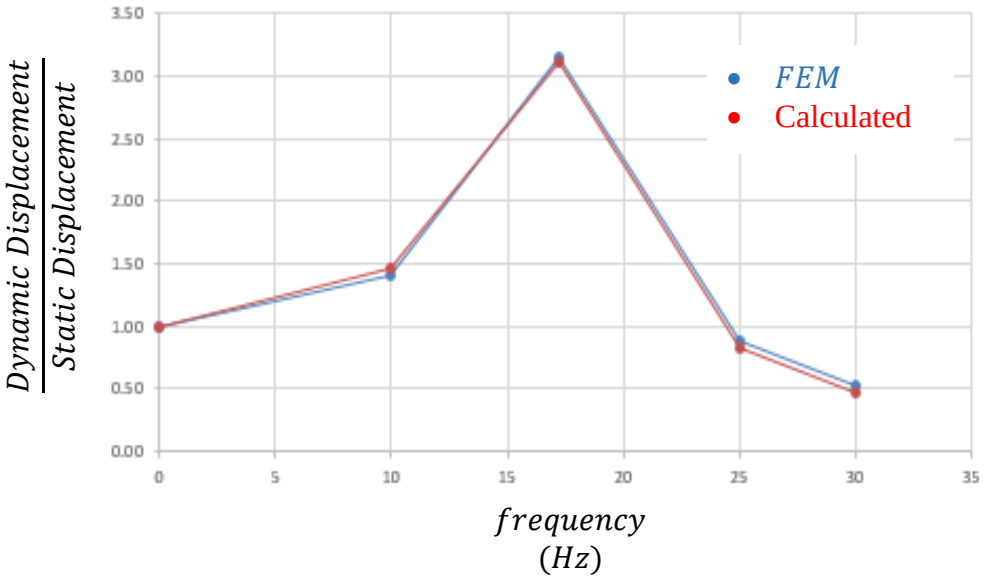

Figure 4.11: Plot of finite element results and that predicted using calculated D value.

After interpreting results for a certain case, the studied variables are adjusted and steps outlined in sections 4.3 and 4.4 are repeated for the new set of variables. After varying parameters, plots of the studied variable against static stiffness and damping are generated. These plots show how the variation in a certain studied variable affects the dynamic response of the system.

In summary, this chapter gives an insight of how data is collected and how the results are interpreted to come up with static stiffness, k, natural frequency, f_n and geometrical damping ratio, D. A flow chart is created to summarize the general study procedure followed throughout this research. It is shown in Figure 4.12.

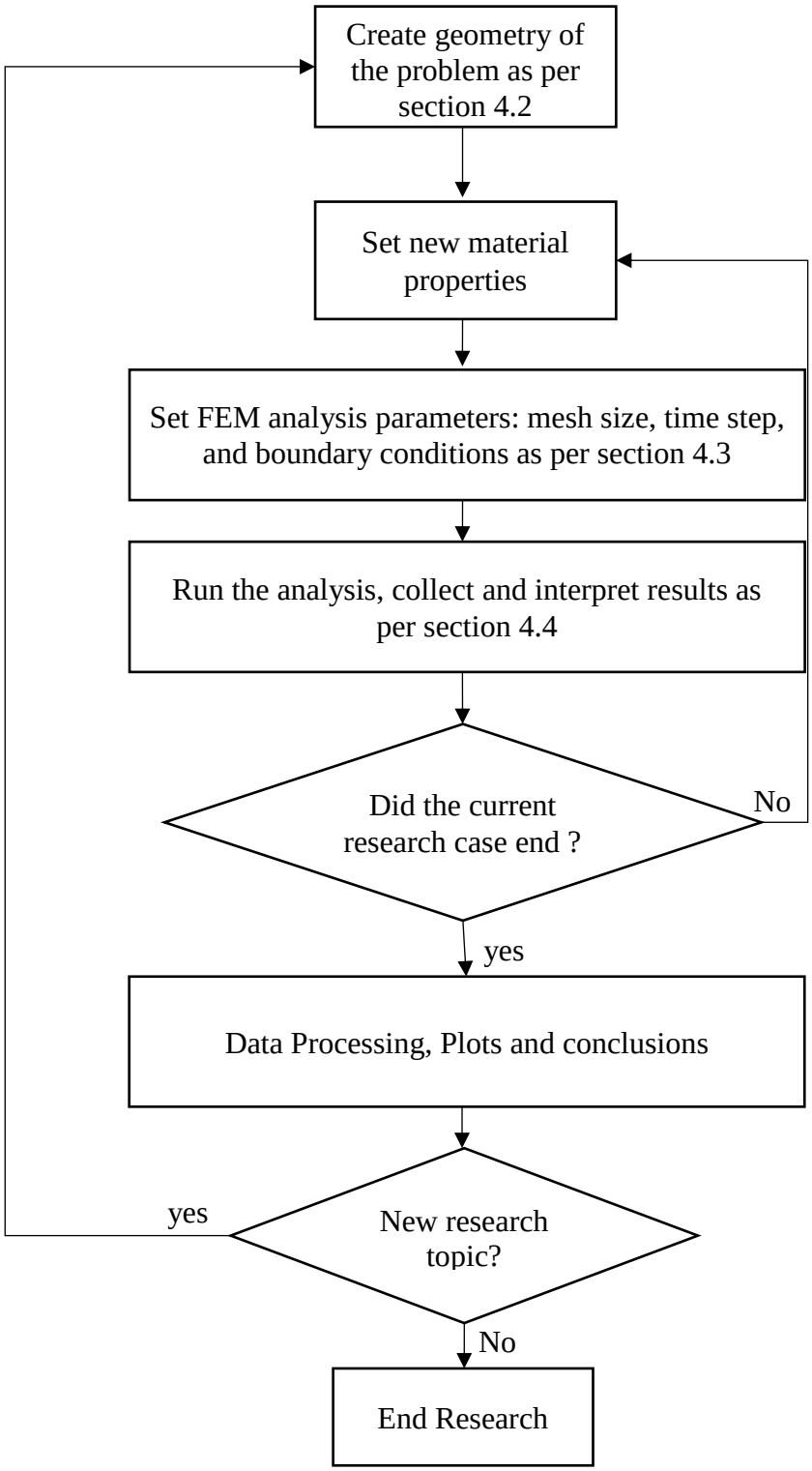

Figure 4.12: Flowchart summarizing research process.

4.5. Verification of the modeling process for dynamic analysis

To verify the modeling process for dynamic analysis, the case of a floating pile in elastic, homogeneous soil is analyzed using the finite element method and compared with results obtained by Novak's (1974) solution. Novak's solution is accurate at a dimensionless frequency, $a_0 = 0.3$. Analysis results at $a_0 = 0.3$ for finite element solution and Novak's solution is shown in Table 4.4. the dimensionless frequency is calculated using $a_0 = \omega r / v_s$. Where ω is the frequency in radians per seconds, r is the pile radius and v_s is the shear wave velocity of the soil. To maintain the value of a_0 at 0.3, both the frequency and the soil modulus of elasticity were varied. Dynamic finite element analysis is used to determine the dynamic displacement at a certain frequency and shear modulus of the soil. Novak solution is used to determine the dynamic displacement analytically. Results of dynamic displacement obtained by dynamic finite element analysis and Novak (1974) are shown in Table 4.4. .Results of both methods are plotted in Figure 4.13. As shown in Figure 4.13, good agreement between the FEM results and Novak's solution was obtained.

Table 4.4: results of verification study.

			u_d		
ω	v_s	G	Novak (1974)	3D FEM	Δ
Radians/second(Hz)	meter/second	Pascals	meter	meter	%
63	52	4.9E+06	2.9E-05	2.3E-05	-21%
126	105	2.0E+07	6.2E-06	6.0E-06	-3%
188	157	4.4E+07	2.5E-06	2.3E-06	-9%
251	209	7.9E+07	1.3E-06	1.2E-06	-11%
314	262	1.2E+08	8.4E-07	8.0E-07	-4%

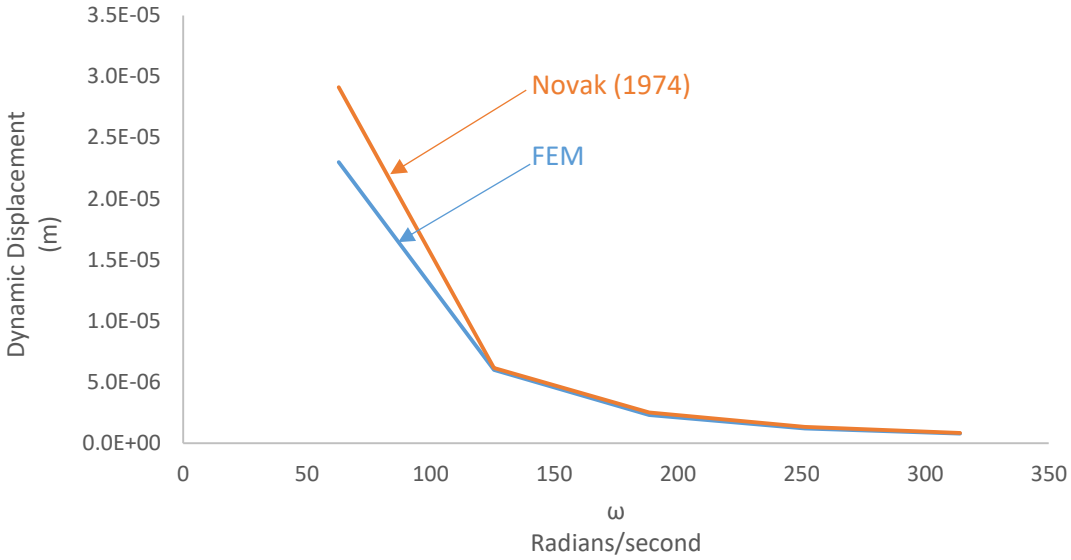

Figure 4.13: Plot of verification study results.

5. Results and Discussion

This chapter presents the results of the research. After defining the process of modeling, analysis and data interpretation in chapter 4, the cases considered in this research are prsented. Results are collected and processed to get the parameters that describe the dynamic behavior of the cases studied.

The cases considered in this research are:

1- Floating pile in homogeneous soil: The pile is elastic embedded in a homogeneous elastic soil. Results of the study give the variation of the stiffness and damping ratio with the variation of the soil modulus of elasticity.

2- Floating pile in nonhomogeneous soil: the study is concerned with a floating pile where the surrounding soil has a modulus of elasticity which increases linearly with depth. The increase stops at a point. Below this point, the soil modulus of elasticity remains constant. Variation of the slope of the increase in soil modulus of elasticity as well as variation of the point at which the modulus remains constant is considered. Their effect on damping ratio and stiffness are considered.

3- End-bearing pile (pile on rock) in homogeneous soil: this case is similar to case 1, but the pile rests on a rock base. This study varies the soil modulus of elasticity. Effect on damping and stiffness are studied.

4- End-bearing pile (pile on rock) in nonhomogeneous soil: this study is concerned with nonhomogeneous soil, where the soil has an increasing modulus of elasticity with depth. The increase stops at a point. Below this point, the soil modulus of elasticity remains constant until the rock base. Variation of the slope of the increase in soil modulus of elasticity as well as variation of the point at

which modulus remains constant is considered. Their effect on damping ratio and stiffness are considered.

5- The pile-to-pile interaction: this study is concerned with the dynamic and static interaction of piles. The simplest case of a pile group (2 piles) is studied in a manner similar to Poulos (1968). Soil modulus of elasticity and pile spacing is also varied. Effect of interaction between the piles is studied. Application to pile groups is discussed.

5.1. Floating pile in homogeneous soil

In this study, an elastic pile in an elastic homogeneous soil is studied via finite element method. An axisymmetric model is used to analyze this problem. Pile modulus of elasticity, E_p is fixed at $2.1 \times 10^{10}\ N/m$ (pre-stressed concrete pile) and its Poisson's ratio, μ_p is fixed at 0.25. Pile diameter, $d_p = 0.5\ m$ and its length, L_p is 10 m. The pile mass density, ρ_p is 2500 Kg/m^3. Soil modulus of elasticity,E_s is varied from $5 \times 10^6\ to\ 8.34\ \times 10^8\ N/m$. The soil Poisson's ratio, μ_s is fixed at 0.45. Soil density, ρ_s is 1800 kg/m^3. Frequency is varied in the dynamic analysis to capture dynamic response of the pile. Frequency variation depends on the soil material. The variation is chosen to best capture the dynamic behavior by choosing frequencies around the resonance area. In general, frequency was between 2.5 and 30 Hz. See Figure 5.1 for a general graphical description of the problem. See Table 5.1 for a summary of values of constants and range of values for varied parameters. The study captured the effect of the varied variables on the stiffness and damping of the pile.

Table 5.1: Values for variables and constants for study of floating pile in homogeneous soil.

Parameter	Symbol	Unit	Value
Pile Modulus of Elasticity	E_p	$Pascal$	$2.1\text{x}10^{10}$
Pile Poisson's Ratio	μ_p		0.25
Pile Mass Density	ρ_p	kg/m^3	2500
Pile Diameter	d_p	m	0.5
Pile Length	L_p	m	10
Soil Modulus of Elasticity	E_s	$Pascal$	$5\text{x}10^6$ to $8.34\text{x}10^8$
Soil Poisson's Ratio	μ_s		0.45
Soil Mass Density	ρ_s	kg/m^3	1800
Mass applied on top of Pile	M	kg	65000
Applied Static Pressure	Q_s	$Pascal$	22000
Dynamic Pressure Amplitude	Q_d	$Pascal$	22000
Frequency	f	Hz	2.5 to 30

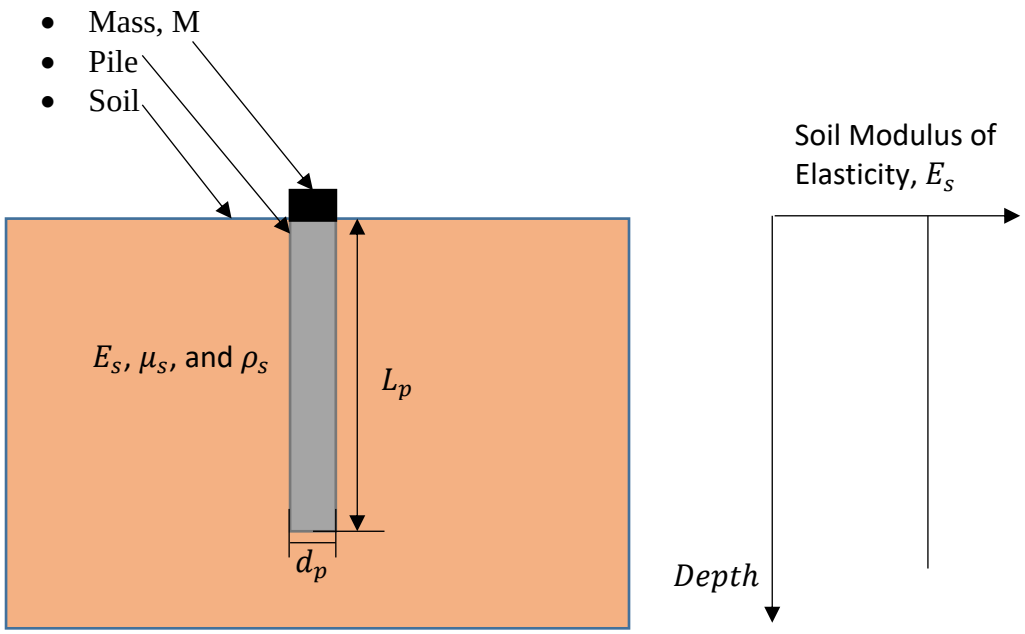

Figure 5.1: Floating pile in an elastic homogeneous soil.

The main two outcomes of this study are the stiffness, k and geometric damping ratio, D. The system stiffness, k as a variation with soil elastic modulus, E_s is given in Figure 5.2 while the variation of geometric damping ratio is given in Figure 5.3. from these two parameters, the critical damping, c_{cr}, the damping, c and the natural frequency, f_n can be calculated using the following Equations.

$$c_{cr} = 2\sqrt{k\,M} \tag{5.1}$$

$$c = D\,c_{cr} \tag{5.2}$$

$$f_n = \frac{1}{2\pi}\sqrt{\frac{k}{M}} \tag{5.3}$$

Variation of these parameters is given in Figures 5.4, 5.5 and 5.6 respectively. For the natural frequency, it is given in Figure 5.6 as a dimensionless natural frequency,a_{0n} which is calculated as

$$a_{0n} = \frac{2\pi f_n (d_p/2)}{v_s} \tag{5.4}$$

Where f_n is the natural frequency, d_p diameter of the pile, v_s is the shear wave velcotiy of the soil.

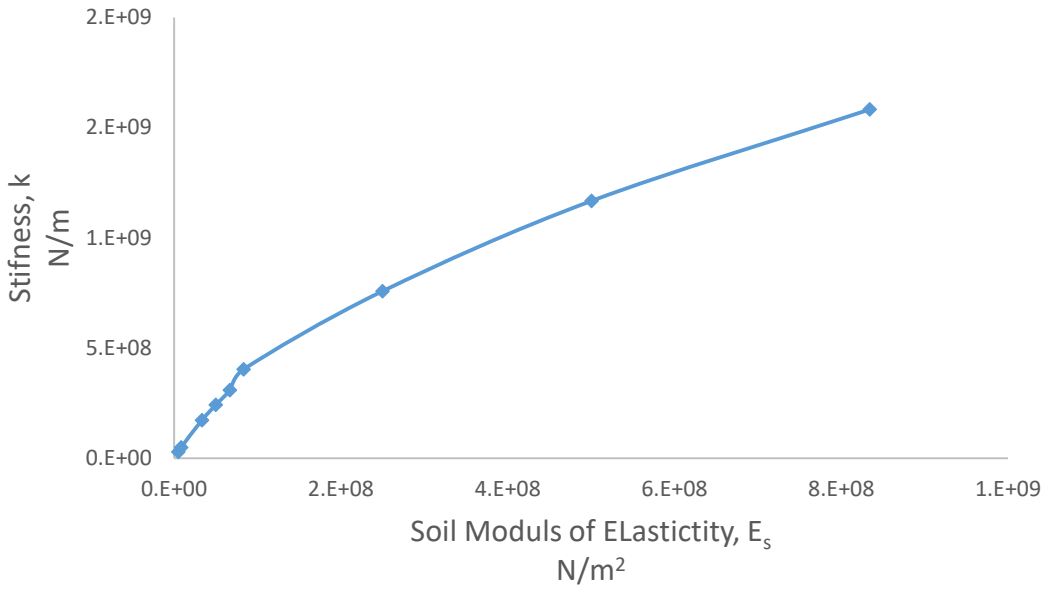

Figure 5.2: Variation of stiffness, k with soil modulus of elasticity, E_s for a floating pile in homogeneous soil.

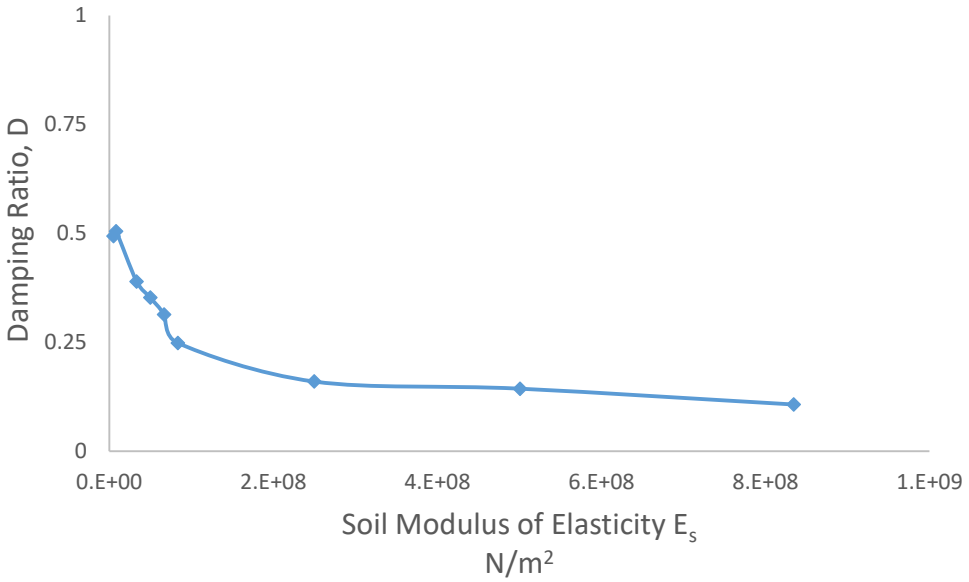

Figure 5.3: Variation of geometric damping, D with soil modulus of elasticity, E_s for a floating pile in homogeneous soil.

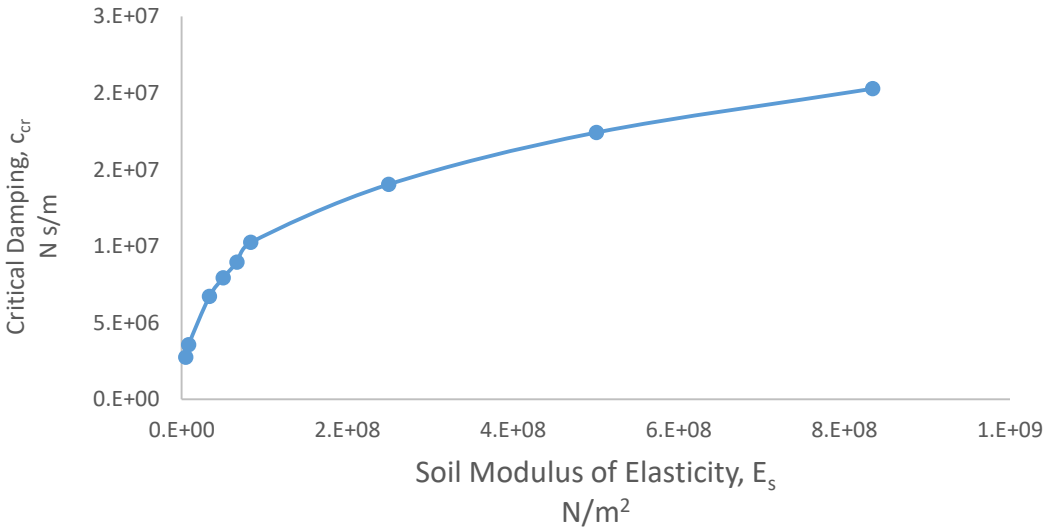

Figure 5.4: Variation of critical damping, c_{cr} with soil modulus of elasticity, E_s for a floating pile in homogeneous soil.

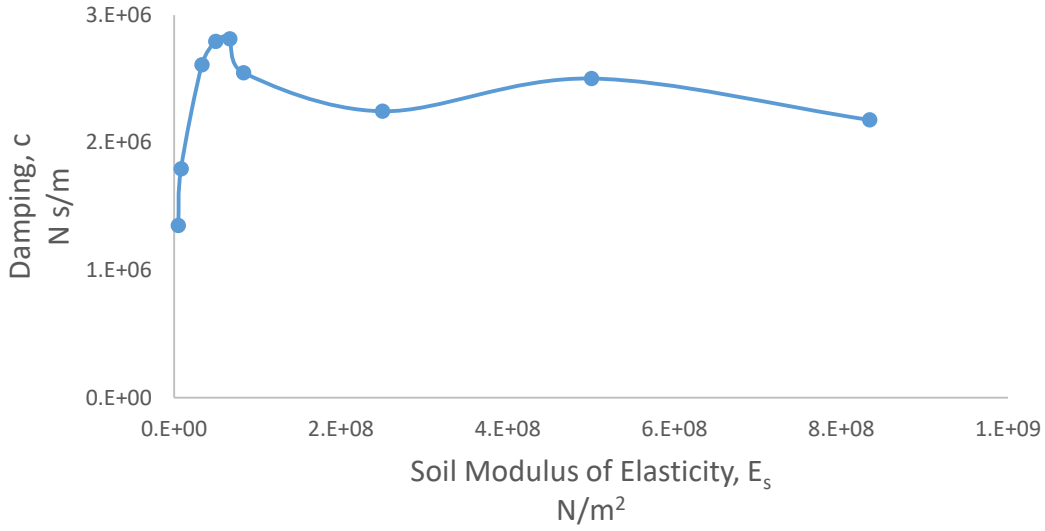

Figure 5.5: Variation of damping, c with soil modulus of elasticity, E_s for a floating pile in homogeneous soil.

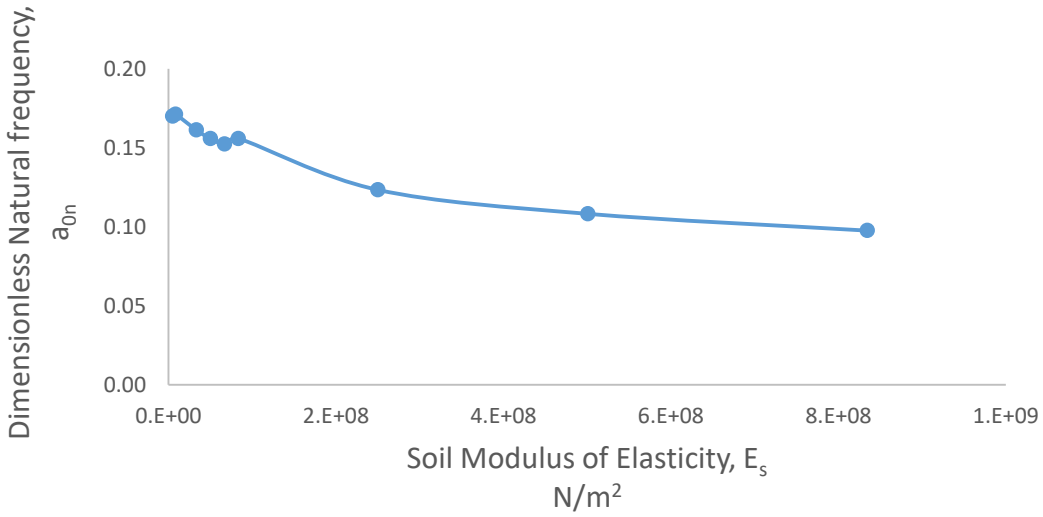

Figure 5.6: Variation of dimensionless Natural frequency, a_{0n} with soil modulus of elasticity, E_s for a floating pile in homogeneous soil.

5.1.1. Results commentary and analysis

- Figure 5.2 shows that the stiffness increases with increase in soil elastic modulus at a slightly nonlinear rate. This increase is expected. As the soil gets stronger, it can sustain the load at lower displacements.
- Figure 5.3 shows that the trend for geometric damping ratio which tends to decrease with an exponential decay function as the elastic modulus of the soil increases.
- From the previous 2 points, it can be concluded that increase in soil elastic modulus provides lower dynamic displacement, u_d and static displacement, u_s but greater amplification of displacement (i.e. u_d/u_s) at resonance. This pattern is shown in Figure 5.7 for value of dynamic displacement and Figure 5.8 for amplification of displacement. From Figure 5.7 it can be seen that the dynamic displacement at resonance is high at low modulus of elasticity and decreases rapidly with increase in soil modulus of elasticity. If the dynamic displacement at resonance is normalized over the static displacement (i.e., dynamic amplification) as in Figure 5.8, it can be seen that amplification increases linearly with increase in soil modulus of elasticity.

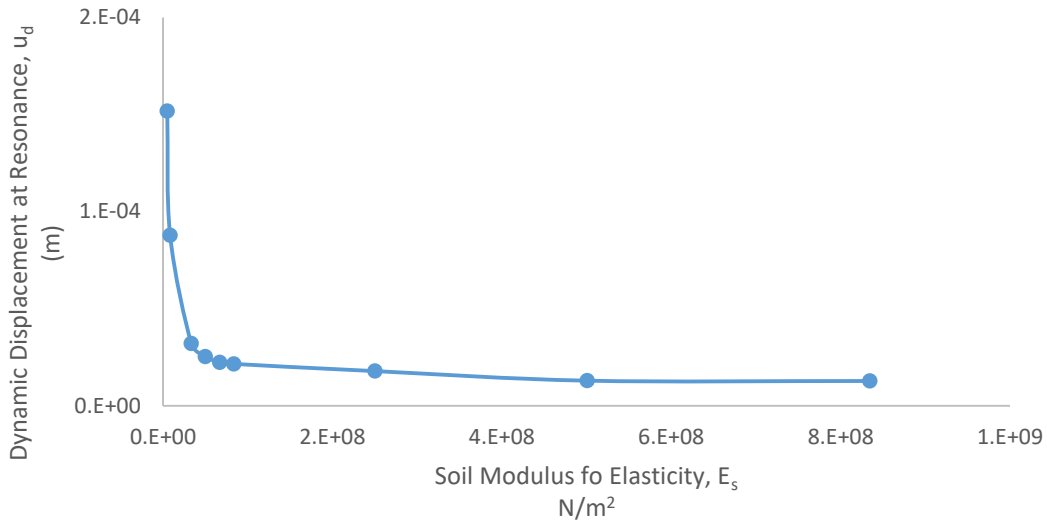

Figure 5.7: Variation of vertical dynamic displacement, u_d at resonance with soil modulus of elasticity, E_s for a floating pile in homogeneous soil.

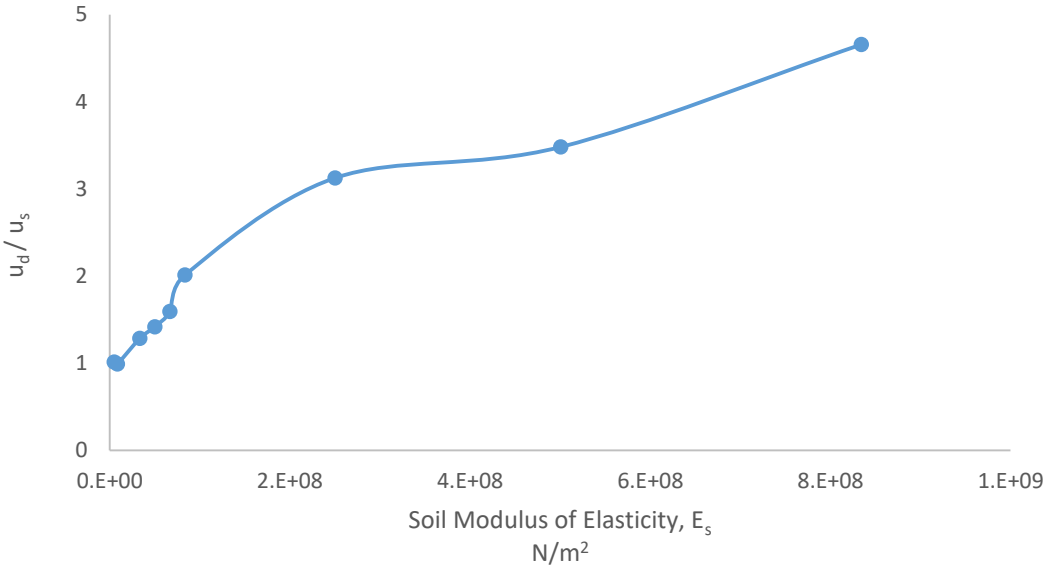

Figure 5.8: Variation of dynamic amplification at resonance with soil modulus of elasticity, E_s for a floating pile in homogeneous soil.

- From Figure 5.4 it is shown that the critical damping increase with the increase in soil stiffness. This is expected since it is mathematically related to the stiffness of the system as described by Equation 5.1.

- From Figure 5.5 it is shown that the damping (which is obtained by multiplying the damping ratio, D with the critical damping, c_{cr}) increases with soil stiffness up to a certain point. At this point the, damping seems to be constant.
- The natural frequency s given in the form of dimensionless frequency in Figure 5.6. It starts high in softer soils and decreases as the soil gets stiffer. The actual natural frequency in Hz increases with increase in soil modulus of elasticity as shown in Figure 5.9.

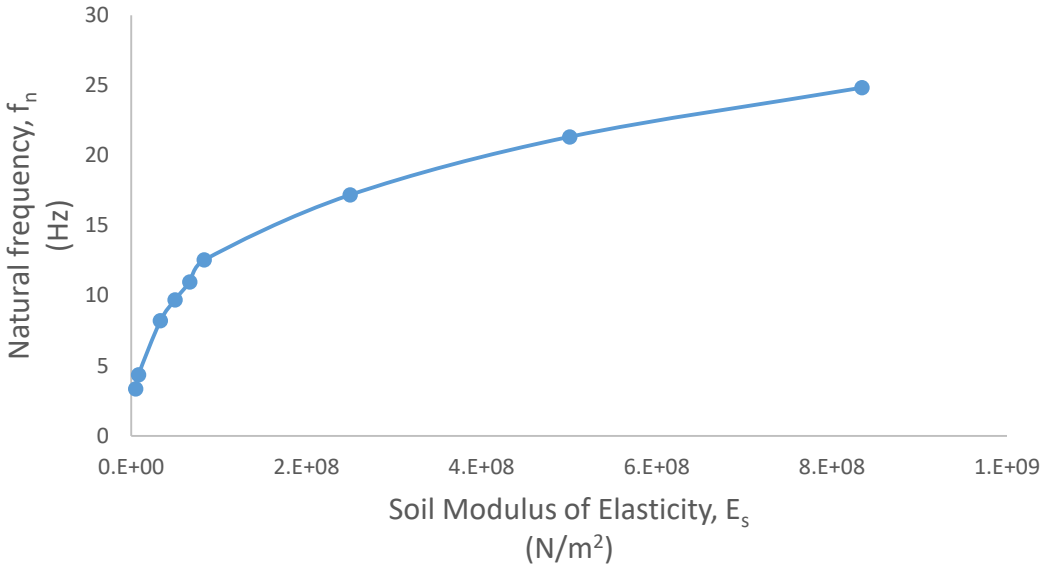

Figure 5.9: Variation of natural frequency, f_n with soil shear wave velocity, v_s for a floating pile in homogeneous soil.

5.1.2. Comparison of finite element solution results with literature

5.1.2.1. Comparison of stiffness

Results obtained by finite element analysis (current study) are compared with the work of others. The first comparison provided is with Novak (1974) solution which is discussed in section 2.2.2. The comparison is shown in Figure 5.10. Relative difference of static stiffness values between finite element analysis and Novak' Solution is calculated using Equation 5.5 and plotted in Figure 5.11.

$$\frac{k_{study} - k_{Novak}}{k_{Novak}} \text{x} 100 \qquad (5.5)$$

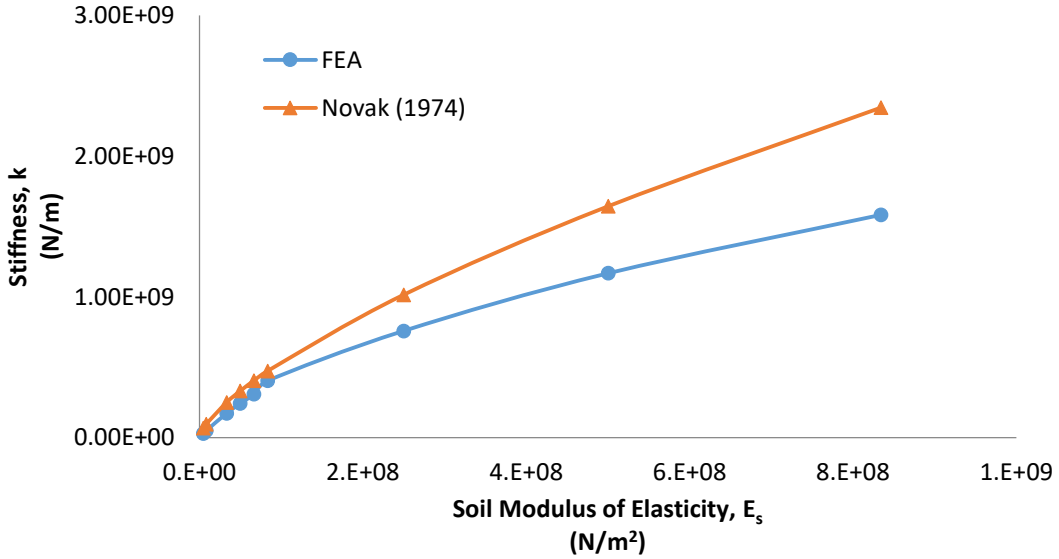

Figure 5.10: Comparison of stiffness,k obtained by finite elemnt method with Novak (1974) for a floating pile in homogeneous soil.

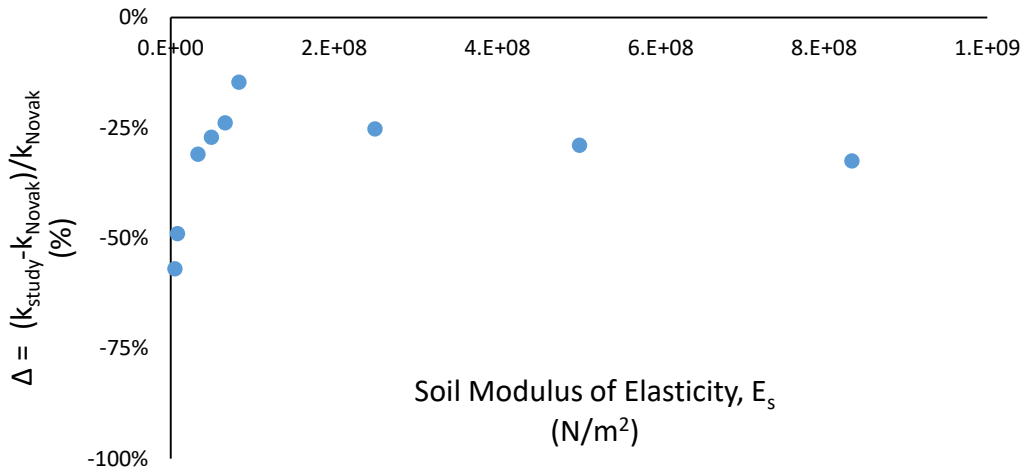

Figure 5.11: Relative Difference of stiffness between 3D FEM and Novak (1974) for a floating pile in homogeneous soil.

From Figure 5.11, it can be shown that there is a great difference between the stiffness obtained by Finite element analysis and that obtained by Novak. The relative difference between the two is between $-57\%\ to -15\%$. In general, Novak's solution over-predicts the stiffness of the system compared to finite element analysis. This difference can be contributed to Novak's simplification of the problem as he idealized the 3D problem to a plane strain 2D plane strain problem. Novak also assumes that the stiffness at the pile tip is similar to a that obtained by elastic solution for a circular loaded area on the surface of an elastic half space. Implications of such difference in stiffness will have its effect extended to other dynamic parameters. Values of natural frequency are directly affected by such difference due to its direct dependency on the stiffness, k as $f_n = (1/2\pi)\sqrt{k/M}$. The critical damping values are also directly affected as $c_{cr} = 2\sqrt{kM}$. Effect on critical damping is extend to the geometrical damping ratio as $D = c/c_{cr}$, where c, is the damping of the system (Geometrical damping in this case).

Another comparison of the stiffness is provided against the work of Gazetas & Mylonakis (1998). The stiffness of a pile in homogeneous elastic soil given is calculated as follows:

$$k = E_p A_p \lambda \frac{\Omega + \tanh(L_p \lambda)}{1 + \Omega \tanh(L_p \lambda)} \tag{5.6}$$

Where λ is calculated using

$$\lambda = \sqrt{\frac{\delta G_s}{E_p A_p}} \tag{5.7}$$

Ω is calculated using the following Equation

$$\Omega = \frac{k_b}{E_p A_p \lambda} \tag{5.8}$$

δ is calculated as

$$\delta = \frac{2\pi}{\ln(\frac{2r_m}{d_p})} \tag{5.9}$$

Where r_m is

$$r_m = 2.5 L_p (1 - \mu_s) \tag{5.10}$$

And k_b is calculated as

$$k_b = \frac{d E_s}{1 - \mu_s}(1 + 0.65 \frac{d_p}{h_b}) \tag{5.11}$$

In Equations 5.6 to 5.11, the following notations apply:

- E_p: Pile modulus of elasticity.
- A_p: Pile cross sectional area.
- λ: a parameter calculated using 5.7.
- Ω: a parameter calculated using 5.8.

- L_p: Pile length.
- k_b; stiffness at pile base given by Randolph & Wroth (1978).
- G_s: soil shear modulus.
- E_s: soil modulus of elasticity.
- d_p: pile diameter.
- h_b: depth to bed rock from pile tip ($h_b = \infty$, if far away and has no effect).
- μ_s: soil Poisson's ratio.
- r_m: radius at which soil settlement is negligible.

Using the Equations defined by Gazetas & Mylonakis (1998), the stiffness was calculated. The problem as defined by Gazetas & Mylonakis (1998) is shown in Figure 5.12. A comparison between this approach and the finite element solution is provided in Figure 5.13 while relative difference $(k_{study} - k_{Gazetas})/k_{Gazetas}$ is given in Figure 5.14.

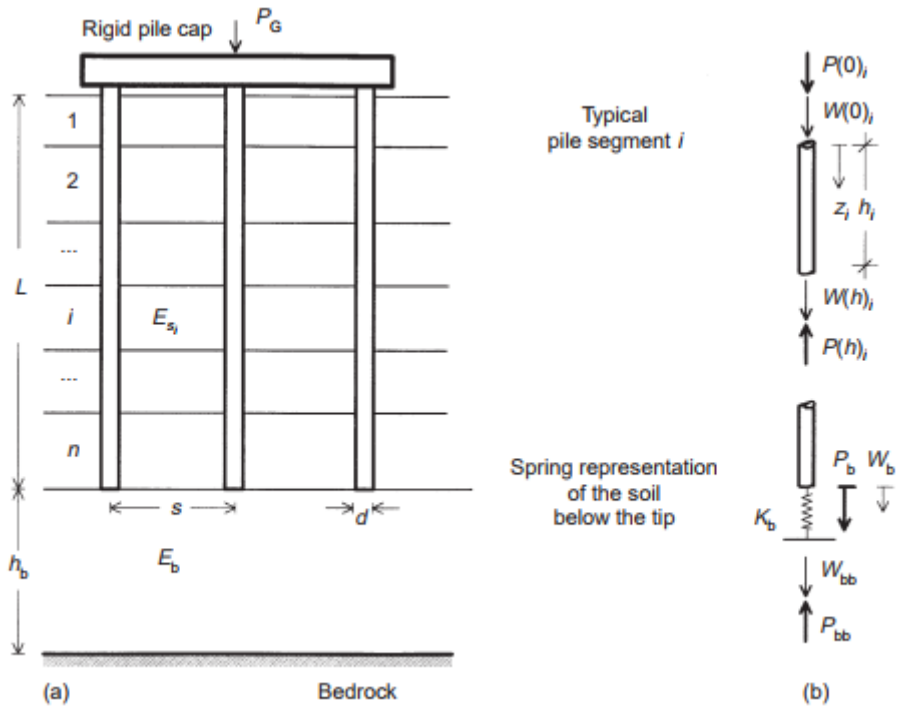

Figure 5.12: Problem layout as studied by Gazetas & Mylonakis (1998).

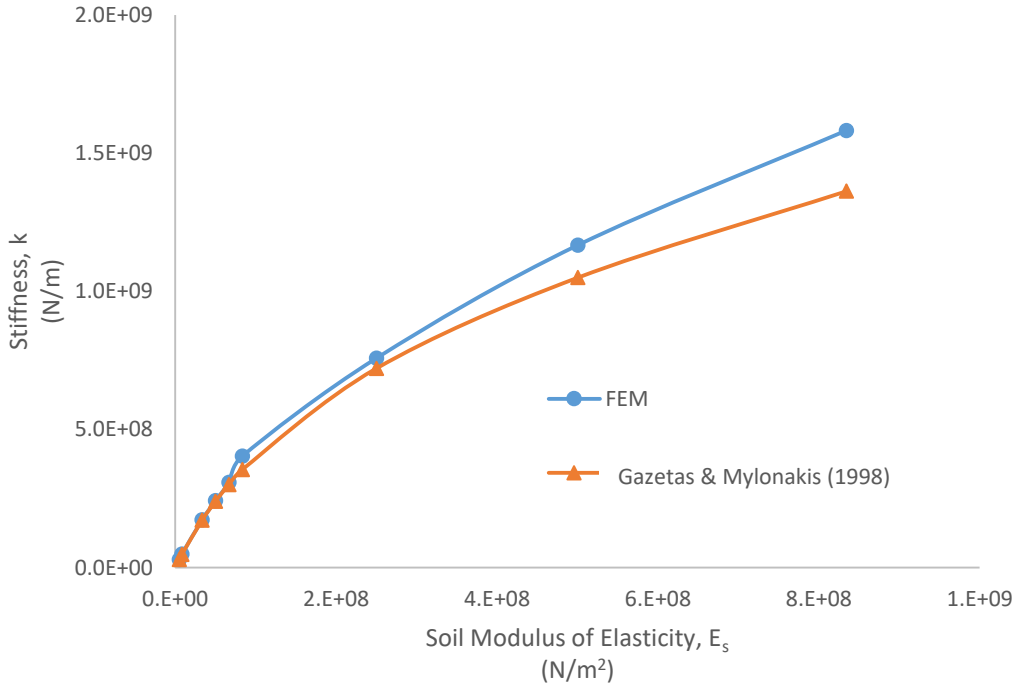

Figure 5.13 Comparison of stiffness,*k* obtained by finite element method with Gazetas & Mylonakis (1998) for a floating pile in homogeneous soil.

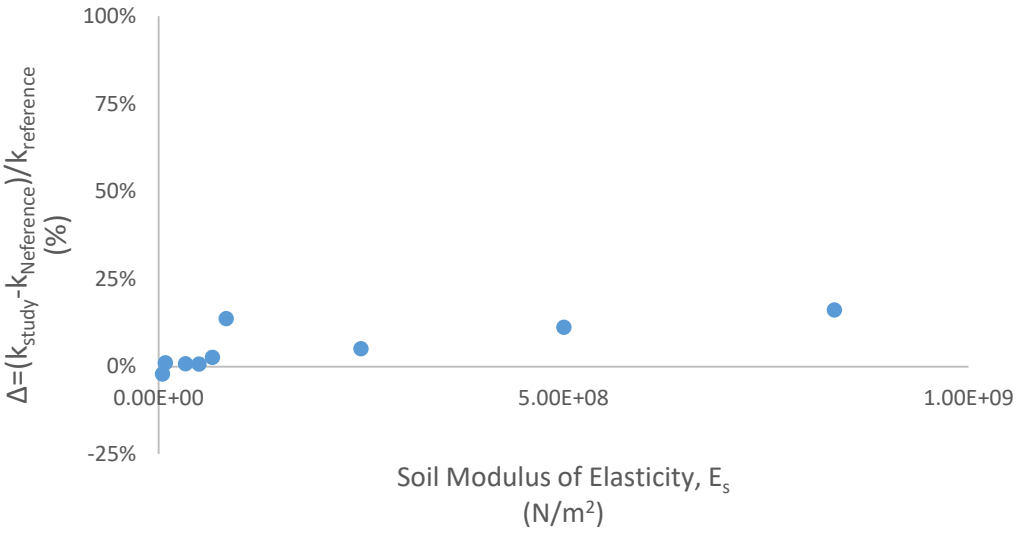

Figure 5.14: Relative difference of stiffness between 3D FEM and Gazetas & Mylonakis (1998) for a floating pile in homogeneous soil.

Comparing the stiffness with Gazetas & Mylonakis (1998) shows very good agreement with that calculated by finite element solution. The relative difference is between $-2\%\ to\ 16.5\%$. In general finite element analysis gives higher values for stiffness than that calculated by Gazetas & Mylonakis (1998).

A solution given in Chowdhury & Dasgupta (2008) and is compared with the FEM results. The solution is a modification of Novak's solution for a rigid cylinder embedded in elastic soil Novak & Beredugo (1972). In this method, the stiffness for a friction pile is calculated as

$$k = \frac{G_S S_1 L_p}{2} \tag{5.12}$$

Where G_s is the soil shear modulus, L_p is the pile length and S_1 is calculated as

$$S_1 = \frac{9.553(1+\mu_s)}{\left(\frac{L}{R}\right)^{1/3}} \tag{5.13}$$

Values of stiffness calculated using this approach compared to finite element results computed by this study are shown in Figure 5.15 while the relative difference is shown in Figure 5.16. From Figure 5.16, it can be seen that the relative difference is low starting at -17% to -30% corresponding to soil modulus of elasticity of $5x10^6$ to 8.34x10^7. The relative difference then continues to increase until it reaches values of -56% to -73%. These results suggest that rigid cylinder assumption might be valid for values of relative rigidity, E_p/G_s greater than 700. Below this values Novak's (1974) solution for pile foundations and Gazetas & Mylonakis (1998) solutions are more agreeable with finite element data and that the pile can't be assumed to be rigid.

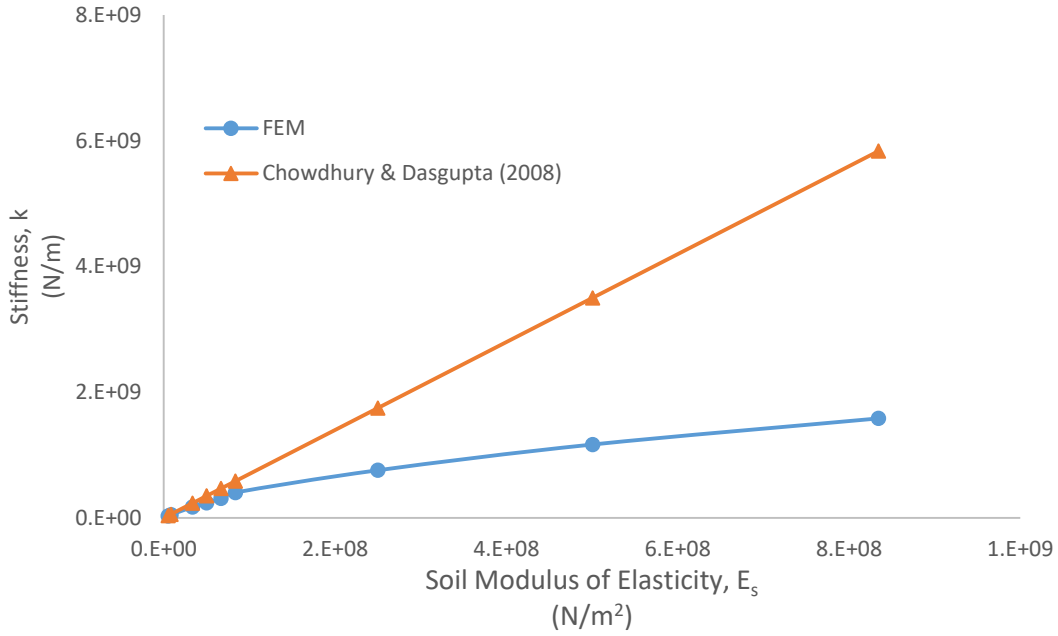

Figure 5.15: Comparison of stiffness obtained by finite element method with work of Chowdhury & Dasgupta (2008) for a floating pile in homogeneous soil.

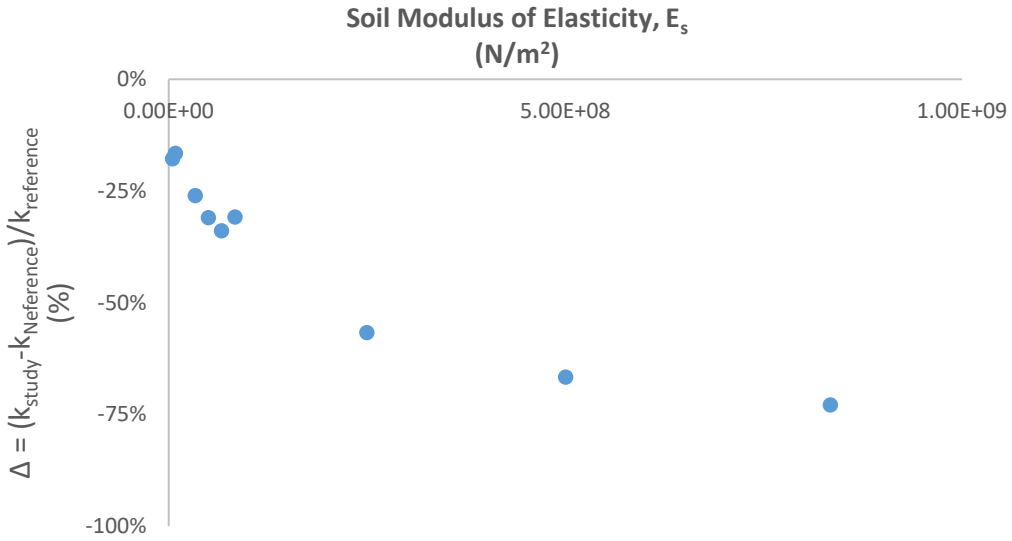

Figure 5.16: Relative difference of stiffness between 3D FEM and Chowdhury & Dasgupta (2008) for a floating pile in homogeneous soil.

5.1.2.2. Comparison of damping

The dynamic response of a pile under dynamic loading is governed by displacement amplification factor, u_d/u_s. This amplification factor describes how much is the static displacement is amplified or reduced at a certain frequency and it is function of the damping of the soil-pile system. Mathematically it can be obtained using the following Equation

$$\frac{u_d}{u_s} = \frac{1}{\sqrt{\left(1 - \frac{f^2}{f_n^2}\right)^2 + 4D^2\frac{f^2}{f_n^2}}} \tag{5.14}$$

Where f is the frequency at which amplification is calculated, f_n is the natural frequency of the system and D is the damping ratio defined as c/c_{cr}. Where c is the damping and c_{cr} is the critical damping of the pile-soil system. The variation of D with soil modulus of elasticity obtained by finite element solution is given in Figure 5.3. Comparison of the damping ratio obtained by finite element method and by Novak is given in Figure 5.17 while relative difference is shown in Figure 5.18. it can be seen from Figure 5.17 that the pattern of variation is similar taking the form of a decay power function. The difference between the two methods starts high at around 90% but then decreases to below 20% at high soil modulus of elasticity. To understand the origin of this difference, the differences of the critical damping component of the geometric damping ratio is studied.

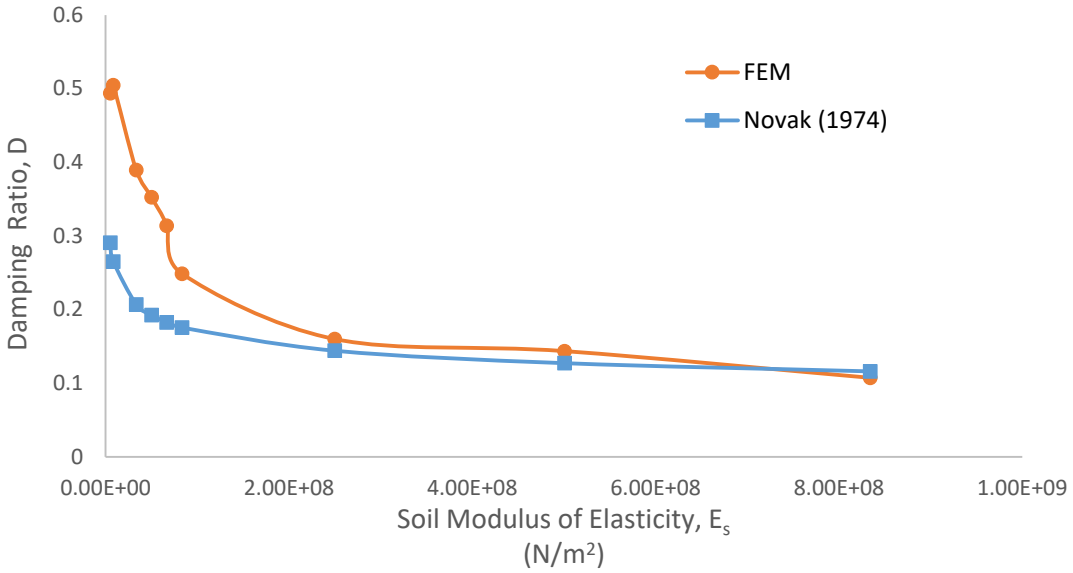

Figure 5.17: Comparison between damping ratio, *D* results Obtained by Finite element method and Novak (1974) for a floating pile in homogeneous soil.

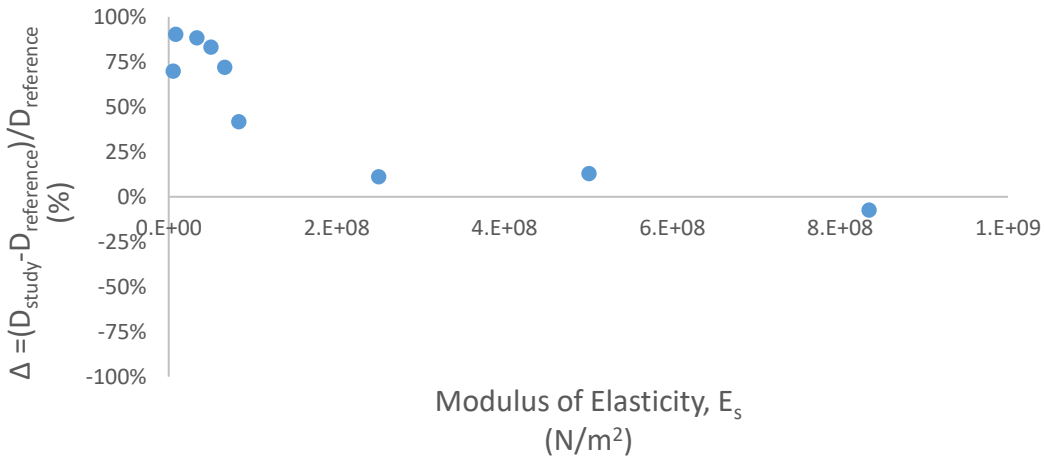

Figure 5.18: Relative difference between Damping ratio, *D* obtained by FEM and by Novak (1974) for a floating pile in homogeneous soil.

Figure 5.19 shows a comparison of critical damping results and 5.20 for relative difference between the results of Novak and the finite element analysis. The difference here would be inherited from the difference in the stiffness since the critical damping is directly dependent on the value of the stiffness. The critical damping difference was 40% but a better agreement is obtained at stiff soils. The greater difference in critical damping values at soft soils might explain the higher difference in damping ratio at the same range of soil properties.

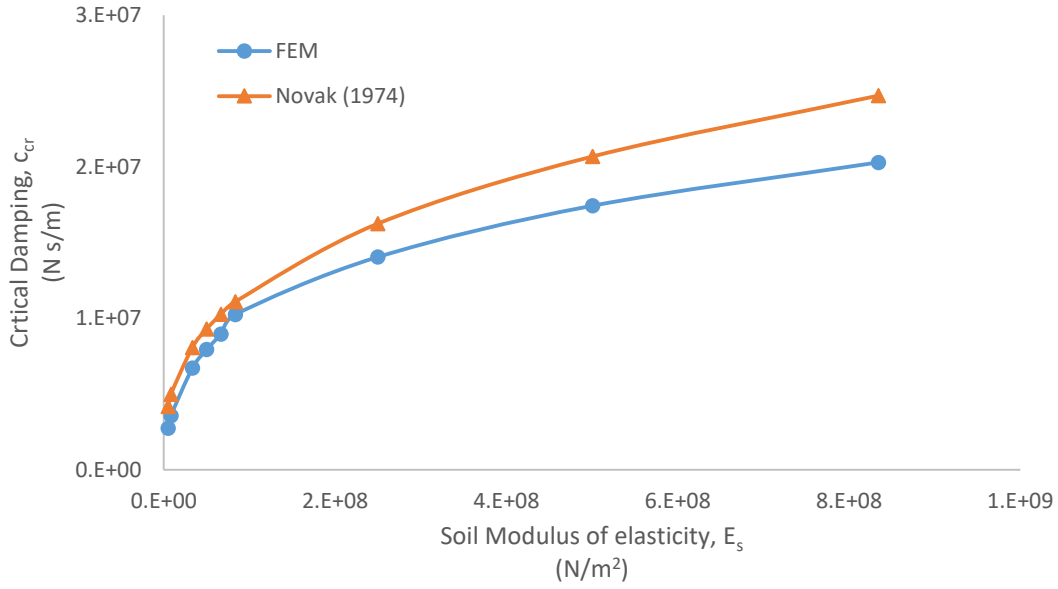

Figure 5.19: Comparison between critical damping results obtained by FEM and Novak (1974) for a floating pile in homogeneous soil.

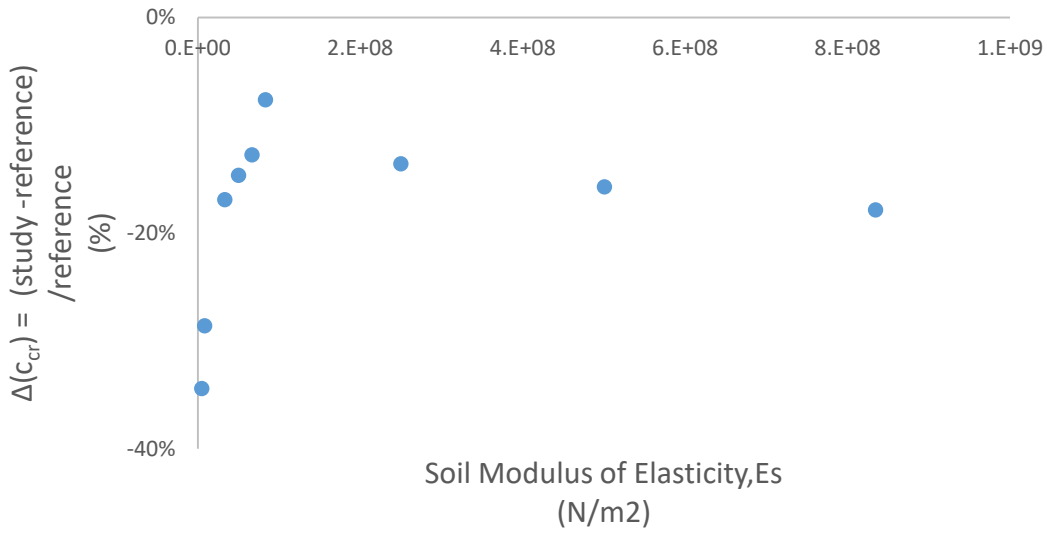

Figure 5.20: Relative difference between critical damping, c_{cr} obtained by FEM and by Novak (1974) for a floating pile in homogeneous soil.

Overall comparison between the two approaches (finite element method and Novak (1974) provided in the form of predicted dynamic displacement value at frequency range used in this research is shown in Figure 5.21. Predicted dynamic displacement values are shown on the y-axis of Figure 5.21 while the dimensionless frequency is shown on the x-axis. The relative difference between both approaches is provided in Figure 5.22. From both Figures, it can be seen that good agreement between the two approaches in predicting dynamic displacement is obtained at values of dimensionless frequency, a_0 greater than 0.2 with relative difference being lower than 20%. In Figure 5.22 as the relative difference between finite element results and Novak's solution is very high at 60% when the dimensionless frequency, a_0 is less than 0.1. The relative difference decreases to values 32% or less at frequencies between 0.1 and 0.2. The difference is less than 20% at $a_0 >$ 0.3. Differences in these two parameters might be contributed to assumptions made by Novak in order to obtain an analytical solution. These assumption as mentioned

earlier are 1) reducing a 3D problem to a 2D plane strain condition. 2) assuming that the stiffness at the tip is similar to that obtained by a loaded circular area on the surface of an elastic half space. Of course the soil at the pile tip is far from being on the surface and will interact with the soil around the pile and above it while supporting the pile.

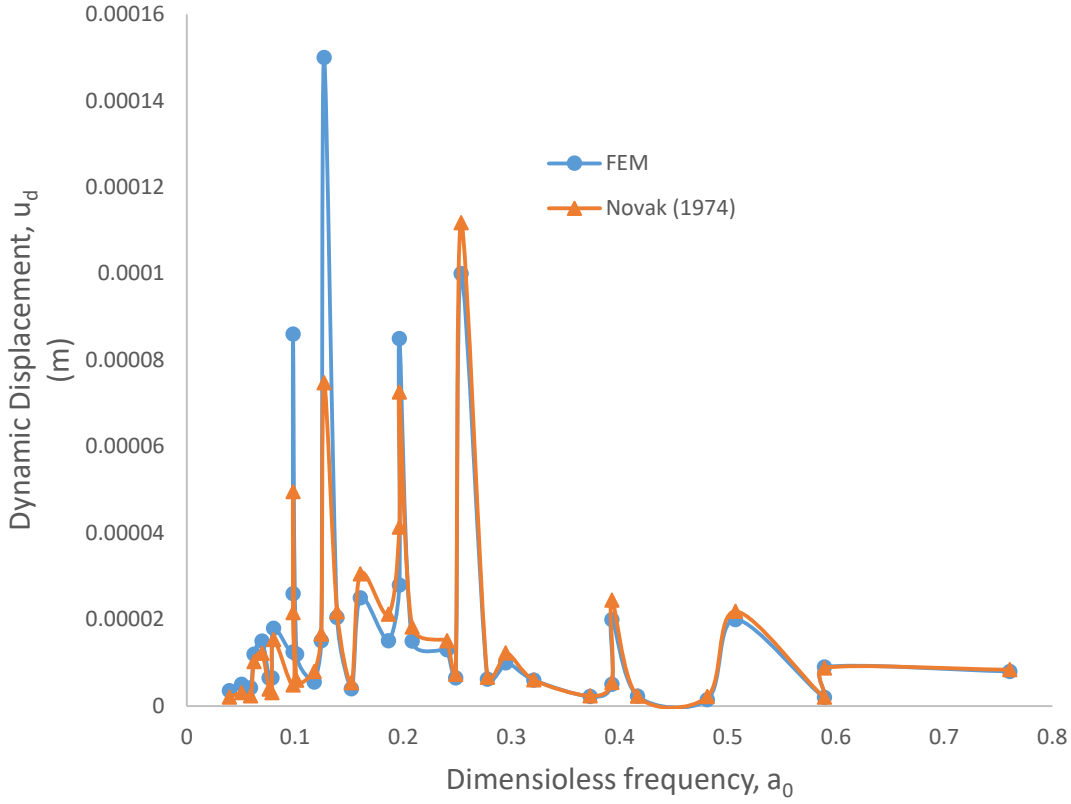

Figure 5.21, Comparison of predicted dynamic displacement values, u_d obtained by finite element method and Novak (1974) for a floating pile in homogeneous soil.

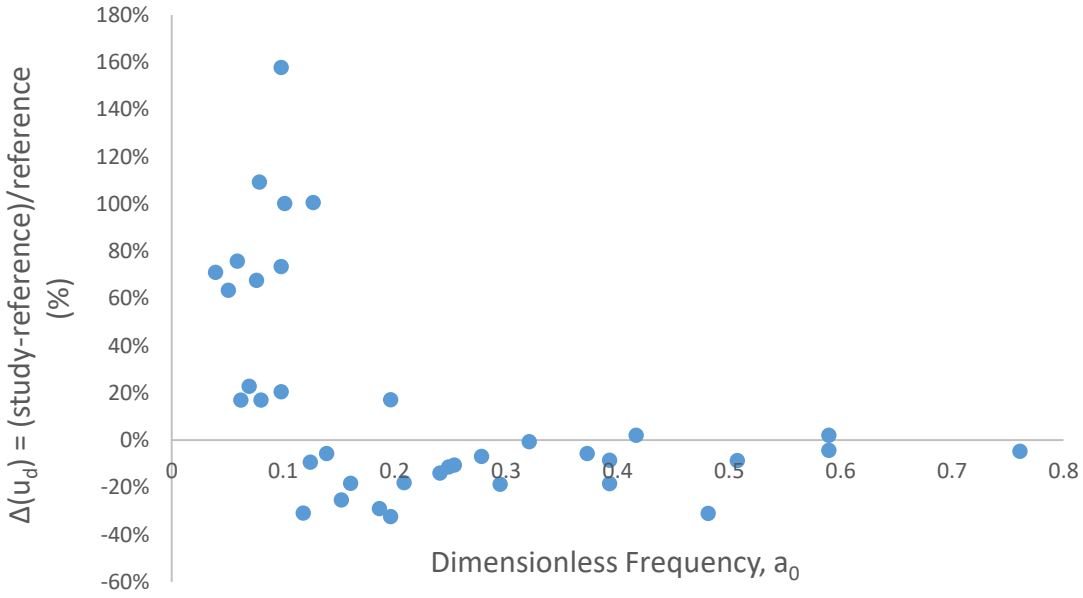

Figure 5.22: Relative difference of dynamic displacement values predicted by finite element method and Novak (1974) for a floating pile in homogeneous soil.

Another comparison of the damping ratio is provided against the work of Chowdhury & Dasgupta (2008) which assumes that the pile acts as a rigid cylinder and is shown in Figure 5.23. it can be shown that there is a wide gap between the two. Damping ratio calculated by Chowdhury & Dasgupta (2008) is under-predicted with values of damping ratio being around 0.04. This is largely due to a low calculated damping and very high critical damping calculated using the method suggested by Chowdhury & Dasgupta (2008). The difference can be seen in Figure 5.24.

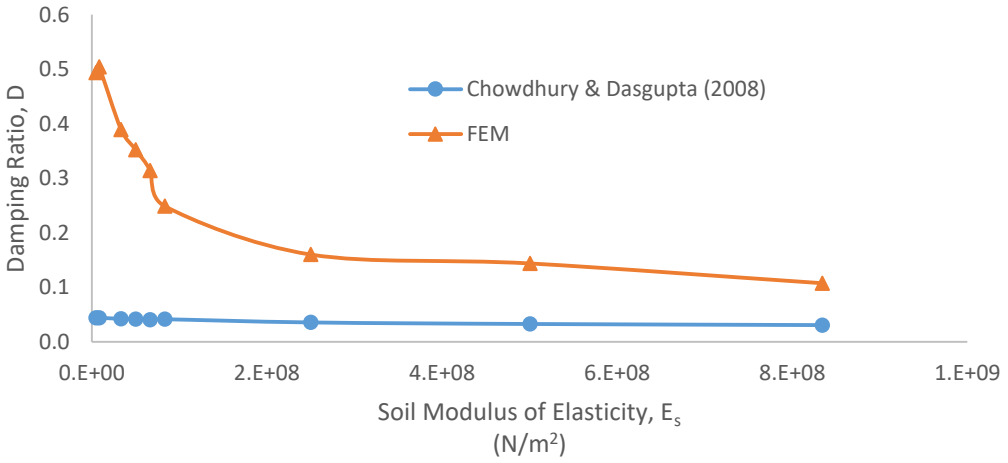

Figure 5.23 Comparison of damping ratio, *D* results Obtained by FEM and Chowdhury & Dasgupta (2008) for a floating pile in homogeneous soil.

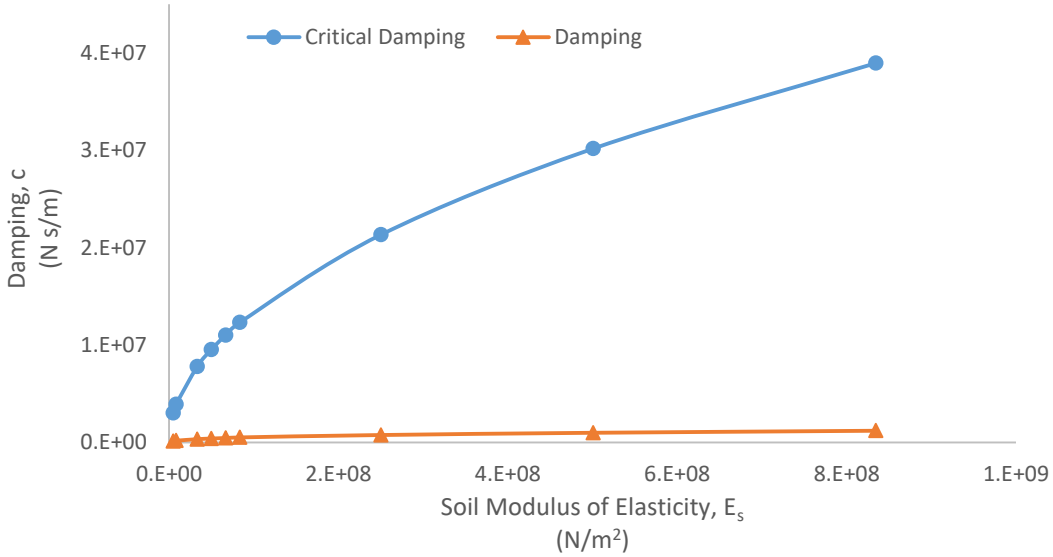

Figure 5.24: Showing great difference between damping and critical damping obtained by Chowdhury & Dasgupta (2008) for a floating pile in homogeneous soil.

The damping, c of rigid cylinder in soil is also calculated by Dobry (2014) . It gives a good agreement with damping, c calculated by finite element method in this research in soft soil. See Figure 5.25. the damping obtained by Dobry (2014) Continue to increase and deviate away from finite element results. Dobry (2014) values are obtained assuming pile acts as a rigid cylinder embedded in an elastic half space. Again the rigid cylinder assumption is not always valid for pile foundation subjected to dynamic loading.

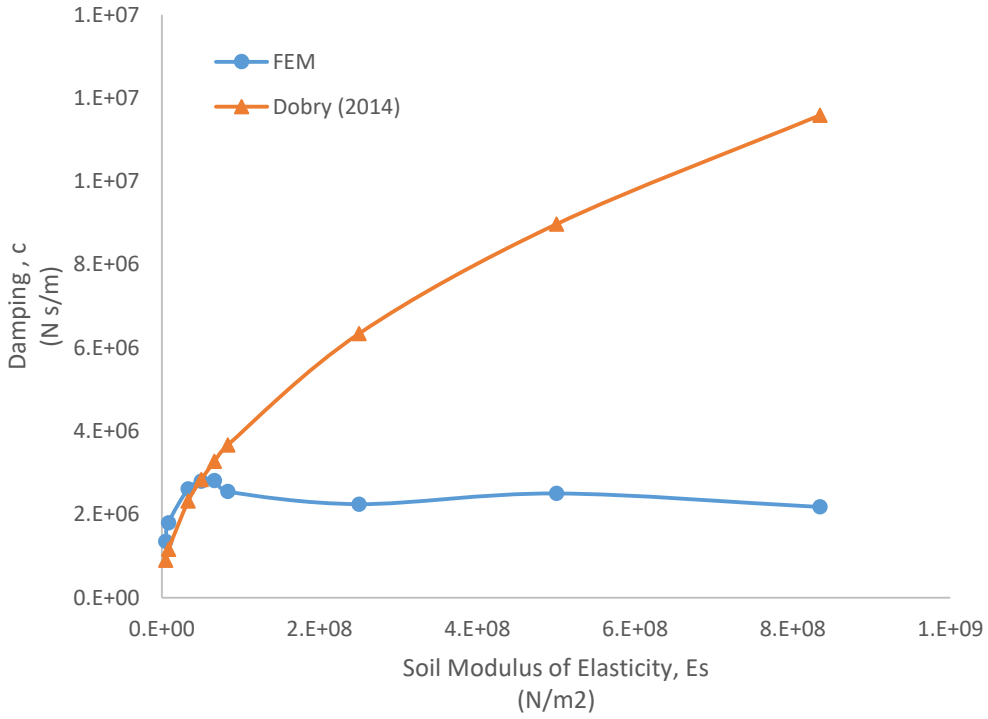

Figure 5.25: Comparison of damping, c obtained by FEM and Dobry (2014) for a floating pile in homogeneous soil.

5.2.Floating pile in nonhomogeneous soil

This is study of this research applies the finite element analysis to obtain the behavior of a floating pile foundation in nonhomogeneous soils. Non-homogeneity here means an increasing soil modulus of elasticity with depth at a rate referred to as S_{E_s} . This is to simulate field conditions where the shear wave velocity increases linearly with depth. This increase however stops at some depth, D_c within the soil. After this point the soil modulus of elasticity becomes constant and this modulus is referred to as E_{sc} The soil rate of increase in modulus of elasticity in this study is varied from 5.56×10^5 to 5.56×10^7 $N/m^2/m$ or $pascal/meter$. The increase stops at a point measured from the surface. The study captures the effect of the varied variables on the stiffness and damping of the pile.

The function describing this soil profile is described mathematically as

$$E_s(z) = \begin{cases} S_{E_s} z\,, & z \leq D_c \\ E_{sc}, & z > D_c \end{cases} \qquad (5.15)$$

In Equation 5.15, $E_s(z)$ is the function of soil modulus of elasticity at any depth, z. S_{E_s} is the rate of increase of soil modulus of elasticity with depth and D_c is the point after which the modulus of elasticity remains constant with depth and is equal to E_{sc}. Graphically this problem is shown in Figure 5.26. For a summary of varied and constant parameters see Table 5.2.

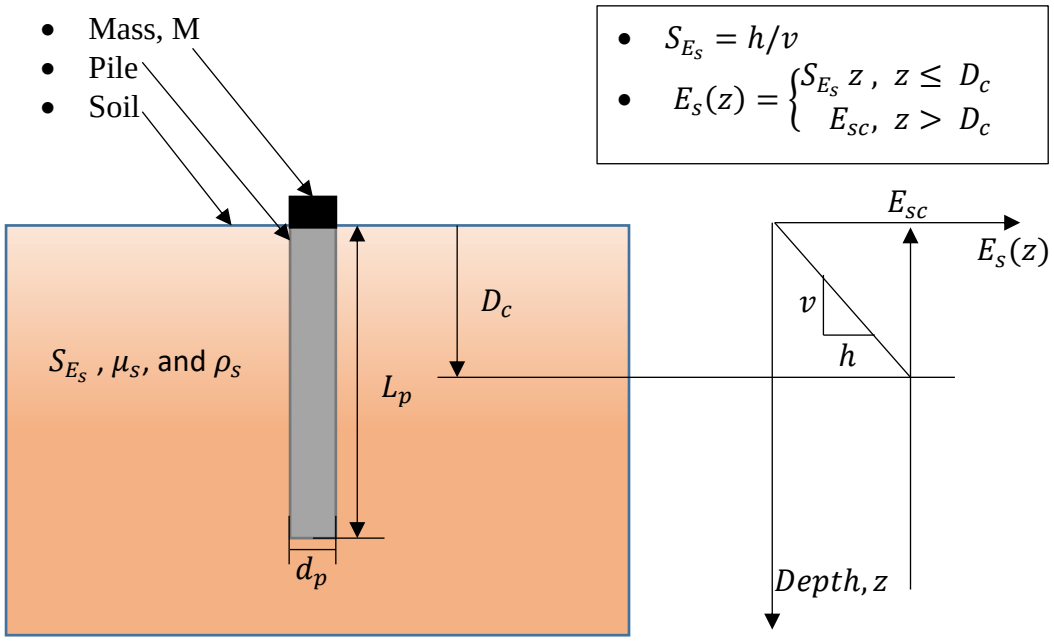

Figure 5.26: Floating pile in nonhomogeneous soil.

Table 5.2: Parameters used in study of pile in nonhomogeneous soil.

Parameter	Symbol	Unit	Value
Pile Modulus of Elasticity	E_p	$Pascal$	$2.1\text{x}10^{10}$
Pile Poisson's Ratio	μ_p		0.25
Pile Mass Density	ρ_p	kg/m^3	2500
Pile Diameter	d_p	m	0.5
Pile Length	L_p	m	10
Soil Modulus of Elasticity	$E_s(z)$	$Pascal$	Function of depth
Rate of Increase in E_s	S_{E_s}	Pascal/m	5.56×10^5 to 5.56×10^7
Point at which increase in E_s stops	D_C	m	$4\ to\ 10\ (0.4L_p\ to\ L_p)$
value of constant modulus of elasticity after D_c.	E_{sc}	$Pascal$	Depends on S_{E_s} and D_c
Soil Poisson's Ratio	μ_s		0.45
Soil Mass Density	ρ_s	kg/m^3	1800
Mass applied on top of Pile	M	kg	65000
Applied Static Pressure	Q_s	$Pascal$	22000
Dynamic Pressure Amplitude	Q_d	$Pascal$	22000
Frequency	f	Hz	$2.5\ to\ 30$

Two parameters are varied in this study, rate of increase in soil modulus of elasticity, S_{E_S} and the point at which E_s remains constant ($E_s(z) = E_{sc}$). The main outcomes of this study are the system stiffness, k and damping ratio, D. The stiffness, k is shown in Figure 5.27 plotted against S_{E_S} while plotted against D_C/L_p in Figure 5.28. The damping ratio is plotted against S_{E_S} in Figure 5.29 and against D_C/L_p in Figure 5.30. from stiffness and damping ratio, the critical damping, the damping and natural frequency can be calculated. They are shown in Figures 5.31, 5.32 and 5.33 respectively.

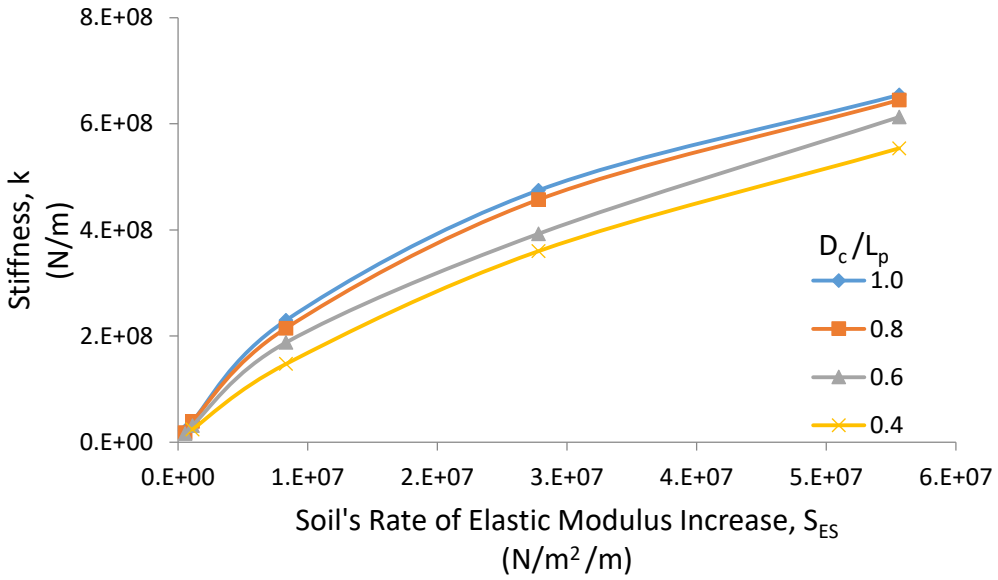

Figure 5.27: Variation of stiffness, k with soil's rate of increase in elastic modulus, S_{E_S} for a floating pile in nonhomogeneous soil.

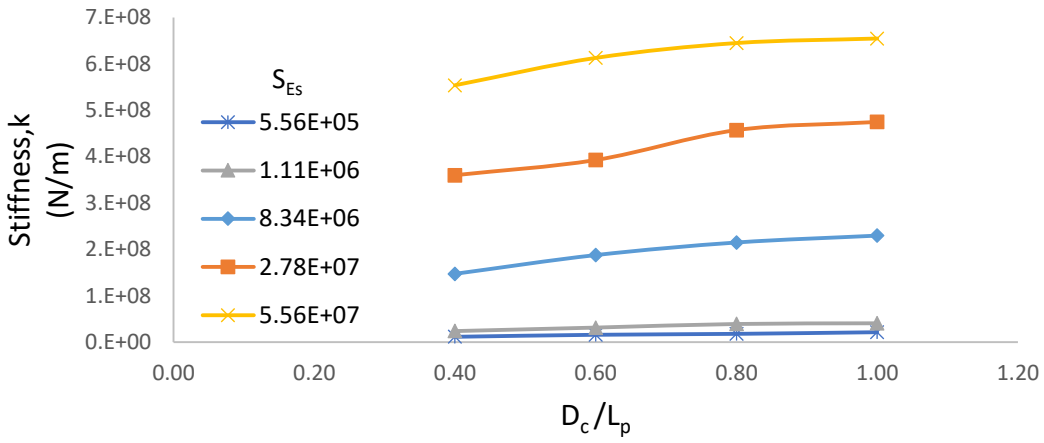

Figure 5.28: Variation of stiffness, k with D_C/L for a floating pile in nonhomogeneous soil.

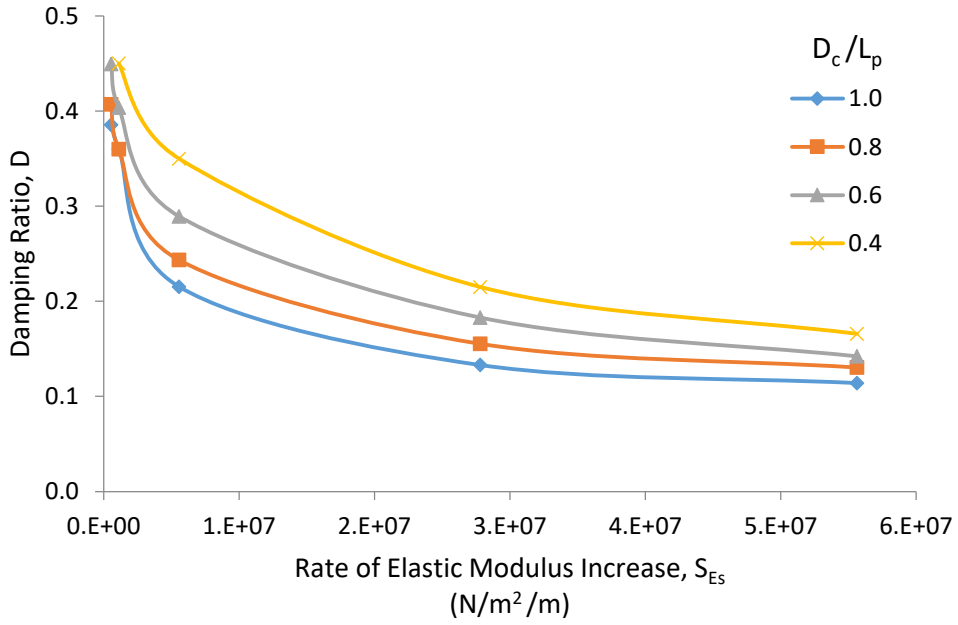

Figure 5.29: Variation of Damping Ratio, D with soil's rate of increase in elastic modulus, S_{E_S} for a floating pile in nonhomogeneous soil.

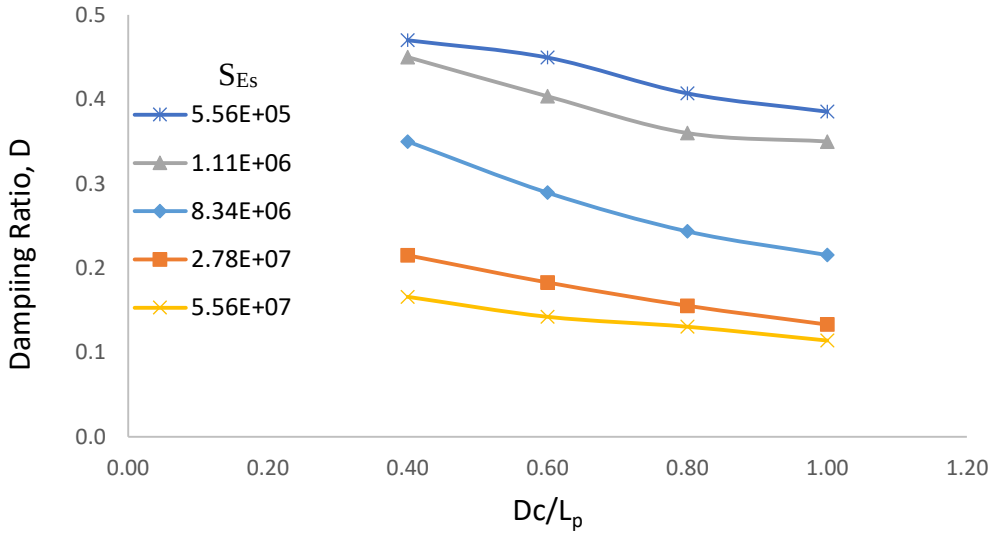

Figure 5.30: Variation of Damping, D Ratio withD_c/L for a floating pile in nonhomogeneous soil.

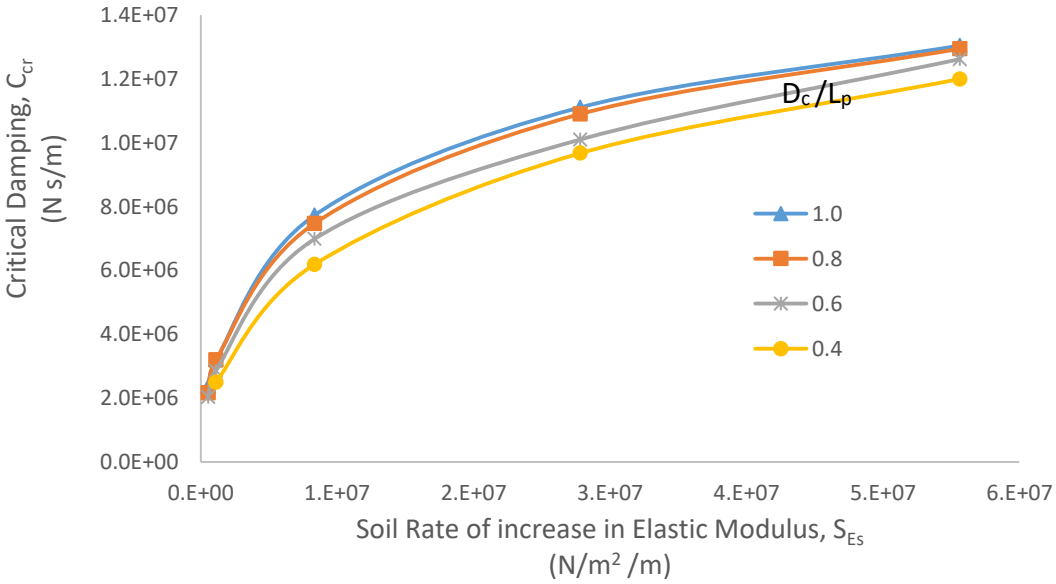

Figure 5.31: Variation of critical damping, c_{cr} with soil rate of increase in elastic modulus, S_{E_S} for a floating pile in nonhomogeneous soil.

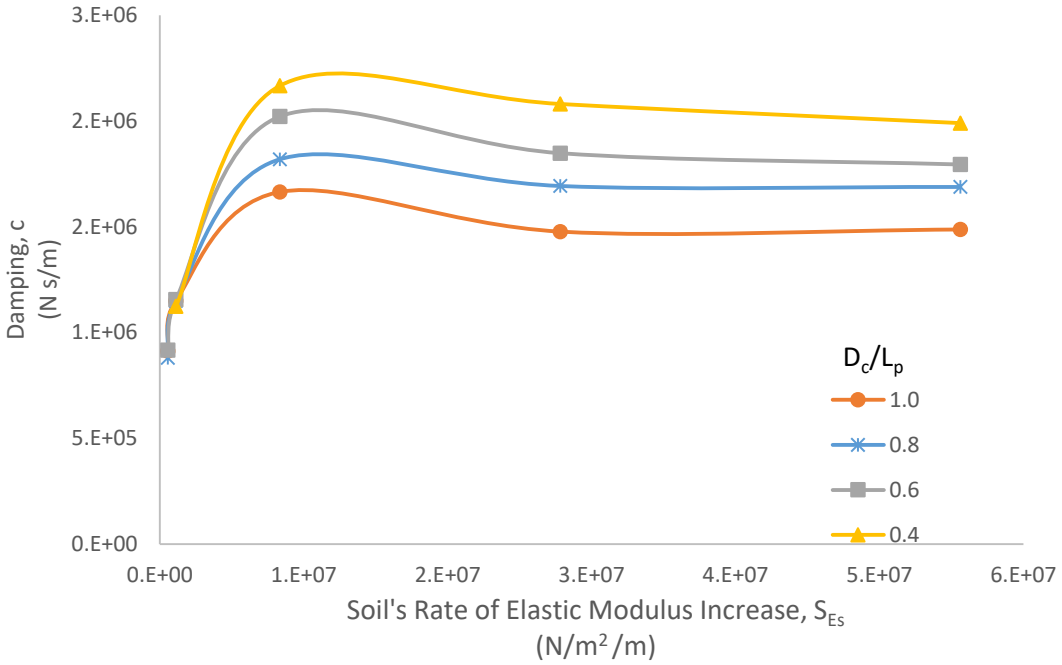

Figure 5.32: Variation of damping, c with soil rate of elastic modulus for a floating pile in nonhomogeneous soil.

5.2.1. Results commentary and analysis

- Increase in stiffness in a nonlinear manner is observed with increase in soil S_{E_s}, where S_{E_s} is the rate of increase of soil modulus of elasticity. The greater the value of S_{E_s} the stronger the soil is, which means that the soil can provide greater support to the applied load at lower displacement. The trend is the same for all values of D_c/L_p in Figure 5.27. It is also observed from Figure 5.27 that at higher values of D_c/L_p the stiffness is higher. This is because higher values of D_c/L_p means that soil modulus of elasticity continues to increase to a greater depth along the pile shaft and stronger stiffness is provided as a result. This trend is observed in Figure 5.28. It can be seen that the stiffness at certain slope,

S_{E_S} is low at low values of D_c/L_p and gets higher for higher values of D_c/L_p. The change in k with D_c/L_p increases in a linear manner

- Damping as plotted in Figure 5.29 seems to decrease with the increase in S_{E_s} values with a power decay function. Damping ratio decreases with D_c/L_p in a linear manner.
- Analysis of stiffness, k and damping ratio, D shows a trend of increasing stiffness and decreasing damping ratio with stiffening soils.. This means increasing natural frequency value and increase in dynamic amplification at this natural frequency with increase in soil S_{E_S} (Note that higher S_{E_s} means more stiff soil). See Figure 5.33 for dynamic displacement values at resonance and Figure 5.34 for amplification factor at the natural frequency.

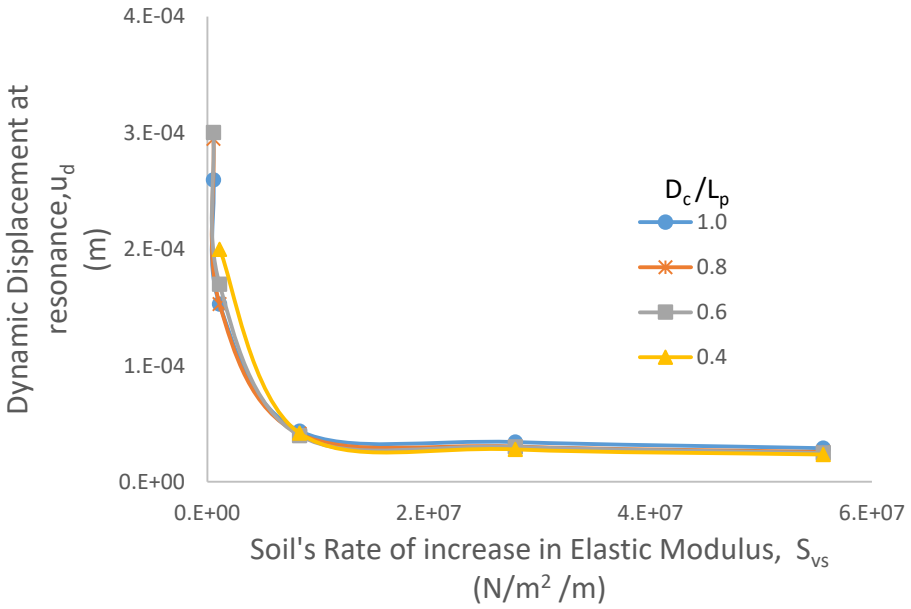

Figure 5.33: Variation of dynamic displacement, u_d at natural frequency with S_{E_s} for a floating pile in nonhomogeneous soil.

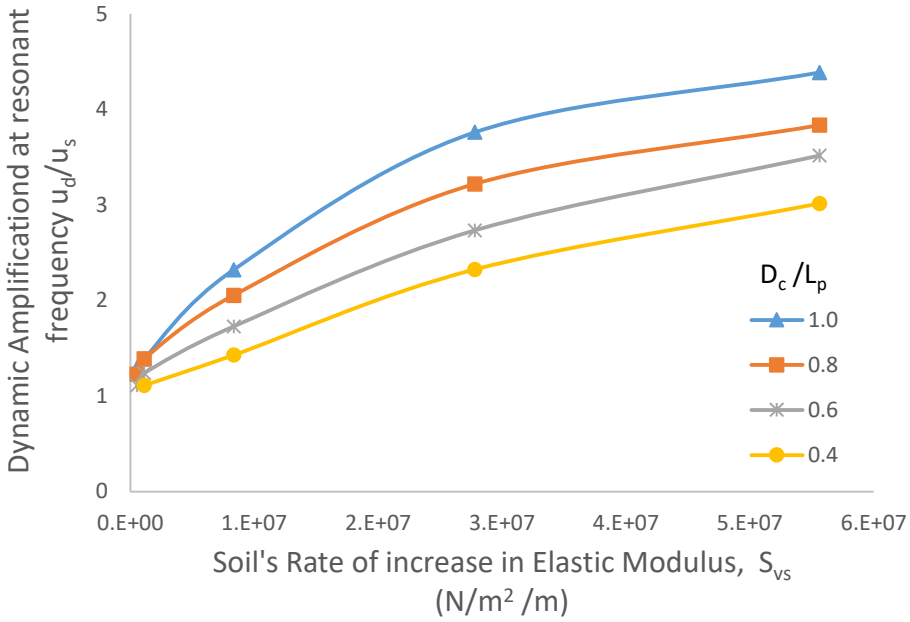

Figure 5.34: Variation of dynamic amplification u_d/u_s at natural frequency with S_{E_s} for a floating pile in nonhomogeneous soil.

- It can be seen from Figure 5.34 that variation of the depth of the point at which soil elastic modulus remains constant, D_c has little effect on the actual value of dynamic displacement but more effect on the amplification of static displacement, u_d/u_s at resonance as shown in Figure 5.35. This means that D_c has little effect on stiffness and more effect on damping.
- From Figure 5.31, it is shown that the critical damping increase with the increase in soil stiffness. This is expected since it is mathematically related to the stiffness of the system as described by Equation 5.1.
- From Figure 5.32, it is shown that the damping which is obtained by multiplying the damping ratio with the critical damping increase with soil stiffness up to a certain point. After this point, the damping seems to be constant.

- The natural frequency in Hz increases with increase in S_{E_s}as shown in Figure 5.35.

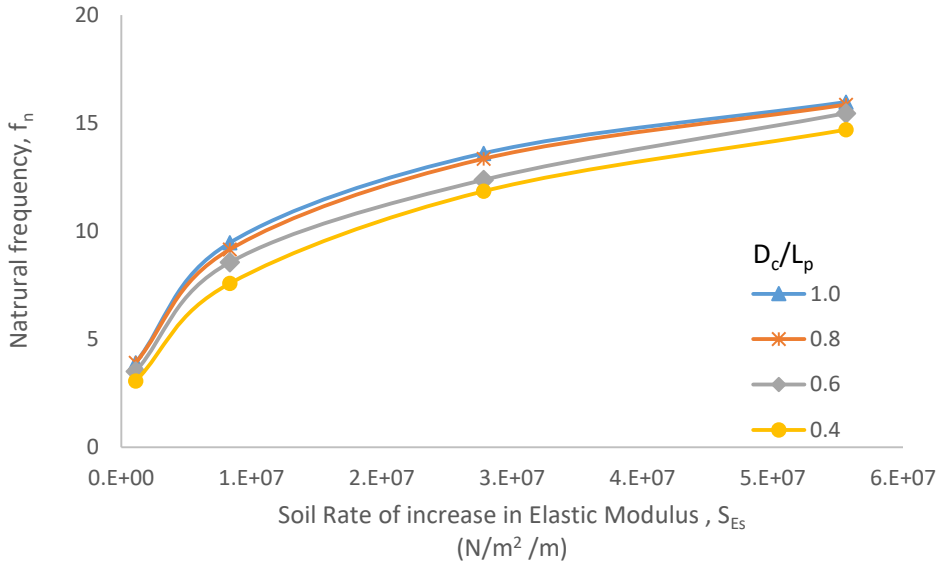

Figure 5.35:Variation of natural frequency, f_n with S_{E_s} for a floating pile in nonhomogeneous soil.

- Another way to look at results of this study is the effect of inhomogeneity ratio, D_c/L_p on stiffness and damping of a single pile. If D_c/L_p = 0, the pile is in homogeneous soil, as D_c/L_p increases, inhomogeneity depth increases. The effect of inhomogeneity on stiffness is shown in Figure 5.36, while effect of inhomogeneity on damping is shown in Figure 5.37.

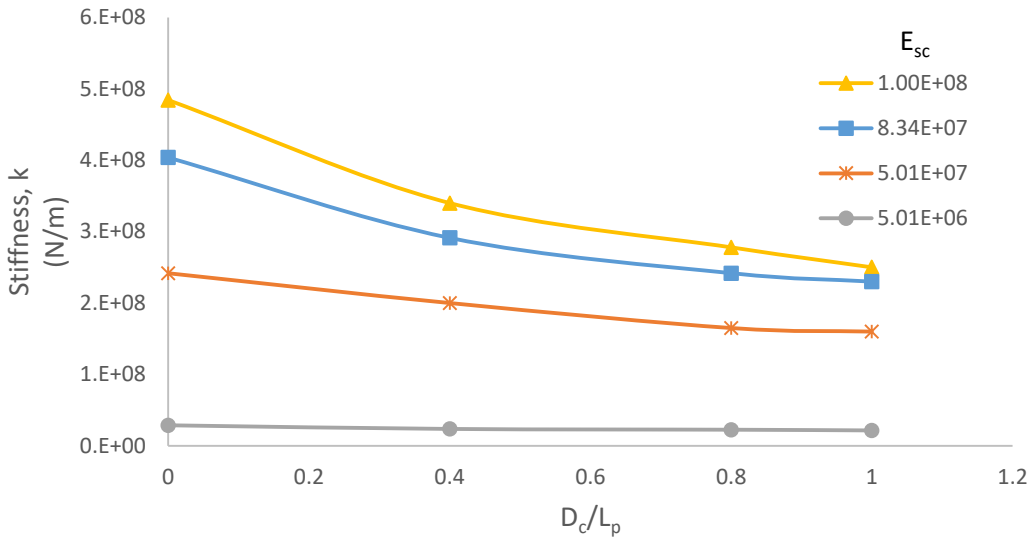

Figure 5.36: Effect of inhomogeneity on stiffness for a floating pile in a nonhomogeneous soil. Note: $D_c/L_p = 0$ means pile in homogeneous soil.

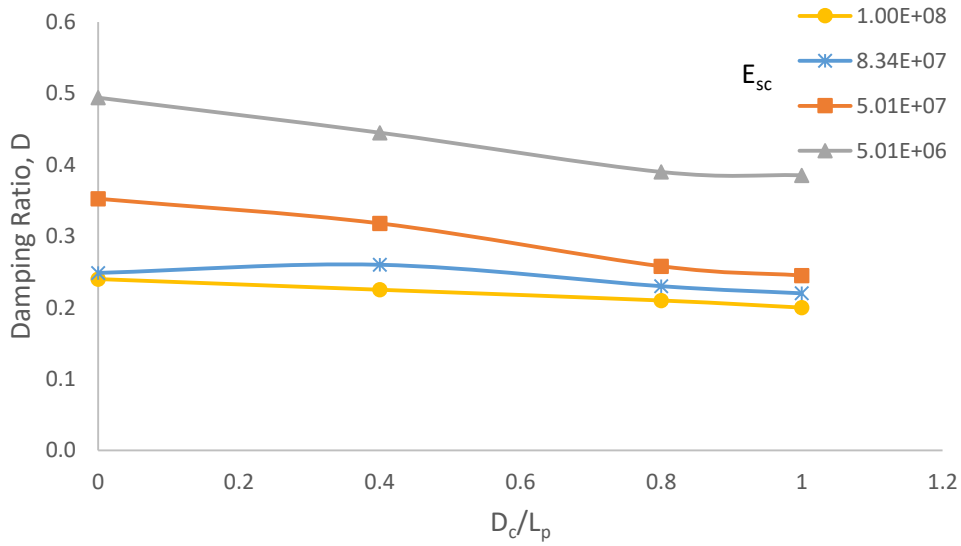

Figure 5.37: Effect of inhomogeneity on stiffness for a floating pile in a nonhomogeneous soil. Note: D_c/L_p= 0 means pile in homogeneous soil.

- From Figure 5.36 and Figure 5.37, it can be seen that both stiffness and damping decrease with increase of inhomogeneity ratio, D_c/L_p compared to a pile in homogeneous soil ($D_c/L_p = 0$).

5.2.2. Comparison of finite element solution results with literature

Floating piles in a nonhomogeneous soil can be analyzed using a simplified one-dimensional finite element approach similar to that described in section 2.3.1 of the dissertation. A program was created using Mathematica® (a programming environment). Details of the program and its code are given in Appendix B of this dissertation while the concept of the approach is described in Section 2.3.1 of this dissertation. The pile was modeled as a 10 segments bar and average shear modulus was calculated at the side at different segments. Side springs and dampers coefficients can be obtained by the following Equations by Randolph & Simons (1986)

$$k_s = \frac{1.375\, G_s}{\pi r_p} \tag{5.16}$$

$$c_s = \frac{G_s}{v_s} \tag{5.17}$$

Where k_s is the side spring coefficient, c_s is the side damper coefficient, G_s is the shear moduls of the soil at the spring location, r_p is the pile radius, and v_s is the shear wave velocity of the soil and is equal to $\sqrt{G_s/\rho_s}$. Where ρ_s is the mass density of the soil.

The base and damper coefficients are obtained using the following equations by Randolph & Simons (1986) are used

$$k_b = \frac{4G_s r_p}{1-\mu_s} \tag{5.18}$$

$$c_b = \frac{3.4 r_p^2}{1-\mu_s}\rho_s v_s \tag{5.19}$$

Where k_b is the base spring coefficient, c_b is the base damper coefficient, G_s is the soil shear modulus, r_p is the pile radius, μ_s is Poisson's ratio, ρ_s is the soil mass density and v_s is the shear wave velocity of the soil. For a graphical representation of the problem of pile modeled as beam with side and base springs and dampers describing soil behavior. See Figure 5.38.

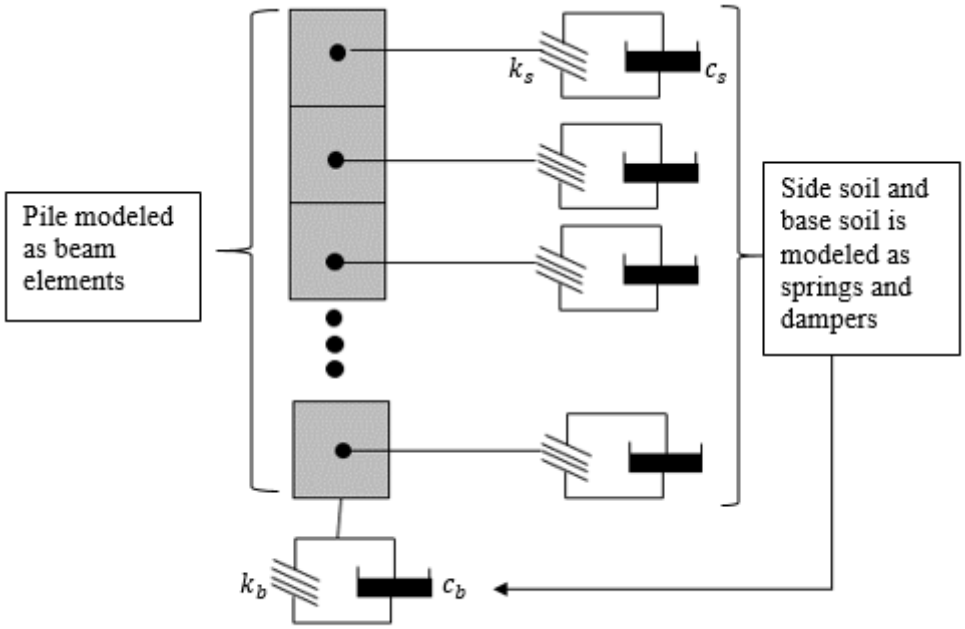

Figure 5.38: Pile modeled as beam segments and soil modeled as springs and dampers.

5.2.2.1. Comparison of stiffness

Comparison of stiffness calculated by 3D finite element and that calculated by 1D Finite element as described in Section 5.2.2 is shown in Figures 5.39, 5.40, 5.41 and 5.42. Summary of numerical results of the comparison is shown in Table 5.3. Good agreement is found between the two approaches in calculating stiffness.

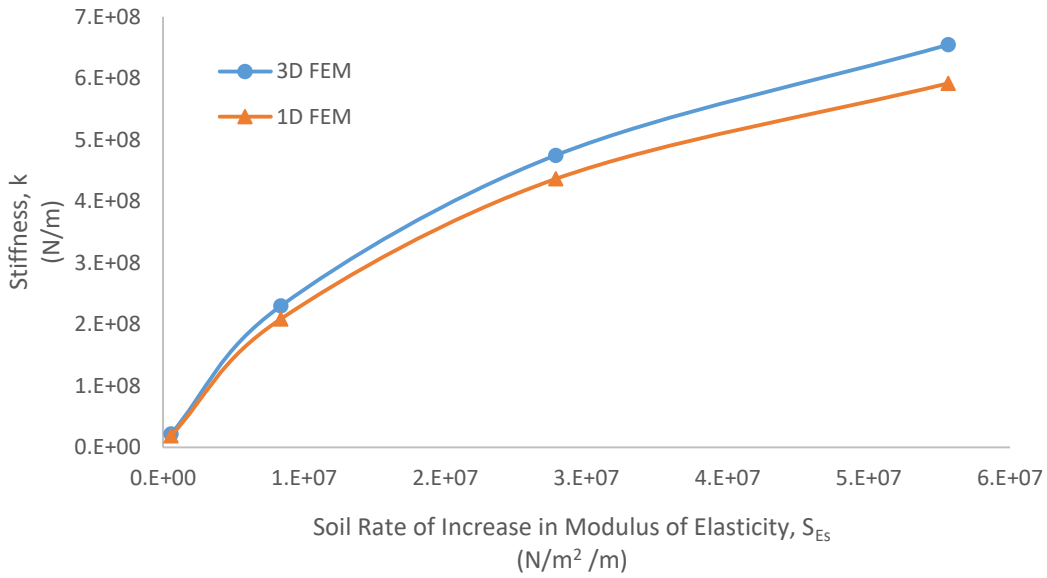

Figure 5.39: Comparison of stiffness for a floating pile in nonhomogeneous soil calculated by 3D FEM and 1D FEM for $D_c/L_p = 1$.

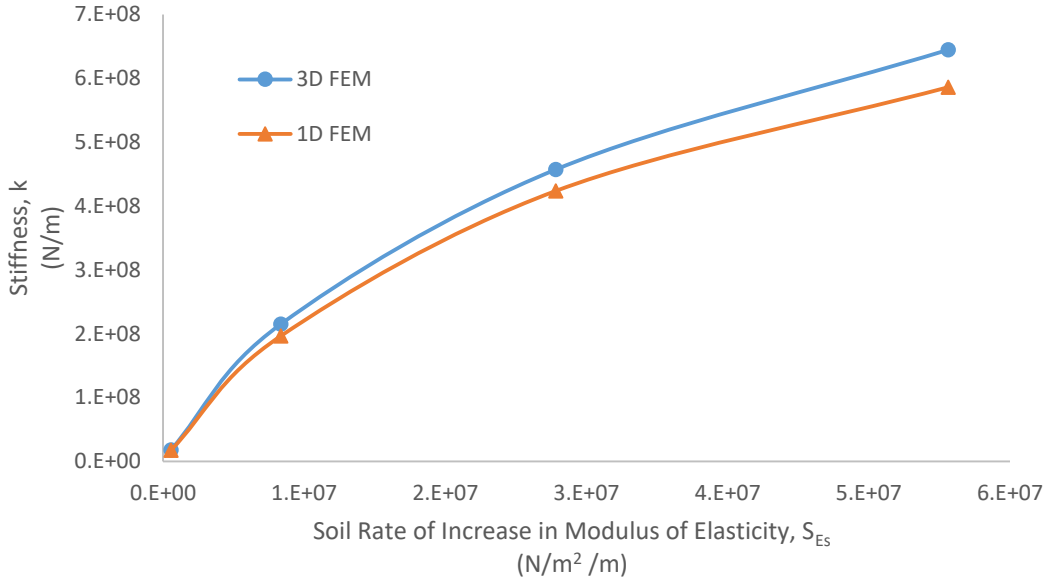

Figure 5.40: Comparison of stiffness for a floating pile in nonhomogeneous soil calculated by 3D FEM and 1D FEM for $D_c/L_p = 0.8$.

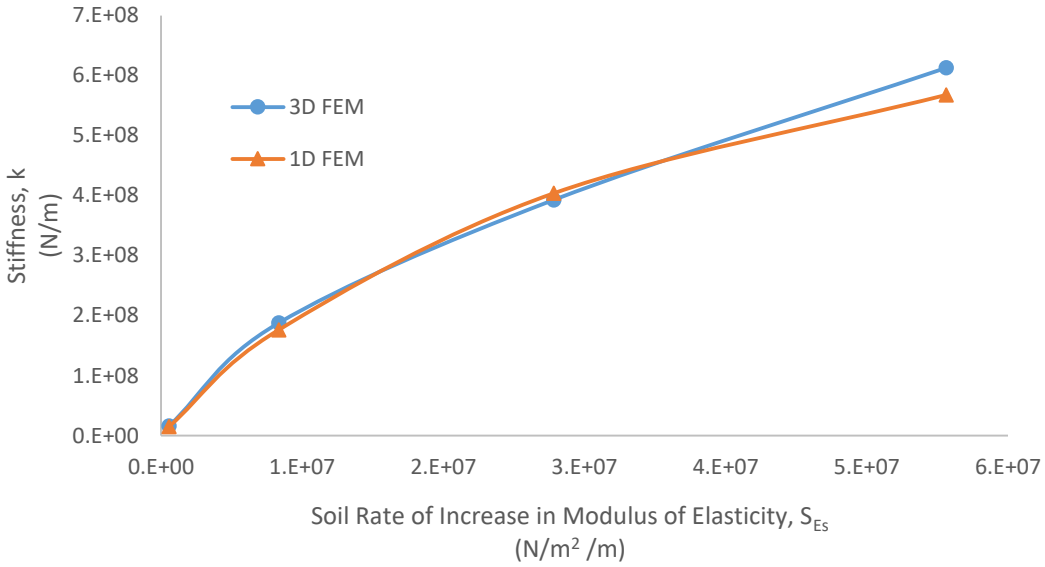

Figure 5.41: Comparison of stiffness for a floating pile in nonhomogeneous soil calculated by 3D FEM and 1D FEM for $D_c/L_p = 0.6$.

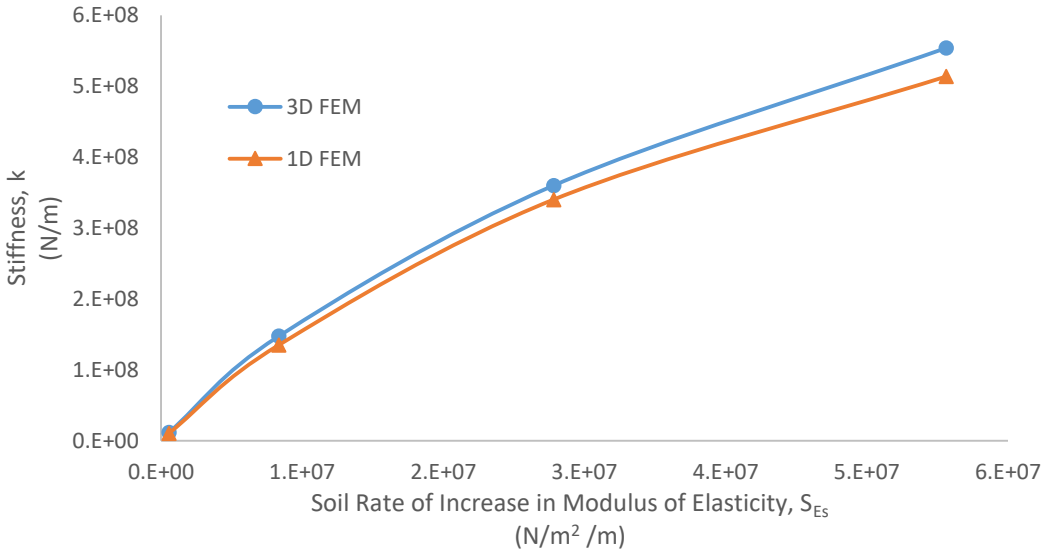

Figure 5.42:Comparison of stiffness for a floating pile in nonhomogeneous soil calculated by 3D FEM and 1D FEM for $D_c/L_p = 0.4$.

5.2.2.2. Comparison of damping

Comparison of geometric damping calculated by 3D finite element and that calculated by the 1D Finite element analysis is shown in Figures 5.43, 5.44, 5.45 and 5.46. Summary of numerical results of the comparison is shown in Table 5.3. Damping is significantly underpredicted by the 1D finite element method.

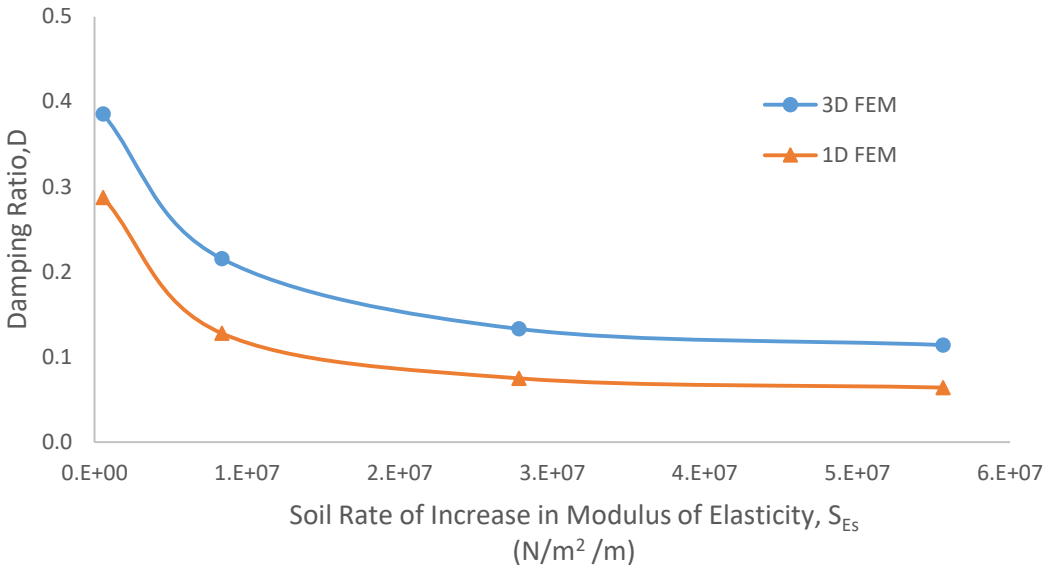

Figure 5.43: Comparison of damping ratio for a floating pile in nonhomogeneous soil calculated by 3D FEM and 1D FEM for $D_c/L_p = 1$.

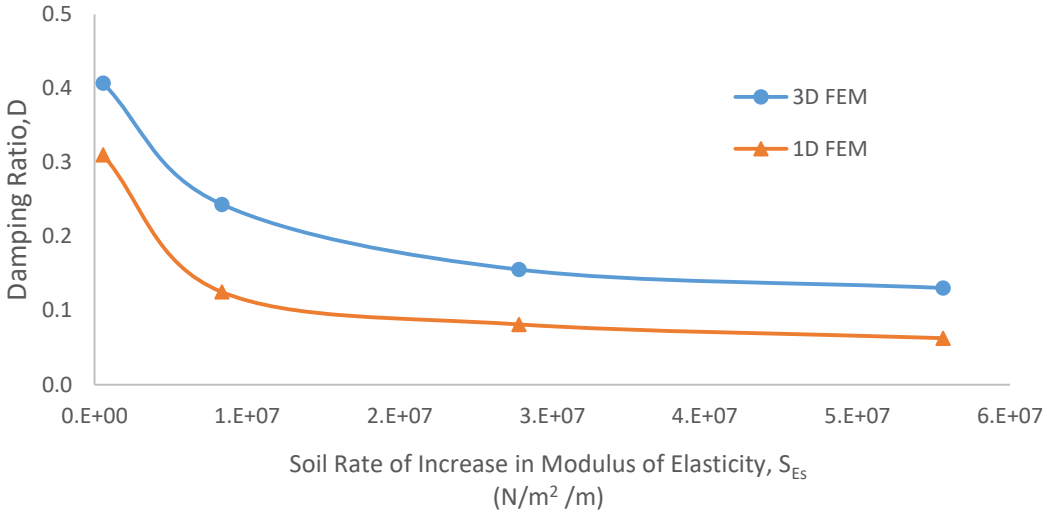

Figure 5.44: Comparison of damping ratio for a floating pile in nonhomogeneous soil calculated by 3D FEM and 1D FEM for $D_c/L_p = 0.8$.

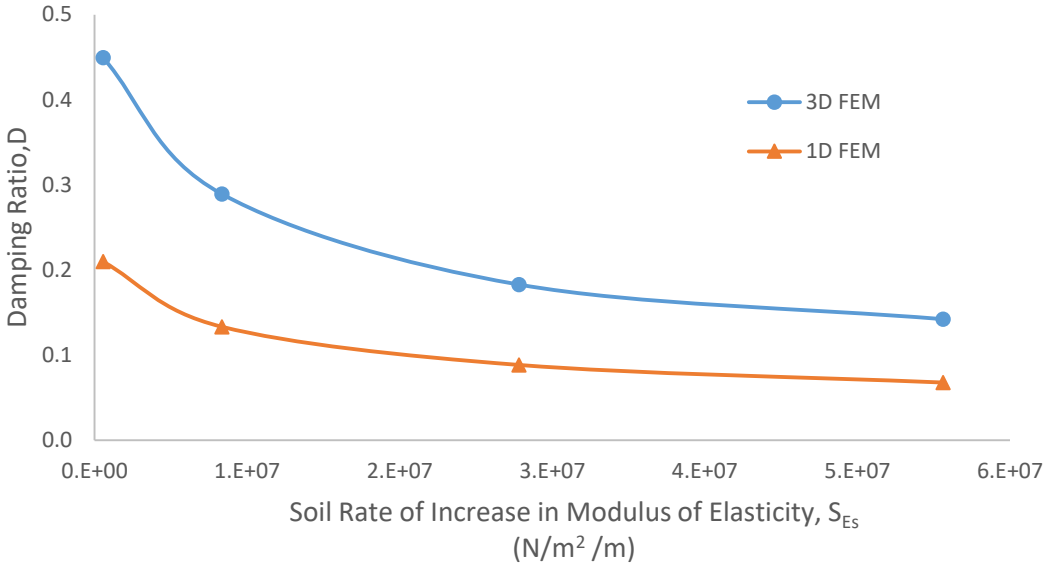

Figure 5.45: Comparison of damping ratio for a floating pile in nonhomogeneous soil calculated by 3D FEM and 1D FEM for $D_c/L_p = 0.6$.

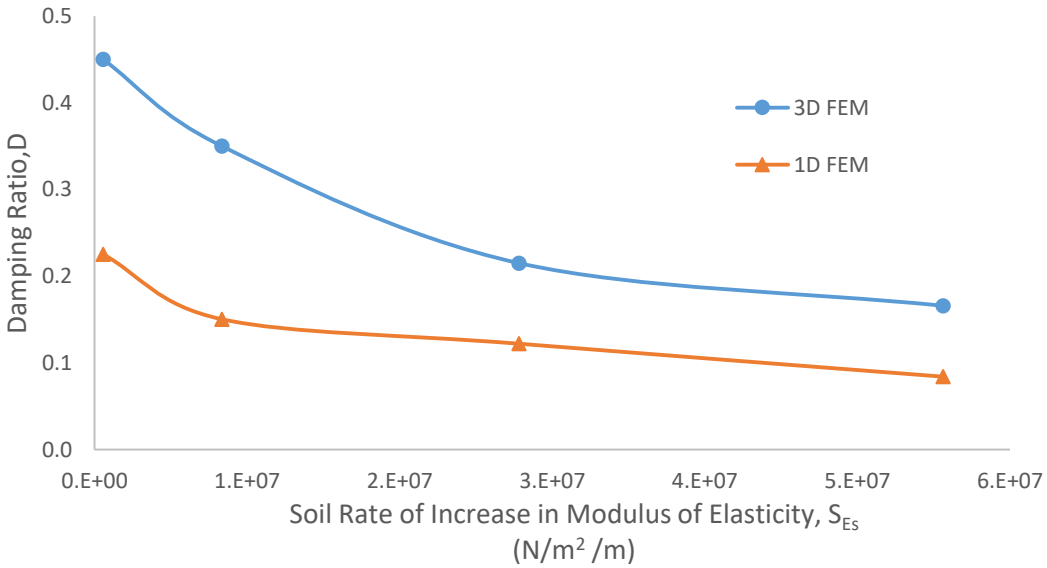

Figure 5.46: Comparison of geometric damping for a floating pile in nonhomogeneous soil calculated by 3D FEM and 1D FEM for $D_c/L_p = 0.4$.

Table 5.3: Numerical results for comparison between 3D and 1D FEM for a floating pile in nonhomogeneous soil.

		k	D	k	D	Δ(k)	Δ(D)
D_C/L_p	S_{E_S}	3D FEM	3D FEM	1D FEM	1D FEM	(%)	(%)
1	5.56E+05	2.16E+07	0.39	1.88E+07	0.29	15%	34%
	8.34E+06	2.30E+08	0.22	2.09E+08	0.13	10%	69%
	2.78E+07	4.75E+08	0.13	4.36E+08	0.07	9%	78%
	5.56E+07	6.54E+08	0.11	5.92E+08	0.06	11%	78%
0.8	5.56E+05	1.80E+07	0.41	1.74E+07	0.31	3%	31%
	8.34E+06	2.15E+08	0.24	1.96E+08	0.13	9%	95%
	2.78E+07	4.57E+08	0.16	4.23E+08	0.08	8%	91%
	5.56E+07	6.45E+08	0.13	5.86E+08	0.06	10%	108%
0.6	5.56E+05	1.60E+07	0.45	1.49E+07	0.21	7%	114%
	8.34E+06	1.88E+08	0.29	1.76E+08	0.13	7%	117%
	2.78E+07	3.93E+08	0.18	4.04E+08	0.09	-3%	107%
	5.56E+07	6.13E+08	0.14	5.68E+08	0.07	8%	110%
0.4	5.56E+05	1.17E+07	0.45	1.05E+07	0.23	11%	100%
	8.34E+06	1.47E+08	0.35	1.35E+08	0.15	9%	133%
	2.78E+07	3.60E+08	0.22	3.40E+08	0.12	6%	76%
	5.56E+07	5.54E+08	0.17	5.14E+08	0.08	8%	97%
					Average Δ->	0.08	0.90

5.3. End-bearing pile in homogeneous soil

In this study, a pile is supported by a firm rock base. Rock base experience deformation that is very low and assumed to be negligible compared to the pile deformation and deformation of the surrounding soil. Rocks have very high shear wave velocity ranging from 760 to $1500\ m/s$. With a density of about 2600 kg/m^3, the shear modulus of rock is between $1.502 \times 10^9\ N/m^2$ and $5.85 \times 10^9\ N/m^2$. The low strains shear modulus of rocks can reach 100 times that of soils. This makes rocks perform as a rigid base for the pile to rest on. For static load design, if the pile is supported on rock, its capacity is considered the actual structural capacity of the pile itself. Richart (1970) extended this assumption to dynamically loaded piles resting on rock. Richart (1970) assumed the pile to

perform as a fixed-free bar ignoring surrounding soil and any geometrical damping. This was presented in Section 2.2.2 of the dissertation. Novak (1974) provided damping and stiffness constants for end-bearing piles while considering surrounding soils. The problem of an elastic pile supported on rock base is shown in Figure 5.47. Constant and varied parameters are shown in Table 5.4. The finite element model of this problem uses fixed boundaries at the base to simulate non deforming rock base. The study captured the effect of the varied variables on the stiffness and damping of the pile.

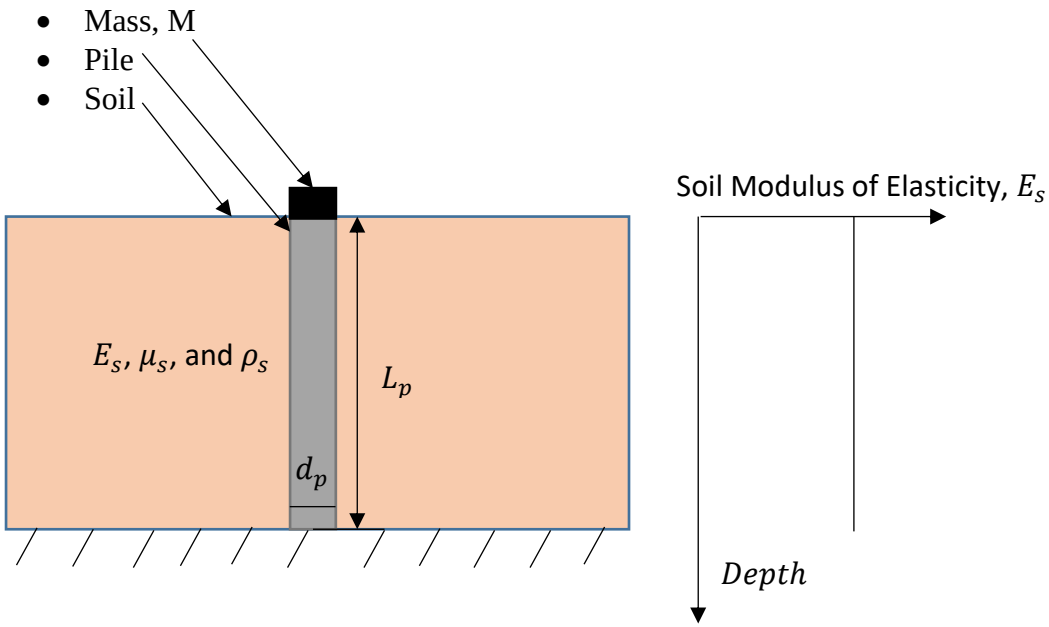

Figure 5.47: End-bearing pile in an elastic homogeneous soil.

Table 5.4: Values for variables and constants for study of end-bearing pile in homogeneous soil.

Parameter	Symbol	Unit	Value
Pile Modulus of Elasticity	E_p	$Pascal$	$2.1\text{x}10^{10}$ and $5.5x10^{10}$
Pile Poisson's Ratio	μ_p		0.25
Pile Mass Density	ρ_p	kg/m^3	2500
Pile Diameter	d_p	m	0.5
Pile Length	L_p	m	10
Soil Modulus of Elasticity	E_s	$Pascal$	$8.34\text{x}10^6$ to $8.34\text{x}10^8$
Soil Poisson's Ratio	μ_s		0.45
Soil Mass Density	ρ_s	kg/m^3	1800
Mass applied on top of Pile	M	kg	65000
Applied Static Pressure	Q_s	$Pascal$	22000
Dynamic Pressure Amplitude	Q_d	$Pascal$	22000
Frequency	f	Hz	2.5 to 30

The main two outcomes of this study are the stiffness, k and damping ratio. Stiffness is plotted in Figure 5.48 while the damping ratio is plotted in Figure 5.49. From these two parameters, the critical damping, damping and dimensionless resonant frequency can be calculated and are shown in Figures 5.50, 5.51, and 5.52 respectively.

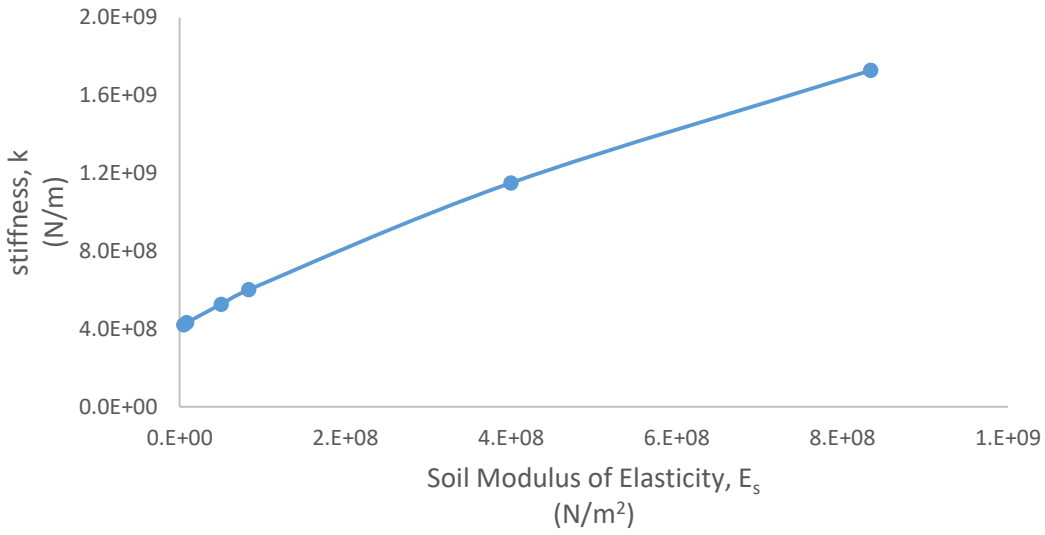

Figure 5.48: Variation of stiffness, k with soil modulus of elasticity, E_s for an end-bearing pile in homogeneous soil.

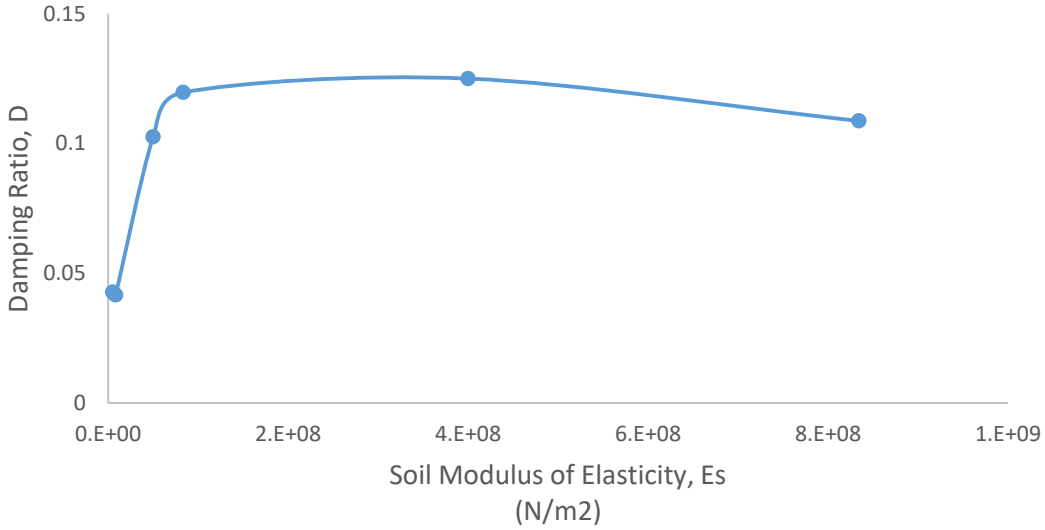

Figure 5.49: Variation of damping ratio, D with soil modulus of elasticity, E_s for an end-bearing pile in homogeneous soil.

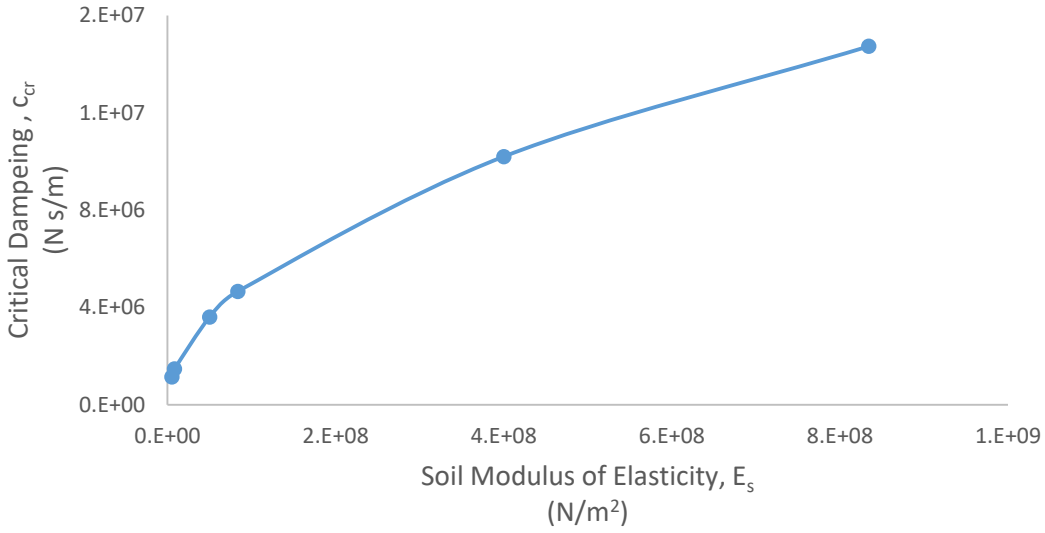

Figure 5.50: Variation of critical damping, c_{cr} with soil modulus of elasticity E_s for an end-bearing pile in homogeneous soil.

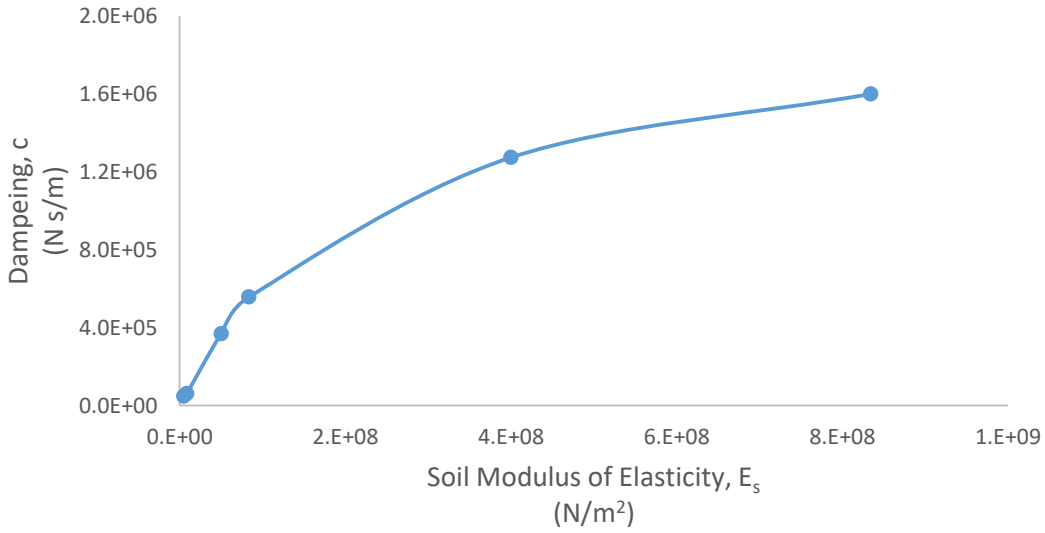

Figure 5.51: Variation of damping, c with soil modulus of elasticity, E_s for an end-bearing pile in homogeneous soil.

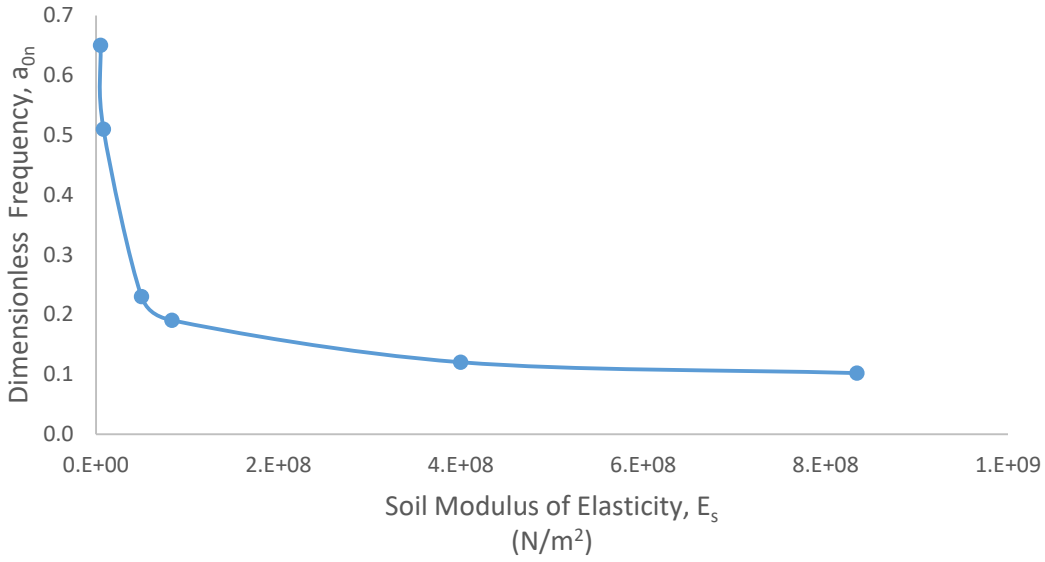

Figure 5.52: Variation of natural dimensionless frequency, a_{0n} with soil modulus of elasticity, E_s for an end-bearing pile in homogeneous soil.

5.3.1. Results commentary and analysis

- Stiffness, k is plotted in Figure 5.48. Stiffness increases with increase in soil modulus of elasticity, E_s. This is expected as soil is stronger it can sustain load at lower deformation. Since this is an end-bearing pile, all increase in stiffness here is provided through the soil along the shaft through friction. Soil around the shaft provide the friction that would increase the pile stiffness.
- Geometric damping ratio is plotted in Figure 5.49. Geometric damping increases with increase in soil modulus of elasticity until a certain point (at $E_s = 8.34 \times 10^7\ Pa$. After this point the geometric damping, D remains almost constant at any modulus of elasticity of the soil, E_s at an average value of 0.12. Any variation of geometric damping is provided by the soil along the shaft. The rock layer wouldn't provide any damping but would reflect the wave back to the pile.

- The combination of the stiffness and damping variation with soil modulus of elasticity would result in decrease in both dynamic displacement, u_d at resonance and amplification of static displacement, u_d/u_s at resonance. Dynamic displacement, u_d at resonance is shown in Figure 5.53 while dynamic amplification of static displacement, u_d/u_s is shown in Figure 5.54.

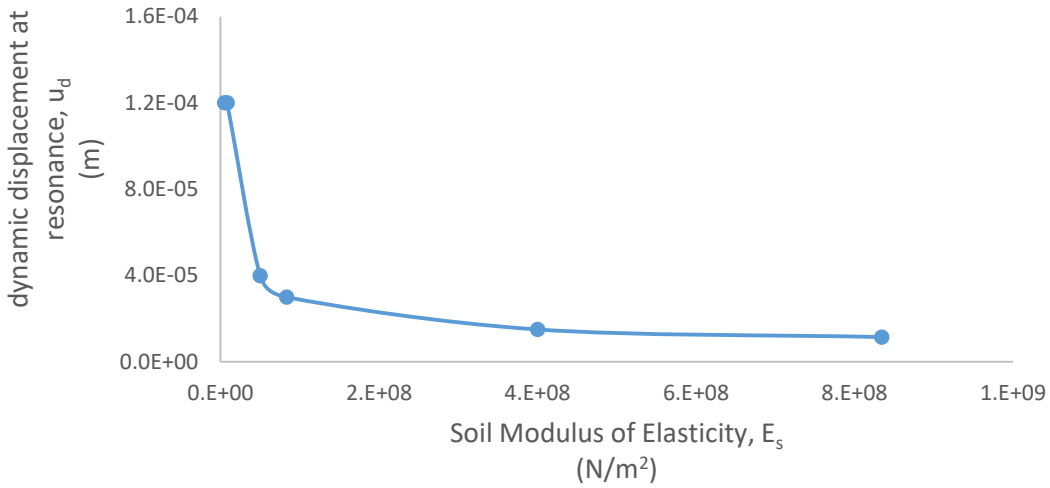

Figure 5.53: Variation of dynamic displacement, u_d at resonance with soil modulus of elasticity, E_s for an end-bearing pile in homogeneous soil

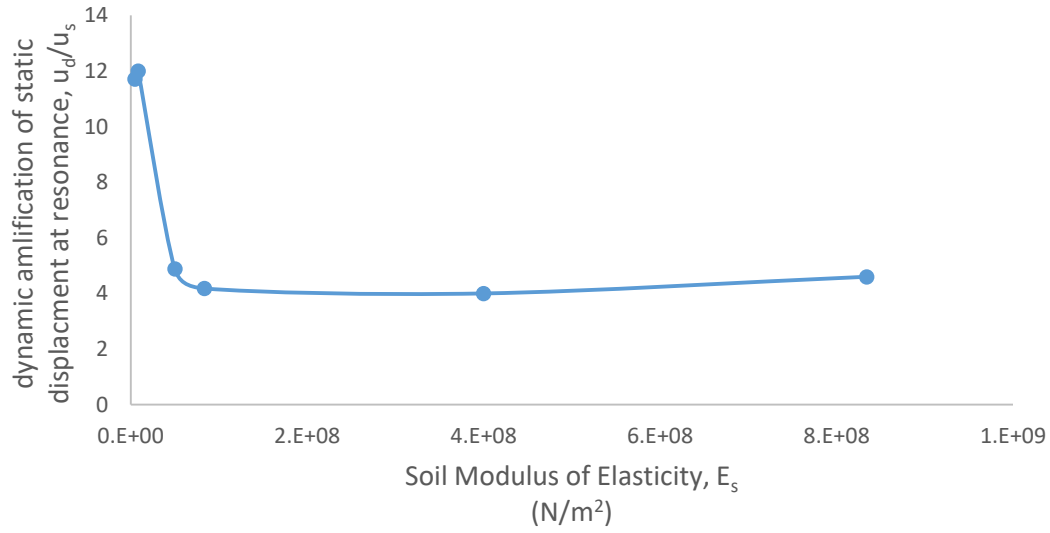

Figure 5.54: Variation of dynamic amplification of static displacement, u_d/u_s at resonance with variation of soil modulus of elasticity, E_s for an end-bearing pile in homogeneous soil.

- It can be seen from Figure 5.53 that the dynamic displacement, u_d at resonance decreases with increase in soil modulus of elasticity. In Figure 5.54 the dynamic amplification of static displacement, u_d/u_s at resonance also decreases with increase in soil elastic modulus.
- The critical damping, c_{cr} is plotted in Figure 5.50. critical damping increases with increase in soil modulus of elasticity. This is expected since the critical damping is proportionally related to the stiffness as shown in Equation 5.1.
- Damping, c which is obtained by multiplying critical damping, c_{cr} by damping ration, D is shown in Figure 5.51. It increases with increase in soil modulus of elasticity, E_s.
- The natural frequency is provided in the form of dimensionless frequency, a_{0n} in Figure 5.52 decreases with the increase in soil modulus of elasticity, E_s. The natural frequency in Hertz is shown in Figure 5.55. The natural frequency, f_n in Hertz increases with increase in soil modulus of elasticity.

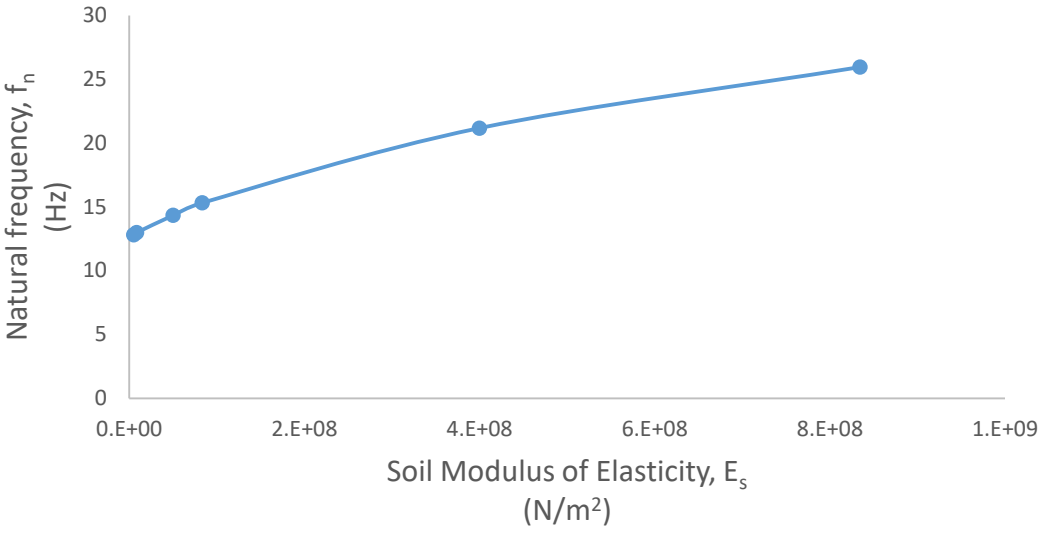

Figure 5.55: Variation of natural frequency, f_n with soil modulus of elasticity, E_s for an end-bearing pile in homogeneous soil.

5.3.2. Comparison of finite element solution results with literature

5.3.2.1. Comparison of stiffness

A comparison of the stiffness for an ending bearing pile calculated using Novak (1974) and 3D Finite element analysis is shown in Figure 5.56, while the relative difference in stiffness between the two approaches is shown in Figure 5.57. No agreement between the two methods is found as 3D FEM is -50% to 350% different than Novak (1974).

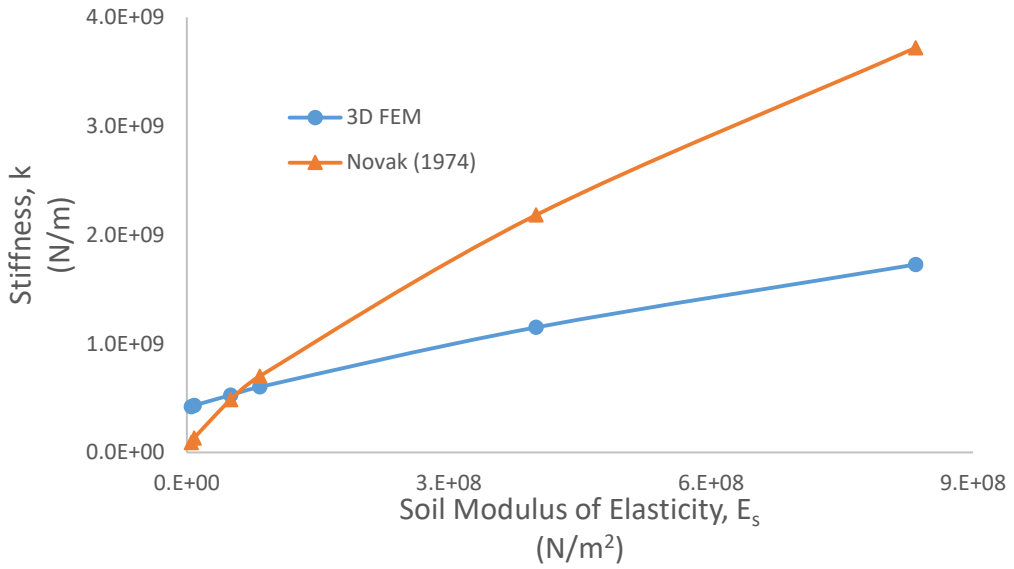

Figure 5.56: Comparison of stiffness calculated using 3D FEM and Novak (1974) for an end-bearing pile in a homogeneous soil.

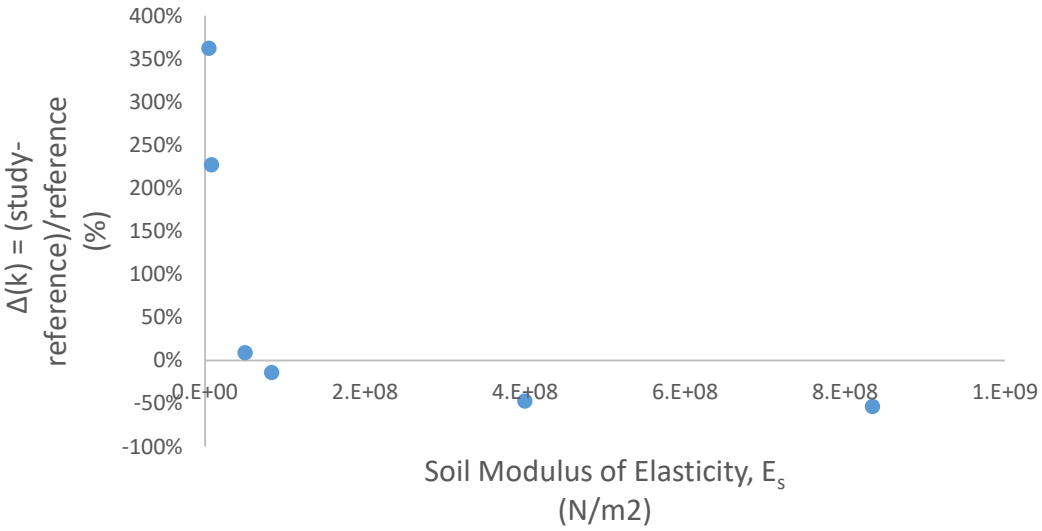

Figure 5.57: Relative difference in stiffness between 3D FEM and Novak (1974) for an end-bearing pile in a homogeneous soil.

Comparison of stiffness, k calculate by 3D FEM and Gazetas & Mylonakis (1998) is provided in Figure 5.58. The relative difference is shown in Figure 5.59. Gazetas & Mylonakis (1998) approach is the same of that provided in Equations 5.6 to 5.10 with a change in Equation 5.10. To be applicable to an end bearing pile the stiffness at the pile tip is calculated using the following Equation

$$k_b = \frac{4G_b r_p}{1-\mu_s} \tag{5.20}$$

In Equation 5.20, G_b is the shear modulus at the pile tip. In order for rigidity of the base to be applicable G_b was assumed to be 1000 times the shear modulus of the soil along the pile shaft. However it was found even if G_b is only 100 times the shear modulus of the soil along the pile shaft, no change in the overall pile stiffness. Good agreement between 3D FEM and Gazetas & Mylonaki (1998). 3D FEM is only 5% to 26% higher in predicting the stiffness.

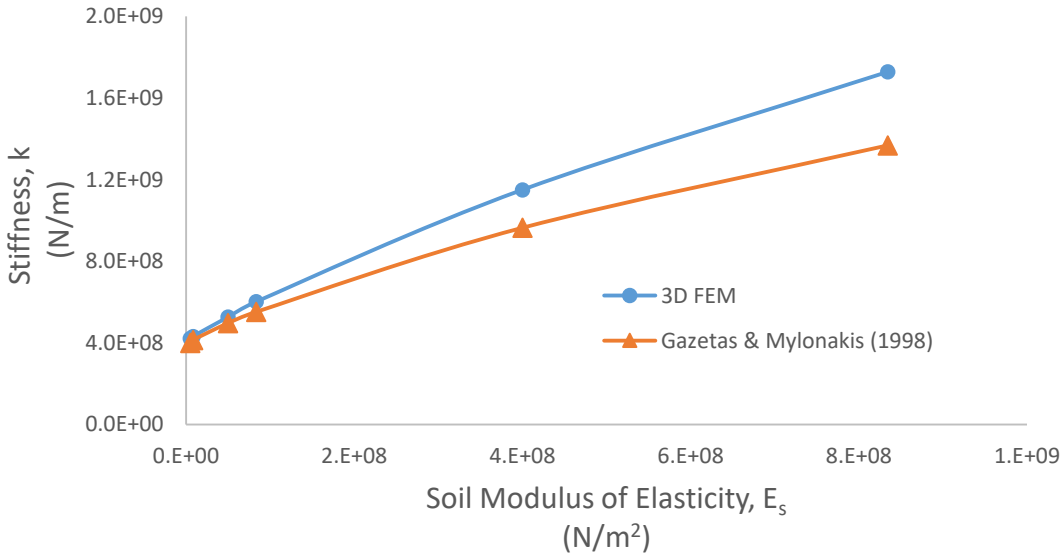

Figure 5.58: Comparison of stiffness, k obtained by finite element method with Gazetas & Mylonakis (1998) for an end-bearing pile in homogeneous soil.

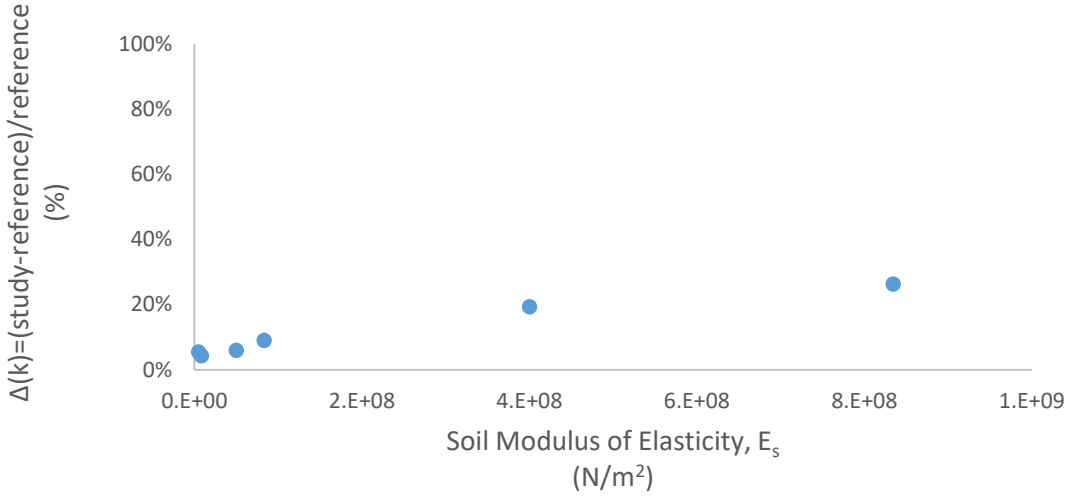

Figure 5.59: Relative difference of stiffness between 3D FEM and Gazetas & Mylonakis (1998), for an end-bearing pile in homogeneous soil.

Chowdhury & Dasgupta (2008) calculated the stiffness of the pile assuming a rigid cylinder embedded in an elastic half-space. Comparison of stiffness calculated using 3D FEM and Chowdhury & Dasgupta (2008) is shown in Figure 5.60 while the relative difference is shown in Figure 5.61. The rigid cylinder assumption might hold valid at low soil modulus of elasticity. As the relative difference is between -38% to -22% for values of soil modulus of elasticity up to $5 \times 10^7\ Pa$. After that the difference reaches values between -72% and -45%. In general, Chowdhury & Dasgupta (2008) over predicts the stiffness of the pile.

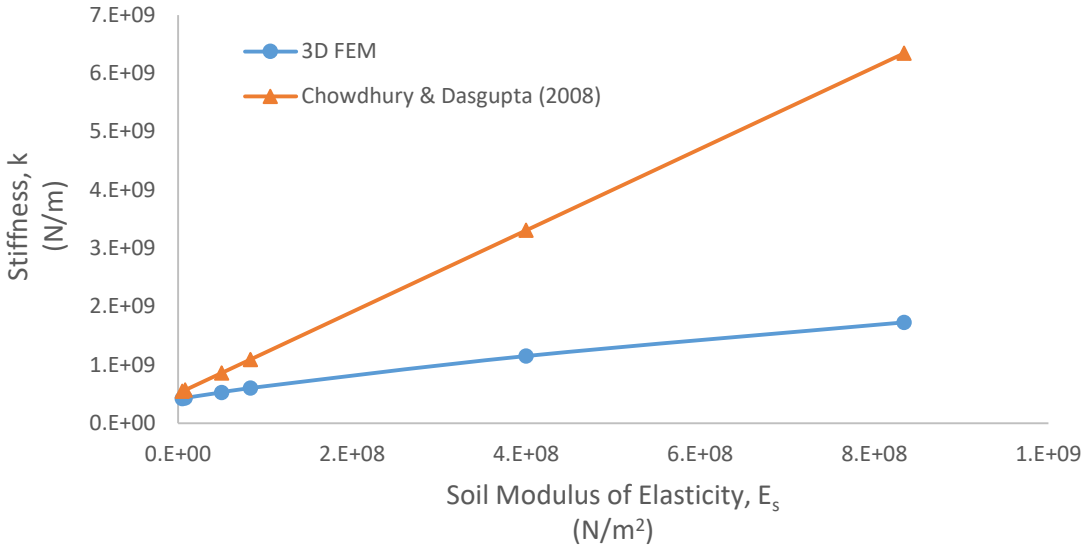

Figure 5.60: Comparison of stiffness obtained by 3D FEM with work of Chowdhury & Dasgupta (2008) for an end-bearing pile in a homogeneous soil.

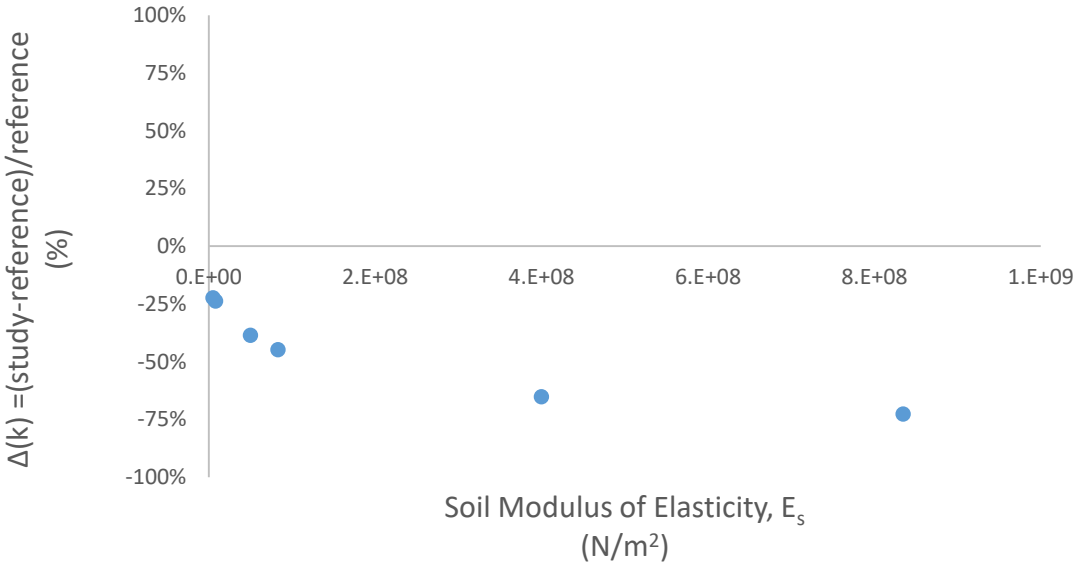

Figure 5.61: Relative difference of stiffness between 3D FEM and Chowdhury & Dasgupta (2008) for an end-bearing pile in a homogeneous soil.

5.3.2.2. Comparison of damping

Damping ratio calculated by the finite element method is compared by the damping ratio calculated using Novak (1974). A comparison between the two approaches is shown in Figure 5.62 while the relative difference between the two approaches is shown in Figure 5.63. It is found that there is a difference in values and in the pattern of the curve. Damping calculated using Novak (1974) decreases with increases in soil modulus of elasticity. On the contrary, damping calculated using finite element method shows a different pattern as damping increases with increase in soil modulus of elasticity until it becomes constant. Difference between the two approaches is between -70% to 45%. No agreement between the two approaches is found.

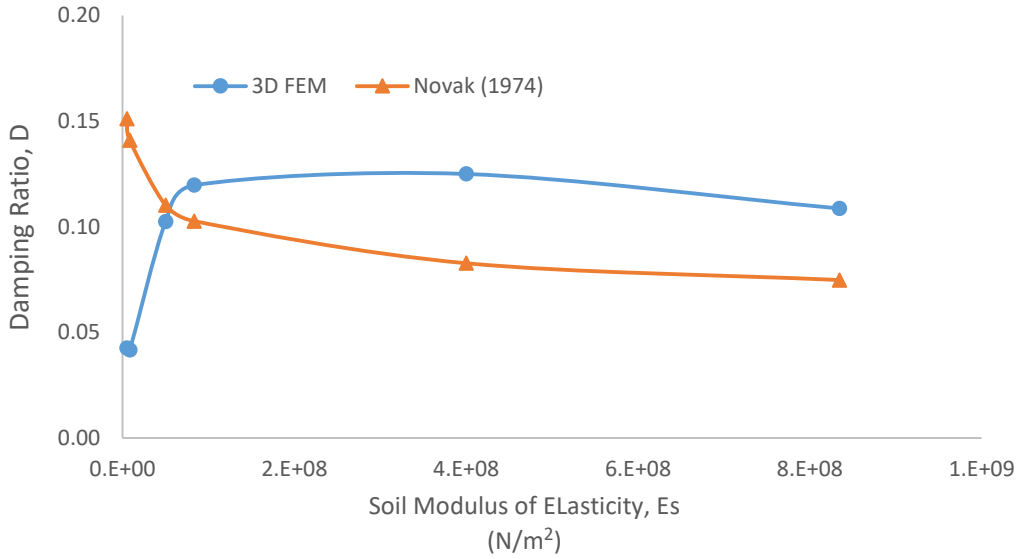

Figure 5.62: Comparison of damping ratio between finite element method and Novak (1974) for an end-bearing pile in a homogeneous soil.

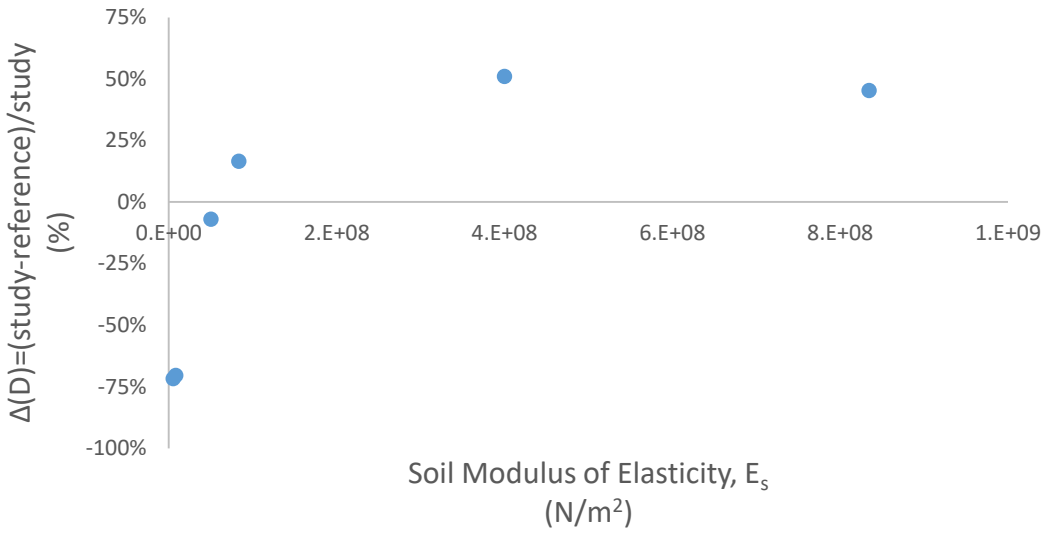

Figure 5.63: Relative difference of stiffness between 3D FEM and Novak (1974) for an end-bearing pile in a homogeneous soil.

The difference in damping can be contributed mathematically to the difference in stiffness. This is because geometric damping is mathematically related to the critical damping ($D = c/c_{cr}$) and the critical damping is a function of the stiffness ($c_{cr} = 2\sqrt{k\,M}$). Comparison of critical damping between the two approaches is shown in Figure 5.64 while relative difference of critical damping between finite element and Novak (1974) is shown in Figure 5.65. Critical damping calculated using finite element method is between 35% and 75% less than that calculated by Novak (1974).

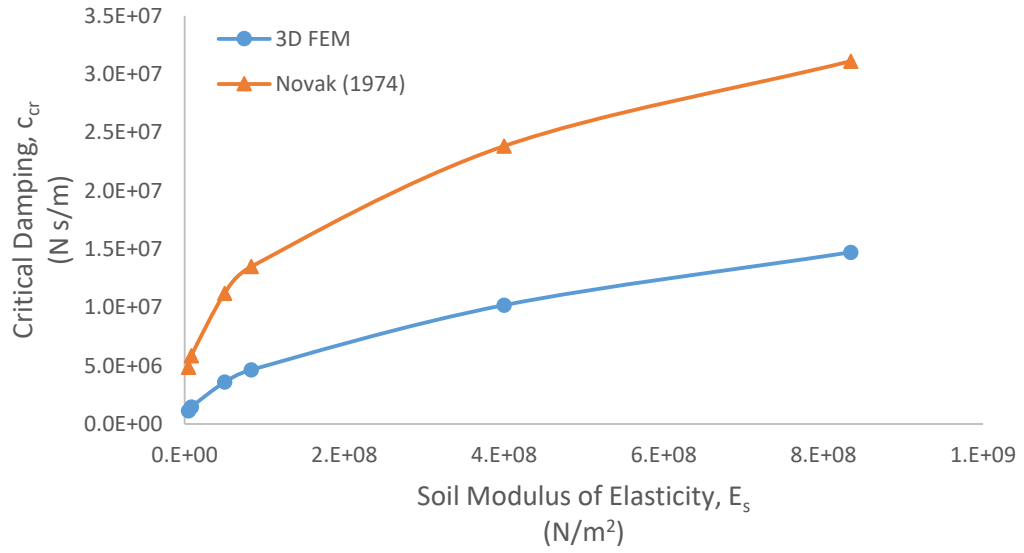

Figure 5.64: Comparison of critical damping between finite element method and Novak (1974) for an end-bearing pile in a homogeneous soil.

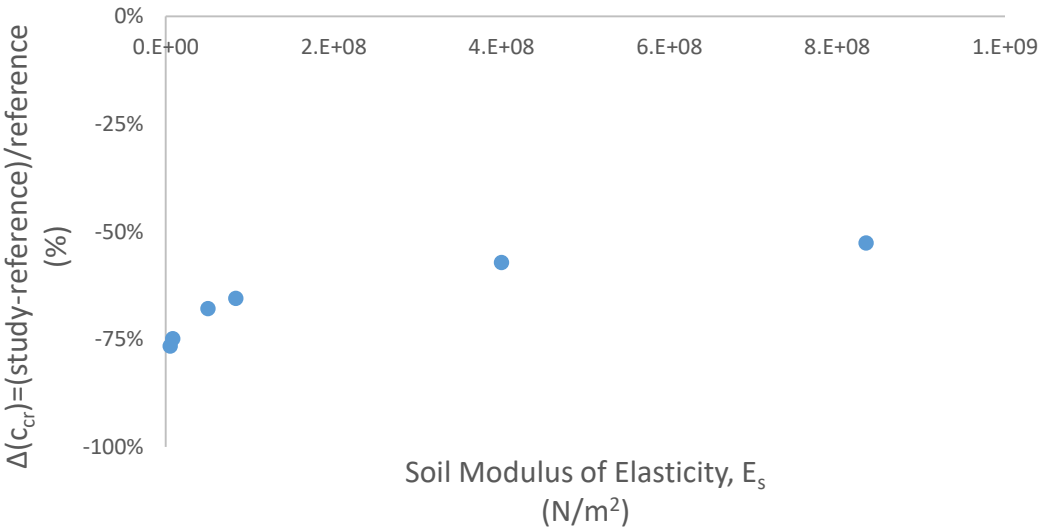

Figure 5.65: Relative difference of stiffness between 3D FEM and Novak (1974) for an end-bearing pile in a homogeneous soil.

Comparison of damping calculated by the finite element method and that calculated by Chowdhury & Dasgupta (2008) is shown in Figure 5.66. Damping calculated by Chowdhury & Dasgupta (2008) is constant at 0.03 regardless of the change in soil modulus of elasticity.

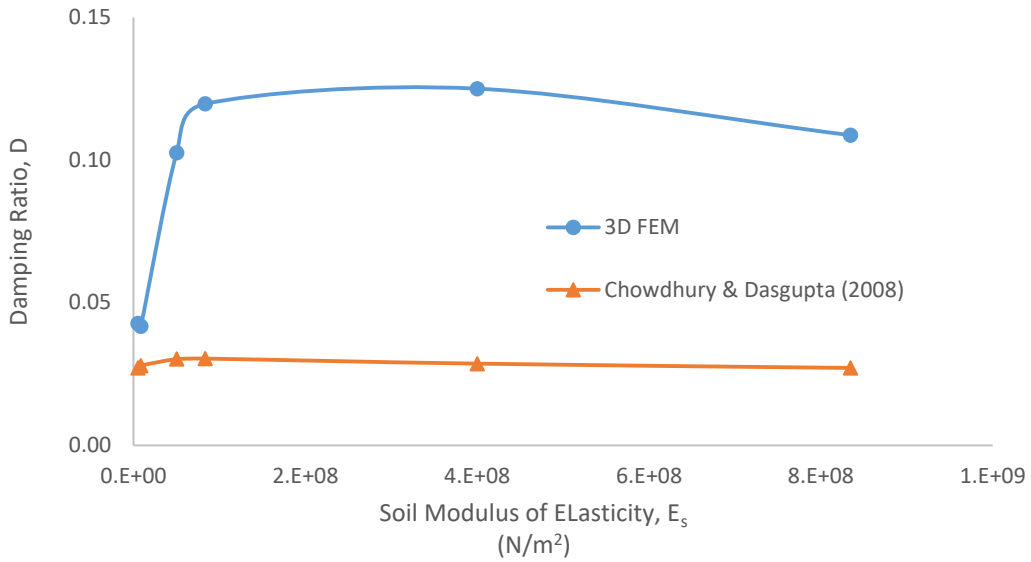

Figure 5.66: Comparison of damping ratio between finite element method and Chowdhury & Dasgupta (2008) for an end-bearing pile in a homogeneous soil.

5.4. End-bearing pile in nonhomogeneous soil

An elastic pile in nonhomogeneous soil supported by a rock base is studied. Inhomogeneity takes the form of an increase in the elastic modulus of the soil with depth. The increase of elastic modulus has a rate of increase that is referred to as S_{E_s}. The increase stops at certain depth, D_c. After this depth the soil mdulus of elasticity remains constant. This constant modulus is referred to as E_{sc}. The problem is graphically described in Figure 5.67 and variables and constants are shown in Table 5.5. The study captures the effect of the varied variables on the stiffness and damping of the pile.

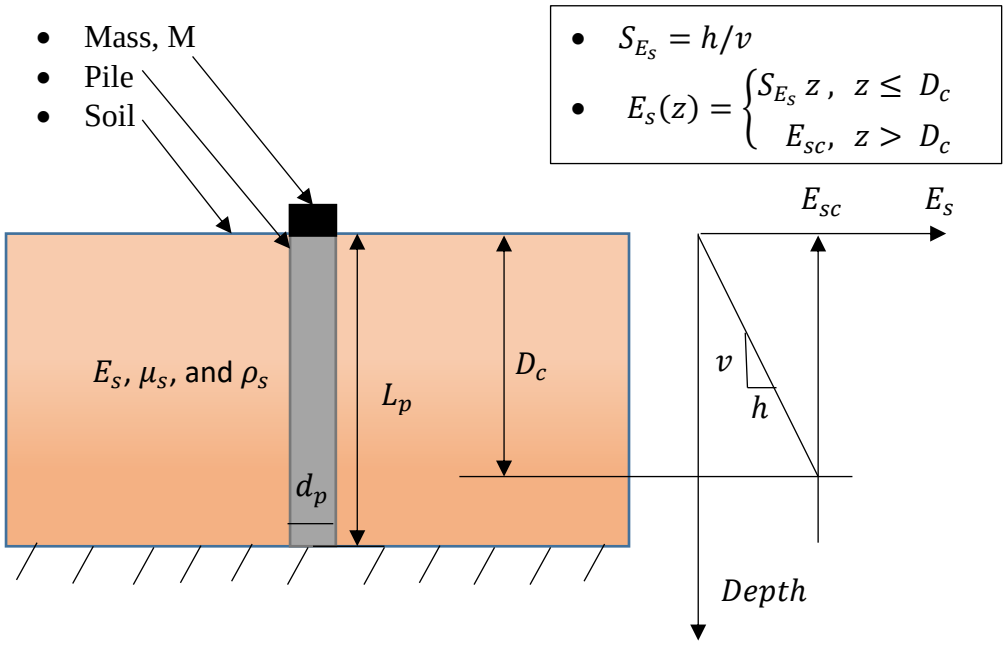

Figure 5.67: End-bearing pile in nonhomogeneous soil.

Table 5.5: Values for variables and constants for study of end-bearing pile in nonhomogenous soil.

Parameter	Symbol	Unit	Value
Pile Modulus of Elasticity	E_p	$Pascal$	$2.1\text{x}10^{10}$
Pile Poisson's Ratio	μ_p		0.25
Pile Mass Density	ρ_p	kg/m^3	2500
Pile Diameter	d_p	m	0.5
Pile Length	L_p	m	10
Soil Modulus of Elasticity	$E_s(z)$	$Pascal$	Function of depth
Rate of Increase in E_s	S_{E_s}	Pascal/m	4.17×10^6 to 8.34×10^7
Constant modulus at D_c	E_{sc}	Pascal	
Point at which increase in E_s stops	D_C	m	$4\ to\ 10\ (0.4L_p\ to\ L_p)$
modulus of elasticity at D_c	E_{sc}		Depends on S_{E_s} and D_c
Soil Poisson's Ratio	μ_s		0.45
Soil Mass Density	ρ_s	kg/m^3	1800
Mass applied on top of Pile	M	kg	65000
Applied Static Pressure	Q_s	$Pascal$	22000
Dynamic Pressure Amplitude	Q_d	$Pascal$	22000
Frequency	f	Hz	$2.5\ to\ 30$

The main two outcomes of this study are the stiffness and damping ratio of the pile. Variation of the stiffness with S_{E_s} is shown in Figure 5.68 while variation of damping with S_{E_s} is shown in Figure 5.69.

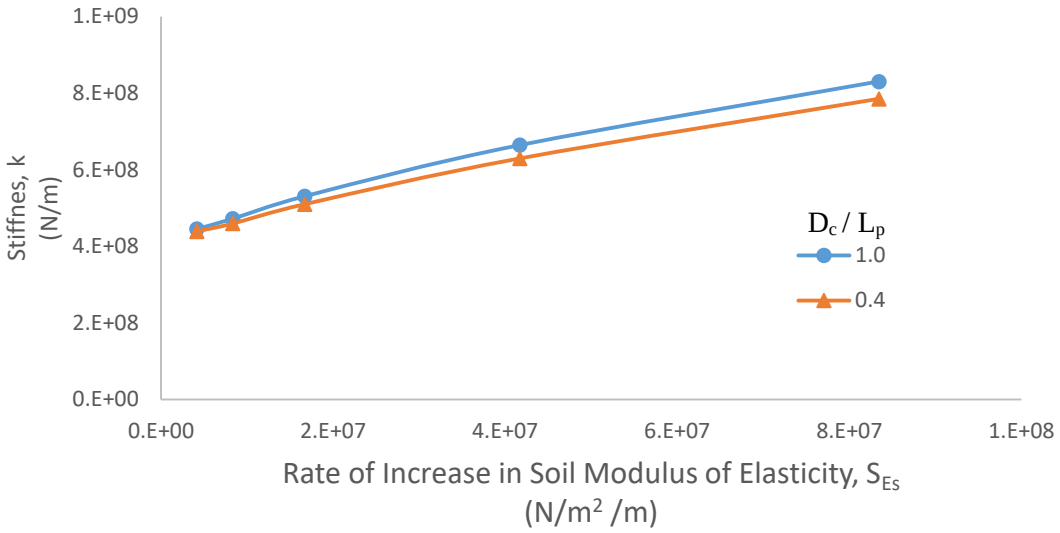

Figure 5.68: Variation of stiffness with S_{E_s} for an end-bearing pile in nonhomogeneous soil.

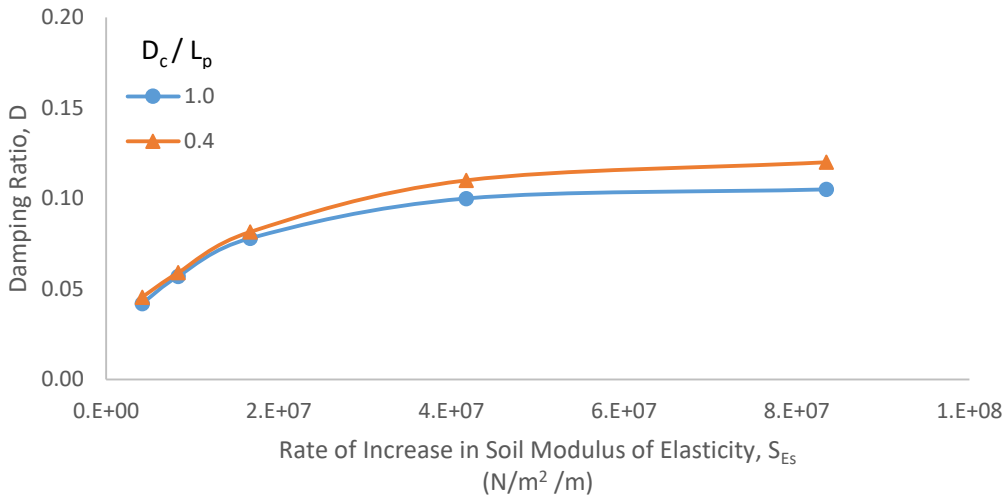

Figure 5.69: Variation of geometric damping ratio with S_{E_s} for an end-bearing pile in nonhomogeneous soil.

From the stiffness and damping ratio, critical damping and damping can be calculated. Critical damping is shown in Figure 5.70 while damping is shown in Figure 5.71.

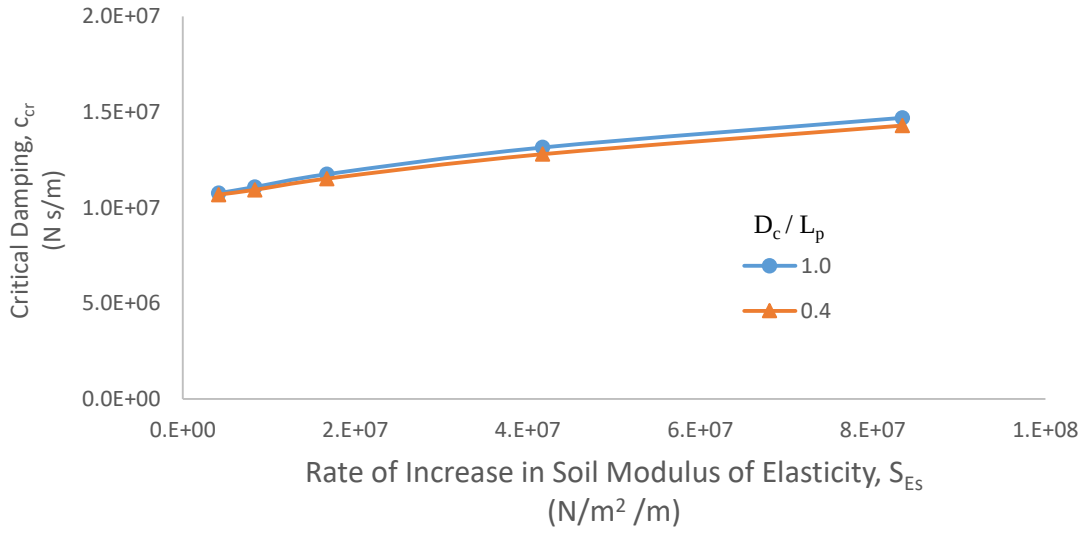

Figure 5.70: Variation of critical damping with S_{E_s} for an end-bearing pile in nonhomogeneous soil.

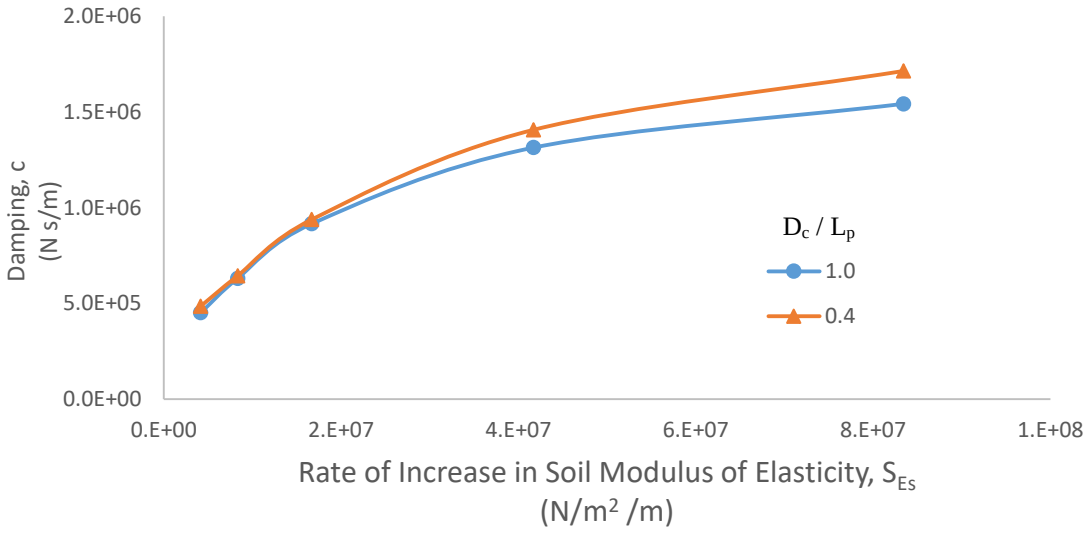

Figure 5.71: Variation of damping with S_{E_s} for an end-bearing pile in nonhomogeneous soil.

5.4.1. Results commentary and analysis

- Stiffness increases with increase in S_{E_s}. As S_{E_s} gets larger, the soil around the pile gets stronger which results in increase the stiffness of the soil-pile system.
- Geometric damping ratio increases with increase in S_{E_s}. All damping of the system is provided from the surrounding soil. The faster the soil can transfer waves away from the pile, the greater is the geometric damping.
- The effect of increasing damping and increasing stiffness is a decrease in dynamic displacement at resonance and decrease in dynamic amplification of static displacement at resonance. Dynamic displacement at resonance is shown in Figure 5.72. Dynamic amplification of static displacement at resonance , u_d/u_s is shown in Figure 5.73.

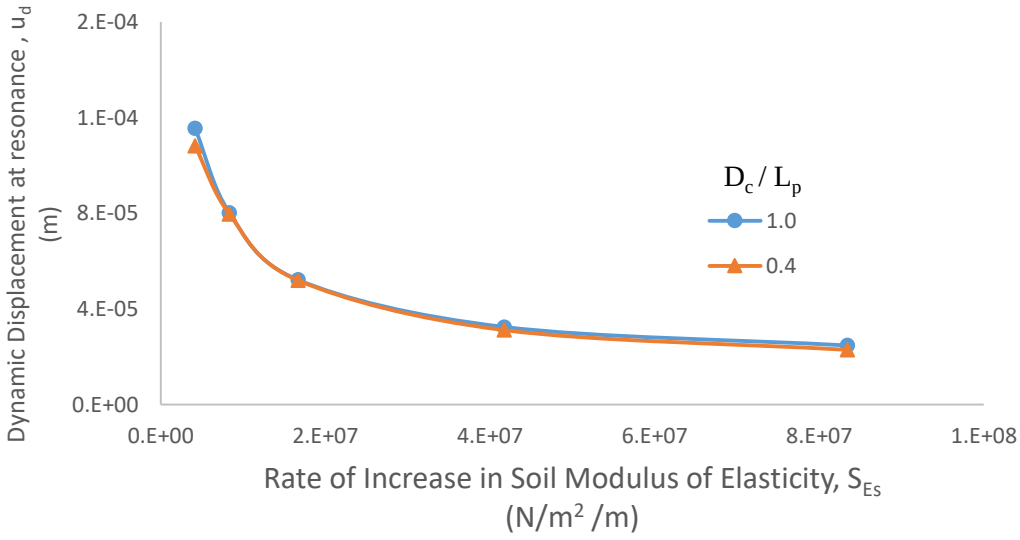

Figure 5.72: Variation of dynamic displacement at resonance with S_{E_s} for an end bearing pile in nonhomogeneous soil.

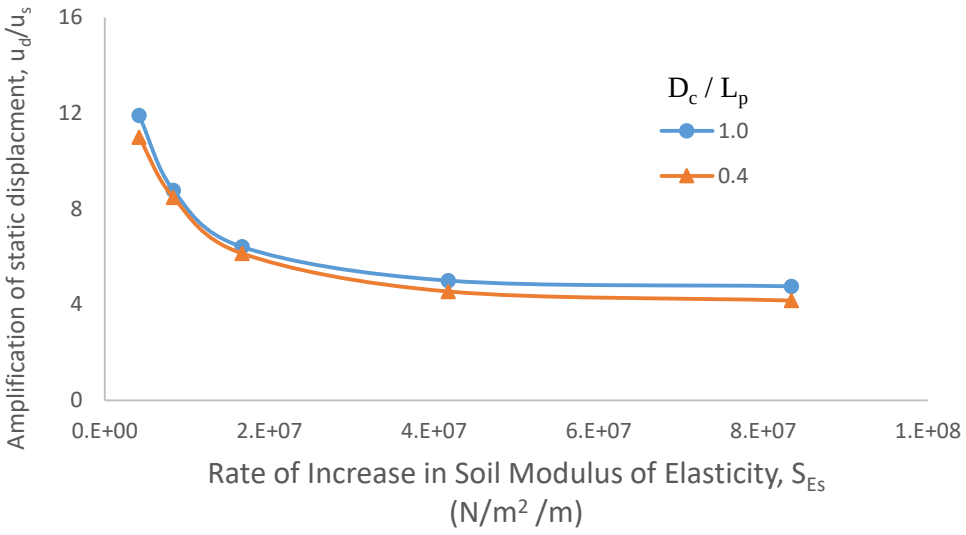

Figure 5.73: Variation of u_d/u_s at resonance with S_{E_s} for an end bearing pile in nonhomogeneous soil.

- Critical damping increases with increase in S_{E_S}. Critical damping is proportionally related to stiffness of the pile.
- Damping of the system also increases with increase in S_{E_s}.
- Variation of D_C/L_p doesn't significantly alter the results. In all Figures 5.68 to 5.69, 2 curves are provided. One for $D_c/L_p = 1$ and the other for $D_c/L_p = 0.4$. In all these Figures the difference between the two curves isn't significant.
- The system natural frequency, f_n increases with increase in S_{E_s}. This is shown in Figure 5.74.

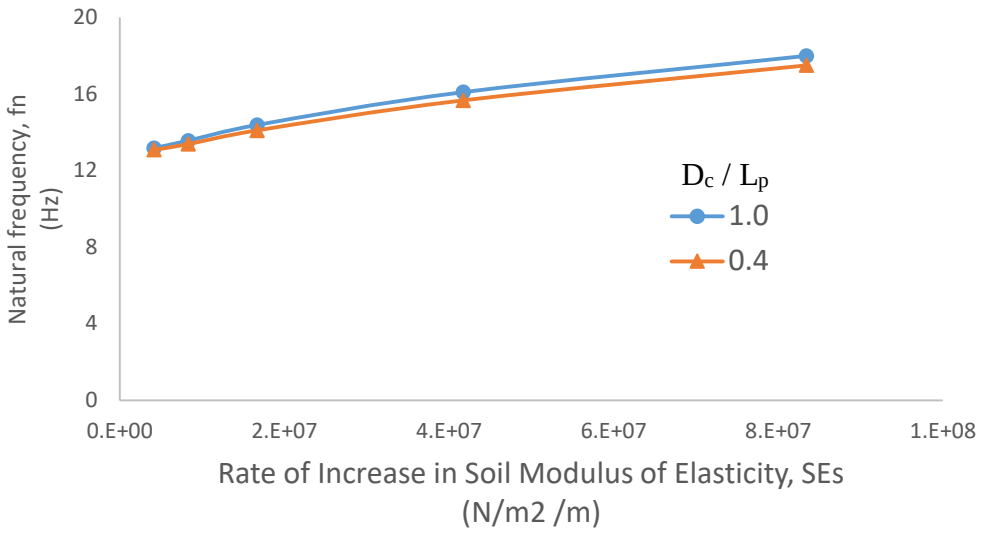

Figure 5.74: variation of natural frequency with S_{E_s} for an end bearing pile in nonhomogeneous soil.

- Another way to look at analysis results is to study effect of an inhomogeneity ratio and the constant modulus of elasticity, E_{sc}. This is shown in Figure 5.75 for stiffness while for damping it is shown in Figure 5.76. Increase in inhomogeneity ratio decreases the stiffness and damping compared to homogeneous soil ($d_c/L_p = 0$).

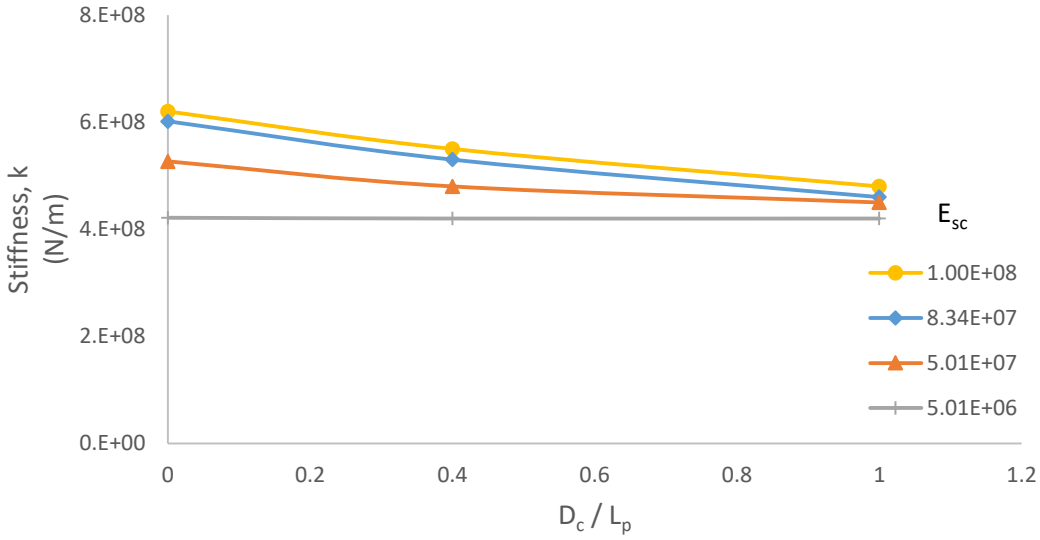

Figure 5.75: Variation of stiffness with inhomogeneity ratio for an end bearing pile.

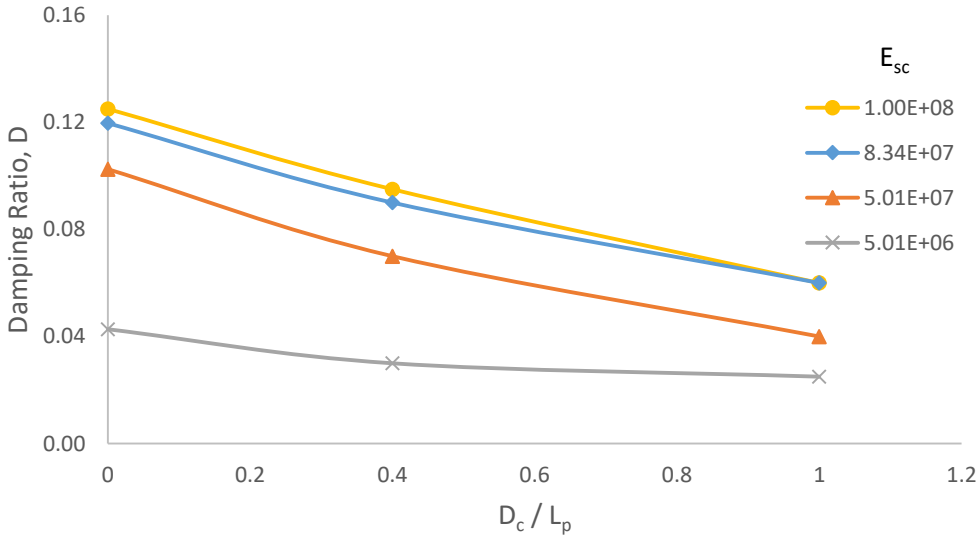

Figure 5.76: Variation of the stiffness with inhomogeneity ratio for an end bearing pile.

5.4.2. Comparison with 1D finite element method

No analytical solution is provided for an end bearing pile subjected to dynamic loads in nonhomogeneous soils. Analysis can be done using the computationally efficient 1D approach described in Section 2.3.1. A comparison of results of the 3D finite element method and the 1D finite element method is presented here for the stiffness and dynamic of the pile. Comparison of stiffness is given in Figure 5.77 while comparison of damping is given in Figure 5.78. Numerical results of the comparison are given in Table 5.6. The comparison provided is for the case where $D_c/L_p = 1$ only. Difference between two approaches in stiffness is below 20% while difference in damping is between 47% to 110%. 1D FEM under predicts stiffness and damping compared to 3D FEM.

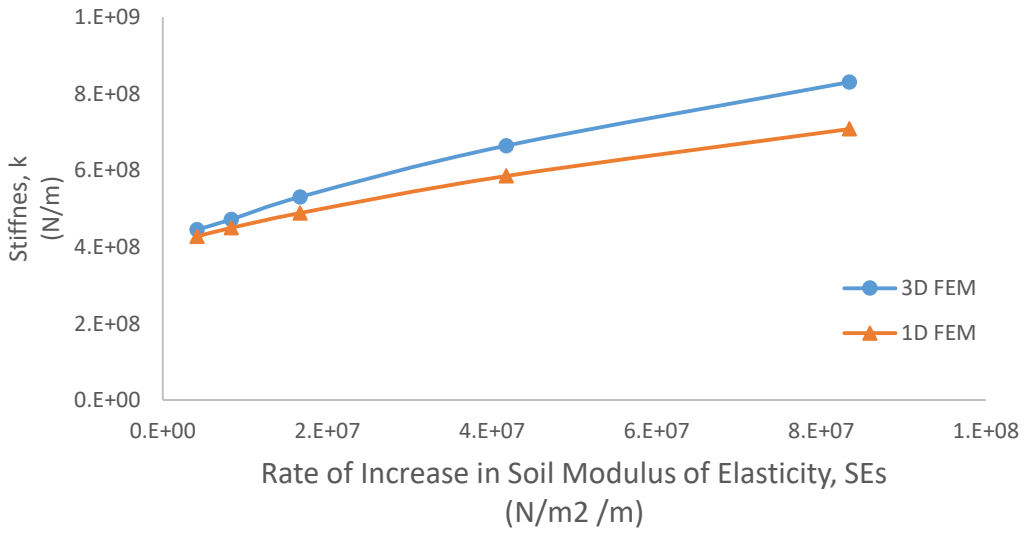

Figure 5.77: Comparison of stiffness calculated by 3D FEM and 1D FEM for an end-bearing pile in nonhomogeneous soil and $D_c/L_p = 1$.

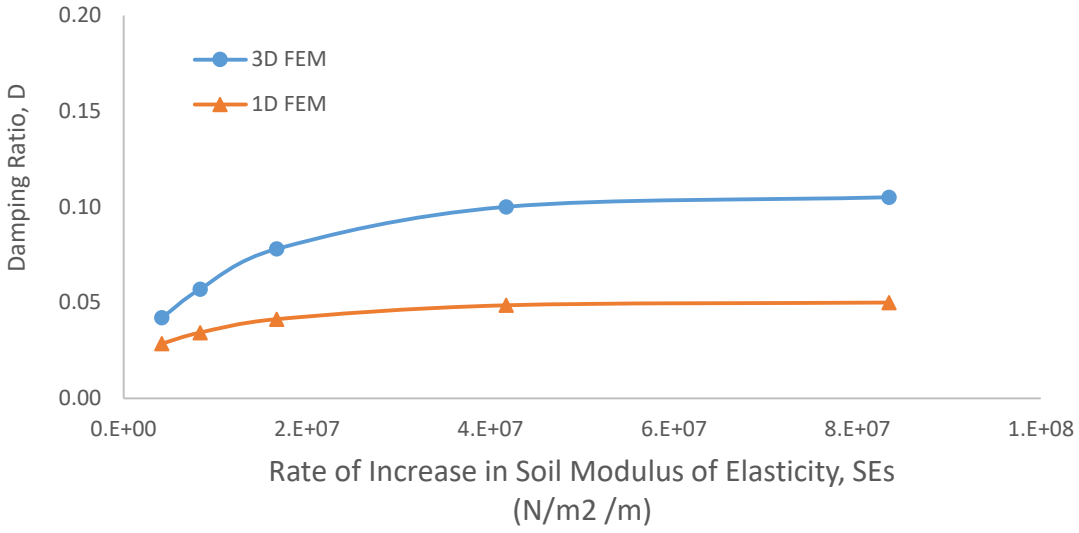

Figure 5.78: Comparison of geometric damping ratio calculated by 3D FEM and 1D FEM for an end-bearing pile in nonhomogeneous soil and $D_c/L_p = 1$.

Table 5.6: Numerical results for Comparison of stiffness and damping calculated by 3D and 1D FEM for an end-bearing pile in nonhomogeneous soil and $D_c/L_p = 1$.

		3D FEM		**1D FEM**			
Dc/L	S_{E_s}	k	D	k	D	Δ(k)	Δ(D)
Unit->	$N/m^2\ /m$	N/m		N/m			
1.0	4.17E+06	4.45E+08	0.04	4.28E+08	0.03	4%	47%
	8.34E+06	4.72E+08	0.06	4.50E+08	0.03	5%	66%
	1.67E+07	5.31E+08	0.08	4.89E+08	0.04	9%	89%
	4.17E+07	6.65E+08	0.10	5.85E+08	0.05	14%	106%
	8.34E+07	8.31E+08	0.11	7.08E+08	0.05	17%	110%

5.5. Pile-to-pile interaction in homogeneous soil

The final study in this research is the study of two floating piles in a homogeneous soil to determine interaction between the two. When piles are constructed in groups, their stiffness and damping are reduced due to stresses from an adjacent interacting pile. The study captures the interaction between two piles by calculating the reduced stiffness and damper coefficients to determine the stiffness and damping interaction factors. The problem is graphically described in Figure 5.79. Two parameters are varied and they are the elastic modulus of the soil and the spacing between the two piles. See Table 5.8 for variables and constants for this study.

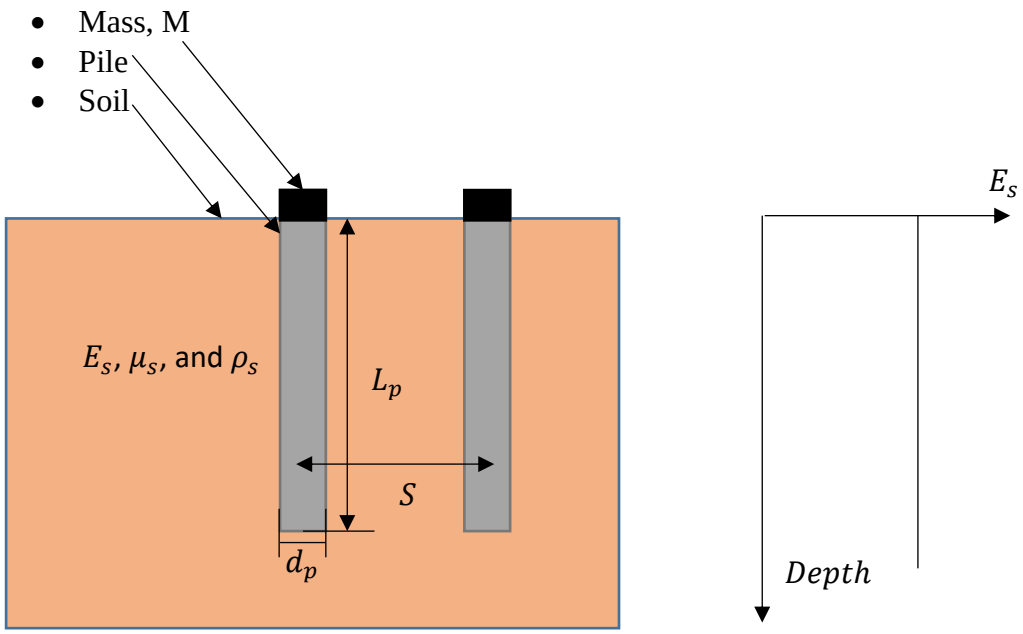

Figure 5.79: 2 Floating piles in homogeneous soil.

Table 5.7: Variables and constants for study of pile to pile interaction.

Parameter	Symbol	Unit	Value
Pile Modulus of Elasticity	E_p	$Pascal$	$2.1\text{x}10^{10}$
Pile Poisson's Ratio	μ_p		0.25
Pile Mass Density	ρ_p	kg/m^3	2500
Pile Diameter	d_p	m	0.5
Pile Length	L_p	m	10
Pile Spacing from center to center	S	m	1 to 3 (2 d_p to 6 d_p)
Soil Modulus of Elasticity	E_s	$Pascal$	$5\text{x}10^6$ to $5\text{x}10^8$
Soil Poisson's Ratio	μ_s		0.45
Soil Mass Density	ρ_s	kg/m^3	1800
Mass applied on top of each Pile	M	kg	65000
Applied Static Pressure per pile	Q_s	$Pascal$	22000
Dynamic Pressure Amplitude per pile	Q_d	$Pascal$	22000
Frequency	f	Hz	2.5 to 30

The piles are assumed to act as two sets of mass, spring, and dashpot vibrating in parallel. This assumption allows the required parameters of the two piles to be obtained (without a cap to eliminate the effect of the cap from interfering with the results) statically to compute stiffness and dynamically to compute damping according to the procedure described in Section 4.4. In a pile-to-pile interaction, the stiffness of single pile in the group is the stiffness of the group

divided by 2. Similarly, damping ratio of a single pile in the group is damping of the group divided by two. The stiffness and damping of a single pile in the group are always less than that a single isolated pile. Interaction is calculated based on this reduction in stiffness and damping as described below.

Since a 2 pile system is the simplest form of a group, the following Equations apply:

$$k_G = \frac{\sum_{i=1}^{n} k_i}{\sum_{i=1}^{n} \alpha_{ki}} \tag{5.21}$$

$$c_G = \frac{\sum_{i=1}^{n} c_i}{\sum_{i=1}^{n} \alpha_{ci}} \tag{5.22}$$

Where k_G is the group stiffness, k_i stiffness calculated for an isolated pile, c_G is the group damping, c_i is the damping calculated for an isolated pile, α_{ki} is stiffness interaction factor and α_{ci} is the damping interaction factor. Finite element analysis is used to calculate k_G and c_G of the 2 pile system. From the study on a single pile in a homogeneous soil, k_i and c_i are calculated. The only remaining factors are $\sum_{i=1}^{n} \alpha_{ki}$ and $\sum_{i=1}^{n} \alpha_{ci}$. Since this is a 2 pile group, $\sum_{i=1}^{n} k_i = 2\ k$ and $\sum_{i=1}^{n} c_i = 2\ c$ where k and c indicates stiffness an damping of an isolated pile. Also, $\sum_{i=1}^{n} \alpha_{ki} = \alpha_{k1} + \alpha_{k2}$ where $\alpha_{k1} = 1$. Similarly, $\sum_{i=1}^{n} \alpha_{ci} = \alpha_{c1} + \alpha_{c2}$ and $\alpha_{c1} = 1$. The value of 1 for α_{k1} and α_{c1} represent interaction of the pile with itself which are always be 1. Since no cap was used in the study, the value of geometric damping, D calculated using the procedure described in section 4.4 yields the geometric damping of the group. This damping is the sum of the geometric damping coming from each pile after being modified for group action.

The following Equation then applies,

$$D_G = D_1' + D_2' \tag{5.23}$$

From 5.23, it can be said that

$$D_G = \frac{c_1'}{2\sqrt{k_1' M_1}} + \frac{c_2'}{2\sqrt{k_2' M_2}} \tag{5.24}$$

The superscript $'$ means modification of the isolated pile stiffness and damping for the group. The stiffness of the group is $K_G = k_1' + k_2'$ and damping is $c_G = c_1' + c_2'$. Since each pile is identical to the other and is subjected to same mass and load, it can be said that $k_1' = k_2' = k'$ and $c_1' = c_2' = c'$. Then the group stiffness calculated from finite element, $k_G = 2k'$ and damping is $c_G = 2c'$. Equations 5.21 and 5.22 become:

$$2k' = \frac{2k}{1 + \alpha_{k2}} \tag{5.24}$$

$$2c' = \frac{2c}{1 + \alpha_{c2}} \tag{5.25}$$

Determining α_{k2} and α_{c2} is the goal of this study. In Equations 5.24 and 5.25, all parameters are calculated using finite element method and α_{k2} and α_{c2} can be obtained.

The following is a sample calculation of values of α_{k2} and α_{c2} using the described procedure for the set of parameters described in Table 5.9.

1- A static load, Q is applied on each pile.

2- The static displacement of each pile can be determined from static analysis and the stiffness of a pile in a 2 pile system,

k' can be calculated as

$$k' = \frac{Q}{u_s} = \frac{22000}{7.23 \times 10^{-6}} = 5.97 \times 10^8 \; N/m \tag{5.26}$$

or

$$k' = \frac{k_G}{2} \tag{5.27}$$

Where k_G is the group stiffness and $k_G = 2Q/u_s$.

Table 5.8: Parameters values for sample calculation of stiffness and damping in a 2 pile system.

Parameter	Symbol	Unit	Value
Pile Modulus of Elasticity	E_p	$Pascal$	$2.1\text{x}10^{10}$
Pile Poisson's Ratio	μ_p		0.25
Pile Mass Density	ρ_p	kg/m^3	2500
Pile Diameter	d_p	m	0.5
Pile Length	L_p	m	10
Pile Spacing from center to center	S	m	1
Soil Modulus of Elasticity	E_s	$Pascal$	2.5×10^8
Soil Poisson's Ratio	μ_s		0.45
Soil Mass Density	ρ_s	kg/m^3	1800
Mass applied on top of Pile	M	kg	65000
Applied Static Pressure	Q_s	$Pascal$	22000
Dynamic Pressure Amplitude	Q_d	$Pascal$	22000
Frequency	f	Hz	$5 \ \ to$ 30

3- For a range of frequencies, dynamic loading is applied and dynamic displacement, u_d at each frequency is determined as shown in Table 5.9.

Table 5.9: results of dynamic displacement for sample calculation of stiffness and damping of 2 pile system.

$E_S = 2.5 \times 10^8\ Pa$		
frequency	Displacement, u_d	u_d/u_s
0	7.23E-06	1.00
5	7.50E-06	1.04
10	1.40E-05	1.94
15	1.80E-05	2.49
20	9.00E-06	1.24
30	2.50E-06	0.35

4- The geometric damping of the group, D_G that correspond to values of dynamic displacement in Table 5.9 was found to be 0.18.

5- The geometric damping contribution from each pile in the group, D' is

$$D' = \frac{D_G}{2} = 0.09 \tag{5.28}$$

6- Damping of a single pile in the group is

$$c' = D' \times 2\sqrt{k'M} = 0.09\left(2\sqrt{5.97 \times 10^8 \times 65000}\right) \tag{5.29}$$

$$c' = 1.12 \times 10^6\ N\ s/m$$

Where in 5.29, $2\sqrt{k'M}$ is the critical damping of a single pile in the group.

7- From elastic analysis of an isolated pile in elastic homogenous soil , the stiffness, $k = 7.58 \times 10^8\ N/m$ and damping $c = 2.25 \times 10^6\ N\ s/m$.

8- Using values of k' and c' obtained from Equations 5.26 and 5.29 and values of stiffness, k and damping c obtained in step 7 in Equations 5.24 and 5.25 after rearranging it to find α,

$$\alpha_{k2} = \frac{k}{k'} - 1 = \frac{7.58 \times 10^8}{5.97 \times 10^8} - 1 = 0.27 \quad (5.30)$$

$$\alpha_{c2} = \frac{c}{c'} - 1 = \frac{2.25 \times 10^6}{1.12 \times 10^6} - 1 = 1.01 \quad (5.31)$$

For the case presented addition of a second pile resulted in a reduction equals to 27% in the stiffness of the isolated pile and 101% reduction in damping of the isolated pile.

9- Steps 1 to 8 are repeated for different soil moduli of elasticity and different spacing to determine the interaction factors for the different cases.

Variation of stiffness interaction factor, α_k with spacing of the piles normalized over the pile diameter is shown in Figure 5.80. Variation of the damping interaction factor with the spacing of the piles normalized over their diameter is shown in Figure 5.81.

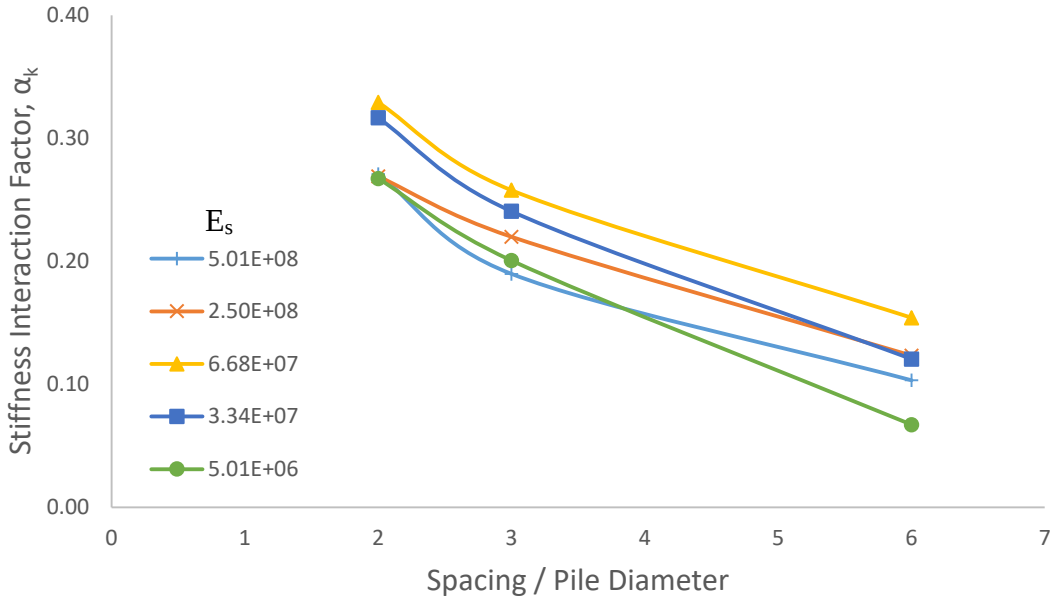

Figure 5.80: Variation of stiffness interaction factors with s/d_p for 2 piles.

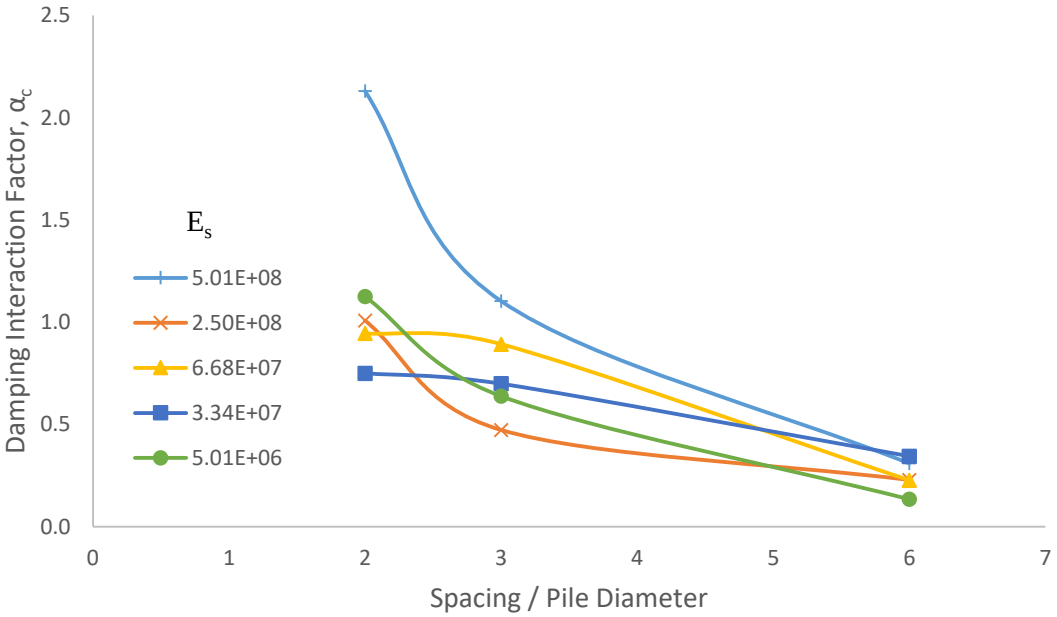

Figure 5.81: Variation of damping interaction factors with s/d_p for 2 piles.

The result of the interaction between the two piles is reduced stiffness and reduced contribution to damping ratio compared to a single isolated pile. Variation

of stiffness of a single pile in the group, k' calculated using 5.26 is shown in Figure 5.82 while damping, D', calculated using Equation 5.28 is shown in Figure 5.83.

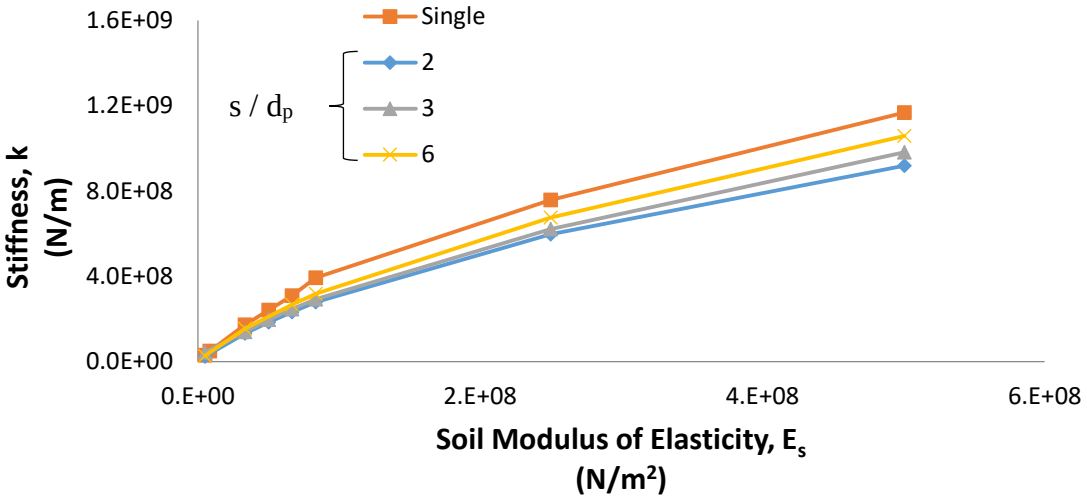

Figure 5.82: Variation of stiffness of a pile in a 2 pile group compared with a single isolated pile.

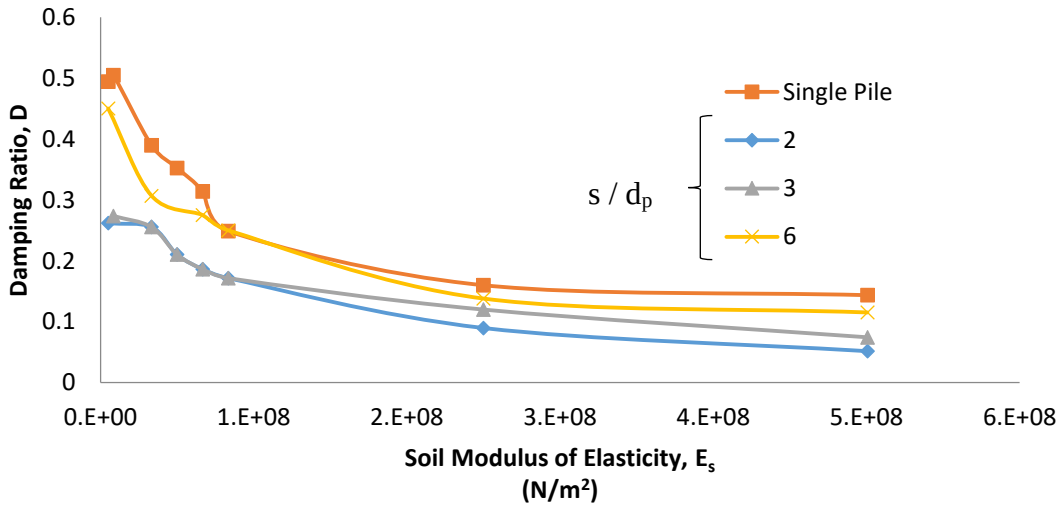

Figure 5.83: Variation of damping of a pile in a 2 pile group compared with a single isolated pile.

Damping of a pile in a 2 pile group calculated as per Equation 5.29 is shown in Figure 5.84.

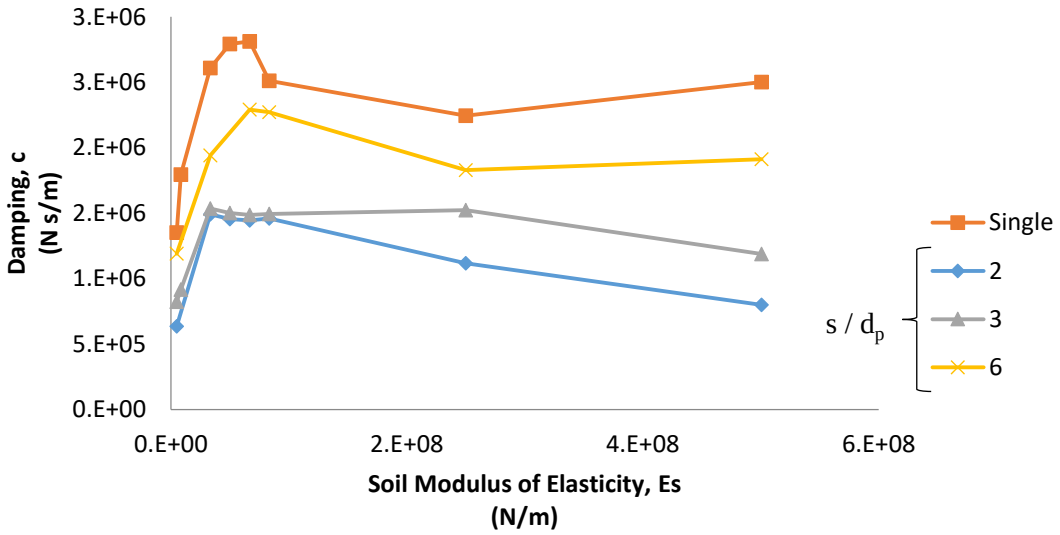

Figure 5.84: Damping of a 2 pile group in homogeneous soil.

5.5.1. Results commentary and analysis

- Results of stiffness interaction factor are plotted in Figure 5.80 for different values of soil modulus of elasticity against the normalized spacing. All curves show that interaction is reduced with increased spacing. This is even more evident in Figure 5.82 that shows that stiffness for different spacing values. The more the spacing is between the pile, the less is the interaction (Figure 5.80). The more the spacing the closer the stiffness curve is to that of a single pile in the same soil (Figure 5.82).
- The interaction means that the spring stiffness that describes the behavior the top of the pile as obtained in Section 5.1 specifically in Figure 5.2 should be reduced if the pile is used in a group. The amount of reduction in the stiffness that should be applied is the interaction factor shown in Figure 5.80.

- The interaction factor shown in Figure 5.80 shows that the effect of soil modulus of elasticity is not perfectly defined. It is then better to describe interaction by an average fitted line. This is shown in Figure 5.85. The R^2 value of the best fit was found to be 0.88, indicating a strong correlation with spacing.

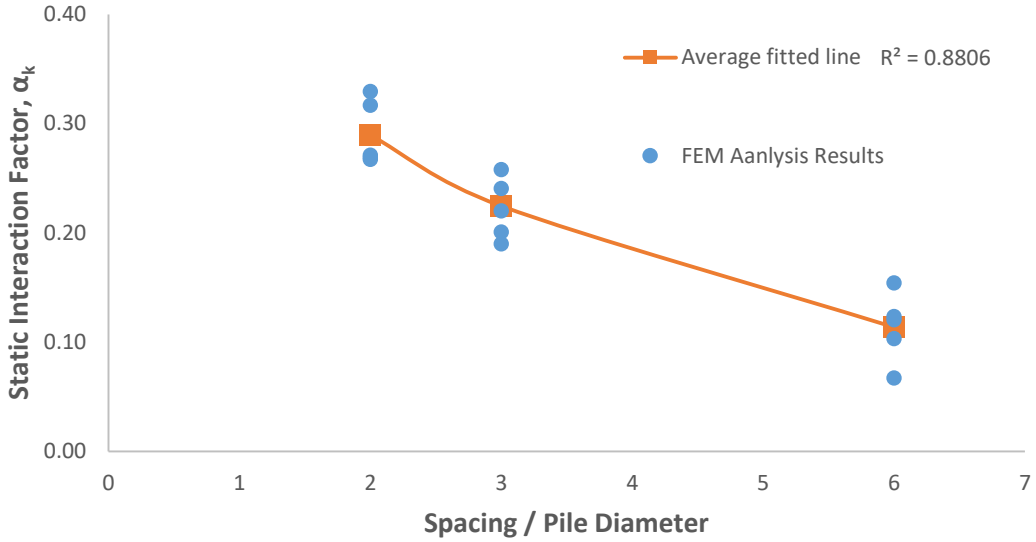

Figure 5.85: Average fitted line for stiffness interaction factor.

- Results of dynamic interaction factors (or damping interaction factors) are plotted in Figure 5.81 for different values of soil modulus of elasticity against the normalized spacing. All curves show that interaction is reduced with increased spacing. This is even more evident in Figure 5.84 that shows that the damping for different spacing values. The more the spacing is between the pile, the less is the interaction (Figure 5.84). The more the spacing is, the closer the damping curves are to the curve of a single isolated pile in the same soil (Figure 5.84).

- The interaction here means that the damping that describes the damping of the top of the pile as obtained in section 5.1 specifically in Figure 5.5 should be

reduced if the pile is used in a group. The amount of the reduction of damping that should be applied is the interaction factor shown in Figure 5.85.

- The interaction factor shown in Figure 5.85 shows that the effect of soil modulus of elasticity is not perfectly defined. It is then better to describe interaction by an average fitted line. This is shown in Figure 5.86. the R^2 value of the best fit was found to be 0.61 indicating a strong correlation with spacing.

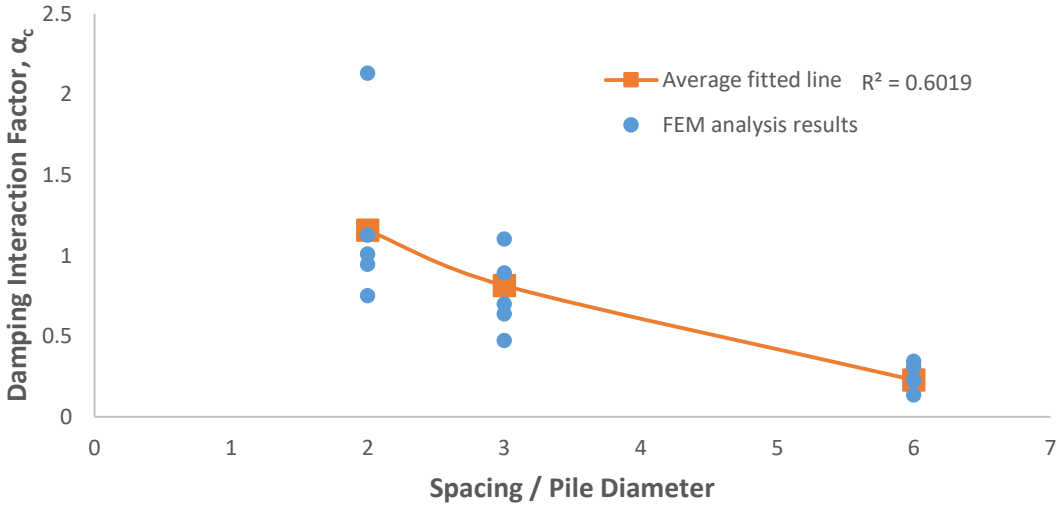

Figure 5.86: Average fitted line for dynamic interaction factor.

5.5.2. Comparison of interaction factors with Poulos (1968)

Interaction factors provided by Poulos (1968) are used in the analysis of pile groups subjected to static loads. In the design of machine foundation, the use of these interaction factors is extended to dynamic loads due to lack of an analytical solution to calculate dynamic interaction factors (Das & Ramana, 2010), (Prakash & Puri 1988) and (Sharnouby & Novak, 1985).

Comparison of static interaction factors provided by Poulos (1968) with stiffness interaction factors obtained by this study (average curve as shown in

Figure 5.85) is shown in Figure 5.87. Comparison of static interaction factors provided by Poulos (1968) with damping interaction factors obtained by this study is shown in Figure 5.88. The static interaction factors given by Poulos (1968) are close to the average line of stiffness interaction factors obtained by this study. The difference may be contributed to the variation in the material properties of the soil which isn't considered in Poulos (1968). The comparison with average damping interaction factors shows that using static interaction factors in the dynamic analysis underpredicts dynamic interaction significantly especially for closely spaced piles.

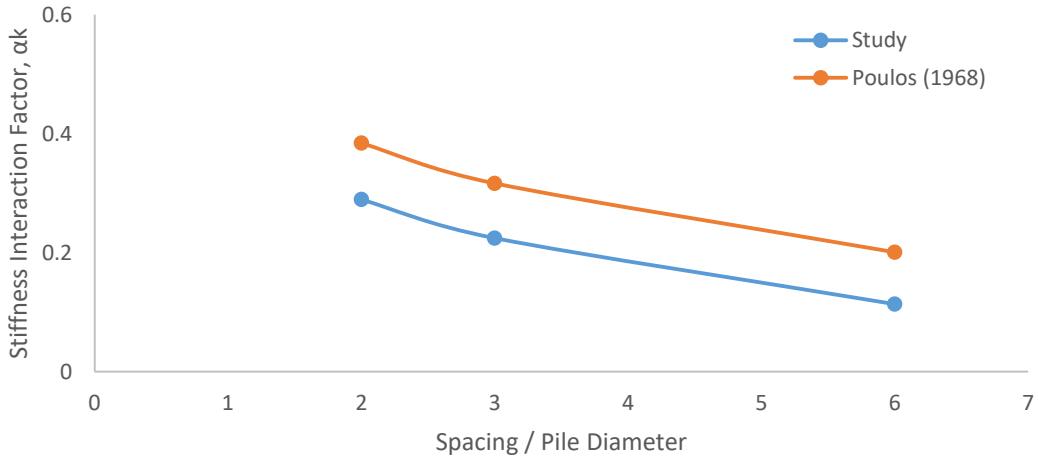

Figure 5.87: Comparison of average stiffness interaction factors with static interaction factors given by Poulos (1968).

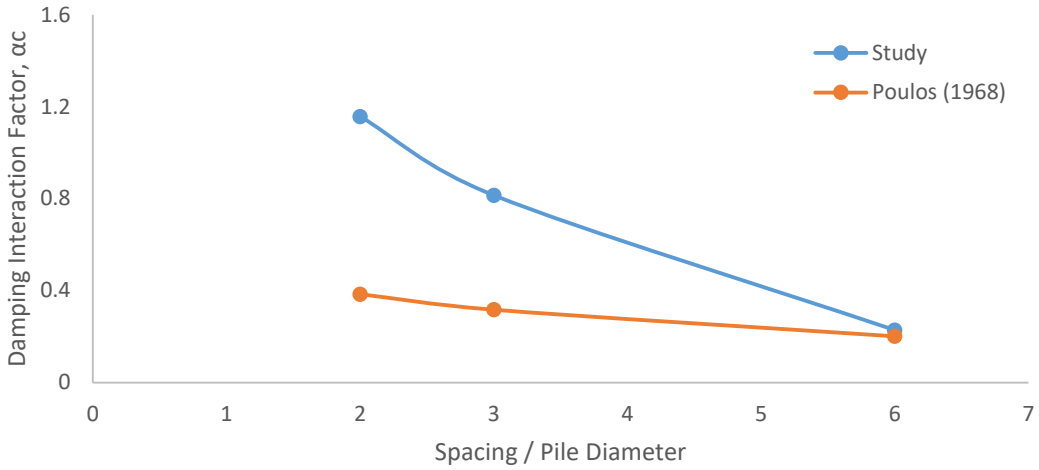

Figure 5.88: Comparison of average damping interaction factors with static interaction factors given by Poulos (1968).

5.6. Frequency independence of the stiffness and damping

In soil dynamics, the stiffness and damping of foundation systems are described using spring and damper analogy. However, the stiffness and damping of foundations provided are dependent on the frequency of the vibration. For example for shallow foundations, Reissner (1936) found a solution for the motion of a rigid disk on the surface of an elastic half-space. The solution simplified to spring and damper analogy by Hsieh (1962). In the latter solution, the stiffness and damping were found to be frequency dependent (i.e. a function of the frequency). Lysmer & Richart (1966) came up with a solution where the stiffness and damping of a shallow foundation were frequency independent. The solution produced accurate results for the response of a shallow foundation within a certain range of frequency. The results were in accordance with Reissner (1936). The stiffness of the foundation was the same obtained from elastic analysis of a statically loaded area over an elastic half-space. The damper is obtained through dynamic analysis.

Novak (1974) solved the Equation of motion for a floating pile foundation. The stiffness and damping of the of the pile were found to be function of the frequency, however at dimensionless frequency, $a_0 = 0.3$, stiffness and damping were found stationary and independent of the frequency. Novak (1974) presented Equations for stiffness and damping independent of the frequency while compromising accuracy at other values of a_0.

A system consisting of a mass, a spring and a dashpot can describe the motion of the pile top when subjected to vertical loading. The mass is the mass supported by the pile; the spring has a spring constant that is equal to the static stiffness of the pile and dashpot that has a coefficient that represents energy loss in the soil-pile system due to radiation damping. A procedure is described in section 4.4 of this thesis of how these parameters were obtained. The concept is extended to different cases of piles in non-homogeneous soils and friction and end bearing pile. The concept is also extended to the case of the pile-to-pile interaction, where the piles are assumed to act as two sets of mass, spring and dashpot vibrating in parallel. This assumption allows the required parameters of the two piles to be obtained by analyzing a group (without a cap to eliminate the effect of the cap from interfering with the results) statically to compute stiffness and dynamically to compute damping using the procedure described in section 4.4. In the pile-to-pile interaction study the stiffness of a single pile in the group is the stiffness of the group divided by 2. Similarly, damping of a single pile in the group is damping of the group divided by 2. The stiffness and damping of a single pile in the group are always less than that of a single isolated pile. Interaction is calculated based on the reduction in stiffness and damping of a pile in a group compared to that of an isolated pile. The

stiffness and damping of all cases in this research are found to be independent of the frequency in the range of the data studied.

In order for the assumption to be valid, the following points should be valid:

1- The stiffness and damping obtained should be able to predict the steady state motion (i.e., dynamic displacement) at the pile top at any frequency using the following Equation:

$$u_d = \frac{Q}{k} \frac{1}{\sqrt{\left(1 - \frac{f^2}{f_n^2}\right)^2 + 4D^2 \frac{f^2}{f_n^2}}} \tag{5.32}$$

Where Q is the dynamic load amplitude, k is the spring constant, f is the frequency at which the dynamic displacement, u_d is calculated, f_n is the natural frequency of the system where $f_n = (1/2\pi)\sqrt{k/M}$, and D is the damping ratio where $D = c/2\sqrt{k\,M}$. The spring constant is equal to the static stiffness of the pile. Damping describes energy loss due to radiation damping only, as no consideration of material damping is applied in this research. Frequencies from 2.5 to 30 Hz are used to calculate D using dynamic finite element analysis while static analysis was used to calculate the stiffness, k. The plot of Equation 5.32 of the frequency range used matches the dynamic displacement calculated by finite element analysis. This means the damping and spring constant calculated are the actual values of stiffness and damping of the pile independent of the frequencies. At least this can be said for the range of the frequencies analyzed and used in calculation. Figure 5.89 is an example of how a plot of Equation 5.32

matches the dynamic displacement calculated by finite element analysis. The dots in Figure 5.89 are finite element results of displacements for specific case while the solid line is a plot of Equation 5.32 using damping and spring constant for that same specific case. The fact that a predicted line fits perfectly with finite element results used in calculation of stiffness and damping was observed in every case analyzed in this research and is an indication of frequency independency of the values of stiffness, k and damping ratio, D obtained in this research at least within the frequency range of 2.5 and 30 Hz. (i.e., fitting Equation 5.32 to a dynamic displacement points similar to those dots shown Figure 5.89 as described in Section 4.4 yields almost a perfect fit in every case analyzed).

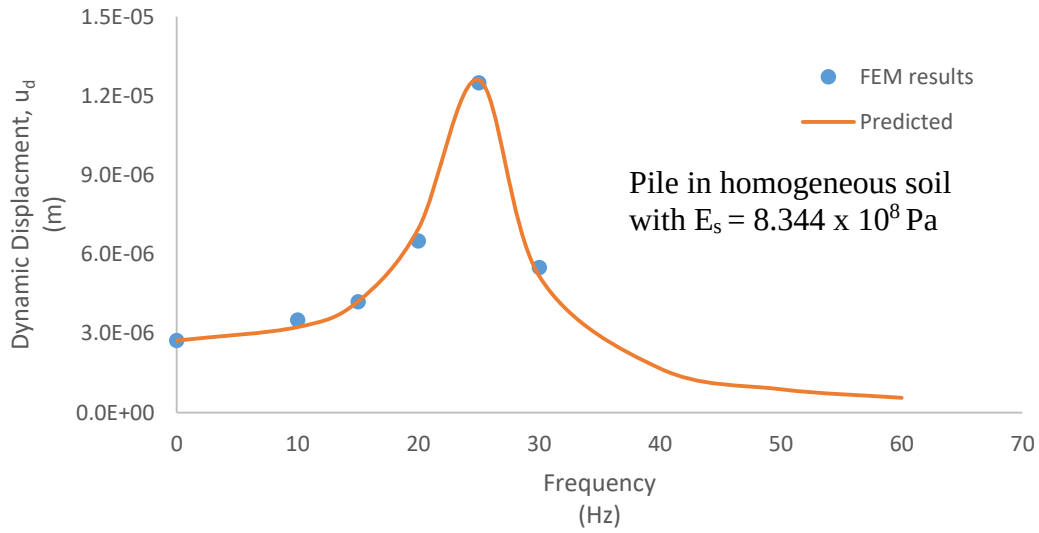

Figure 5.89: Dynamic displacement results plotted using Equation 5.32 (solid line) and finite element results (dots).

2- Using a frequency range of 2.5 to 30 Hz, the stiffness and damping calculated and presented the ability to match finite element analysis results. A test to see if the spring and damping are also valid for frequencies greater than 30 Hz was performed. The frequencies investigated were 40, 50 and 60. The test was performed only at the minimum and the maximum value of study variables used in each case. The results of this test found that the stiffness and damping calculated can be used to predict the steady-state dynamic displacement at the top of the pile for frequencies greater than 30 Hz. No change in stiffness and damping is observed. Dynamic displacement results obtained using finite element analysis for frequencies greater than 30 Hz agrees with Equation 5.32. As an example see Figure 5.90 that shows values of dynamic displacements obtained by finite element analysis fall on the curve used to predict the displacement.

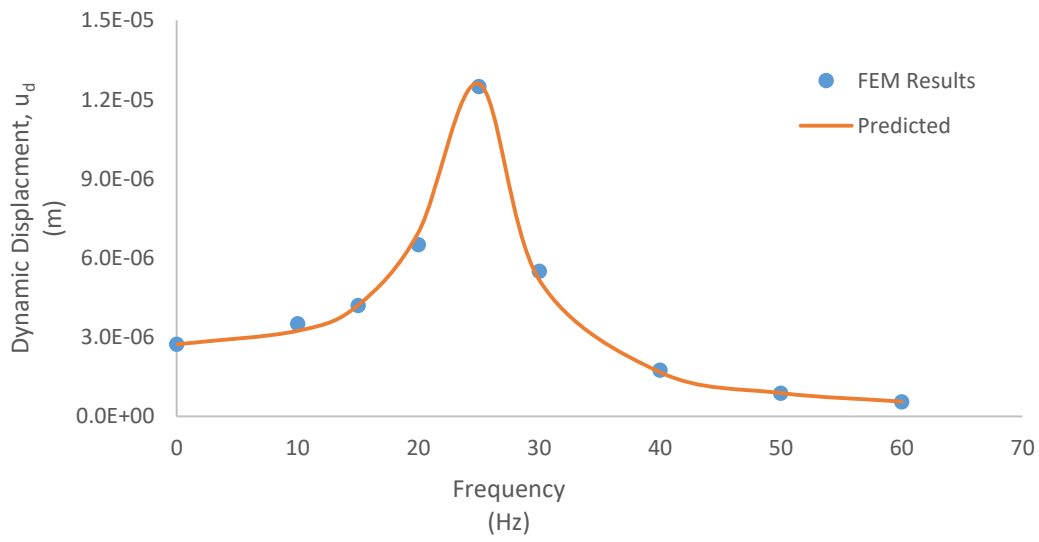

Figure 5.90: Dynamic displacement results plotted using Equation 5.32 (solid line) and finite element results (dots).

3- The resonance (frequency of maximum displacement), f_n is calculated using the spring constant, k and the mass supported by the pile, M where $f_n = 1/(2\pi)\sqrt{k\,M}$. As an example, see Figure 5.89. In Figure 5.89 a pile embedded in a homogeneous soil with soil modulus of elasticity of 8.344 x 10^8 Pa, the natural frequency was calculated to be 25 Hz. The resonance frequency from finite element analysis is found at this number as shown in Figure 5.89. Agreement of frequency of maximum dynamic displacement (obtained from FEM) with resonant frequency calculated from spring constant is observed in all cases studied in this research. This means that maximum dynamic displacement obtained via finite element occurs near resonant frequency, f_n obtained from spring constant. If this is true, it can be said the stiffness and damping computed are the true stiffness and damping of the system.

4- If the stiffness and damping are frequency independent, they should be able to predict the motion at the top of the pile in the time domain for any frequency of loading. This means that time history analysis of a single degree of freedom consisting of a mass, a spring, and a damper with stiffness and damping calculated using the procedure described in section 4.4 should be similar and close to time history analysis using finite element simulation of the actual soil-pile system. This was also found to be true in several tests at different frequencies. Examples of time history comparison between the single degree of freedom and finite element analysis of a pile are shown in Figure 5.91 (a) to Figure 5.90 (d) . It can be seen from Figure 5.91 that the single degree of freedom (SDOF) time history matches the time history analysis of finite element simulation of the pile.

Figure 5.91: (a) to (d): Examples of time history analysis for FEM and SDOF.

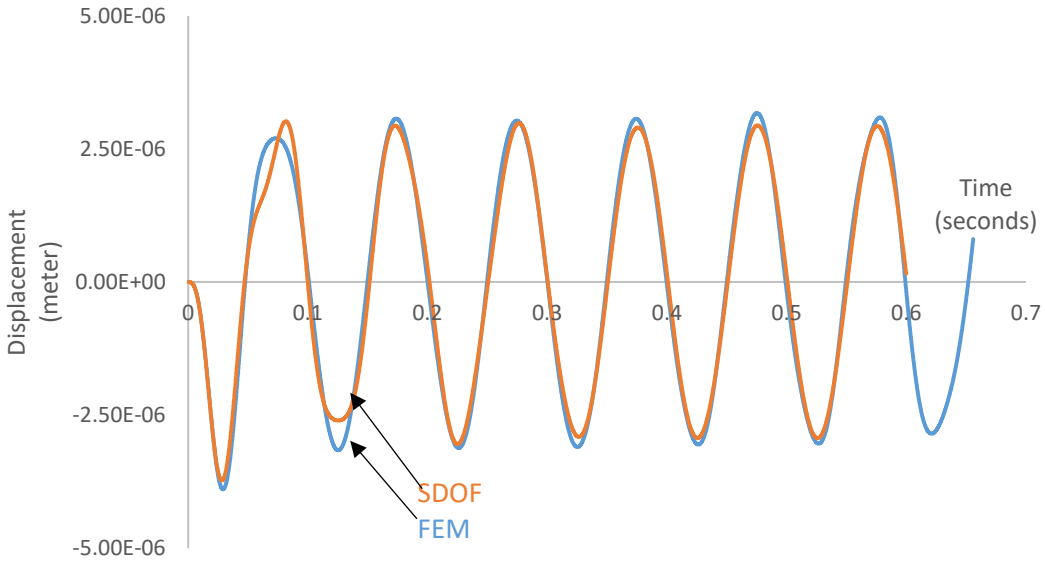

Figure 5.91 (a) Time history analysis for end bearing pile and SDOF representing the case. Frequency = 10 Hz. Homogeneous soil with modulus of Elasticity = 8.344×10^8 $Pascals$.

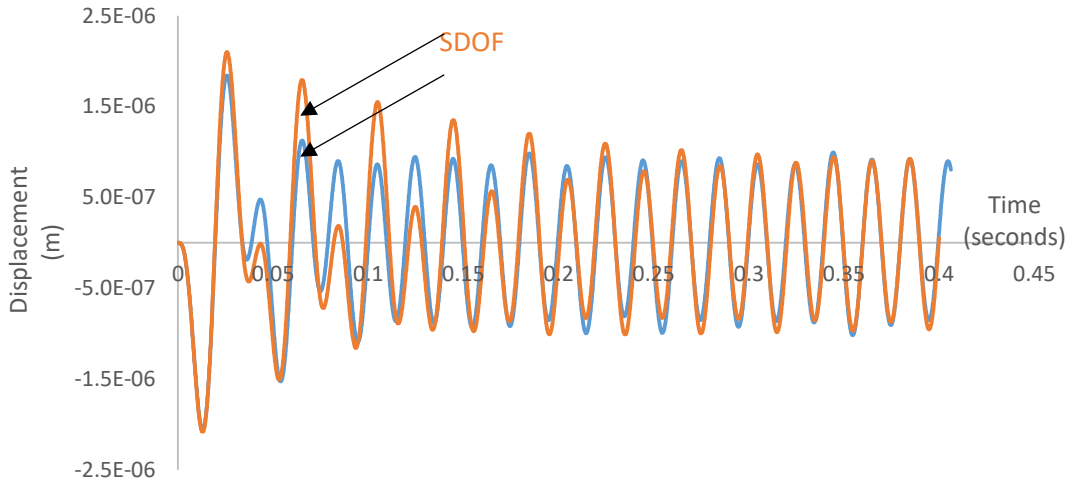

Figure 5.91 (b) Time history analysis for an end bearing pile and SDOF representing the case. Frequency = 50 Hz. Homogeneous soil with modulus of Elasticity = 8.344×10^8 $Pascals$.

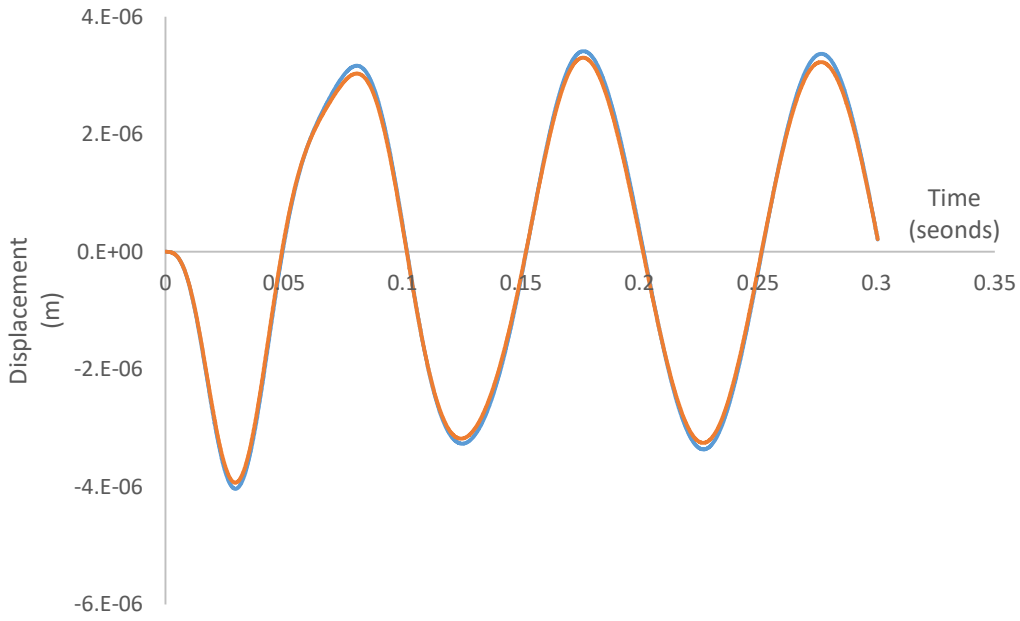

Figure 5.91 (c) Time history analysis for a floating pile and SDOF representing the case. Frequency = 10 Hz. Homogeneous soil with modulus of Elasticity = 8.344×10^8 $Pascals$.

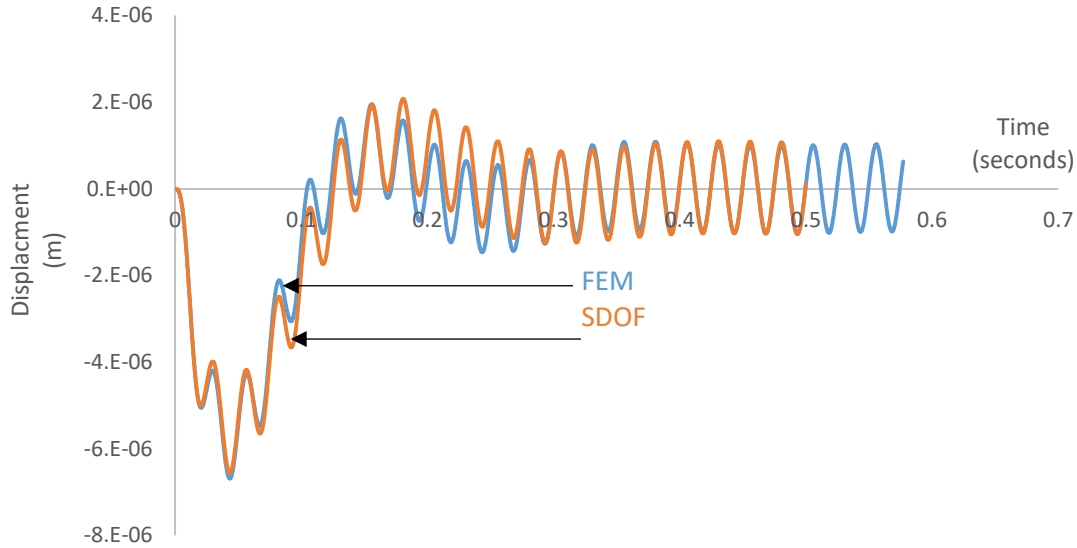

Figure 5.91 (d) Time history analysis for a floating pile and SDOF representing the case. Frequency = 40 Hz. Homogeneous soil with modulus of Elasticity = 8.344×10^8 $Pascals$.

5.7. A discussion on design applications

5.7.1. Design of a pile in homogenous soil

Comparison of stiffness obtained by this study with Novak (1974) shows a great difference in stiffness and damping. Comparison of stiffness and damping with Chowdhury & Dasgupta (2008) shows good agreement of stiffness only at a low modulus of elasticity of the soil. However, comparison of damping ratio shows no agreement as damping ratio calculated by Chowdhury & Dasgupta (2008) was constant at any value of the soil modulus of elasticity. To show how analyzing a pile subjected to vertical dynamic load using stiffness and damping obtained by Novak (1974) and Chowdhury & Dasgupta (2008) differ from finite element analysis, see Figure 5.92. The graph shows differences in resonance frequency and displacement at resonance. The displacements values are agreeable after resonant frequency. Pile properties in this examples are the same used in this research.

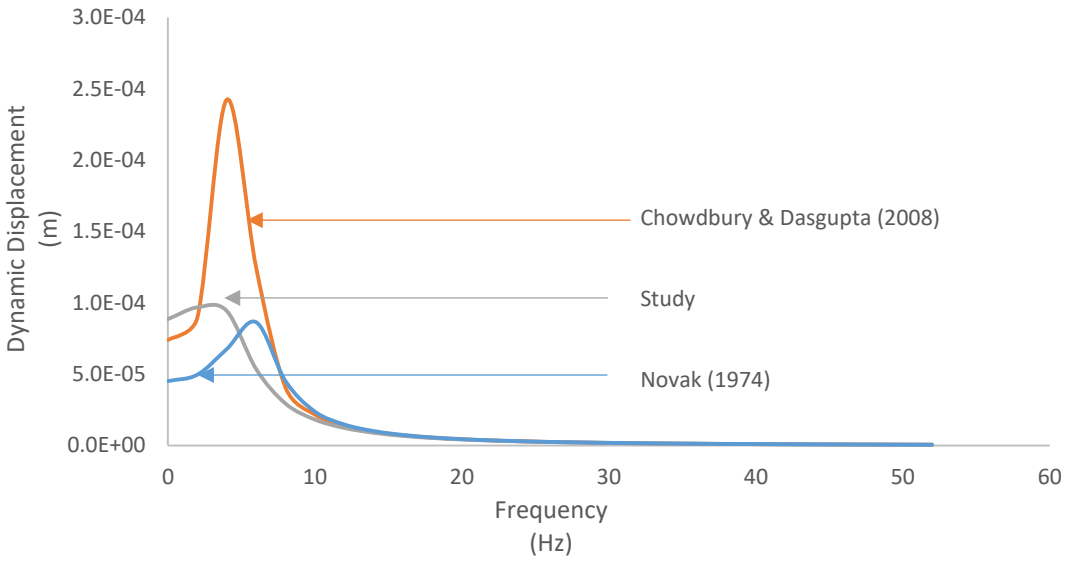

(a)

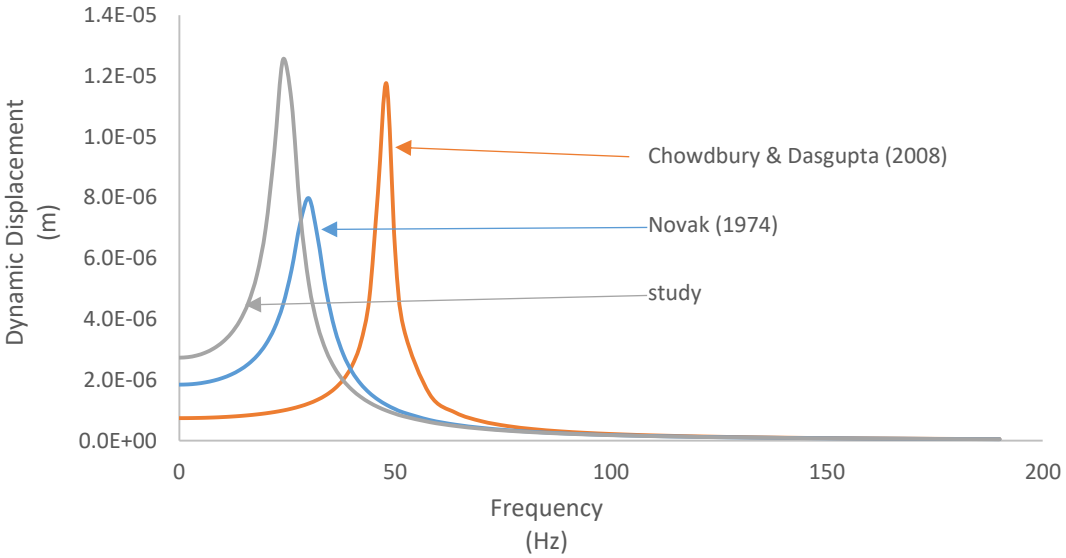

(b)

Figure 5.92: Comparison of dynamic displacement at different frequencies.

(a) $E_s = 8.344 \times 10^6\ pa$ (b) $E_s = 8.34 \times 10^8\ Pa.$

Comparison of stiffness and damping obtained by this research with Novak (1974) is provided. The stiffness values obtained by Novak (1974) were significantly different and higher than those obtained in this research. Damping

ratio decreases with increase in soil elastic modulus if obtained by Novak (1974). Damping ratios calculated by this research were found to be increasing with the increase in soil modulus of elasticity. Comparison of stiffness and damping obtained by Chowdhury & Dasgupta (2008) and those obtained by this research found no agreement. Stiffness obtained by Chowdhury & Dasgupta (2008) was significantly higher than that obtained in this research. Figure 5.93 shows how using stiffness and damping obtained by Novak (1974) and Chowdhury & Dasgupta (2008) compare with those obtained by this study in predicting dynamic displacement at any frequency. The methods differ in predicting resonance frequency and displacement at resonance. After resonance, both methods show agreement in predicting dynamic displacements.

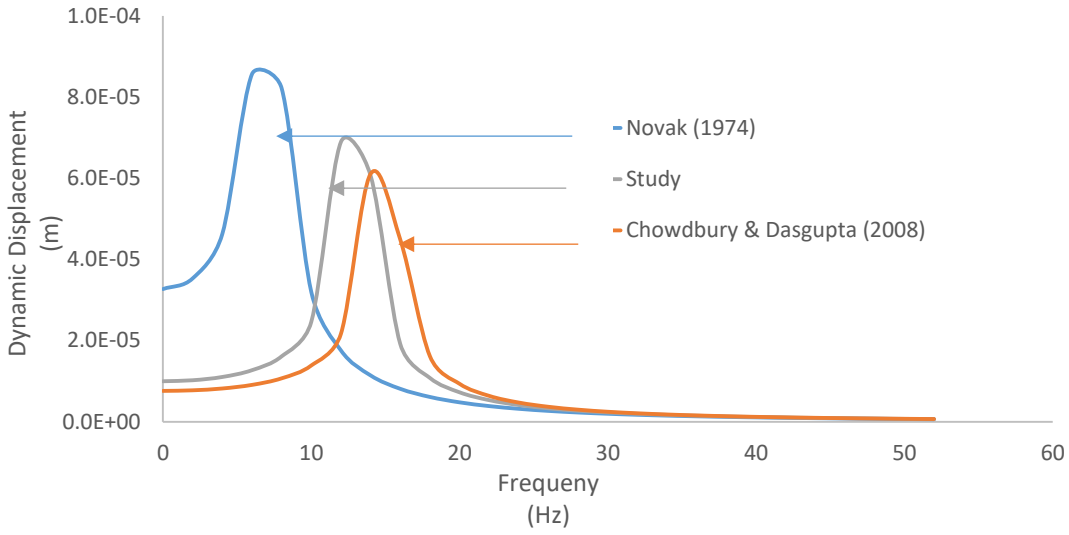

(a)

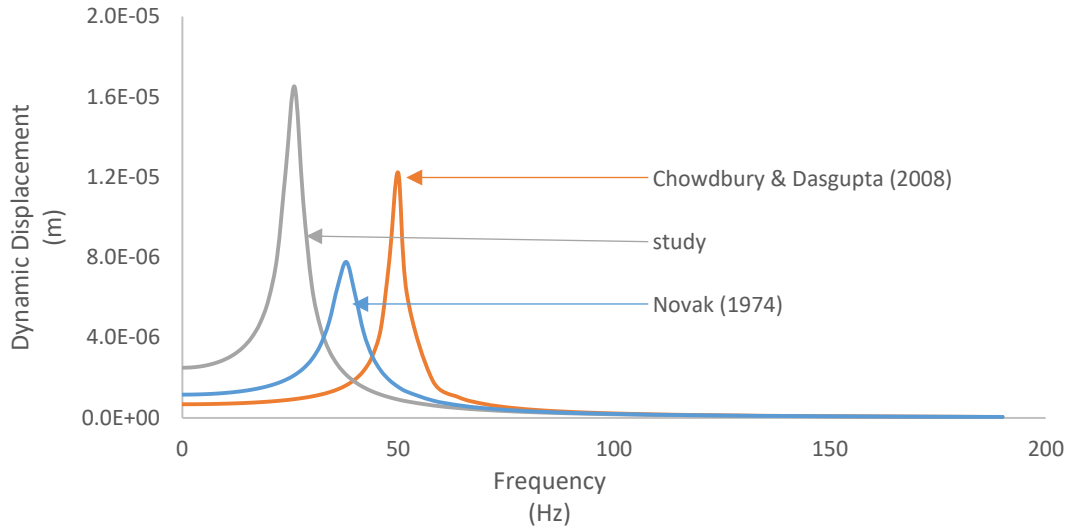

(b)

Figure 5.93: Comparison of dynamic displacement at different frequency.

(α) $E_s = 8.344 \times 10^6\ pa$ (b) $E_s = 8.34 \times 10^8\ Pa.$

In the case of designing a floating or an end-bearing pile in a homogeneous soil, comparison of stiffness obtained by finite element analysis with Novak (1974) found that stiffness obtained by Novak (1974) is overestimated. This overestimation in stiffness lead to overestimation in critical damping, c_{cr} , and the damping ratio which is equal to c/c_{cr}. It also affects the value of the natural frequency. However, calculating damping, c using Novak (1974) is more agreeable with finite element results. As a result, ıt is suggested to use an analytical solution based on static elastic analysis of piles to obtain stiffness of the pile. One method was presented earlier in section 5.1.2.1 by Gazetas & Mylonakis (1998). In fact using such a method for stiffness makes Novak solution more agreeable with finite element data in determining dynamic displacement at any frequency as well as determining resonant frequency. This is because adjusting the stiffness automatically adjusts the value of the damping ratio, D as shown in Figure 5.94 for damping of a floating pile and 5.95 for damping of an end bearing pile. It can be seen from Figures 5.94 and 5.95 that using a static stiffness reduces the difference in damping between finite element and Novak (1974). In fact, using a stiffness computed by static analysis makes the damping ratio curve obtained by Novak (1974) agreeable with finite element results not only in values but also in the pattern (i.e. increasing with increase in soil modulus of elasticity) for the case of an end bearing pile.

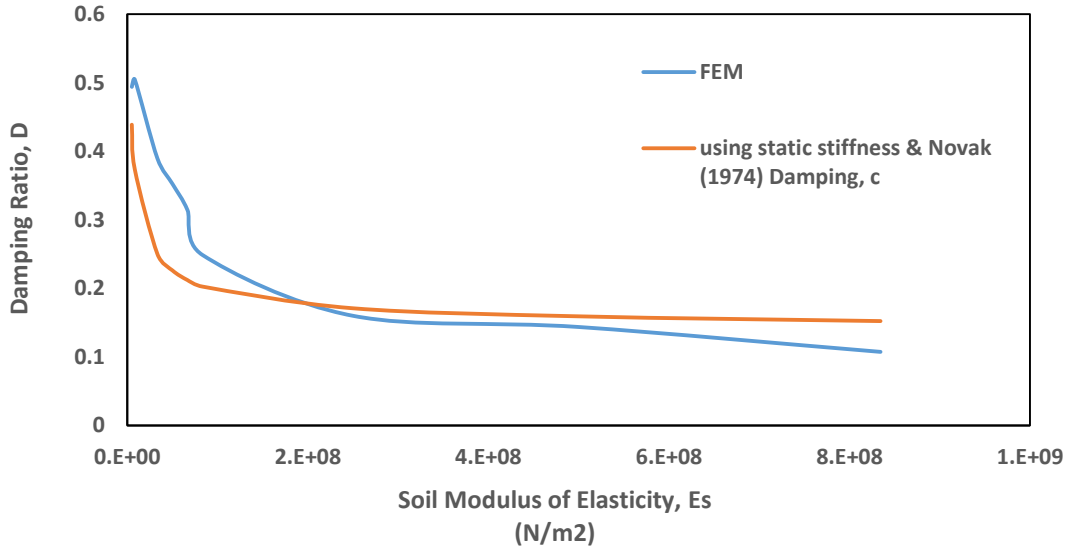

Figure 5.94: Comparison of Damping ratio between FEM and Novak (1974) after adjusting stiffness for a floating pile.

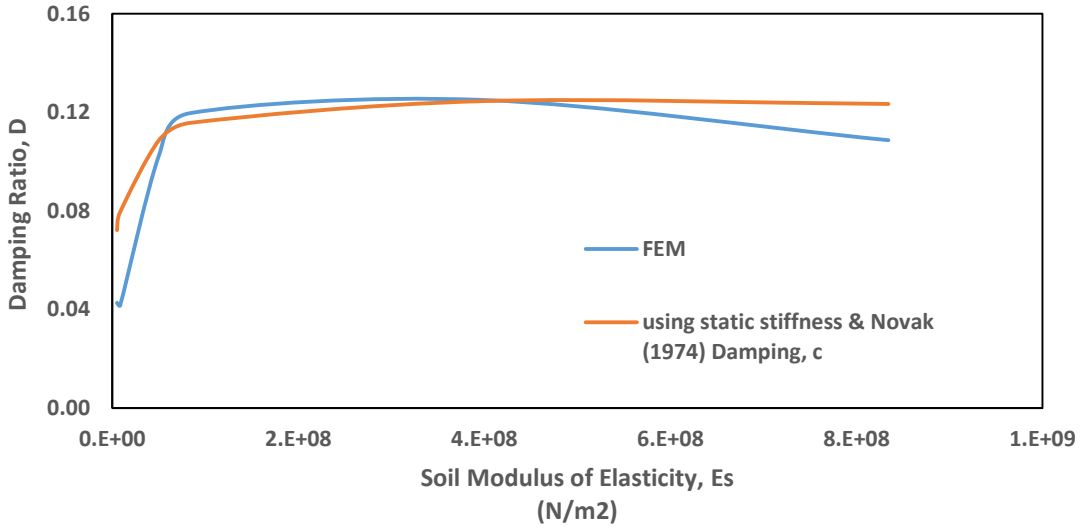

Figure 5.95: Comparison of Damping ratio between FEM and Novak (1974) after adjusting stiffness for an end-bearing pile.

5.7.2. Design of a pile group

An example is provided to show how interaction factors are used in designing a pile group using static and dynamic interaction factors. The example considers 2 approaches: (1) the currently used one where Poulos (1968) interaction factors are applied to both stiffness and damping and (2) The new interaction factors obtained by FEM are applied to stiffness of the group and damping interaction factors are applied to damping of the group. The parameters of the soil and the pile are summarized in Table 5.10. The problem is shown graphically in Figure 5.9

Table 5.10:Summary of soil and pile parameters for example of design of pile groups.

Parameter	Symbol	Unit	Value
Pile Modulus of Elasticity	E_p	$Pascal$	$2.1x10^{10}$
Pile Poisson's Ratio	μ_p		0.25
Pile Mass Density	ρ_p	kg/m^3	2500
Pile Diameter	d_p	m	0.5
Pile Length	L_p	m	10
Pile Spacing from center to center	S	m	1 .5
Cap thickness	t	m	1
Cap width	w	m	5
Cap Length	L_C	m	5
Cap mass density	ρ_C	kg/m^3	2500
Soil Modulus of Elasticity	E_s	$Pascal$	5.0×10^8
Soil Poisson's Ratio	μ_s		0.45
Soil Mass Density	ρ_s	kg/m^3	1800

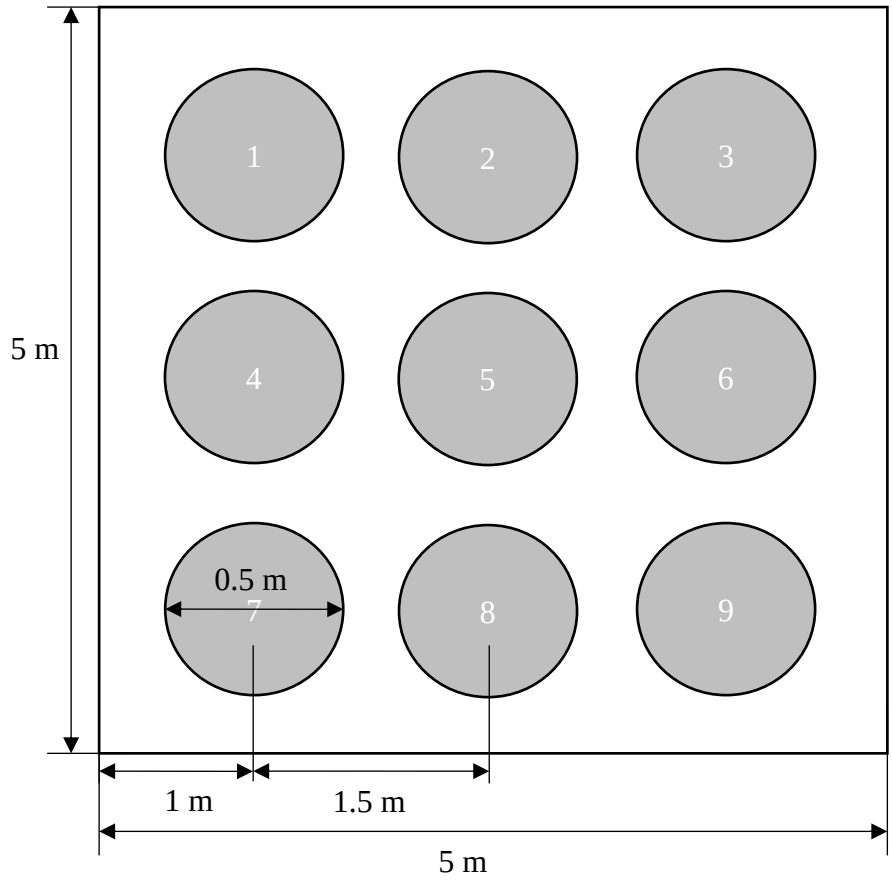

Figure 5.96: Outline of pile group for design example.

The stiffness and damping of an isolated pile of that group is found from finite element analysis to be $1.17 \times 10^9\ N/m$ and $2.5 \times 10^6\ N\ s/m$ respectively. Using pile number 1 as the reference pile, stiffness interaction factors are calculated. Values of interaction factors are shown in Table 5.11.

Table 5.11: Values of interaction factors for pile group design example.

		Poulos (1968)	stiffness	damping
Pile	spacing from reference pile	αk	αk	αc
1	0.00	1.00	1.00	1.00
2	1.50	0.59	0.34	0.81
3	3.00	0.37	0.22	0.23
4	1.50	0.59	0.34	0.81
5	2.12	0.48	0.28	0.52
6	3.35	0.34	0.21	0.13
7	3.00	0.37	0.22	0.23
8	3.35	0.34	0.21	0.13
9	4.24	0.27	0.17	0.00
	Σα	4.35	2.98	3.87

Based on interaction factors shown in Table 5.11, the stiffness and damping of the group using Poulos method are:

$$k_G = \frac{nk_p}{\Sigma\alpha} = \frac{9(1.17 \times 10^9)}{4.35} = 2.42 \times 10^9\ N/m \tag{6.1}$$

$$c_G = \frac{nc_p}{\Sigma\alpha} = \frac{9(2.5 \times 10^6)}{4.35} = 5.30 \times 10^6\ N\ s/m \tag{6.2}$$

While based on the second approach, the stiffness and damping of the group are

$$k_G = \frac{nk_p}{\Sigma\alpha} = \frac{9(1.17 \times 10^9)}{2.98} = 3.35 \times 10^9\ N/m \tag{6.3}$$

$$c_G = \frac{nc_p}{\Sigma\alpha} = \frac{9(2.5 \times 10^6)}{3.87} = 5.81 \times 10^6\ N\ s/m \tag{6.4}$$

The response of the foundation is shown in Figure 5.97. In Figure 5.97 it is shown that there is 45% difference in stiffness and 10% difference in damping between the two methods. These numbers might differ from problem to problem as the interaction factors are dependent on pile spacing.

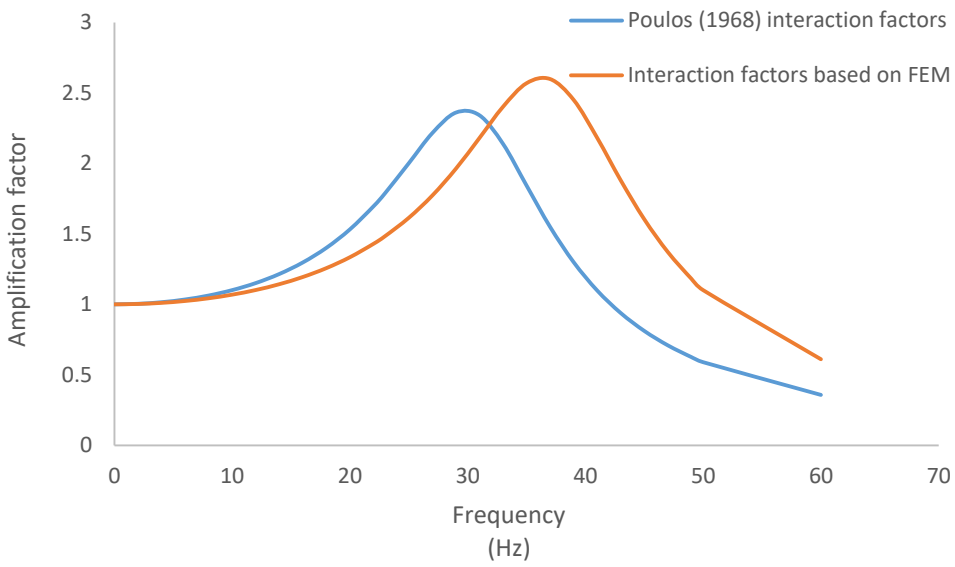

Figure 5.97: response of pile group in design example.

6. Design Charts and Conclusion

6.1. Design Charts

In the case of inhomogeneity in the soil profile along the pile. The stiffness, k and damping, c should be reduced. Reduced stiffness, k_r and reduced damping, c_r charts are provided in Figure 6.1 and 6.2 for floating piles and Figures 6.3 and 6.4 for an end bearing pile. To use Figures 6.1, 6.2 , 6.3 and 6.4:

a. Stiffness and damping are calculated based on a homogenous soil with a modulus of elasticity equal to E_{sc}.
b. The inhomogeneity ratio is calculated as D_c/L_p.
c. From D_c/L_p , the reduction in stiffness and damping k_r/k_h and c_r/c_h could be obtained using Figures 6.1 6.2 , 6.3 and 6.4.
d. finally k_r and c_r could be obtained.

E_{sc} is the constant modulus of elasticity at a depth D_c below the ground surface, L_p is the pile length, k_r and c_r are reduced stiffness and damping due to inhomogeneity, and $k_h$and c_h are the stiffness and damping of the soil if it were homogeneous with a modulus of elasticity equal to E_{sc}.

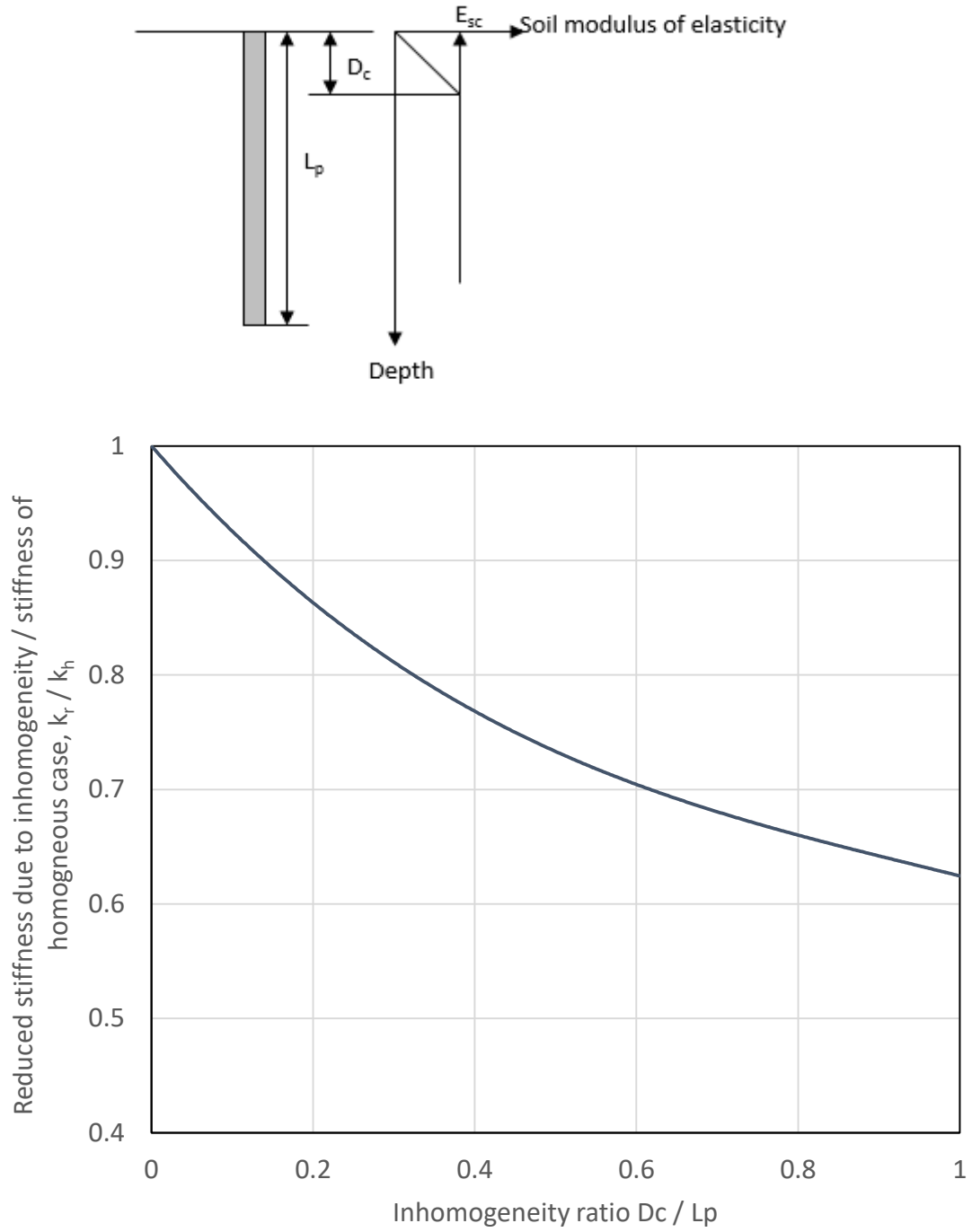

Figure 6.1: Reduction in stiffness of a floating pile due to inhomogeneity of soil profile.

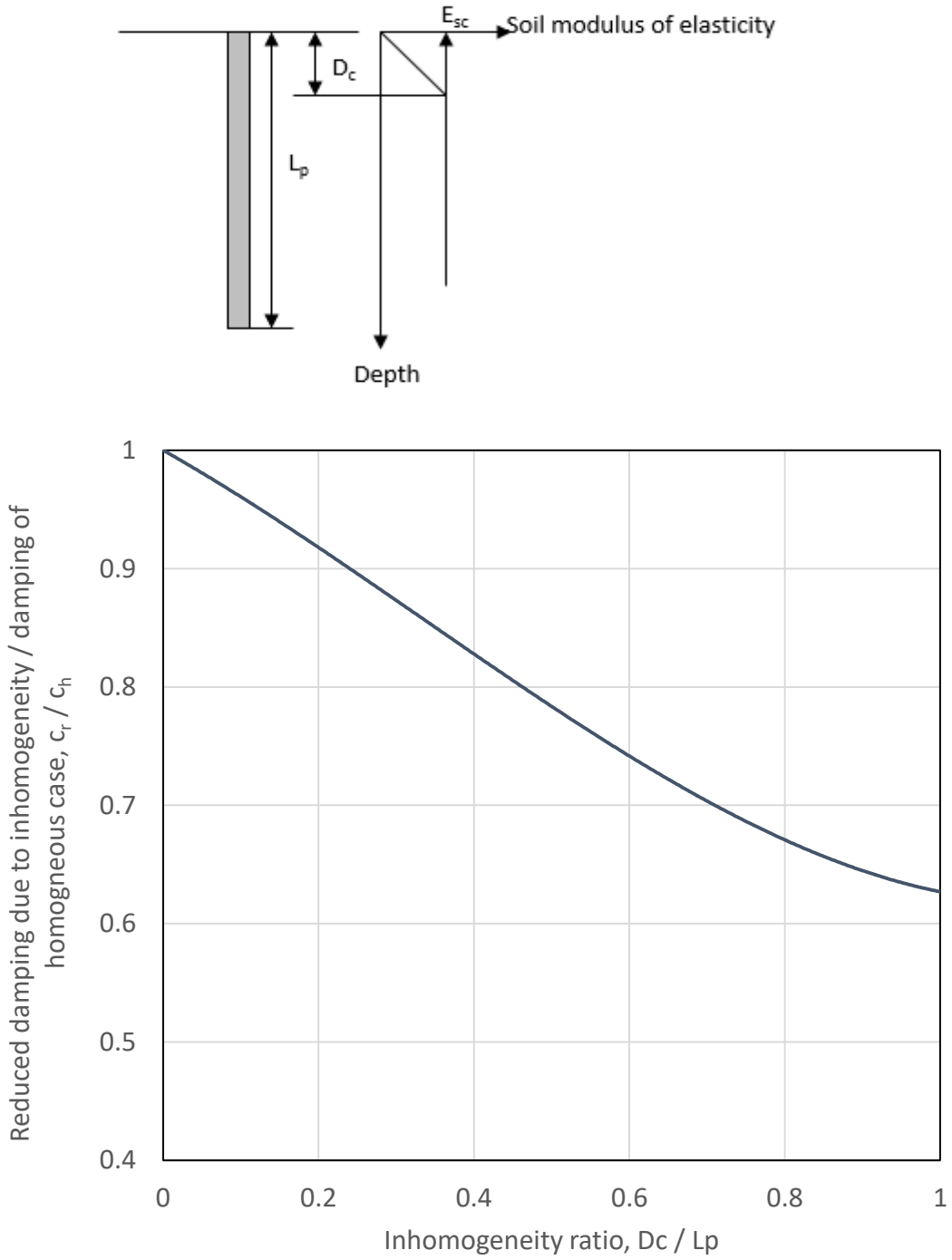

Figure 6.2: Reduction in damping of a floating pile due to inhomogeneity of soil profile.

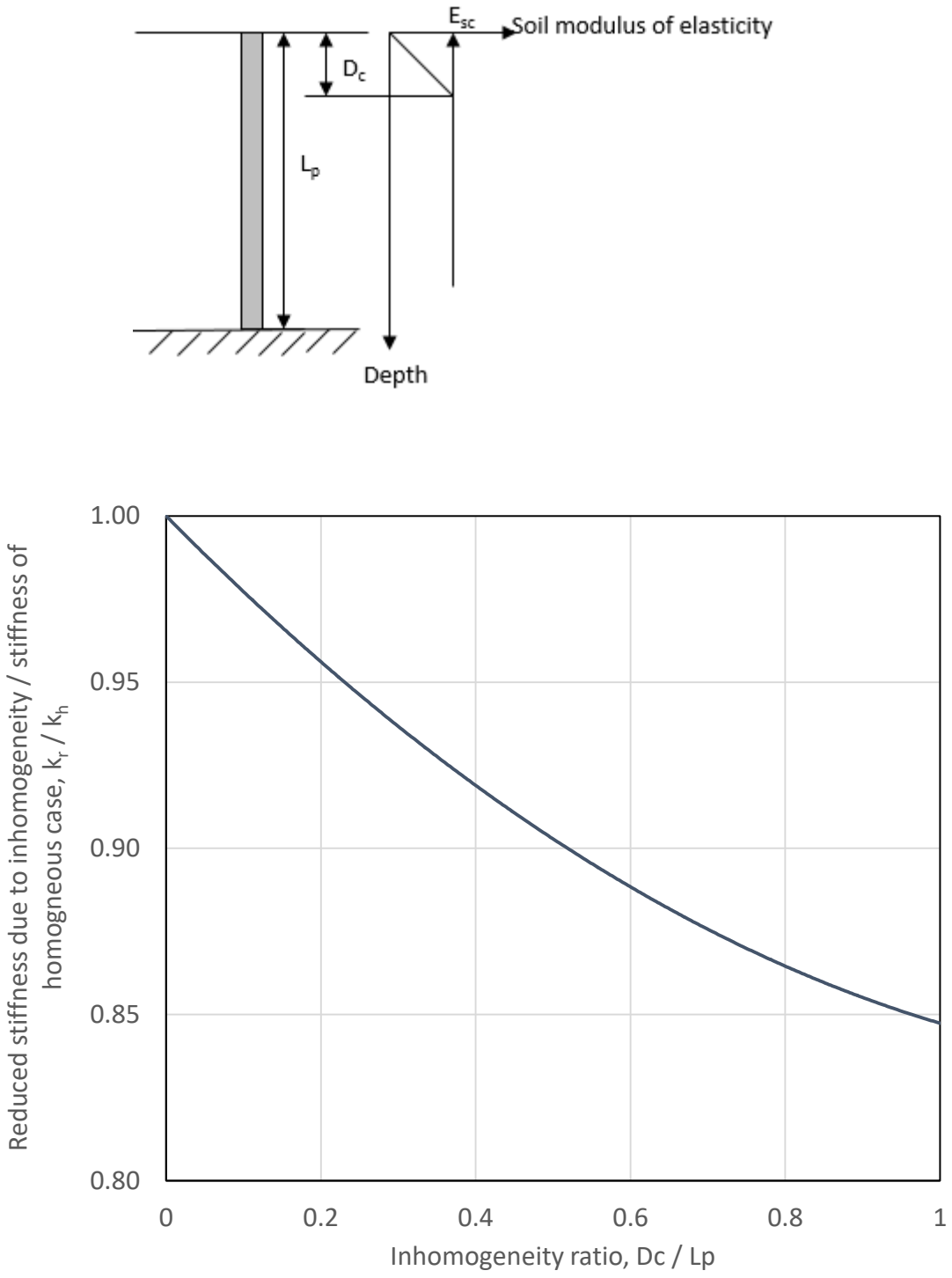

Figure 6.3: Reduction in stiffness of an end bearing pile due to inhomogeneity of soil profile.

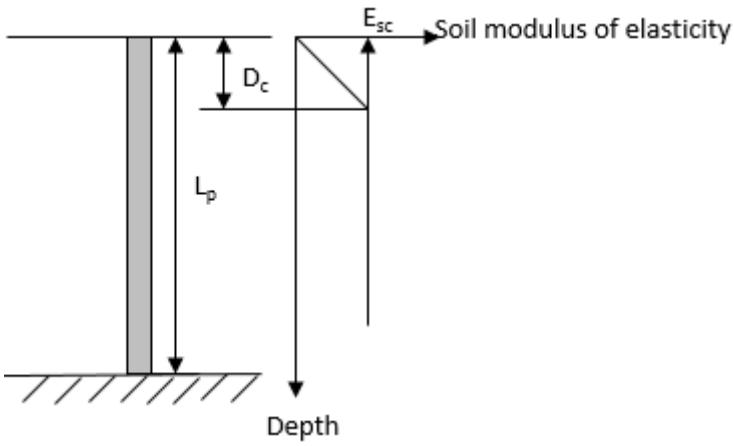

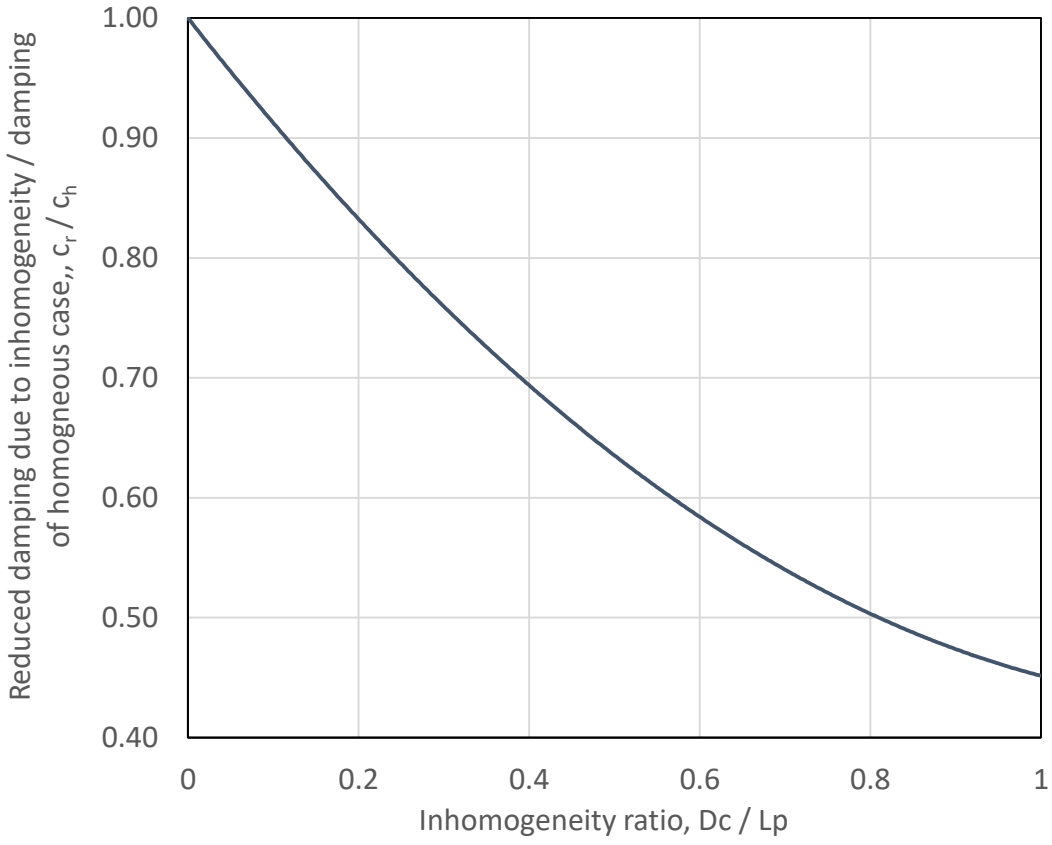

Figure 6.4: Reduction in Damping of an end bearing pile due to inhomogeneity of soil profile.

In the case of pile group, Average interaction factors that should be applied to stiffness and damping of a pile group are introduced in section 5.5. The

interaction factors suggested to be applied on stiffness and damping interaction factors are shown in Figure 6.5.

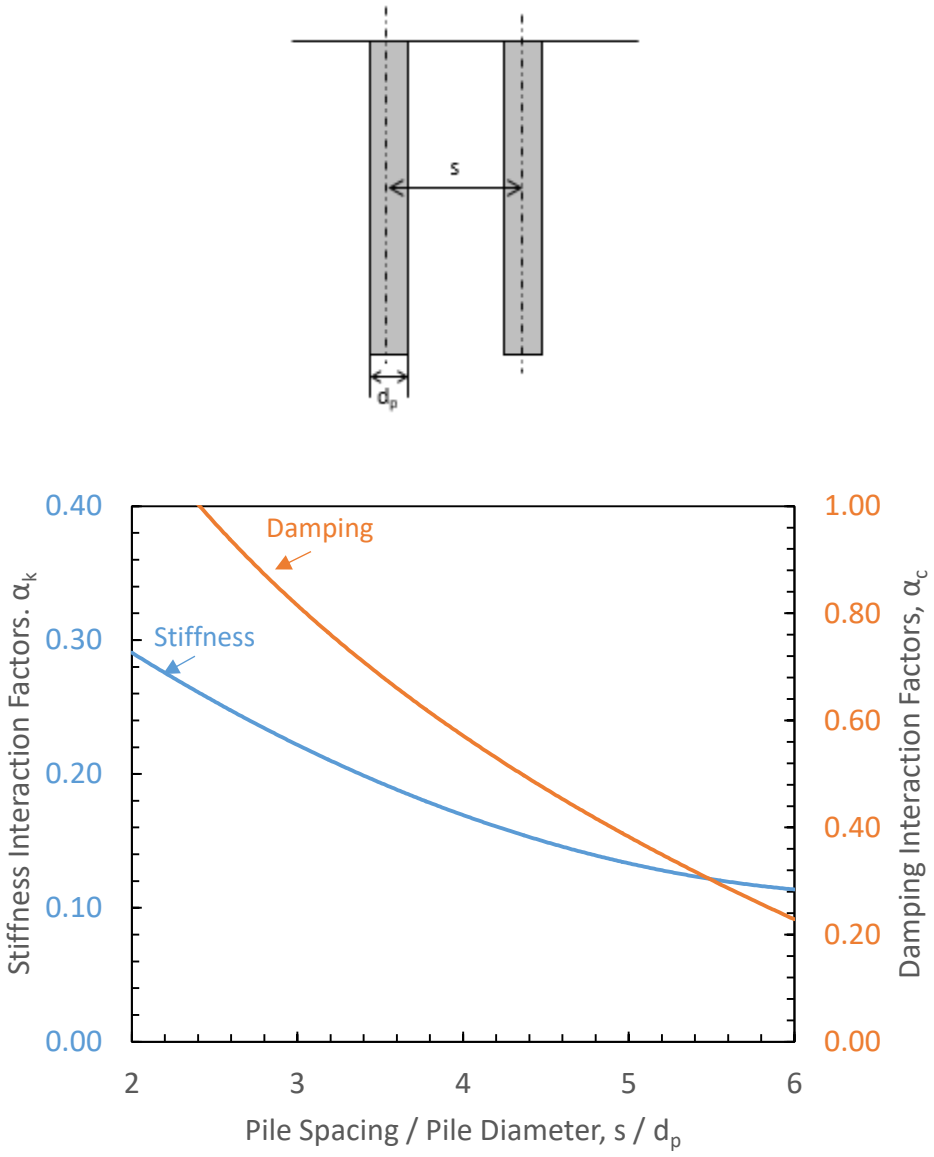

Figure 6.5: Stiffness and damping interaction factors.

6.2. Conclusion

The stiffness and damping of a pile top when subjected to vertical vibration are needed for the design of a pile subjected to dynamic loading.

Piles are mostly used in groups. The stiffness and damping of individual piles within a pile group are less than that of an isolated pile due to pile-to-pile interaction. The interaction between piles is accounted for in design by using interaction factors. The process of designing a pile group begins by designing an individual pile and then modify the design to account for interaction using interaction factors. Interaction factors that are currently in use are the ones provided by Poulos (1968). However, these interaction factors are based on static analysis of pile to pile interaction.

This research focuses on variation in the conditions of the soil surrounding the pile and the soil at the pile tip. The research studies floating and end bearing piles in homogeneous and nonhomogeneous soils. The research also studies pile to pile interaction in homogeneous soils. In all the cases studied, the response at the top of the pile can be represented by a single degree of freedom system consisting of a mass, a spring, and a damper. The spring stiffness is the same as the stiffness of the pile and the damper represents energy loss due to radiation damping. The mass represents the mass supported by the pile. A method described in section 4.4 of this dissertation was used to obtain the stiffness and damping of the pile-soil system. Charts of the variation of stiffness and damping with variation in soil conditions are provided for each case studied in this research.

The concept of replacing the pile with a mass, spring and damper system is extended to the study of the pile-to-pile interaction. The two piles are replaced by 2

parallel sets of spring and damper. The piles interact with each other which results in a reduction in stiffness and damping compared to an isolated pile. The interaction factor between the two pile is based on this reduction of stiffness and damping. A stiffness interaction factor is introduced to represent the reduction in stiffness and a damping interaction factor represents the reduction in damper coefficient.

The main outcomes of this research is as follows:

1- Floating pile in homogeneous soil

- The stiffness, k of a single pile increases with increase in soil modulus of elasticity.
- The geometric damping ratio, D decreases with increase in soil modulus of elasticity.
- A change in soil modulus of elasticity from 8×10^6 to 8×10^8 Pascal (i.e., a 100-fold increase) results in 32-fold increase in stiffness and 5 fold decrease in damping.
- Critical damping, c_{cr} increases with increase in soil modulus of elasticity.
- Damper coefficient increases until it reaches a point where it remains practically constant.
- The natural frequency of the soil-pile system increases with increase in soil modulus of elasticity.

2- End bearing pile in homogeneous soil

- For an end bearing pile, the stiffness of the pile system increase with an increase in soil modulus of elasticity.
- Geometrical damping ratio was found to increase until a certain value of the soil modulus of elasticity. After this value, the geometric damping remains almost constant.
- Critical damping increases with increase in soil modulus of elasticity.
- Damping increases with increase in soil modulus of elasticity.
- Natural frequency increases with increase in soil modulus of elasticity.
- An increase in soil modulus of elasticity from 8×10^6 Pascal to 8×10^8 Pascal will increase the stiffness by 400 % while the damping ratio increased by 200%.

3- Comparison Between End-Bearing Piles and Floating Piles in Homogeneous Soil

- In weak soils, the stiffness of end-bearing piles is 1300% greater than the stiffness of floating piles. However, damping of floating piles is 1000% higher than damping of end-bearing piles.
- In strong soils, similar values of stiffness and damping are obtained for both floating and end-bearing piles.

4- Floating pile in nonhomogeneous soil

- An increase in top weak soil layer results in reduction in stiffness, damping ratio, damper coefficient and natural frequency.

5- If the top weak soil layer increases in thickness to become equal to the pile length (i.e. 100% inhomogeneity), both the stiffness and damping are reduced by 40%.

6- End bearing pile in nonhomogeneous soil

- An increase in the thickness of the top weak soil layer reduces stiffness and damping of the soil-pile system.
- If the top weak soil layer increases in thickness to become equal to the pile length (i.e. 100% inhomogeneity), the stiffness is reduced by 20% while damping is reduced by 60%.

7- Pile to Pile Interaction

- The stiffness and damping interaction factors were found to be dependent on the spacing between the piles. The greater the spacing, the less is the value of the interaction factor. This is because when piles are placed far from each other, the transferred stresses between the two piles is reduced.
- The values of damping interaction factors found to be different than static interaction factors.
- Damping interaction can be greater than one. This was found in cases of piles placed at 0.5 meters away from each other.
- Dynamic stiffness interaction factors are lower than the static interaction factors currently used in practice.
- Damping interaction factors are higher than the static interaction factors.

6.3. Summary

For design of a pile supported machine, the stiffness and damping of the soil-pile system at the level of the pile head are needed. The research provides a methodology to determine both the stiffness and damping for a wide range of variables, both in material and geometry.

Floating Pile in Homogeneous Soil

- Increase in soil modulus of elasticity results in increase in stiffness, decrease in damping ratio, increase in damping and increase in natural frequency.
- An increase in soil modulus of elasticity from 8×10^6 Pascal to 8×10^8 Pascal will increase the stiffness by 3200 % while the damping ratio decreases by 500%.

End-Bearing Pile in Homogeneous Soil

- Increase in soil modulus of elasticity results in increase in stiffness, increase in damping ratio, increase in damping and increase in natural frequency.
- An increase in soil modulus of elasticity from 8×10^6 Pascal to 8×10^8 Pascal will increase the stiffness by 400 % while the damping ratio increased by 200%.

Comparison Between End-Bearing Piles and Floating Piles in Homogeneous Soil

- In weak soils, the stiffness of end-bearing piles is 1300% greater than the stiffness of floating piles. However, damping of floating piles is 1000% greater than damping of end-bearing piles.
- In strong soils, similar values of stiffness and damping are obtained for both floating and end-bearing piles.

Floating Pile in Non-Homogeneous Soil

- An increase in the thickness of the top weak soil layer will reduce the stiffness and damping of the soil-pile system.
- If the top weak soil layer increases in thickness to become equal to the pile length, both the stiffness and damping are reduced by 40%.

End-Bearing Pile in Non-Homogeneous Soil

- An increase in the thickness of the top weak soil layer reduces stiffness and damping of the soil-pile system.
- If the top weak soil layer increases in thickness to become equal to the pile length, the stiffness is reduced by 20% while damping is reduced by 60%.

Pile to Pile Interaction Factors

- As spacing between piles increases, the interaction factor decreases.
- Dynamic stiffness interaction factors are lower than the static interaction factors currently used in practice.
- Damping interaction factors are higher than the static interaction factors.

Design Charts

- Design charts are provided to account for inhomogeneity in the soil profile for both floating and end-bearing piles.
- Stiffness and damping interactions factors are provided to account for dynamic pile to pile interaction.

Appendices

A. An Introduction To Soil Dynamics

A.1. Vibrating systems

Consider a system of a single degree of freedom system as shown in Figure A.1. Such system consists of a rigid mass, a supporting elastic spring and viscous dashpot damper. Applying a force F to the system; in which F is dynamic in nature that varies with time t. In such a system the inertia takes effect and Newton's second Equation of motion applies to the system. The following differential Equation can be used

$$M\frac{d^2u}{dt^2} = F(t) \qquad (A.1)$$

In Equation A.1, M is the mass and u is the displacement. In said system, the spring will respond to the displacement caused by the force while the damper will respond to the velocity. Equation A.1 is now adjusted to include the spring and damper reactions to becomes

$$M\frac{d^2u}{dt^2} + c\frac{du}{dt} + ku = F(t) \qquad (A.2)$$

Where c is the damper viscosity coefficient and k is the spring constant. Understanding such a system is critical in Machine foundation and soil dynamics in general. In many cases, the soil response to an applied dynamic load is reduced to an analogous spring and a viscous dashpot damper. This makes the problem easy to solve. The engineers only need to conduct experiments to determine c and k values and solve the problem.

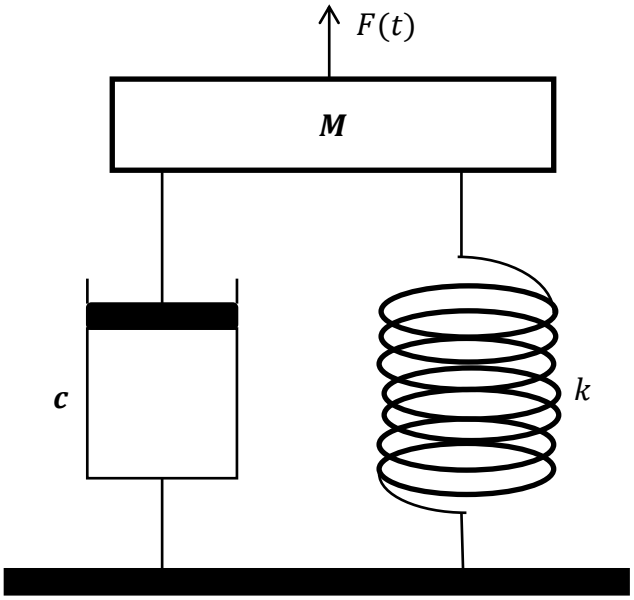

Figure A.1: Single degree of freedom system consists of a mass, a spring and a viscous damper.

A.2. Free vibration

If the force F is set to zero (i.e., the system is unloaded) the system will then vibrate freely for a period of time and then stops. Equation A.2 then becomes

$$M\frac{d^2u}{dt^2} + c\frac{du}{dt} + ku = 0 \qquad (A.3)$$

Depending on the damping of the system and the value of the displacement at the time the force is set to zero , the response can be identified mathematically. Defining the damping ratio of the system which is the ratio of the damper coefficient on the critical damping of the system is Mathematically represented by

$$\zeta = \frac{c}{2\sqrt{kM}} \qquad (A.4)$$

Where the denominator is the value of the critical damping of the system. Also the natural frequency ω_0 of such a system can be written as

$$\omega_0 = \frac{f_n}{2\pi}\left(\frac{radians}{second}\right) \; where \; f_n = \sqrt{\frac{\kappa}{M}}(Hz) \qquad (A.5)$$

The response of the system can be characterized by using the response time t_r also called the relaxation time which is defined as

$$t_r = c/k \qquad (A.6)$$

The value of t_r defines the response time of the system. At any time less than the response time, the system is considered stiff and the response depends on the damper. The system response depends more on the spring when the time is greater than the response time. From Equations A.4, A.5 and A.6 the damping can be related to the damping ratio and the natural frequency of the system as $c = 2\zeta\omega_0$. Using $c = 2\zeta\omega_0$ into Equation A.3, gives the following

$$M\frac{d^2u}{dt^2} + 2\zeta\omega_0\frac{du}{dt} + \omega_0^2 u = 0 \qquad (A.7)$$

Equation A.7 represents a differential Equation in which the solution can be assumed to take the form

$$u = Ae^{at} \qquad (A.8)$$

Where A is a constant related to the initial value of the displacement when F was set to zero. and a is an unknown value.

Substituting Equation A.8 in Equation A.7 will give

$$a^2 + 2\zeta\omega_0 a + \omega_0^2 = 0 \qquad (A.9)$$

a now can be found by finding the roots of Equation 2.9. The solution might be real or complex, and it takes the form

$$a_{1,2} = -\zeta\omega_0 \pm \omega_0\sqrt{\zeta^2 - 1} \qquad (A.10)$$

It is clear from Equation 2.10 that the response of the system depends on the value of the damping ratio ζ. In general, three outcomes can be obtained as shown in the upcoming sections.

A.2.1. when the damping ratio, ζ is less than 1

When the damping ratio ζ is less than 1($\zeta < 1$), the solution of Equation A.10 takes the form complex roots.

$$\alpha_{1,2} = -\zeta\omega_0 \pm i\omega_0\sqrt{1 - \zeta^2} \qquad (A.11)$$

Where i is the imaginary part of the complex number and($i = \sqrt{-1}$). The dynamic displacement u can be obtained as

$$u = A_1 e^{i\omega_1 t} e^{-\zeta\omega_0 t} + A_2 e^{i\omega_1 t} e^{-\zeta\omega_0 t} \qquad (A.12)$$

And $\omega_1$is defined as the damped natural frequency where $\omega_1 = \omega_0\sqrt{1 - \zeta^2}$. $e^{i\omega_1 t}$ Can be rewritten as $\cos(\omega_1 t) + i\sin(\omega_1 t)$. Equation 2.12 then becomes

$$u_d = C_1 \cos(\omega_1 t)\, e^{-\zeta\omega_0 t} + C_2 \sin(\omega_1 t)\, e^{-\zeta\omega_0 t} \qquad (A.13)$$

Where C_1 and C_2 values depend on the displacement u_0 which is the displacement when the force F is set to zero. Finally the solution of the dynamic displacement u_d relative to the initial displacement u_0 can be given as

$$\frac{u}{u_0} = \frac{\cos(\omega_1 t - \psi)}{\cos(\psi)}\, e^{-\zeta\omega_0 t} \qquad \text{(A.14)}$$

Where ψ is the phase angle and $\tan(\psi) = \frac{\omega_0 \zeta}{\omega_1}$. This behavior of the system is represented graphically in Figure A.2 for various damping values. In general, the system will continue to vibrate in a sinusoidal form but its amplitude will decay depending on the exponent of the damping $e^{-\zeta\omega_0 t}$. This decay will continue until it reaches at rest conditions.

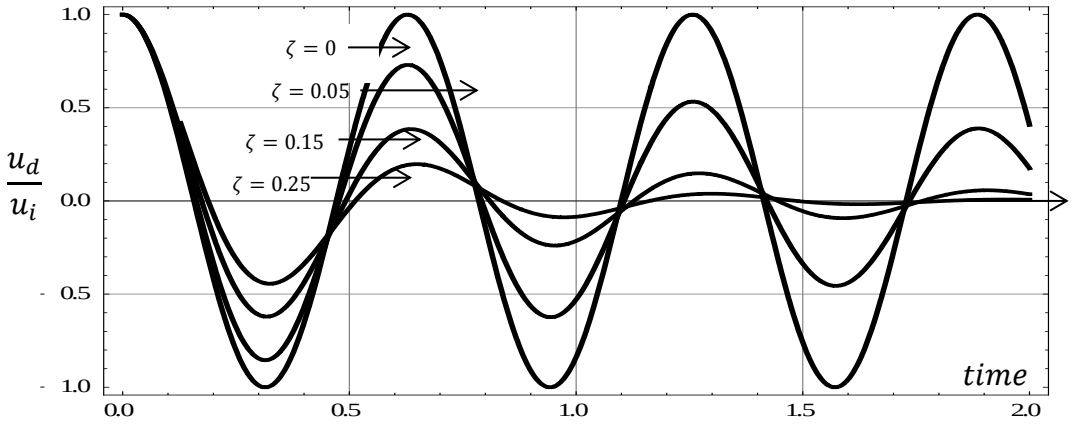

Figure A.2: Free vibration of damped systems.

A.2.2. Critically Damped Systems

When the Damping Ratio of the system is set to 1 (i.e., $\zeta = 1$) the system is said to be critically damped. The response is entirely different than that when $\zeta < 1$. The sinusoidal behavior is no longer applicable here; instead a, smooth curve is obtained for the decay of the amplitude with time. This behavior is represented in Figure A.3. The solution of Equation A.9 has two roots of equal values and $\alpha_1 =$

$\alpha_2 = -\omega_0$. The ratio of the amplitude of the displacement at any time to that at $t = 0$ is given by

$$\frac{u}{u_0} = (1 + \omega_0 t)\, e^{-\omega_0 t} \tag{A.15}$$

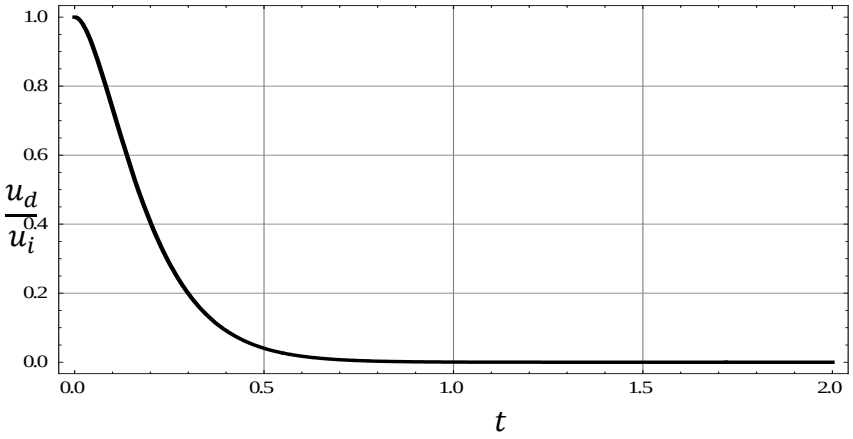

Figure A.3: Critically damped systems.

A.2.3. When the Damping Ratio is Greater than 1

In such a case where $\zeta > 1$, the solution to Equation 2.9 has two roots that are real and different. The following Equation describes the ratio of the amplitude of displacement at any time relative to that at $t = 0$.

$$\frac{u_d}{u_0} = \frac{\omega_2}{\omega_2 - \omega_0}\, e^{-\omega_1 t} - \frac{\omega_1}{\omega_2 - \omega_1}\, e^{-\omega_2 \tau} \tag{A.16}$$

A.3. Forced vibrations

The previous sections dealt with the solution of the dynamic differential Equation A.2 when the force F equals zero (i.e., free vibration). In this section, the response of the system is investigated under a loading that varies with time. The loading considered is periodic sinusoidal in nature and takes the form

$$F(t) = F_0 \cos(\omega t) \tag{A.18}$$

Where ω is the frequency of the periodic load in $radians/seconds$. The solution of Equation A.2 is now obtained and is

$$u = u_d \, Cos(\omega t - \psi) \tag{A.19}$$

Where u_d is the dynamic displacement and is given by

$$u_d = \frac{F_0/k}{\sqrt{\left(1 - \frac{\omega^2}{\omega_0^2}\right)^2 + \left(2\zeta \frac{\omega}{\omega_0}\right)^2}} \tag{A.20}$$

Where ζ and ω_0 are defined as per Equations A.4 and A.5 respectively. Equation A.20 can also be written in terms of k and c only as shown in the following Equation

$$u_d = \frac{F_0/k}{\sqrt{\left(1 - m\frac{\omega^2}{k}\right)^2 + \left(c\frac{\omega}{k}\right)^2}} \tag{A.21}$$

If the system has no mass, the solution is reduced to

$$u_d = \frac{F_0/k}{\sqrt{1 + \left(c\frac{\omega}{k}\right)^2}} \tag{A.22}$$

Equations A.20 is represented graphically in Figure A.4. It is important to note that $u_s = F_0/k$ and u_s is defined as the static displacement.

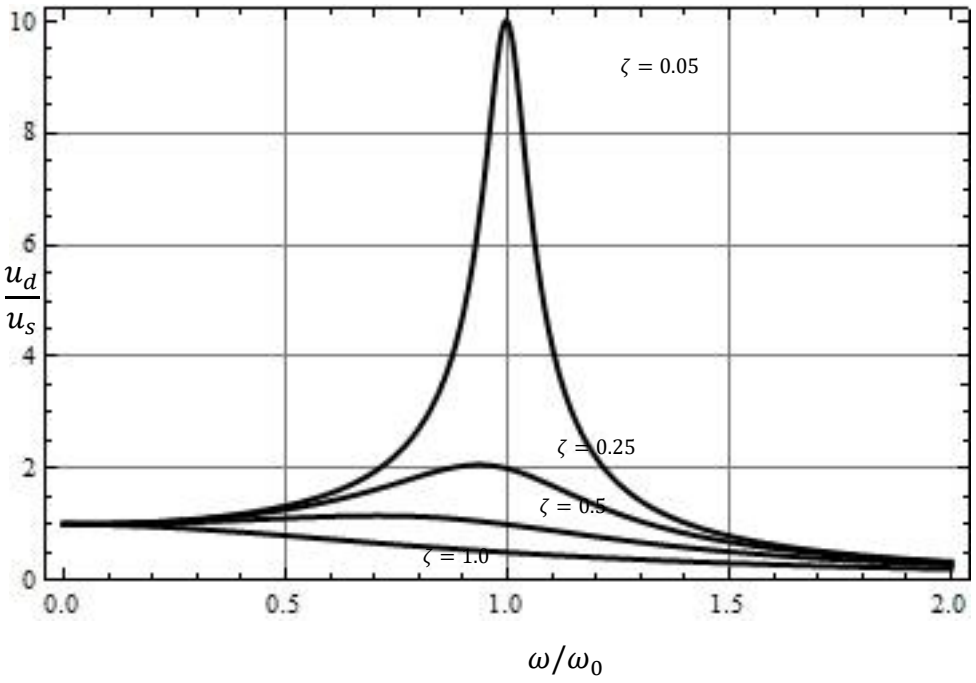

Figure A.4: Oscillation of forced vibration.

So far, an introduction to vibrating systems of a single degree of freedom is presented in the previous sections based on texts (Das & Ramana, 2010; Verruijt, 2010). It is convenient to use such systems to represent the response of the soil to a footing subjected to periodic loading. It is also can be used for single piles in a homogeneous elastic half-space (Verruijt, 2010). While the finite element method and the boundary element method can be used in engineering practices, it is easier and faster to deal with the reduced system. It also allows the engineers to focus on the problem at hand, not on the complexity that is associated with using the numerical methods. This also allows making changes on the problem parameters and decision making much faster and easier. In the upcoming sections, a review of the developments of the soil dynamics field with a focus on the response of the soil supporting shallow foundation subjected to a harmonic load shall be presented.

A.4. Waves in three-dimensional elastic medium

Waves in the soil are better represented by a three dimensional elastic half space. This section will present the mathematical preliminaries required for waves in a three-dimensional space.

A.4.1 The Equation of motion in a three-dimensional elastic medium

For a small finite elastic cube similar to that shown in Figure A.5 (a), If that cube has experienced motion in any directions it would be similar to that presented in Figure A.5 (b). The differential Equations that represent this are driven by summing the forces in all directions.

$$\frac{\partial \sigma_x}{\partial x} + \frac{\partial \tau_{yx}}{\partial y} + \frac{\partial \tau_{zx}}{\partial z} = \rho \frac{\partial^2 u}{\partial t^2} \tag{A.23}$$

$$\frac{\partial \sigma_y}{\partial y} + \frac{\partial \tau_{xy}}{\partial x} + \frac{\partial \tau_{zy}}{\partial z} = \rho \frac{\partial^2 v}{\partial t^2} \tag{A.24}$$

$$\frac{\partial \sigma_z}{\partial z} + \frac{\partial \tau_{xz}}{\partial x} + \frac{\partial \tau_{yz}}{\partial y} = \rho \frac{\partial^2 w}{\partial t^2} \tag{A.25}$$

Where $u, v\ and\ w$ are the displacements in the $x, y\ \ and\ z$ directions respectively, σ_i is the normal stress on the i axis, τ_{ij} is the shear stress acting normal on The i plane and its directed towards the j axis and ρ is the mass density of the medium. Strain which is defined as the change in shape relative to the original shape and is given by

$$\varepsilon_x = \frac{\partial u}{\partial x} \tag{A.26}$$

$$\varepsilon_y = \frac{\partial v}{\partial y} \tag{A.27}$$

$$\varepsilon_z = \frac{\partial w}{\partial z} \tag{A.28}$$

$$\gamma_{xy} = \frac{\partial v}{\partial x} + \frac{\partial u}{\partial y} \tag{A.29}$$

$$\gamma_{yz} = \frac{\partial w}{\partial y} + \frac{\partial v}{\partial z} \tag{A.30}$$

$$\gamma_{z\chi} = \frac{\partial w}{\partial x} + \frac{\partial u}{\partial z} \tag{A.31}$$

Where ε_ι is the normal strain in the i direction, γ_{ij} is the shear strain acting normal on the i axis directed towards the j axis. The rotation about a certain axis is defined by

$$\overline{\omega}_x = \frac{1}{2}\left(\frac{\partial w}{\partial y} - \frac{\partial v}{\partial z}\right) \tag{A.32}$$

$$\overline{\omega}_y = \frac{1}{2}\left(\frac{\partial u}{\partial z} - \frac{\partial w}{\partial x}\right) \tag{A.33}$$

$$\overline{\omega}_z = \frac{1}{2}\left(\frac{\partial v}{\partial x} - \frac{\partial u}{\partial y}\right) \tag{A.34}$$

Where $\overline{\omega}_\iota$ is the rotation around the i axis. The mathematical derivation of those Equations is given in many books on the Theory of elasticity such as Elasticity and Soil Mechanics by (Davis & Selvadurai, 1996).

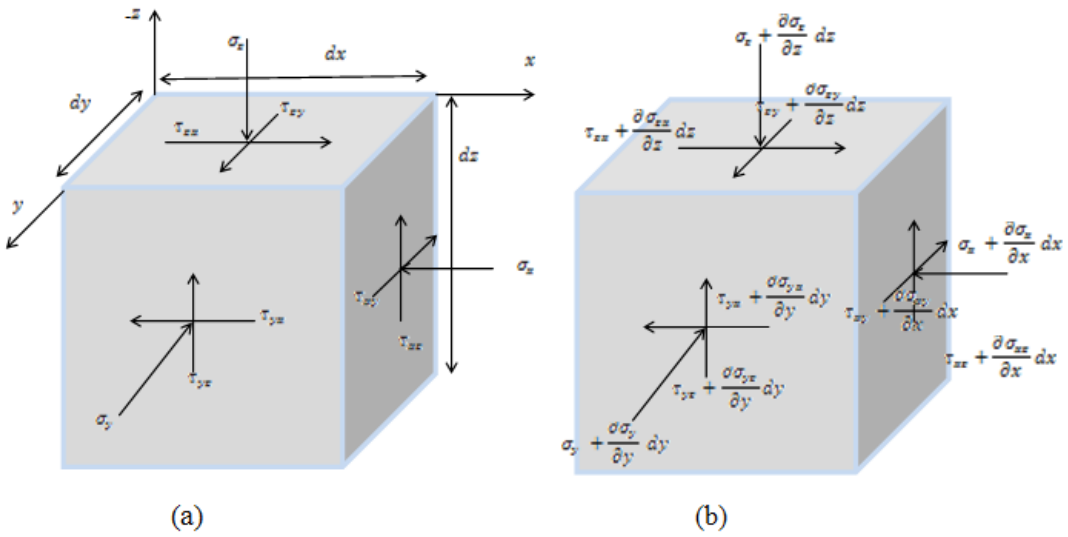

Figure A.5: (a) A finite cube under static stress. (b) The same cube undergoing some motion.

A.4.2. Hooke's law

In a linear elastic medium, the stress and strain are related by Hooke's Law and are given by

$$\varepsilon_x = \frac{1}{E}[\,\sigma_x - \mu(\sigma_y + \sigma_z)] \tag{A.35}$$

$$\varepsilon_y = \frac{1}{E}[\,\sigma_y - \mu(\sigma_x + \sigma_z)] \tag{A.36}$$

$$\varepsilon_z = \frac{1}{E}[\,\sigma_z - \mu(\sigma_y + \sigma_x)] \tag{A.37}$$

Where E is Young's Modulus of Elasticity and μ is Poisson's ratio. Similarly the shear stresses and strains are related by

$$\tau_{xy} = G\gamma_{xy} \tag{A.38}$$

$$\tau_{yz} = G\gamma_{yz} \tag{A.39}$$

$$\tau_{zx} = G\gamma_{zx} \tag{A.40}$$

G is the shear modulus and is related the Young's Modulus Poisson's ratio by

$$G = \frac{1}{2}\, E\,(1+\mu) \tag{A.41}$$

The solution to Equations A.35 to A.37 that relates the normal stresses to the normal strains is

$$\sigma_x = \lambda\overline{\varepsilon} + 2G\varepsilon_x \tag{A.42}$$

$$\sigma_y = \lambda\overline{\varepsilon} + 2G\varepsilon_y \tag{A.43}$$

$$\sigma_z = \lambda\overline{\varepsilon} + 2G\varepsilon_z \tag{A.44}$$

Where

$$\lambda = \mu E/[(1+\mu)(1-2\mu)] \tag{A.45}$$

$$\overline{\varepsilon} = \varepsilon_x + \varepsilon_y + \varepsilon_z \tag{A.46}$$

A.4.3. Equations for compression stress waves in an infinite elastic medium

Equation A.23 can be rewritten using Equations A.38, A.40 and A.42 to become

$$\rho\frac{\partial^2 u}{\partial t^2} = \frac{\partial}{\partial x}(\lambda\overline{\varepsilon} + 2G\varepsilon_x) + \frac{\partial}{\partial y}\left(G\gamma_{xy}\right) + \frac{\partial}{\partial z}(G\gamma_{xz}) \qquad \text{(A.47)}$$

The values of ε_x, γ_{xy} and γ_{xz} can be substituted using Equations A.26, A.29 and A.31 so that Equation A.47 becomes

$$\rho\frac{\partial^2 u}{\partial t^2} = \frac{\partial}{\partial x}(\lambda\overline{\varepsilon} + 2G\varepsilon_x) + G\frac{\partial}{\partial y}\left(\frac{\partial v}{\partial x} + \frac{\partial u}{\partial y}\right) + G\frac{\partial}{\partial z}\left(\frac{\partial w}{\partial x} + \frac{\partial u}{\partial z}\right) \qquad \text{(A.48)}$$

The previous Equation can be rearranged so that it becomes

$$\rho\frac{\partial^2 u}{\partial t^2} = \lambda\frac{\partial \overline{e}}{\partial x} + G(\frac{\partial^2 u}{\partial x^2} + \frac{\partial^2 v}{\partial x\partial y} + \frac{\partial^2 w}{\partial x\partial z} + \frac{\partial^2 u}{\partial x^2} + \frac{\partial^2 u}{\partial y^2} + \frac{\partial^2 u}{2\partial z^2}) \qquad \text{(A.49)}$$

Yet $\overline{\varepsilon} = \varepsilon_x + \varepsilon_y + \varepsilon_z$ which values can be taken from Equations A.26, A.27 and A.28 so that

$$\frac{\partial^2 u}{\partial x^2} + \frac{\partial^2 v}{\partial x\partial y} + \frac{\partial^2 w}{\partial x\partial z}$$

can be rewritten as $\frac{\partial\overline{\varepsilon}}{\partial x}$. Using the previous derivation, Equation A.49 is simplified to be

$$\rho\frac{\partial^2 u}{\partial t^2} = (\lambda + G)\frac{\partial\overline{\varepsilon}}{\partial x} + G\nabla^2 u \qquad \text{(A.50)}$$

Where

$$\nabla^2 = \frac{\partial^2}{\partial x^2} + \frac{\partial^2}{\partial y^2} + \frac{\partial^2}{\partial z^2} \qquad \text{(A.51)}$$

Similarly in the y and z directions

$$\rho \frac{\partial^2 v}{\partial t^2} = (\lambda + G) \frac{\partial \overline{\varepsilon}}{\partial y} + G\nabla^2 v \tag{A.52}$$

$$\rho \frac{\partial^2 w}{\partial t^2} = (\lambda + G) \frac{\partial \overline{\varepsilon}}{\partial z} + G\nabla^2 w \tag{A.53}$$

By differentiating Equations A.50, A.52 and A.53 with respect to x, y and z respectively and then summing the Equations all together, the result would be

$$\rho \frac{\partial^2 \overline{\varepsilon}}{\partial t^2} = (\lambda + 2G)(\nabla^2 \overline{e}) \tag{A.54}$$

By dividing both sides on ρ

$$\frac{\partial^2 \overline{\varepsilon}}{\partial t^2} = \frac{(\lambda + 2G)}{\rho} \nabla^2 \overline{\varepsilon} = v_p \nabla^2 \overline{\varepsilon} \tag{A.55}$$

Where $v_p$is defined as the compressional wave velocity and is given by

$$v_p = \frac{\lambda + 2G}{\rho} \tag{A.56}$$

For the rest of this text, Compression waves can be referred to as Primary waves or P-waves.

A.4.4. Equations for shear waves in an infinite elastic medium

By differentiating Equation A.52 with respect to z and Equation A.53 with respect to y the following Equations are obtained

$$\rho \frac{\partial^2}{\partial t^2}\left(\frac{\partial v}{\partial z}\right) = (\lambda + G)\frac{\partial \overline{\varepsilon}}{\partial y \partial z} + G\nabla^2 \frac{\partial v}{\partial z} \tag{A.57}$$

$$\rho \frac{\partial^2}{\partial t^2}\left(\frac{\partial w}{\partial y}\right) = (\lambda + G)\frac{\partial \overline{\varepsilon}}{\partial y \partial z} + G\nabla^2 \frac{\partial w}{\partial y} \tag{A.58}$$

By subtracting the two previous Equations, the following is obtained

$$\rho \frac{\partial}{\partial t^2}\left(\frac{\partial w}{\partial y} - \frac{\partial v}{\partial z}\right) = G\nabla^2 \left(\frac{\partial w}{\partial y} - \frac{\partial v}{\partial z}\right) \tag{A.59}$$

And it is already known from Equation A.32 that $\left(\frac{\partial w}{\partial y} - \frac{\partial v}{\partial z}\right) = 2\overline{\omega}_x$. Equation A.59 can be rewritten as

$$\rho \frac{\partial^2 \overline{\omega}_x}{\partial t} = \frac{G}{\rho}\nabla^2 \overline{\omega}_x = v_s^2 \nabla^2 \overline{\omega}_x \tag{A.60}$$

Where v_s is defined as the shear wave velocity. For the rest of this text Shear waves are refereed to S-Waves.

A.4.5. Rayleigh waves (R-Wave)

Another type of elastic waves is the Rayleigh wave. This type travels at or near the free surface boundary of an elastic medium. Its velocity is close to that of a shear wave. Figure A.6 shows variation of v_r/v_s with the Poisson's ratio. Where v_r is the Rayleigh wave velocity.

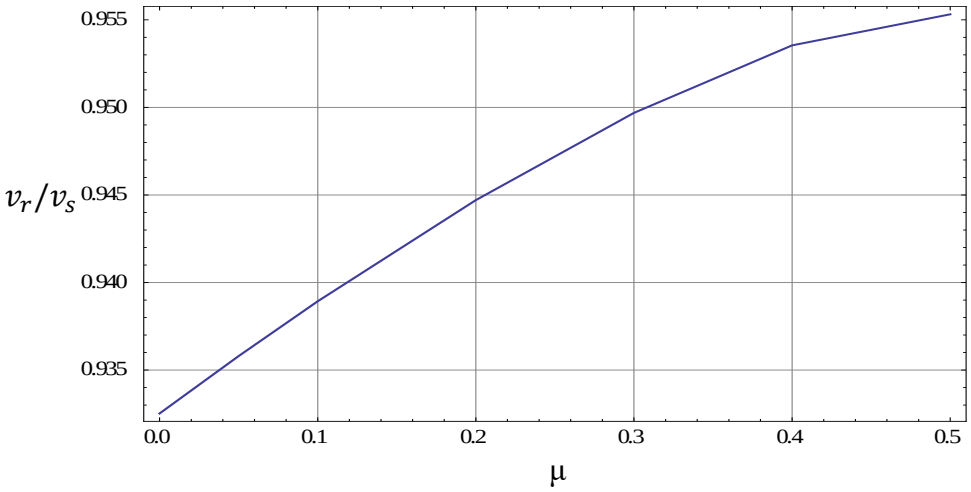

Figure A.6: Variation of v_r/v_s with the Poisson's ratio.

A.4.6. Attenuation of elastic waves with distance from source of vibration

As waves travel through an elastic medium, they lose energy. Part of this energy is absorbed by the medium due to what is known as damping, geometrical and hysteretic. Geometrical damping is the loss of amplitude due to spreading away from the source, while the hysteretic damping of the medium is related to the material properties or dry friction of a medium in case of soil. Body waves decay with distance faster than surface waves and Rayleigh waves. The decay of elastic waves follows the Equation

$$u_{ydr} = \frac{u_{yd0}}{r^n} \tag{A.61}$$

Where

$$n = \begin{cases} 2 \; for \; compression \; and \; shear \; wave \; at \; the \; surface \\ 1 \; for \; body \; waves \; within \; the \; elastic \; medium \\ \frac{1}{2} \; for \; Rayleigh \; Waves \end{cases}$$

In Figure A.7-a, a disturbance at a source point is shown and in Figure A.7-b, the arrival time and amplitudes of the waves are shown. From Figure A.7, it is obvious that a Rayleigh wave will arrive last at a time close to the S-wave and the R-wave will have the highest amplitude compreaed to the compressional and shear wave. A P-wave is the fastest among the waves.

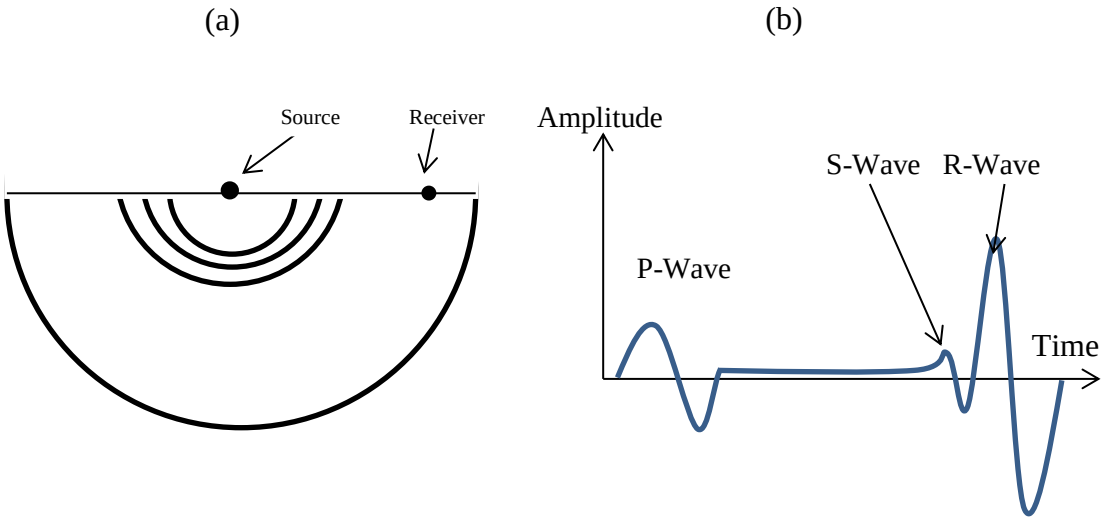

Figure A.7: (a) Disturbance caused at a point on the surface. (b) the amplitude of different wave and their arrival time.

A.5. Reflection and refraction of elastic waves within a horizontally layered elastic medium

When traveling body waves (P-waves and S-waves) reaches the boundary between two elastic layers with different elastic properties, some of the waves will be reflected and some will be refracted and will continue traveling through the second layer. P-waves and S-waves behave differently in multilayered systems. The particle motion in the case of P-wave propagation is continuous to the original P-wave ray (see Figure A.8-a), whereas the particle motion of in the case of S-wave propagation can be divided to two directions:

1- SH-waves which cause the particles to move in the plane of propagation as presented in Figure A.8-b.
2- SV-waves that cause the particles to move in a direction that is perpendicular to the plane of propagation as shown in Figure A.8-c.

In the case of a P-wave at the interface of two layers, there will be two reflected waves and two refracted waves. The first of the reflected waves will be of the same nature of the source wave, a P-wave, while the second one will be of the nature of an SV-wave. As for the refracted waves, the same applies; a P-wave and SV-wave will be generated (see Figure A.8-a).

For the first type of an S-wave which is an SH-wave, there would be a reflected SH-wave and a refracted SH-wave as result of facing a new elastic layer. See Figure A.8-b.

As for SV-waves, the result of facing a new layer would be two reflected waves which are a P-wave and an SV-wave and two refracted waves, a P-wave and an SV-wave as shown in Figure A.8-c.

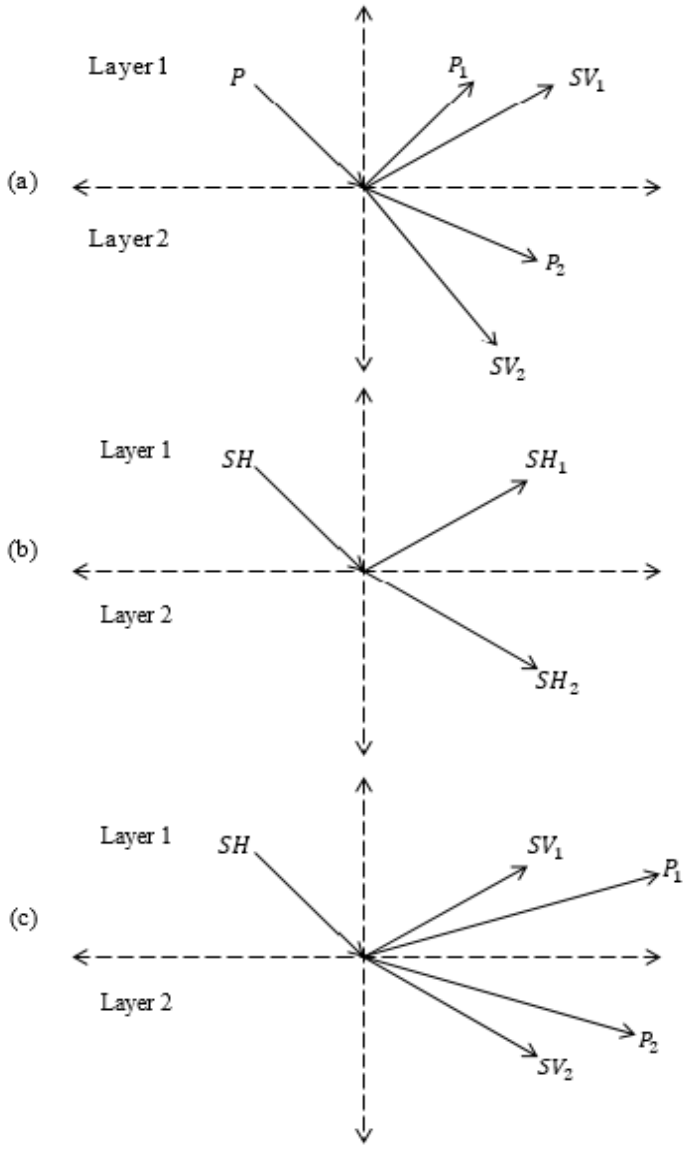

Figure A.8: Reflection and refraction of body waves at the interface between two layers.

A.6. Theories and applications for dynamic soil-foundation interaction

Consider a footing similar to that presented in Figure A.9. The footing has a mass, m, a radius, r_0 and is subject to a dynamic force Q with an amplitude of Q_0. The elastic properties of the half space are the shear modulus, G, Poisson's ratio, μ, and a mass density ρ. Several solutions for such a problem exist to find the dynamic displacement of the elastic half space under such conditions. The upcoming sections will present some of these solutions along with assumptions made to simplify the problem. Furthermore, a comparison between some of the theories and field testing will also be presented.

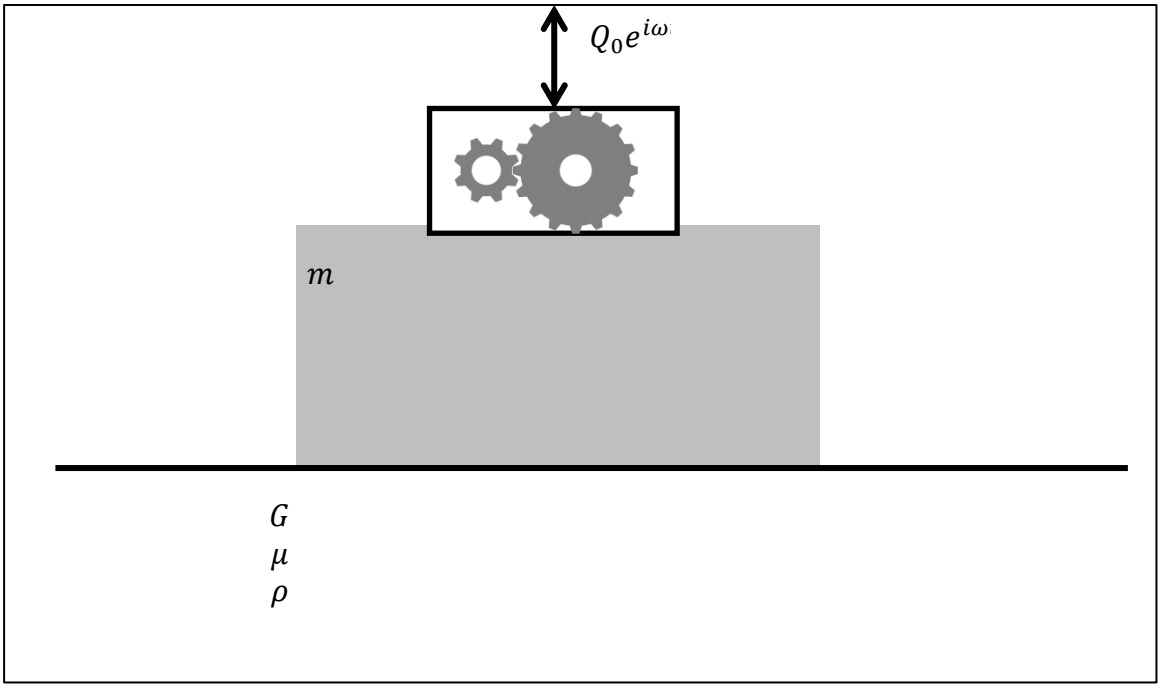

Figure A.9: Foundation subject to dynamic load.

A.1.1. The work of Reissner (1936)

Lambe in 1904 studied the problem of a vertical point load acting dynamically over an elastic half-space. The problem is known as "the Dynamic Boussinesq Problem." Reissner, (1936) studied the case where a uniformly

distributed load is acting dynamically on a circular flexible foundation. The nature of the pressure distribution under the footing for such a load case is presented in Figure A.10-a. This was done by integrating the problem of a point load which was studied by (Lambe, 1904). The vertical displacement was found to be

$$u = (\frac{Q_0 e^{i\omega\tau}}{G r_0})(f_1 + f_2) \quad \text{(A.62)}$$

where Q_0 is the amplitude of the load applied, u is the dynamic displacement at the center of the foundation, G is the shear modulus of the elastic medium, r_0 is the radius of the foundation and f_1 and f_2 are called displacement functions which are functions of a dimensionless frequency a_0 and are shown in Figure A.11 and Figure A.12 respectively, while a_0 is obtained as per Equation A.63.

$$a_0 = \frac{\omega r_0}{v_s} \quad \text{(A.63)}$$

Where ω is the frequency of motion in radians per second and v_s is the shear wave velocity in meters per second and r_0 is the radius of said footing.

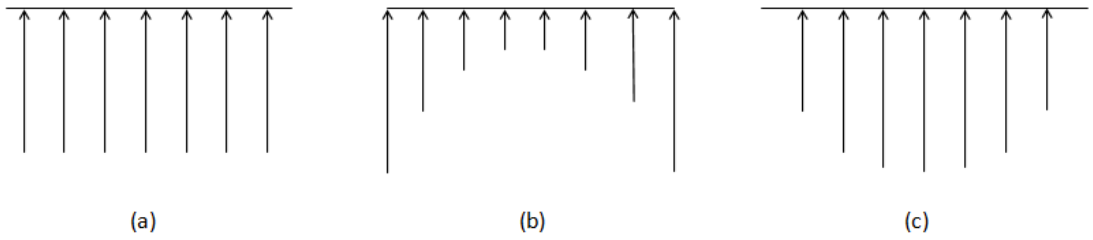

Figure A.10:Pressure distribution under footing subject to dynamic load. (a) Uniform pressure distribution, (b) Pressure distribution under a rigid footing and (c) Parabolic pressure distribution.

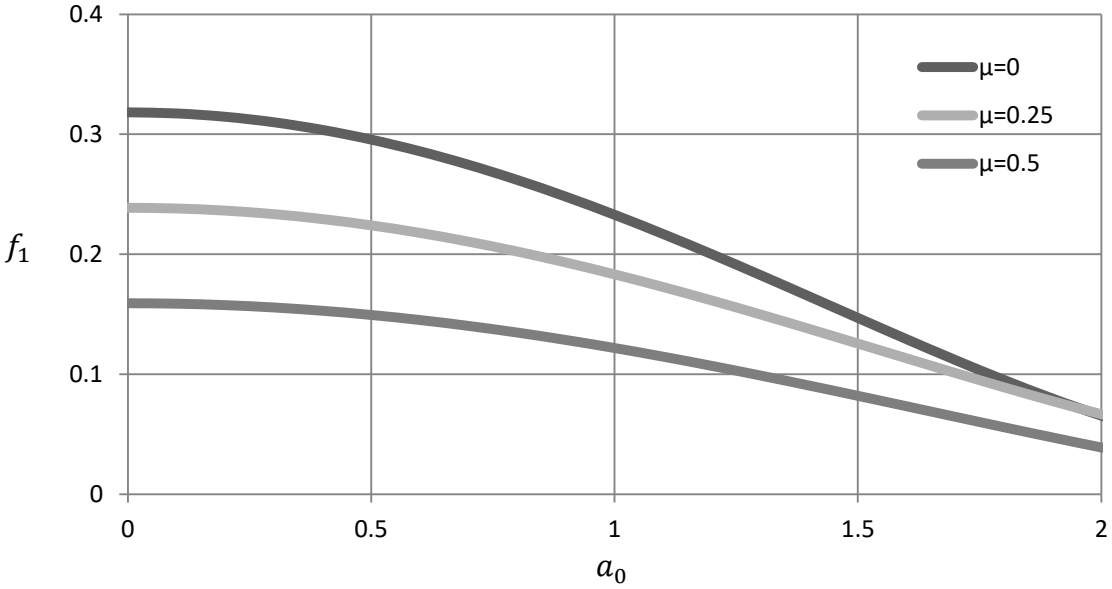

Figure A.11: Values of f_1 vs. dimensionless frequency a_0 for different Poisson's ratios.

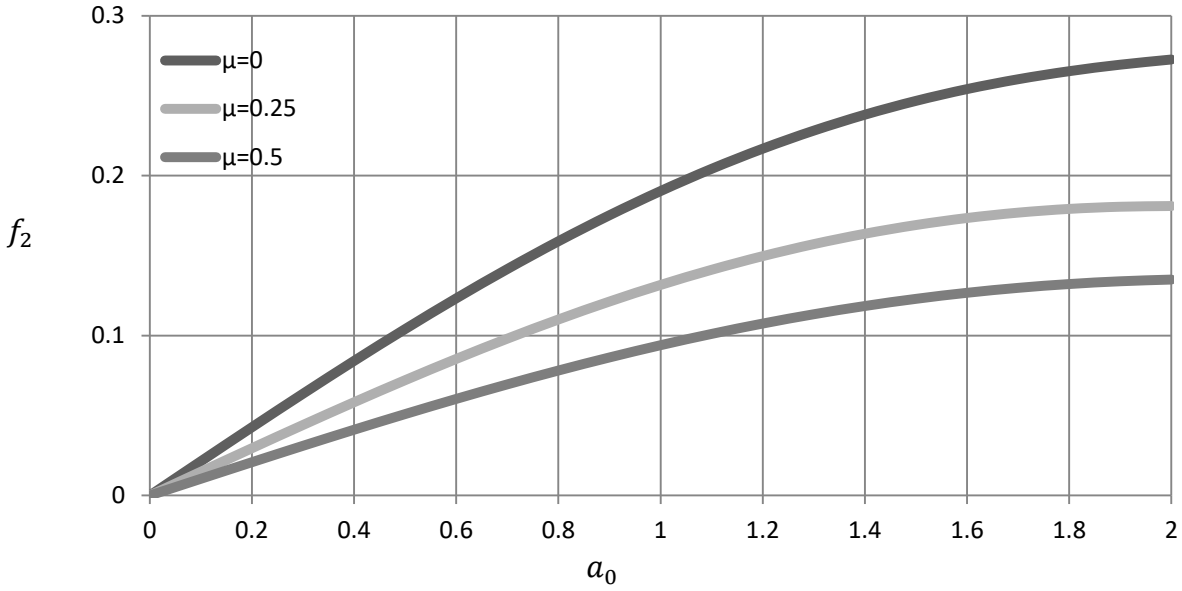

Figure A.12: : Values of f_2 vs. dimensionless frequency a_0 for different Poisson's ratios.

Using Equation A.62 and applying equilibrium in forces, the following Equation for the amplitude of motion can be derived

$$A_z = \left(\frac{Q_0}{Gr_0}\right) Z \tag{A.64}$$

Where Z is a dimension-less amplitude and is given by

$$Z = \sqrt{\frac{f_1^2 + f_2^2}{(1 - ba_0^2 f_1)^2 + (ba_0^2 f_2)^2}} \tag{A.65}$$

The term b refers to a dimensionless mass ratio that relates the mass of the foundation, m, and the machine with the mass density of the soil, ρ, and is defined as

$$b = \frac{m}{\rho r_0^3} = \frac{W}{\gamma r_0^3} \tag{A.66}$$

Where γ is the unit weight of the soil and W is the weight of the foundation plus that of the machine. So far the dynamic elastic response for the case of a uniformly distributed pressure on a flexible foundation was given (Figure A.10-a). Quinlan (1953) and Sung (1953) picked up on Reissner's work and studied the response of a load distribution that is similar to that show in Figure A.10-b and A.10-c. Equations A.64 and A.65 applies to the case of a rigid foundation (Figure A.10-b) but the values of f_1 and f_2 are different and are shown in Figure A.13 and A.14.

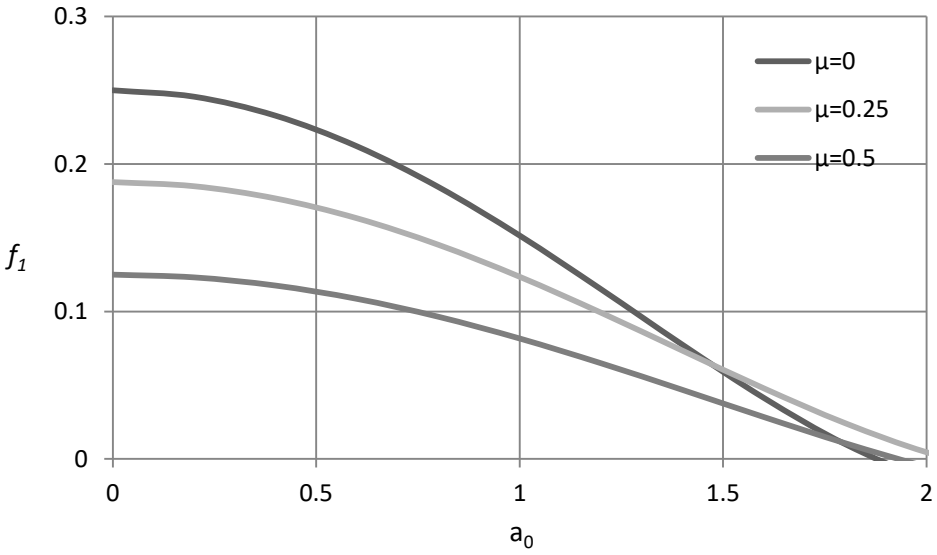

Figure A.13: Values of f_1 for a rigid foundation.

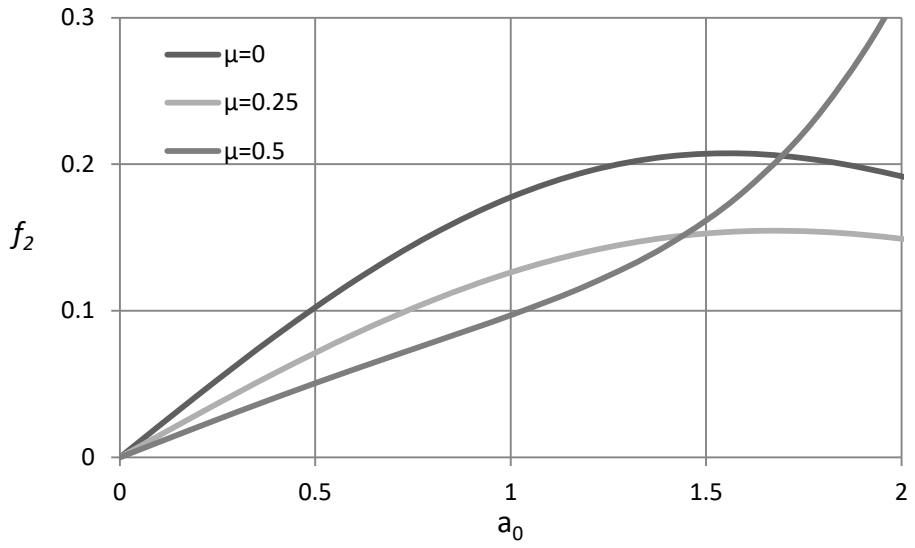

Figure A.14: Values of f_2 for a rigid foundation.

A.4.7. The Work of Lysmer & Richart (1966) on Lumped Parameter System for Vertical Motion

Lysmer & Richart (1966) work reduces the problem of the elastic half-space theory to a model of a single degree of freedom consists of a mass, a spring and a dashpot damper similar to that shown in Figure A.1. The required spring and dashpot constants are obtained from the elastic theory. The mass is equal to the mass of the vibrating machine and the supporting footing.

Generally, the Equations for calculating the required parameters are

$$k = \frac{4Gr_0}{1-\mu} \tag{A.67}$$

$$c = \frac{3.4}{1-\mu} r_0^2 \sqrt{\rho G} \tag{A.68}$$

Where G is the shear modulus of the soil, ρ is the density of the soil, μ is Poisson's Ratio, and r_0 is the radius of the supporting footing. After these two constants are

calculated, the response of the soil can be obtained using the procedure presented in sections A.1-A.3 to calculate the response of the single degree of freedom system.

Lysmer and Richart work is of importance because of its simplicity. Moreover, his work showed that any elastic dynamic system could be reduced to a single degree of freedom at the point of interest by identifying the equivalent spring and dashpot constants. Since then development in the area of machine vibrations has continued with different loading settings (e.g., horizontal and rocking vibrations) different ground conditions (e.g., rock base). The mass ratio B, spring constant k, and damping ratio D for a rigid foundation under different types of loading are in shown Table A.1. The Equations in Table A.1 are based on continuation of Lysmer Solution.

Table A.1: Values of mass ratio, spring constant and damping ratio for different types of dynamic loadings.

Degree of freedom	Mass ratio	Spring constant	Damping ratio
Vertical	$B_v = \frac{(1-\mu)}{4}\frac{m}{\rho r_0^3}$	$K_v = \frac{4Gr_0}{1-\mu}$	$D_v = \frac{0.425}{\sqrt{B_z}}$
Sliding	$B_h = \frac{(7-8\mu)}{32(1-\mu)}\frac{m}{\rho r_0^3}$	$K_h = \frac{8Gr_0^3}{2-\mu}$	$D_h = \frac{0.288}{\sqrt{B_h}}$
Rocking	$B_r = \frac{3(1-\mu)}{8}\frac{I_r}{\rho r_0^3}$	$K_r = \frac{8Gr_0^3}{3(1-\mu)}$	$D_r = \frac{0.15}{(1+B_r)\sqrt{B_r}}$
Torsional	$B_t = \frac{I_t}{\rho r_0^3}$	$k_t = \frac{16Gr_0^3}{3}$	$D_t = \frac{0.5}{1+2B_t}$

A.7. Dynamic properties of soil

Although soil is not an elastic medium nor is it homogeneous, the dynamic properties and mathematics of an elastic medium can be used to obtain reasonable approximations for the response of soil to dynamic loading. The mathematics of a dynamic elastic medium forms the basis of theories presented before. It is then of importance to be able to obtain the dynamic properties of soil. Several laboratory tests are available to determine these mechanical properties that are needed to apply the theory of elasticity to soil dynamics. From these tests, several correlations between soil properties are made to further aid in the analysis.

Soil tends to behave nonlinearly when under stress. If the applied loading is cyclic, the behavior is called the backbone curve and looks like that shown in Figure A.15. This nonlinear behavior can be reduced to a linear behavior using two parameters, the shear modulus and the damping ratio. It is important that this reduction will require prior knowledge of the expected strain level the soil will be exposed to. This is due to the fact that the two said parameters; the shear modulus and the damping ratio; vary with the strain level. With prior knowledge of the strain level, a dynamic soil test can be selected to determine the required parameters. When the shear modulus and the damping ratio are obtained, the soil behavior can be modeled within a reasonable accuracy using the elastic theory.

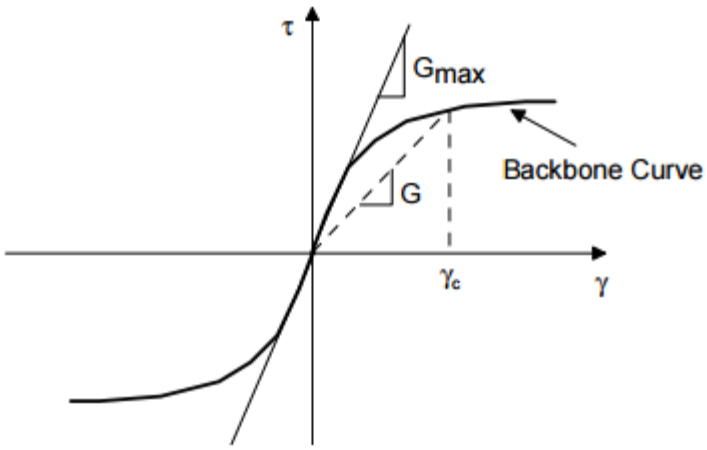

Figure A.15: Backbone curve.

A.7.1. Laboratory testing and correlations for dynamic soil properties

A.7.1.1. Resonant column test

In the Resonant column test, a soil sample is excited to vibrate until it reaches one of its natural modes. Once resonated, the frequency at resonance is obtained to calculate the wave velocity of the soil. If the soil is excited in torsion, the wave velocity calculated will be that of a shear wave. On the other hand, if the

soil is excited longitudinally, the wave velocity obtained will be that of the compression wave.

Two types of the resonant column test are used. They differ in the applied boundary conditions on the soil sample. The two types are free-fixed and free-free boundary conditions. Figure A.16 shows a schematic drawing of the setup for the resonant column test. Sinusoidal force is applied to the specimen through the power source and an amplifier. Together, they deliver the force to the driver. The pick-up end is used to obtain the soil specimen response. Obtaining of dynamic soil properties ($G\ and\ \zeta$) depends on the type of the boundary condition and the force (vertical or torsional) applied to the soil sample.

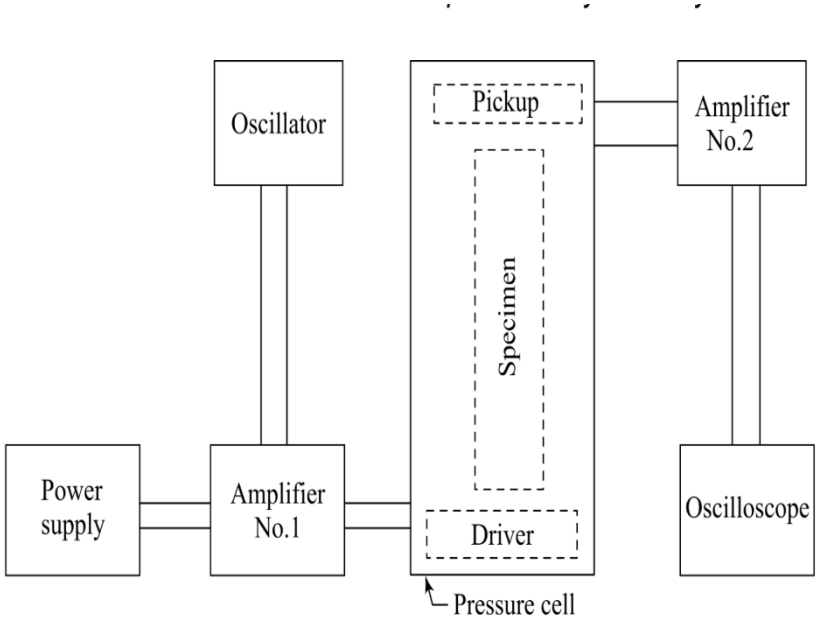

Figure A.16: : Schematic drawing of the resonant column test.

Equations for obtaining E and v_p from a fixed free resonant column test with vertical dynamic loading are

$$E = 39.48\left(\frac{f_n^2 * L^2}{\alpha^2}\right)\rho \tag{A.69}$$

$$v_p = \frac{2\pi f_n L}{\alpha} \tag{A.70}$$

Where $\alpha\tan(\alpha) = \frac{AL\gamma}{W}$, L is the length of the specimen, W is the weight of the attachments on top of the soil sample, γ is the unit weight of the soil sample, f_n is the natural frequency obtained and ρ is the density of the soil sample.

Similarly, Equations from a torsional load applied to the soil for obtaining v_s and G of the soil sample are

$$G = 39.48\left(\frac{f_n L}{\alpha}\right)^2 \rho \tag{A.71}$$

$$v_s = \frac{2\pi f_n L}{\alpha} \tag{A.72}$$

Here, $a = \frac{2\pi f_n}{v_s}\tan\left(\frac{2\pi f_n L}{v_s}\right) = \alpha\tan(\alpha)$. Other symbols definitions are similar to that of Equations A.69 and A.70.

Other laboratory tests include cyclic shear test and cyclic tri-axial test. These tests are better used to determine soil strength parameters for large strains and when nonlinearity is expected. Figure A.17 shows different laboratory and field tests with the range of strain level each test will produce.

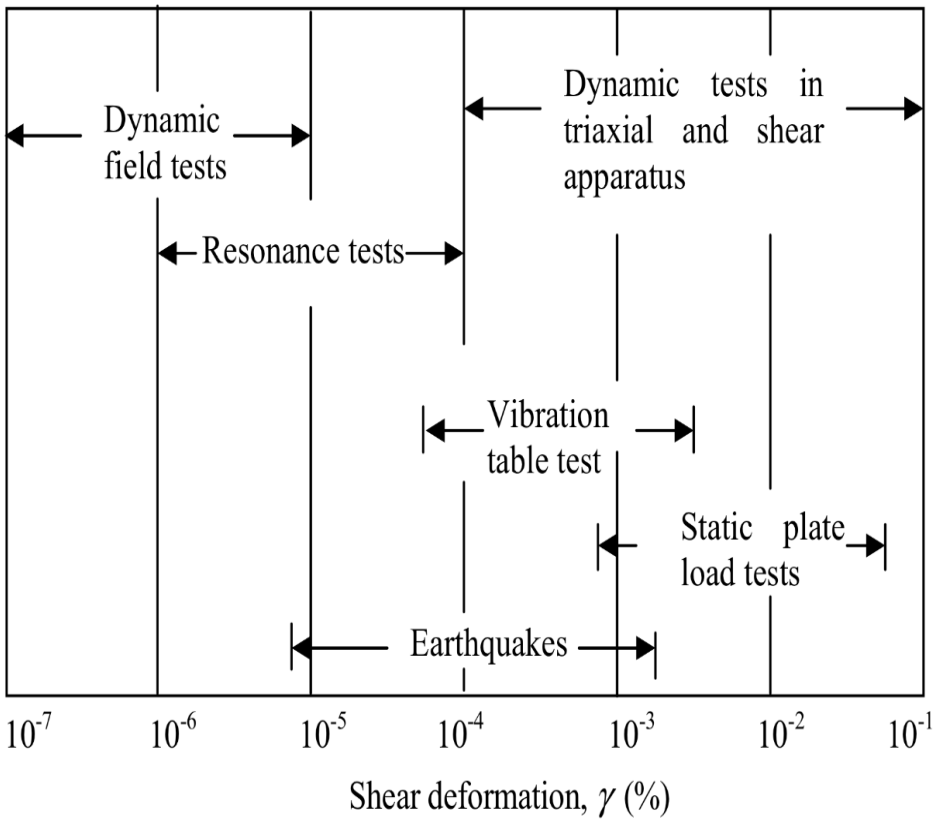

Figure A.17: : Range of strain levels produced by different shear tests (Das & Ramana, 2010).

A.7.1.2. Correlations for shear modulus at low strains in cohesion-less soils

B. O. Hardin & Richart (1963) conducted several resonant column tests on dry Ottawa sands. The shear strain amplitude was at 10^{-3} %. The results of their experiments showed that the shear wave velocity is independent of the grain-size distribution, soil gradation and the relative density of the specimen. Instead, the resulting shear wave velocities were dependent on the void ratio and the effective confining pressure. The results of these experiments are shown in Figure A.18.

From Figure 2.18, it can be seen that the higher the confining pressure, the higher the resulting shear wave velocities. This finding is in accordance to the fact that at deeper earth strata, the shear wave velocities are higher than those at

shallower depths. It is also shown in Figure A.15 that at the same confining pressure higher void ratios has shear wave velocity that is lower than at low void ratios (i.e., the shear wave velocity is inversely correlated with the void ratio). The correlation of the shear wave velocity with the confining pressure and the void ratio apply indirectly with the shear modulus.

A.7.1.3. Correlations for shear modulus at low strains for normally consolidated cohesive soils

B.O. Hardin & Black (1968) experimented with normally consolidated kaolinite and Boston Blue clay with a resonant column test. Their findings are presented in Figure A.19. The shear modulus was found dependent on the void ratio at a certain confining pressure and can be estimated as

$$G = 1230 \frac{(2.973 - e)^2}{(1 + e)} {\sigma_c'}^{1/2} \quad \text{(A.69)}$$

In Equation A.69 the shear modulus G and the effective confining pressure are both in lbs/in^2.

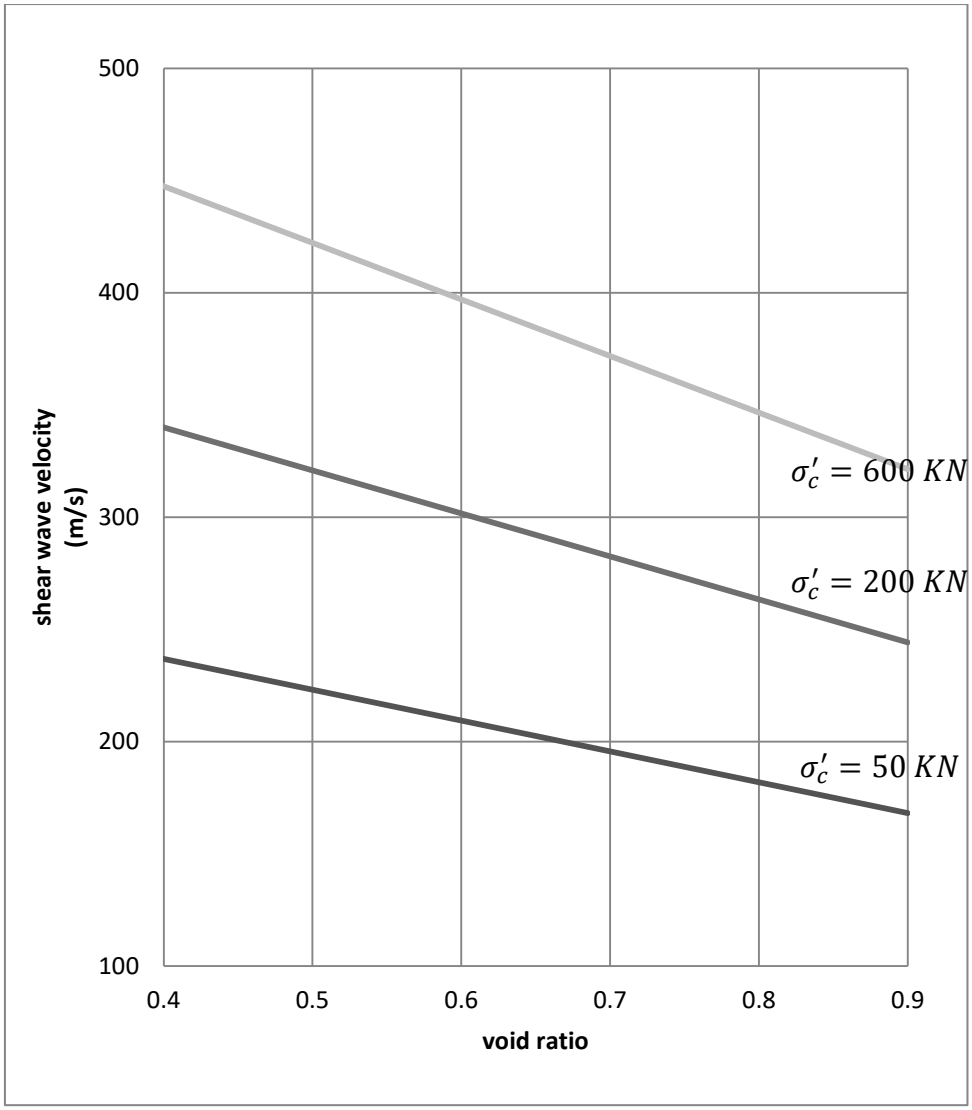

Figure A.18: Variation of shear wave velocity with the void ratio for different confining pressures (B O Hardin & Richart, 1963).

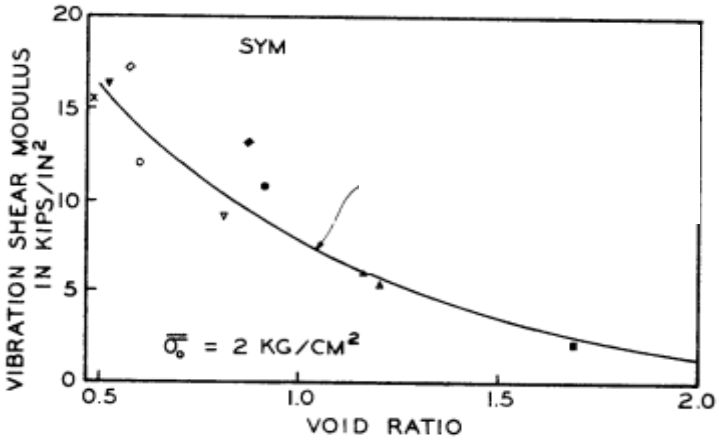

Figure A.19: Correlation of shear modulus with void ratio for normally consolidated clays (B. O. Hardin & Black, 1968).

A.7.1.4. Correlations for shear modulus at low strains for overly consolidated cohesive soils

B. O. Hardin & Black (1968) consolidated some specimens before testing to see how pre-consolidation pressure might affect the correlation between shear modulus and void ratio. Equation A.69 will be modified so that the shear modulus will be calculated as

$$G = 1230\frac{(2.973-e)^2}{(1+e)}(OCR)^k {\sigma_c'}^{1/2} \qquad \text{(A.70)}$$

In (A.70) the term k depends on the plasticity index of the clay specimen. This variation is shown in Figure A.20.

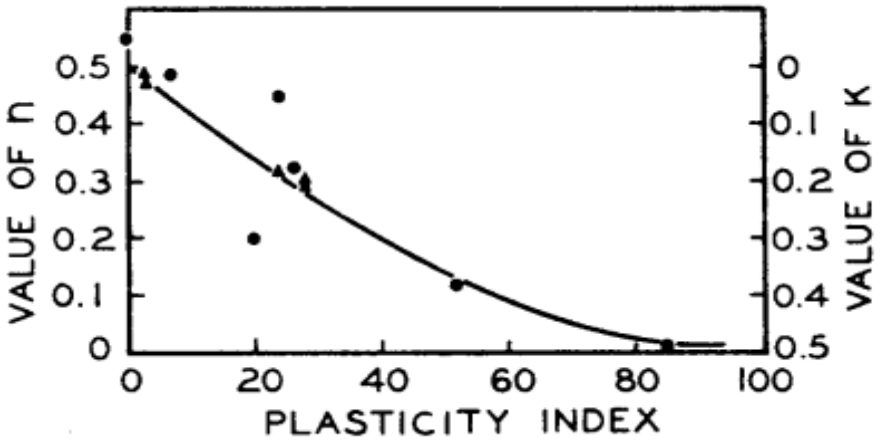

Figure A.20: Variation of the term k in Equation 2.70 with the plasticity index (B. O. Hardin & Black, 1968).

A.7.1.5. Correlations for shear modulus and damping ratio with strain level

In order to obtain a reliable approximation of soil response to a dynamic load, the shear modulus and the damping ratios must be identified correctly and at the strain level for the case at hand. A machine generating a dynamic load of low amplitude will induce a low strain in the soil skeleton. At this low strain level, the shear modulus and the damping ratio will defer greatly from those at higher strain level produced by something like an earthquake or an explosion. Generally, at low strains, the soil will respond with a high shear modulus and low damping. At higher strains, the soil will respond with a low shear modulus but with higher damping. This unique relation is reported by several scholars of geotechnical engineering and their results are shown in Figure A.21 for the shear modulus and in Figure A.22 for the damping ratio.

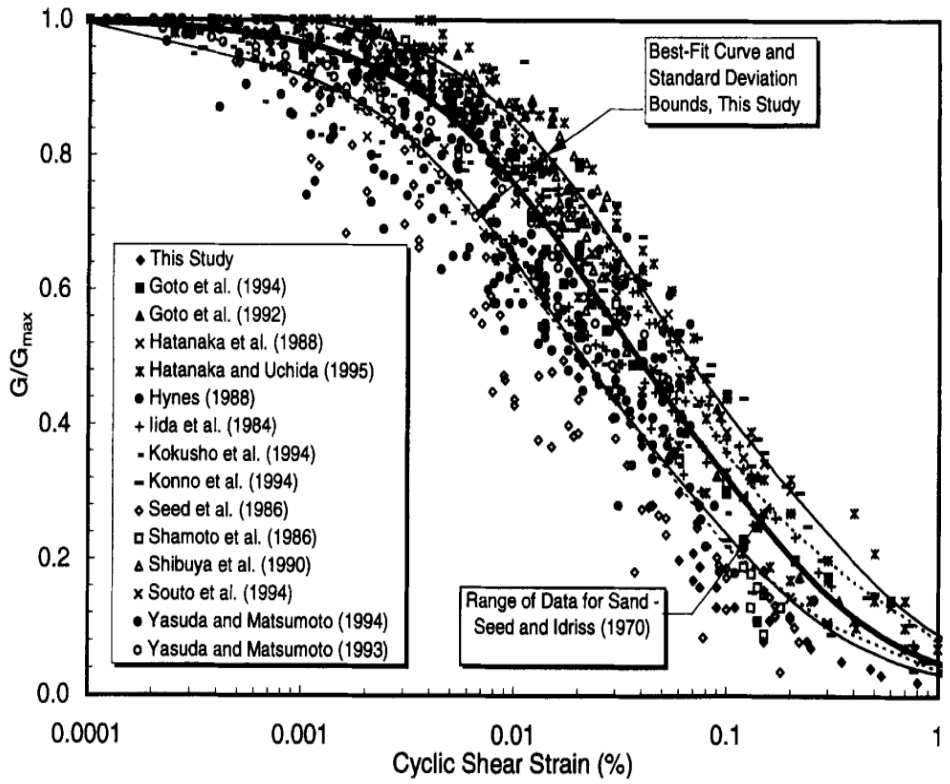

Figure A.21: Normalized shear modulus values at different strain levels (Rollins & Evans, 1998).

From the data, a best-fit curve reported by Rollins & Evans (1998) is shown in Figure A.21. The curve is a hyperbolic curve and the shear modulus according to this curve is

$$\frac{G}{G_{max}} = \frac{1}{1.2 + 16\gamma(1 + 10^{-20\gamma})} \tag{A.70}$$

Where G is the shear modulus and G_{max} is the maximum shear modulus, which is the shear modulus measured at very a low strain level of $10^{-4}\%$ (Rollins & Evans, 1998).

A similar correlation for the damping ratio with the shear strain is reported by Rollins & Evans (1998). The damping is correlated with shear strain as

$$D = 0.8 + 18(1 + 0.15\gamma^{-0.9})^{-0.75} \quad \text{(A.71)}$$

These relations are important to accurately and easily model a dynamic problem. If the expected strain level is known, the non-linear soil stress-strain curve can be reduced to an equivalent shear modulus and damping ratio. This correlation will also help aid in selecting the proper dynamic soil testing method as some testing methods produce higher strains than others which will yield a higher damping ratio while the shear modulus will be lower than a low strain inducing laboratory test.

B. A program for static and dynamic analysis of single piles subjected to vertical loading

A program that analyzes piles subjected to vertical loading is created using 1-dimensional finite element approach such as that described in section 2.3.1 of this thesis. The purpose of the program is to use it in comparing results with the 3D finite element method used in this research in cases where no analytical solution is available. The following will discuss the math behind the program. A step by step discussion on how the program is created is provided and the full code is provided afterward. The program was created in Mathematica®. Mathematica is computational language that can be used in programming engineering applications. A graphical representation of the problem is shown in Figure B.1. In Figure B.1, it is shown that the pile is divided into segments. Each segment represents a bar element. Each element is then connected to a spring and a damper along the shaft. These springs and dampers represent soil behavior along the pile shaft. The spring represent friction provided by the soil and the damper will represent geometrical damping of the soil at the side. At the base, the bar is connected to a spring and a damper both at the side and from beneath. The bottom spring and damper attached to the bottom segment represent soil behavior at the tip of the pile.

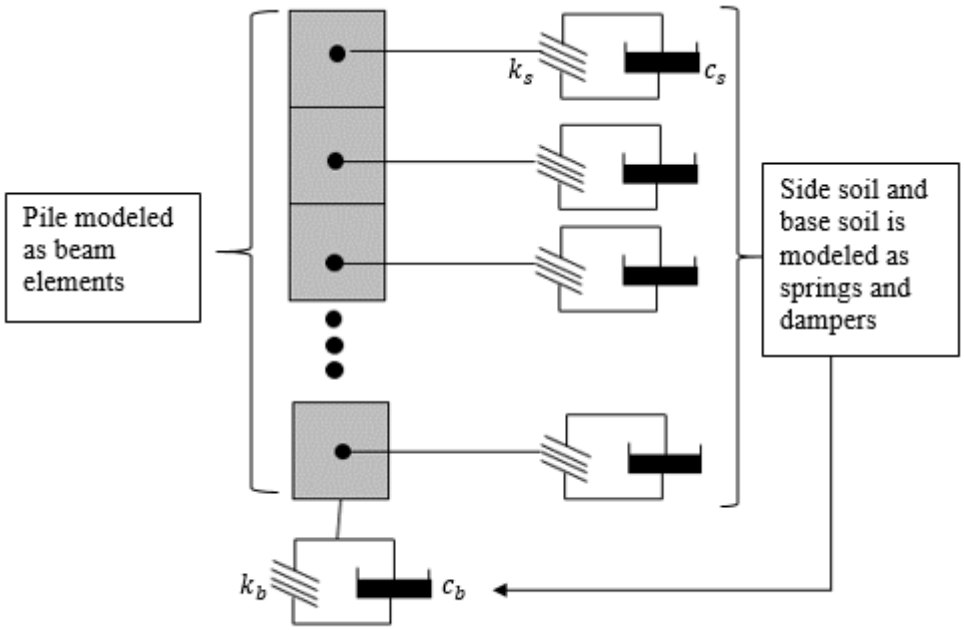

Figure B.1: Graphical representation of the problem of a pile subjected to vertical static and dynamic load modeled as 1-D bar elements.

B.1. Program Input and analysis

The program input variables are the load, its frequency, pile modulus of elasticity, pile density, pile geometry (i.e., length, radius and cross-sectional area), mass supported at the top, and finally, soil material properties (Shear modulus, Poisson's ratio, and density) . These inputs are related to the problem. another input is needed for analysis which includes time step size and number of segments the pile is divided into.

The program will take the input and generate data for analysis. Data required for analysis includes pile segment stiffness, pile segments mass matrices and side and base soil spring and dampers coefficients. The program then creates global stiffness, mass and damping matrices needed for analysis. A load vector is created depending on loading data. A static and a dynamic analysis are run, and static and dynamic displacements can be determined. The following is a step by step explanation of the math behind the program.

1- The input of pile data:

1- E_p: pile modulus of elasticity.

2- $\rho_{p:}$: pile density.

3- A_p: pile cross-sectional area.

4- L_p: pile length.

5- r: pile radius

6- $segments$: number of segments the pile is cut into.

7- M: mass supported at the top of the pile.

2- The generation of pile segment stiffness and mass matrices.

8- The stiffness matrix of the pile is 2 by 2 matrix and is calculated as

$$k_p = \frac{E_p A_p}{(L_p/segments)} \begin{bmatrix} 1 & -1 \\ -1 & 1 \end{bmatrix} \qquad \text{(B.1)}$$

9- The length of the pile is divided by the number of segments in Equation B.1 since each bar element length is equal to total pile length over the segment number.

10- The mass matrix of a pile segment is calculated as

$$M_p = \rho_p \, A_p \left(\frac{L_p}{segments}\right) \begin{bmatrix} 1/2 & 0 \\ 0 & 1/2 \end{bmatrix} \quad \text{(B.2)}$$

3- The input of soil profile data which includes shear modulus, the mass density, and Poisson's ratio. These data need to be in Mathematica table format.

4- From soil profile properties table, a table is created by the program. This table contains the springs and dampers coefficients that represent soil along the shaft and at the tip of the pile. For side spring and damper, the following Equations are used to determine the coefficients per unit length of pile (Randolph & Simons, 1986)

$$k_s = \frac{1.375 \, G_s}{\pi r_p} \quad \text{(B.3)}$$

$$c_s = \frac{G_s}{v_s} \quad \text{(B.4)}$$

In B.3 and B.4, k_s is the side spring coefficient, c_s is the damper coefficient, G_s is the side soil shear modulus at a segment, r_p is the pile radius, and v_s is the soil shear modulus of elasticity.

For the spring and the damper at the bottom, the following Equations are used

$$k_b = \frac{4 G_s r_p}{1 - \mu_s} \quad \text{(B.5)}$$

$$c_b = \frac{3.4 r_p^2}{1 - \mu_s} \rho_s v_s \quad \text{(B.6)}$$

8- Now that the stiffness and damping are calculated, the global stiffness, damping and mass matrices are assembled. It will have a size of (segments+1) by (segments+1). Note the mass supported on top the pile will be added to the first entry of the global mass matrix (i.e., entry [row 1, column 1].

9- The force vector is created and the static force is applied.

10- Static displacement vector is calculated as

$$\{u_s\} = [K_G]^{-1}\{F\} \quad \text{(B.7)}$$

Where $\{u_s\}$ is the global displacement vector, $[K_G]$ is the global stiffness matrix, and $\{F\}$ is the global force vector.

11- From $\{u_s\}$, the static displamcent at the top of the pile is calculated and static stiffness of the pile is determined by

$$k = \frac{applied\ force}{displacement\ at\ the\ top\ of\ the\ pile} \quad \text{(B.7)}$$

12- The frequency of the dynamic load is set.

13- A trapezoidal algorithm is used to calculate the dynamic displacement see flow chart in Figure B.2.

14- From dynamic analysis, the dynamic displacement can be calculated at a certain frequency.

15- Using these steps, stiffness, and damping can be obtained according to section 4.4 of this thesis.

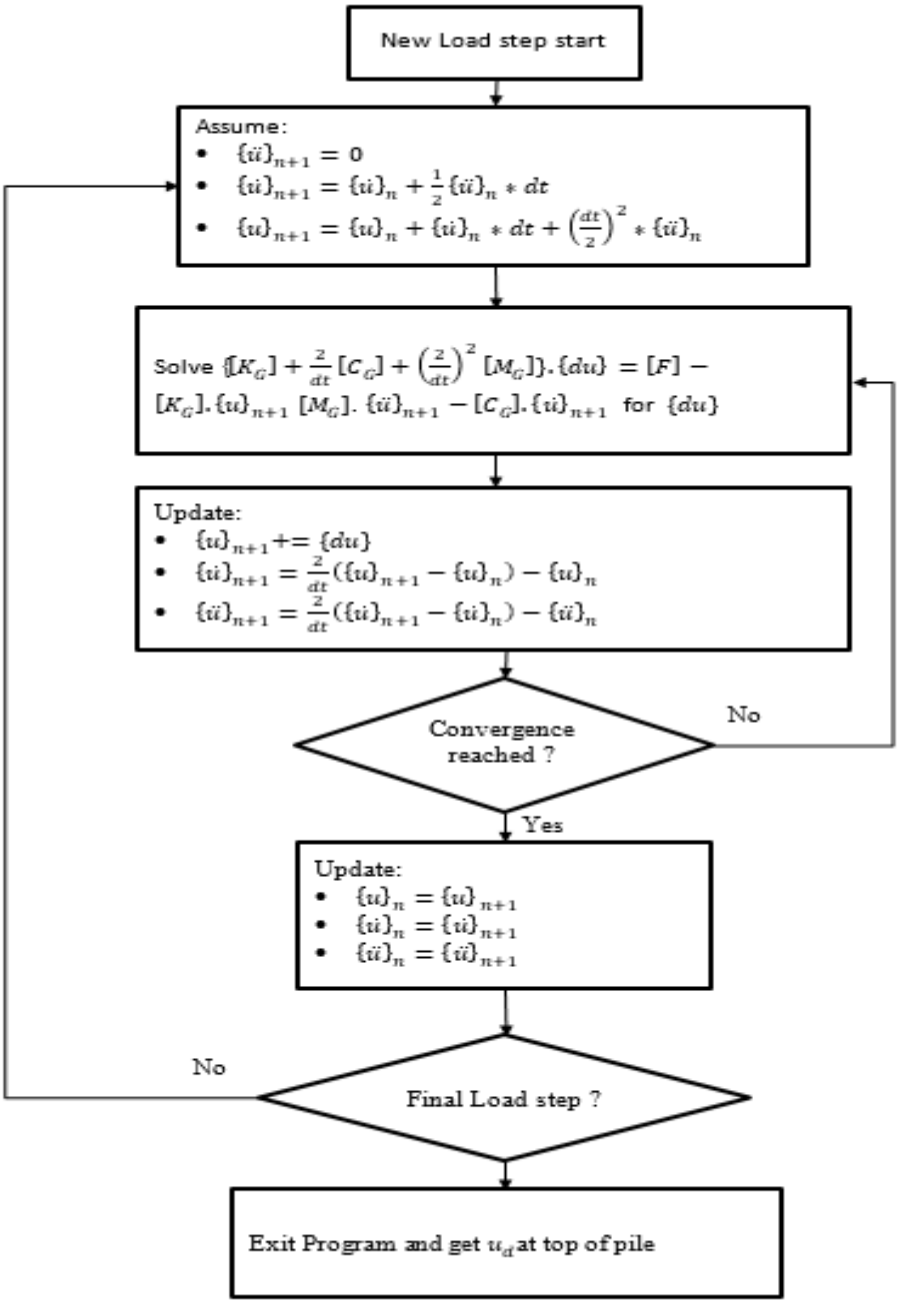

Figure B.2: Flowchart of a trapezoidal algorithm for dynamic analysis.

B.2. Program verification

The program's dynamic and static capabilities are compared to results of a pile in homogeneous soil obtained by this study. 3 different values of the soil shear modulus are chosen and a plot of displacement against frequency is plotted using the two methods, 1D FEM (i.e., this program) and finite element analysis using axisymmetric finite elements (i.e., study results). The results are plotted in Figures B.3, B.4 and B.5. Note that in these Figures, the displacement at frequency equals to zero is the static displacement of the pile. other than the displacement at the resonant frequency, the program was able to obtain results within less 10% in difference. At resonance, the program computes a dynamic displacement that is 40% to 50% higher than that computed using finite element analysis with axisymmetric elements.

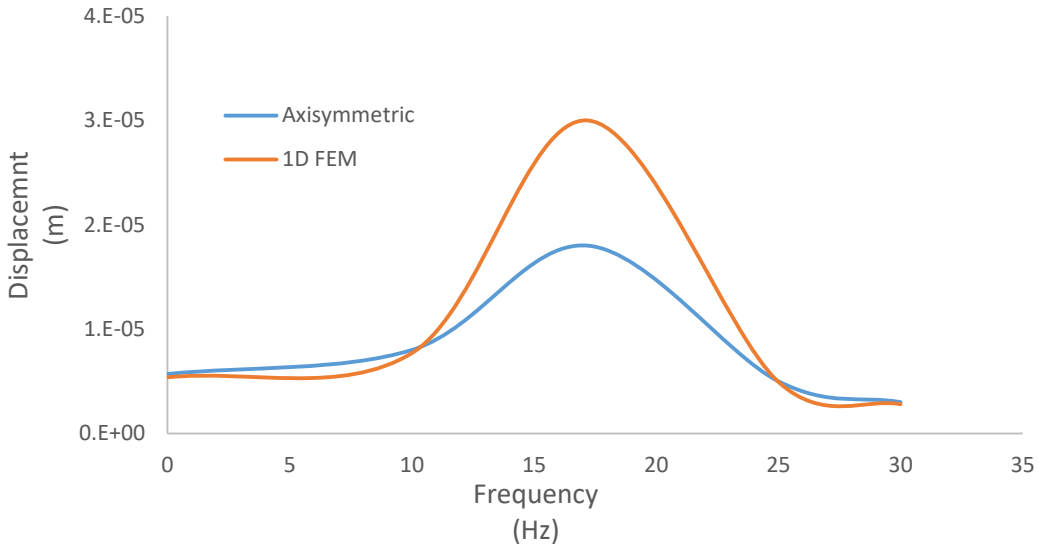

Figure B.3: Comparison of dynamic displacement computed using axisymmetric finite elements and program for soil shear modulus of $8.6 \times 10^7 Pa$.

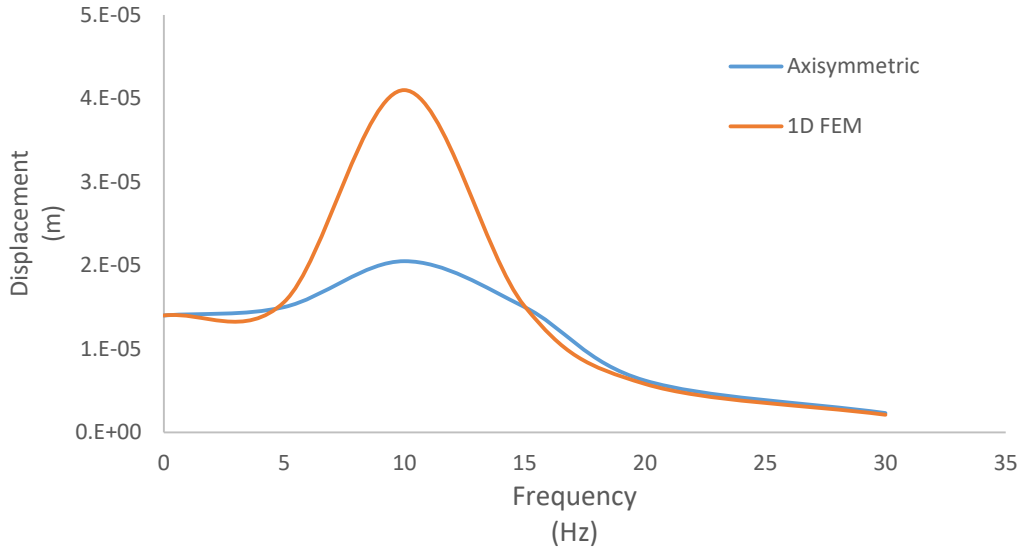

Figure B.4: Comparison of dynamic displacement computed using axisymmetric finite elements and program for soil shear modulus of $2.3 \times 10^7 Pa$.

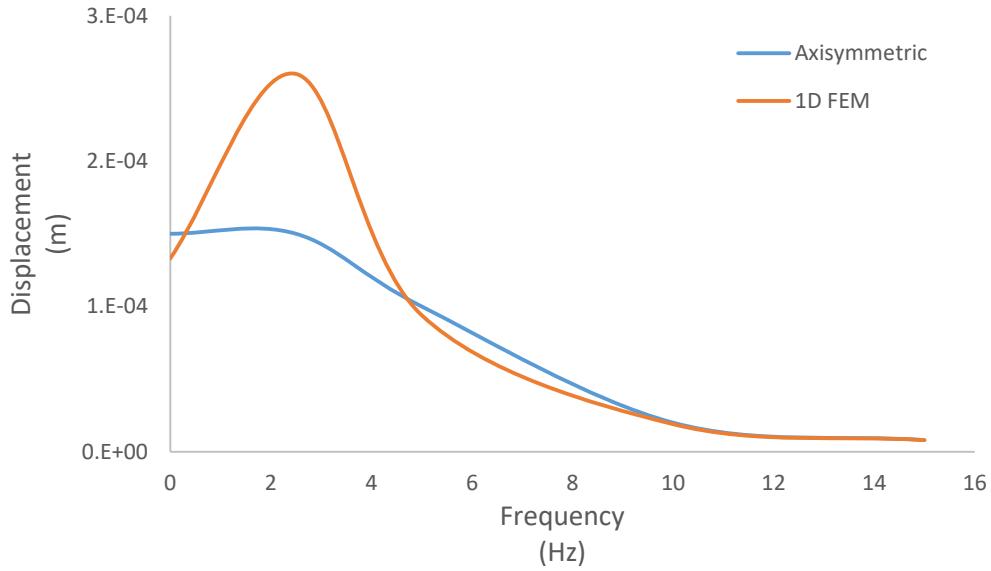

Figure B.5: Comparison of dynamic displacement computed using axisymmetric finite elements and program for soil shear modulus of $1.7 \times 10^6\ Pa$.

Appendix B.2 discusses the program created by the author for static and dynamic analysis of pile foundation subjected to vertical dynamic loading. The purpose of the program is to compare its analysis results with 3D finite element analysis results obtained by this research in cases where no analytical solution is available. The program details are discussed. It was compared with 3D finite element analysis for homogenous elastic soil cases and it was found that the program yields comparable results and is suitable to use in this research.

The following text is the actual program code:

```
(*Program dynamic vertical pile on springs and damper*)
(*load data*)
p = 22000*0.25*0.25*Pi;
(*frquency*)
freq = 16.35;
(*pile properties*)
Ep = 2.1*10^10; (*Modulus of elasticity*)
Ap = 0.25*0.25*3.14;(*cross sectional area*)
Lp  = 10; (*Pile length*)
r = 0.25; (*pile radius*)
rp = 2500; (*pile density*)
(* the pile is divided into segments*)
segments = 10;

(*mass on top of pile*)
m = 65000;
```

```
(*stiffness matrix of one segment*)
kp = ({
    {Ep*Ap/(Lp/segments), -1*Ep*Ap/(Lp/segments)},
    {-1*Ep*Ap/(Lp/segments), Ep*Ap/(Lp/segments)}
   });
(*mass matrix of a pile segment*)
mp = ρp*Ap*(Lp/segments) ({
     {1/3, 0},
     {0, 1/3}
    });
(*time step size*)
dt = 0.0001;
(*soil properties*)
ρ = 1800; (*soil density. might change to be varied according to layers, would require significant program changes. in the calculation of the spring and damper coefficients  a matrix would be used instead of one variable *)
μ = 0.45 ;(*soil Poisson's ratio*)
(*shear modulus profile a matrix of size (segments+1) by 1 could be \
uniform or varied depending onlayers*)
Gs = Array[2.88*10^8 &, {segments + 1, 1}];
(*soil spring modulus: a(segments+1) by 1 matrix describe spring \
constant at pile shaft and then
spring constant at base at entry segments+1*)
ks = Array[0 &, {segments + 1, 1}];
```

```
(*soil damper coefficient: an 11 (segments+1) by 1 matrix describes damper constant at pile shaft and then spring constant at base at entry segments+1*)
cs = Array[0 &, {segments + 1, 1}];
(*fill in the soil spring constant and damper constants by randolph and simons (1986)*)
Do[

        cs[[i, 1]] += Gs[[i, 1]]/Sqrt[Gs[[i, 1]]/\[Rho]] *Lp/segments;
        ks[[i, 1]] += 1.375*Gs[[i, 1]]/(3.14*r)*Lp/segments;
        , {i, 1, segments, 1}];
(*fill the base spring and damper constants*)
ks[[segments + 1, 1]] += 4*Gs[[segments + 1, 1]]*r/(1 - \[Mu]);
cs[[segments + 1, 1]] +=
  3.4*r^2/(1 - \[Mu])*Sqrt[Gs[[segments + 1, 1]]/\[Rho]];
(*construct the global stiffness matrix m damping and mass matrices \
size = (segments+1) by (segments+1) *)
kg = Array[
  0 &, {segments + 1, segments + 1}]; (*global stiffness matrix*)
cg = Array[
  0 &, {segments + 1, segments + 1}];(*global damper matrix*)
mg = Array[0 &, {segments + 1, segments + 1}];(*global mass matrix*)
(*fill these matrices*)
(*1 fill kg with pile stiffnesses*)
(*loop on eleemnts = # of segments*)
```

```
Do[
        (*fill global stiffness*)
        kg[[i, i]] += kp[[1, 1]];
        kg[[i, i + 1]] += kp[[1, 2]];
        kg[[i + 1, i]] += kp[[2, 1]];
        kg[[i + 1, i + 1]] += kp[[2, 2]];
        (*fill golbal dampign marix*)
        cg[[i, i]] += cs[[i, 1]];
        cg[[segments + 1, segments + 1]] = cs[[segments + 1, 1]];
        (*fill global mass*)
        mg[[i, i]] += mp[[1, 1]];
        mg[[i, i + 1]] += mp[[1, 2]];
        mg[[i + 1, i]] += mp[[2, 1]];
        mg[[i + 1, i + 1]] += mp[[2, 2]];
        , {i, 1, segments, 1}];
(*add soil stifffness to global mstiffness matrix*)
Do[
        kg[[i, i]] += ks[[i, 1]];
        , {i, 1, segments + 1, 1}];
(*add mass on top of pile*)
mg[[1, 1]] += m;
(*Global Force Matrix*)
F = Array[0 &, {segments + 1, 1}];
F [[1, 1]] = 22000*Pi*0.25^2;
```

```
us = (Inverse[kg].F)[[1, 1]];(*static displacement*)
Print["static displacement =" ]
Print[us];
(*Begin Dynamic Analysis here using trapezoidal algorithm*)
(*applied variable force vector*)
F = Array[0 &, {segments + 1, 1}];
(*incremental displacement vector size segments +1*)
dunew = Array[0 &, {segments + 1, 1}];
(*displacment vector at step n at iteration i*)
unow = Array[0 &, {segments + 1, 1}];
(*displacment vector at step n+1 at iteration i*)
unew = Array[0 &, {segments + 1, 1}];
(*acceleration at n i*)
accnow = Array[0 &, {segments + 1, 1}];
(*acceleration at n+1 at iteration i*)
accnew = Array[0 &, {segments + 1, 1}];
(*velocity at n *)
velnow = Array[0 &, {segments + 1, 1}];
(*velocity at n+1 at i*)
velnew = Array[0 &, {segments + 1, 1}];
(*internal loadvector*)
fintg = Array[0 &, {segments + 1, 1}];
(*ud Table to record dynamic displacment results)*)
udTable = Table[0, {i, 10001}, {j, 1}];
```

```
(*begin trapezoidal algorithm*)
(*load step number*)
sn = 1;
(*loop on steps n*)
Do[
    (*set the accleration at n+1 to 0*)
    accnew = Array[0 &, {segments + 1, 1}];
    (*get veleocity at n+1 and displacment at n+1*)
    velnew = velnow + 0.5*accnow*dt;
    unew = unow + velnow*dt + (dt/2)^2*accnow;
    (*get load at current step*)
    F[[1, 1]] = p*Sin[n*freq*2*Pi];

    (*start iteration to get unow velnow and accnow at n+1*)
    Do[
        (*get big trapezoidal Equation*)
        TeqL = kg + (2/dt)*cg + (2/dt)^2*mg;(*left side*)
        TeqR = F - kg.unew - mg.accnew - cg.velnew;
        dunew = Inverse[TeqL].TeqR;
        unew += dunew;
        velnew = (2/dt)*(unew - unow) - velnow;
        accnew = (2/dt)*(velnew - velnow) - accnow;
        (*get convergence*)
        (*intiate values*)
```

```
            convTop = 0;
            convBot = 0;
            Do[
                convTop += dunew[[k, 1]]^2;
                convBot += unew[[k, 1]]^2;
                , {k, 1, segments + 1, 1}];
            (*check convergence*)
            If[And[n != 0, Sqrt[convTop]/Sqrt[convBot] <= 0.0001], Break[];];
            (*If[And[n\[NotEqual]0,Sqrt[F[[1,1]]-(kg.unew)[[1,
 1]]\[LessEqual]0.0001]],Print["Converged"];Break[];]*)
            , {i, 1, 200, 1}];
            (*udate values at n*)
            unow = unew;
            velnow = velnew;
            accnow = accnew;
            (*record results*)
            udTable[[sn, 1]] += unow[[1, 1]];
            sn += 1
        , {n, 0, 1, dt}]
(*export dynamic analysis results to excel for processing*)
Export["udTable.csv", udTable];
```

Bibliography

1- ACI 351 (2004). Foundations for Dynamic Equipment, American Concrete Institute, 351.34, Farmington Hill, MI.

2- Ali, Osama (2015). Vertical Dynamic Soil-Pile Interaction for Machine Foundations. University of Maryland, College Park, MD, U.S.A.

3- Autodesk Simulation Mechanical 2014-2017, Autodesk. Retrieved from: https://www.autodesk.com/education/free-software/simulation-mechanical.

4- Bathe, K. J. (2006). Finite element procedures. Klaus-Jurgen Bathe. Retrieved from: http://web.mit.edu/kjb/www/Books/FEP_2nd_Edition_4th_Printing.pdf

5- Baxter, R. L. & Bernhard, D. L. (1967, January). Vibration Tolerances for Industry. ASME-American Society of Mechanical Engineers. Vol. 89(7).

6- Bharathi, M. Raj, D. & Dubey, D.R. (2014). Codal Provisions for Design of Machine Foundations–A Review. International Symposium Geohazards: Science: Engineering and Management, Kathmandu, Nepal, November, pp. 20-21.

7- Butterfield R. & Banerjee, P. K. (1971). The problem of pile group–pile cap interaction. Geotechnique, Vol. 21(2), pp. 135-142.

8- Chow, Y.K. & Teh, C.I. (1991). Pile-Cap-Pile-Group Interaction in Nonhomogeneous Soil. Journal of Geotechnical Engineering, Vol. 117(11), pp. 1655-1668.

9- Chowdhury, I. & Dasgupta, S.P. (2006). Dynamic Response of Piles Under Vertical Loads. Indian Geotechnical Journal, Vol. 115(143).

10- Chowdhury, I. & Dasgupta, S. P. (2008). Dynamics of Structure and Foundation-A Unified Approach: 1. Fundamentals (Vol. 1). CRC Press.

11- Coyle, H. M. Lowery, L. L. & Hirsch, T. J. (1977). Wave Equation Analysis of Piling Behavior. Numerical Methods in Geotechnical Engineering, pp. 272–296. Mcgraw-Hill.

12- Das, B. & Ramana, G.V. (2010). Principles of Soil Dynamics. Cengage Learning.

13- Davis, R.O. & Selvadurai, A.P.S. (1996). Elasticity and Geomechanics. Cambridge University Press.

14- Desai, C.S. & Zaman, M. (2013). Advanced Geotechnical Engineering: Soil-Structure Interaction using Computer and Material Models. CRC Press.

15- DIN 4024: Machine Foundations. (1955).

16- Dobry, R. (2014). Simplified Methods in Soil Dynamics. Soil Dynamics and Earthquake Engineering, Vol. 61, pp. 246-268.

17- Dobry, R. & Gazetas, G. (1988). Simple Method for Dynamic Stiffness and Damping of Floating Pile Groups. Geotechnique, Vol. 38(4), pp. 557-574.

18- El Naggar, H. & El Naggar, M.H. (2007). Simplified Approximate Approach to Group Effect in Pile Dynamics. Fourth International Conference on Earthquake Geotechnical Engineering, Greece, 1325.

19- Elkasabgy, M. & El Naggar, M.H. (2013). Dynamic Response of Vertically Loaded Helical and Driven Steel Piles. Canadian Geotechnical Journal, Vol. 50(5), pp. 521-535.

20- Gazetas, G. & Makris, N. (1991). Dynamic Pile-Soil-pile Interaction. Part I: Analysis of Axial Vibration. Earthquake Engineering & Structural Dynamics, Vol. 20(2), pp. 115-132.

21- Gazetas, G. & Mylonakis, G. (1998). Settlement and Additional Internal Forces of Grouped Piles in Layered Soil. Géotechnique, Vol. 48(1), pp. 55–72.

22- Hardin, B.O. & Black, W.L. (1968). Vibration Modulus of Normally Consolidated Clay. Journal of the Soil Mechanics and Foundations Division, Vol. 94, pp. 353–370.

23- Hardin, B.O. & Richart, J.F.E. (1963). Elastic Wave Velocities in Granular Soils. ASCE Proceedings Journal of the Soil Mechanics and Foundations Division, Vol. 89, pp. 33–65.

24- Holeyman, A.E. (1988). Modelling of Dynamic Behavior at the Pile Base. Proceedings of the 3rd International Conference on the Application of Stress-Wave Theory to Piles, pp. 174–185.

25- Hsieh, T.K. (1962), Foundation Vibrations, Proceedings, Institute of Civil Engineers, London, Vol. 22, pp. 211-226.

26- Kagawa, B.T. (1991). Dynamic Soil Reaction to Axially Loaded Piles. Journal of Geotechnical Engineering, Vol. 117(7), pp. 1001–1020.

27- Lambe, H. (1904). On the Propagation of Tremors Over the Surface of an Elastic Solid. Philosophical Transactions of the Royal Society of London, Vol. 203, pp. 1–42.

28- Logan, D. L. (2011). A first course in the finite element method. Cengage Learning.

29- Lysmer, J. (1978). Finite Element Analysis of Soil-Structure Interaction. Report No. UCB/EERC-78/29, University of California, Berkeley, CA.

30- Lysmer, J. and Richart, F. E. (1966). Dynamic Response of Footings to Vertical Loading. Journal of the Soil Mechanics and Foundations Division. ASCE, Vol. 92(1), pp. 65-91.

31- Mathematica 10. Wolfram Alpha. Retrieved from: http://www.wolfram.com/mathematica/?source=nav.

32- Novak, M. (1974). Dynamic Stiffness and Damping of Piles. Faculty of Engineering Science, University of Western Ontario, London, Ontario.

33- Novak, M. (1977). Vertical Vibration of Floating Piles. Journal of the Engineering Mechanics Division, Vol. 103(1), pp. 153–168.

34- Novak, M. & Beredugo, Y.O. (1972). Vertical Vibration of Embedded Footings, Journal of the Soil Mechanics and Foundations Division, ASCE, Vol. 98 (SM12), pp. 1291-1310.

35- Potts, D. M. & Zdravkovic, L. (1999). Finite Element Analysis in Geotechnical Engineering: Theory. Thomas Telford.

36- Potts, D. M. & Zdravkovic, L. (2001). Finite Element Analysis in Geotechnical Engineering: Application. Thomas Telford.

37- Poulos, H. G. (1968). Analysis of Settlement of Pile Groups, Geotechnique, Vol. 18(4), pp. 449-471.

38- Prakash, S. & Puri, V.k. (1988). Foundations for Machines. John Wiley and Sons.

39- Quinlan, P. (1953). The Elastic Theory of Soil Dynamics. ASTM Special Technical Publication.

40- Randolph, M.F. and Simons, H.A. (1986). An Improved Soil Model for One Dimensional Pile Driving Analysis. Proceedings of the 3rd International Conference of Numerical Methods in Offshore Piling, pp. 3-17.

41- Randolph, M.F. & Wroth, P. (1978). Analysis of Deformation of Vertically Loaded Piles. Journal of the Geotechnical Engineering Division, Vol. 104(12), pp. 1465–1488.

42- Reissner, E. (1936). Stationäre, axialsymmetrische, durch eine schüttelnde Masse erregte Schwingungen eines homogenen elastischen Halbraumes. Ingenieur-Archiv, Vol. 7(6), pp. 381–396.

43- Richart, F.E. Hall, J.R., and Woods, R.D. (1970). Vibration of Soils and Foundations. Prentice-Hall, Inc., Englewood Cliffs, NJ.

44- Rollins, K. & Evans, M. (1998). Shear Modulus and Damping Relationships for Gravels. Journal of Geotechnical Engineering Vol. 124(5)

45- SAES-Q-007: Foundations and Supporting Structures for Heavy Machinery. (2009), Saudi Aramco, SA

46- Seidel, M. & Coronel, M.C. (2011). A New Approach for Assessing Offshore Piles Subjected to Cyclic Axial Loading. Geotechnik, Vol. 34(4), pp. 276–284.

47- Sharnouby, B. & Novak, M. (1985). Static and Low-Frequency Response of Pile Groups. Canadian Geotechnical Journal, Vol. 22(1), pp. 79–94.

48- Smith, E.A.L. (1960). Pile-Driving Analysis by the Wave Equation. Journal of Soil Mechanics and Foundations Division, Vol. 86(EM 4), pp. 35-61.

49- Stokoe, K. & Woods, R. (1972). In Situ Shear Wave Velocity by Cross-Hole Method. Journal of the Soil Mechanics and Foundations Division, Vol. 98(SM5), pp. 443–457.

50- Sung, T. (1954). Vibrations in Semi-Infinite Solids due to Periodic Surface Loading. In Symposium on Dynamic Testing of Soils. ASTM International.

51- Varga, R. S. (2009). Matrix Iterative Analysis. Springer Science & Business Media.

52- Verruijt, A. (2010). An Introduction to Soil Dynamics. Springer Science & Business Media.

53- Wilson, E.L. (2002). Three-Dimensional Static and Dynamic Analysis of Structures, Computers and Structures, Inc.

54- Zhang, J. & Tang, Y. (2007). Radiation Damping of Shallow Foundations on Nonlinear Soil Medium, 4th International Conference on Earthquake Geotechnical Engineering.